

The Role of the Guanine Nucleotide Exchange Factor Rab3GEP in the regulation of Rab27a

Paolo Sanzà

University of Nottingham
School of Life Sciences

2017

ai miei Genitori

Abstract

In mammalian cells vesicle transport is an important process, many diseases are caused by defects of trafficking. Key elements for organelle trafficking are Rab proteins which regulate this system. Rabs are GTPases and belong to the Ras superfamily proteins. Rab27a is one of the main actors of this process, it promotes the recruitment of secretory vesicles at the release site, the plasma membrane, by its role of interconnection between the vesicle and the motor protein myosin V. Dysfunction leads to disease such as Griscelli syndrome. Rab27a is a molecular switch, in the active state is able to bind effectors. The switching from the GDP-bound to the GTP-bound is catalysed by Rab3GEP. Furthermore, to function properly Rab27a has to be targeted to the organelle membrane, this function has been attributed to the guanine exchange factor as well. Rab3GEP contains a DENN domain (*differentially expressed in normal versus neoplastic*) at the N-terminus and a death domain at the C-terminus. Rab3GEP belongs to the family of DENN domain proteins, in general DENN domains are considered as domains with a guanine exchange factor activity. Down-regulation of this Rab3GEP in melan-a melanocytes induces to melanosome clustering at the perinuclear area. There is no knowledge about the mechanism of Rab3GEP in the activation and targeting of Rab27a to the vesicle membranes. To better characterise Rab3GEP protein, truncations and point mutations of this GEF were performed and they were tested in cell based assays (using melanocytes with Rab3GEP knock out) and in pull down assays (using the capacity to activate Rab27a as a read out of the GEF activity). Moreover, Rab3GEP wild type, and some mutants were mis-targeted from the cytosol (normal localisation) to mitochondria, in order to investigate their capacity to rescue melanosome distribution in melan-Rab3GEP KO cells and to examine their ability to re-target Rab27a to a different membrane organelle. Results reported in this thesis indicate that point mutations within the DENN domain impair the ability of Rab3GEP to rescue the melanosome disperse distribution and to activate Rab27a in vitro assay, suggesting the crucial role of this domain for the Rab3GEP activity. However, the DENN domain alone is not sufficient to rescue melanosome distribution and to activate Rab27a. This suggests an essential role of the other parts of the protein. Moreover,

evidence in this thesis indicate that the cytosolic localisation of Rab3GEP is essential for the ability of Rab3GEP to rescue melanosome distribution, and that the targeting activity of Rab3GEP towards Rab27a is dependent on its GEF activity. However, evidence obtained by studying melan-Rab3GEP KO cells indicate that despite the important role of Rab3GEP in Rab27a activation/targeting, it is not essential.

Table of Contents

Abstract i

Table iii

Acknowledgments vii

Declaration viii

List of Figures and Tables ix

Abbreviations xiv

1 Introduction 1

1.1 Ras proteins overview 2

1.2 Rab proteins 3

1.2.1 Rab proteins structure 3

1.2.2 Rab proteins regulation 7

1.2.3 Rab proteins cycle 8

1.2.4 Rab GEFs 11

1.2.4.1 DENN domain proteins 13

1.2.4.2 Vps9 domain proteins 16

1.2.4.3 Sec2 domain proteins 17

1.2.4.4 TRAPP domain proteins 17

1.2.5 Rab GAPs 18

1.3 Rab27 proteins 20

1.3.1 Rab27 Cycle 21

1.3.2 Guanine nucleotide exchange factor of Rab27 22

1.3.3 Rab27 GAPs 25

1.3.4 Rab27 Effectors 25

1.3.5 Diseases correlated with Rab27 29

1.3.6 Melanosome maturation and trafficking 31

1.3.7 Aims 37

2 Materials and Methods 38

2.1 Cell culture 38
2.1.1 Murine Melanocytes 38
2.1.2 Human Embryonic Kidney (HEK)-293a cell line 38
2.1.3 Sub-culturing of cells 39
2.1.4 Cell cryopreservation 39
2.1.5 Transfections 40
2.1.5.1 Plasmid DNA 40
2.1.5.2 siRNA Transfection 40
2.1.6 Counting cells 41
2.2 DNA Techniques 42
2.2.1 Transformations 42
2.2.2 Small scale purification plasmid DNA 42
2.2.3 Polymerase chain reaction (PCR) 42
2.2.4 Site-directed mutagenesis 43
2.2.5 Agarose gel Electrophoresis 43
2.2.6 Restriction endonuclease digestion 44
2.2.7 Ligation 44
2.2.8 Plasmid constructs 44
2.2.9 DNA sequencing 45
2.2.10 Adenovirus generation 46
2.3 Protein Techniques 47
2.3.1 Western Blot analysis 47
2.3.1.1 Preparation Sodium dodecyl sulphate polyacrylamide gel 47
2.3.1.2 Preparation of samples 48
2.3.1.3 Protein quantification 49
2.3.1.4 Electrophoresis 49
2.3.1.5 Transferring to membrane and immunoblotting 49
2.3.2 GST Pulldown Assay 50
2.3.3 Antibodies for Western Blot 51

2.4 Microscopy....52
2.4.1 Cells seeding on coverslips....52
2.4.1.1 Free growing cells....52
2.4.1.2 Micropattern....52
2.4.2 Fixation and Immunostaining....52
2.4.3 Mitotracker staining....53
2.4.4 Microscopes used for imaging....53
2.4.5 Cell phenotype analysis....54
2.4.6 Micropattern Cells analysis....55
3 Characterisation melan-Rab3GEP knockout cells....56
3.1 Introduction....56
3.2 Active Rab27a in melan-Rab3GEP KO cells with disperse melanosome distribution....60
3.3 Discussion....72
4 Integrity of Rab3GEP protein is crucial for the GEF activity....74
4.1 Introduction....74
4.2 Truncated Rab3GEP mutant expression in HEK293a....78
4.3 Expression of truncated Rab3GEP mutants in melan-Rab3GEP K.O. cells....81
4.3.1 Visualization of Rab3GEP truncations in melan-Rab3GEP KO cells with high magnification....87
4.3.2 Analysis of the function of truncated Rab3GEP proteins using micropattern chip....90
4.3.3 Truncated mutants of Rab3GEP are not able to activate Rab27a....95
4.4 Expression of point Rab3GEP mutant in melan-Rab3GEP KO cells....101
4.4.1 Visualization of point mutants Rab3GEP in melan-Rab3GEP KO cells with high magnification....112
4.4.2 Analysis of the function of Rab3GEP DENN domain point mutants using micropattern chip transport assay....114

4.4.3 I353D point mutation of Rab3GEP causes impairment of the GEF activity of Rab3GEP 118

4.5 Discussion 122

5 Rab3GEP distribution and its activity 126

5.1 Introduction 126

5.2 The cytoplasmic distribution of Rab3GEP is essential for its function in melanosome transport 128

5.3 Rab27a follows Rab3GEP to mitochondrial localisation 137

5.4 Deletion of the Death Domain of Rab3GEP abolish its capacity to target Rab27a 145

5.5 I353V point mutation reduce the capacity to re-target Rab27a to mitochondria 150

5.6 Discussion 155

6 Conclusion 157

7 Appendix 159

7.1 The proportion of cells with melanosomes clustered mirrors the rate of cell proliferation 159

7.2 Defect of anterograde melanosomes trafficking during cell growth 161

References 164

Acknowledgments

Firstly, I would like to thank my supervisor Alistair Hume for allowing me to carry out my PhD in his Lab, for his guidance and support during the past three years. I would like to thank my co-supervisor Sally Wheatley for having kindly given me antibodies and drugs important for my research and for her suggestions and support.
I would like to thank Debs Briggs for her availability in the Lab and for her "tolerance" every time I bothered her.
I would like to thank Raghdan Al-Saad for his support in the lab, and for the long conversations.
I would like to thank Chris Robinson and Richard Evans for their support in the lab.

Moreover, I would love to thank Daniele Bergamaschi for believing in me while I was in London and for giving me the opportunity to learn a lot regarding cell signalling in his lab.
A special thank goes to Anissa Chikh for believing in me in difficult moments, for her training, help and support. I would like to thank all my friends wherever they are all around the world. Finally, but not for importance I would love to thank my Family, no word can explain my huge gratitude for my Brothers and my Parents.

Declaration

I declare that this manuscript and the work presented in it have been generated by me as result of my own research under the supervision of Dr Alistair Hume. Any contributes are referenced accordingly.

Paolo Sanzà

List of Figures and Tables

Figure 1 Conserved sequences between Rab proteins 4

Figure 2 Human Rab family divided in subfamilies 5

Figure 3 Rab activation and deactivation 7

Figure 4 General Rab cycle 9

Figure 5 Models of Rab targeting to the membranes 10

Figure 6 Multistep reactions of GEFs 11

Figure 7 Structures of nucleotide-free Rab-GEF complex 12

Figure 8 DENN domain protein families in human 14

Table 1 Specificity GEF activity of the DENN Family 16

Figure 9 RabGAPs Mechanism 19

Figure 10 Model of Rab27 cycle 21

Figure 11 Structure of human Rab3GEP protein 22

Figure 12 The double role of MADD/DENN/Rab3GEP 24

Figure 13 Rab27 effectors 26

Table 2 Rab27 effectors and functions 28

Figure 14 Melanosome stages I-IV 31

Figure 15 Eumelanin and pheomelanin biosynthetic pathways 32

Figure 16 Melanosome anterograde trafficking models 34

Figure 17 Model activation and targeting of Rab27a on melanosome membrane 35

Figure 18 Melanosome redistribution due to defect of the anterograde trafficking 36

Table 3 Volume used for passaging tissue culture cells 39

Table 4 Table siRNA 41

Table 5 Setting used for PCR reaction.....43

Table 6 Setting used for site-directed mutagenesis 43

Table 7 List of primers.....45

Table 8 Components of Stacking Gel 48

Table 9 Components of Separating Gel 48

Table 10 Antibodies used for Western Blot 51

Table 11 Antibodies used for immunostaining.....53

Figure 19 Example of cells with clustered and dispersed melanosome distribution counted with ImageJ 54

Figure 20 Cell cycle regulation by Retinoblastoma and p53.....58

Figure 21 Rab3GEP knockdown in melan-ink4 melanocytes induces perinuclear distribution of melanosomes 61

Figure 22 Representative image of melan-Rab3GEP KO cells show a mixed population of cells with different melanosome distribution.....62

Figure 23 Images showing the mixed phenotype of the #1, #2 and 3# melan-Rab3GEP cell lines.....63

Figure 24 melan-Rab3GEP KO cells do not express Rab3GEP protein 64

Figure 25 Disperse melanosome distribution in melan-Rab3GEP KO cell is driven by Rab27a.....65

Figure 26 Lower expression of endogenous melanophilin and Rab27a in melan-Rab3GEP KO cell lines compared to melan-a cell line 67

Figure 27 Endogenous localisation and expression of melanophilin in melan-Rab3GEP KO, melan-a and Leaden cell lines.....71

Figure 28 Schematic representation of the cell based assay of Rab3GEP function 75

Figure 29 Schematic representation of the GST-Slp1 pull-down assay 77

Figure 30 Schematic representation of truncated mutations of Rab3GEP ..78

Figure 31 Similar GFP signal between the different truncation of Rab3GEP protein in HEK293a 79

Figure 32 Truncated mutations of Rab3GEP present the predicted molecular weight in melan-Rab3GEP KO cells.....82

Figure 33 Overexpression of the truncation mutant of Rab3GEP in melan-Rab3GEP KO cells do not rescue melanosome distribution.....85

Figure 34 High magnification images of in melan-Rab3GEP KO cells expressing GFP-labelled truncated mutants of Rab3GEP.....88

Figure 35 Melanosome distribution in GFP-Rab3GEP and GFP expressing melan-Rab3GEP KO cells grown on micropattern substrates 91

Figure 36 Schematic representation of micropattern chip analysis.....92

Figure 37 Truncation of Rab3GEP lose the ability to disperse melanosomes toward the cell periphery 94

Figure 38 GFP expression truncation isoforms of Rab3GEP and their controls full-length and GFP, and expression level of Rab27a between all the samples 97

Figure 39 Truncation isoforms of Rab3GEP are not able to activate Rab27a 99

Figure 40 3D model of DENN domain of Rab3GEP based on DENND1B and point mutations 104

Figure 41 The location of point mutations in Rab3GEP protein 105

Figure 42 Expression of Rab3GEP point mutants in HEK293a 106

Figure 43 Expression of the point mutation of Rab3GEP in melan-Rab3GEP KO cells do not restore the dispersed distribution of melanosomes 110

Figure 44 Expression of Rab3GEP point mutants and melanosome distribution in free growing melan-Rab3GEP KO cells.....112

Figure 45 Point mutations of Rab3GEP expressed in cells visualised in Micro Pattern 116

Figure 46 I353D of DENN domain of Rab3GEP and correspond to I226 of DENND1B 118

Figure 47 GFP and mCherry expression in HEK293a before protein collection 119

Figure 48 Pull-down assays indicate lack of GEF activity of the point mutation I353D and activity of R514A.....120

Figure 49 The intracellular distribution of GFP-Rab3GEP in melan-Rab3GEP KO melanocytes.....129

Figure 50 Schematic representation of Rab3GEP-FKBP/FRB-Tomm70 system 130

Figure 51 Schematic representation of predicted results using GFP-Rab3GEP-FKBP 131

Figure 52 Drug treatment allows the formation of the heterodimer FKBP-FRB and co-localisation of Rab3GEP with Tomm70.....132

Figure 53 Formation of the heterodimer Rab3GEP-FKBP-FRB-Tomm70 reduces the percentage of cells with disperse melanosome distribution..135

Figure 54 Tomm70-GFP-Rab3GEP is localised to mitochondria 137

Figure 55 Expression of Tomm70-GFP-Rab3GEP protein does not restore melanosome distribution in melan-Rab3GEP KO cells.....139

Figure 56 Expression of Tomm70-GFP-Rab3GEP in melan-Rab3GEP KO cells results in mis-targeting of Rab27a to mitochondria 142

Figure 57 ΔDD truncation loss the capacity to re-target Rab27a to mitochondria 147

Figure 58 Point mutant Rab3GEP^{I353V} loss the capacity to re-target Rab27a to mitochondria 152

Figure 59 Relationship between total number of melan-Rab3GEP ko cells and cells with clustered melanosomes 160

Figure 60 PMA increases cell number and proportion of cells with clustered melanosome distribution in melan-Rab3GEP KO #1.....162

Abbreviations

APS - Ammonium Persulfate
Arf - ADP-ribosylation factor
BSA - Bovine Serum Album
DAPI - 4’,6-diamidino-2-phenylindole
Dbl - diffuse B-cell lymphoma
DD – Death domain
dDENN- downstream DENN
DENN - Differentially Expressed in Normal versus Neoplastic
DH - Dbl-homology
DMEM - Dulbeco’s Modified Eagle Medium
DMSO - Dimethyl sulfoxide
DNA - desoxyribonucleic acid
dNTP - deoxynucleotide triphosphate
DrrA - defect in Rab1 recruitment A
EDTA - ethylene-diamine-tetraacetic acid
F-actin - Filamentous actin
FADD -.Fas-associated death domain
FBS - Fetal Bovine Serum
FKBP - FK506-binding protein domain
FRB - FKBP-rapamycin-binding domain
G-actin - Globular actin
GAP- GTPase-activating protein
GDF - GDI-displacement factor
GDI - GDP dissociation inhibitor
GDP - guanosine diphosphate
GEF - guanine-nucleotide exchange factor
GFP - green fluorescent protein
Grb2 - Growth factor receptor-bound protein 2
GST - glutathione S-transferase
GTP - guanosine triphosphate
GTPase - guanosine triphosphatase
HEK - human embryonic kidney
KIF - kinesin superfamily protein
LCV - Legionella-containing vacuole
M&M -Materials and Methods

MADD - MAPK activating death domain
MAPK - mitogen activated protein kinase
Mlph - melanophilin
Mst1- Macrophage stimulating 1
MyoVa – MyosinVa
PBS - Phosphate Buffered Saline
PCC - Pearson Correlation Coefficient
PMA - Phorbyl 12-myristate 13-acetate
PMEL17 - pre-melanosome protein
PVDF - polyvinylidene fluoride
Rab - Ras-like proteins in brain
Rab3GEP - rab3 GDP/GTP exchange protein
Rabex5 - rabaptin-5 associated exchange factor for Rab5
Ran- Ras-related Nuclear protein
Ras- Small rat sarcoma
RCC1 - regulator of chromosome condensation 1
REP - Rab escort protein
RGGT- Rab-geranylgeranyl transferase
Rho-Ras homolog
Rin - ras interaction/interference
RIP - receptor interacting protein
SDS - sodium dodecyl sulphate
SH2 - Src-homology 2
SHD - Slp homology domain
siRNA - small interfering RNA
Slac2 - synaptogmin-like protein lacking C2 domains
Slp - synaptotagmin-like proteins
Sos1/2 - Son of sevenless homolog
TRADD - TNFR-associated death domain
TRAF2 - TNFR-associated factor 2
TRAPP - Transport Protein Particle
uDENN- upstream DENN
ULK - Unc-51 like autophagy activating kinase 1
Varp - Vps9-ankyrin-repeat protein
Vps9 - Vacuolar Protein Sorting 9

1 Introduction

The cell contains membrane bounded organelles each of them with precise roles. Each of these organelles contains specific components and has specific functions. Organelles communicate with one another to perform their function in the cell. Plasma membranes, endoplasmic reticulum, Golgi apparatus are examples of organelles that are linked by vesicular transport. Vesicles are released by the donor organelle, move through the cytosol to reach the acceptor organelle, here they release their contents (1). Budding, transport, tethering and fusion are the essential four steps for the correct communication between organelles by vesicles. Trafficking of these vesicles is not random, but it is tightly regulated. In fact, the vesicles do not move in the cytosol indiscriminately but rather they are anchored to the microtubules and actin filaments, and they are directed to precise target. The Rab (*Ras-like proteins in brain*) family is known to regulate vesicular trafficking, this family of protein belongs to the Ras (*Rat sarcoma*) superfamily (2). Ras proteins are small GTPases with low molecular weight (20-30kDa) that play a crucial role in the regulation of cell signal transduction and in the physiology of the cell. Ras superfamily of small GTPases, together with their effectors and regulators, control a large number of activities of the cell. Trafficking, cell signalling, cytoskeletal regulation are some of the functions performed by the subfamilies of Ras GTPases (3). Ras superfamily proteins are molecular switches, and their state, active or inactive is tightly controlled by regulators known as GEFs (*Guanine nucleotide Exchange Factors*) and GAPs (*GTPase-activating proteins*). GEFs regulate the activation of the GTPase instead GAPs favour their inactivation (4).

Since the 1950s, many studies have been performed to understand the mechanisms involved in vesicular trafficking and how specific vesicles can reach their targeting in a spatial and temporal ways. A great contribution to our understanding has been the discovery of Rab proteins as key factors in the regulation of these processes.

Melanosomes are pigment storage vesicles and they are present in skin melanocytes, in choroidal melanocytes and in retinal pigment epithelial (5). Melanosome trafficking has been extensively studied, and one protein crucial for their trafficking is Rab27a (6). This protein, as other proteins belonging to the Ras superfamily, is regulated by GEFs and GAPs (7,8).

This thesis will discuss the melanosome trafficking in melanocytes depleted of Rab3GEP, a GEF for Rab27a. Moreover, in this thesis the role of Rab3GEP

in targeting and activation of Rab27a will be characterised. In order to understand the behaviour of Rab27a and its GEF, this introduction will discuss the main features of the Rab Family, describing the main structures and regulators of the molecular switch. Subsequently, it will narrow in the main characteristics and regulation of Rab27a in melanosome trafficking.

1.1 Ras proteins overview

The Ras superfamily is constituted by five distinct branches: Ras, Rho, Ran, Arf, Rab. Genomic studies have revealed 167 proteins belonging to the Ras superfamily in human, these proteins are grouped into the five families except for ten of them which are defined as unclassified (2).
The family of Ras proteins are involved in proliferation, differentiation, signal transduction and apoptosis (3,9). Rho proteins (*Ras homolog*) are involved in cell cycle, regulation of actin organisation, gene expression, in cell shape, regulation of cell polarity as well as cell movement and they seem to be involved in the processes of exocytosis and endocytosis (10,11). Ran GTPases (*RAs-related Nuclear protein*) are involved in the trafficking of RNA and proteins across the nuclear envelope, as well as in the assembly of the mitotic spindle, nuclear envelope and in DNA replication (12,13). Arf proteins (*ADP Ribosylation Factors*) are involved in trafficking of membranes and proteins as well as into the reorganisation of the cytoskeleton (3).
Rab proteins (*Ras-like proteins in brain*) represent the largest family of the Ras superfamily, 11 Rabs have been identified in yeast and more than 60 Rab genes have been recognised in humans (14). Rabs are crucial in the intracellular vesicular transport, both in exocytosis and endocytosis as well as between organelles. They regulate the budding of vesicles, transport along the microtubules and actin filament, tethering and fusion with the acceptor organelle (15).

Ras superfamily proteins are able to bind GTP/GDP which allows them to switch between two states, a GTP bound active state and an inactive state when GDP is bound. The hydrolysis of the γ-phosphate group of the GTP causes a change of conformation which determines the active/inactive state (16).

1.2 Rab proteins

Rab proteins represent the largest family of Ras GTPase proteins, Sec4/Ypt from *Saccharomyces cerevisiae* was the first Rab gene discovered (17). This gene encodes for a protein crucial in the trafficking from the Golgi apparatus to plasma membrane (18). Since the discovery of the first Rab protein have been identified more than 60 Rab proteins in mammals (14). Rab GTPases are ubiquitous proteins and they are present in many compartments such as of the endomembrane system, in mitochondria, and in the plasma membrane. Despite this, the best known role of Rab proteins is in exocytic and endocytic membrane trafficking (19). They regulate the specificity of anterograde and retrograde trafficking of vesicles between compartments. Although the expression of some Rab proteins is largely ubiquitous some of them are present only in specific tissue and cells. Rab27a, for example, is mainly express in hemapoietic cell lineage (15), Rab3a has been found exclusively in the synaptic vesicle of neurons (20), Rab17 and Rab13 are present in epithelial cells (21,22).

1.2.1 Rab proteins structure

Rab proteins contain some features in common with all the other members of the Ras superfamily proteins, such as they share 30-50% of similarity in primary structure (23), and they present a conserved domain named "G domain". This domain is one of the most ancient protein domain known and it is responsible for the guanine nucleotide binding and hydrolysis (24). The structure of G domain consists of a central 6-stranded β-sheet encircled by 5 *α*-helices. Within this domain there are five conserved motifs that represent the nucleotide-binding site, and two switch regions. These high conserved motifs compose the G boxes and each of them is numerated G1-G5 (24).

The G1 box, also known as a P-loop is an important motif for the binding with the β and γ phosphates of the nucleotide. The G2 motif is part of the switch I region, this part of the protein changes its conformation in relation of the presence of GTP or GDP (24). The G3 box is located close to the switch II region and to the Mg^{2+} ion, nevertheless, it does not necessarily bind the cation (24). The switch II region has no similarity between the Ras

superfamily. Both switch I and II are involved in the interaction with the effectors and they are important for the activity of the GEF and GAP proteins (24). G4 box and G5 box are crucial to distinguish GTP from ATP. The switch regions I and II assume a close position when GTP is present. Instead when GDP is bound, therefore, in the absence of the γ phosphate, the switch regions are flexible and dynamic, changing their position with speed between pico- to nanosecond timescale (24).

A feature that characterize Rab proteins from the other members of the Ras superfamily is the presence of conserved sequences named F motifs (F1-F5) (25). These motifs are distributed in and around the switch regions I and II. RabF1 (IGVDF) is located in the loop 2 (β2) so it is part of the switch I region, this sequence is highly conserved between Rabs. The G residue is present also in Arf family proteins but it is absent in Ras and Rho (see Figure 1) (25). The other F motifs (F2-F5) are close or in the switch II region and their sequence is: KLQIW (RabF2/β3), RFRSIT (RabF3/loop4), YYRGA (RabF4/α2-loop5) and LVYDIT (RabF5/β4-loop6). Some of these motifs present one or two residues in common with other proteins of the Ras superfamily (see Figure 1).



Figure 1 Conserved sequences between Rab proteins

Alignment profile using Hidden Markov Model (HMM) sequence of Ras, Rab, Rho and Arf. All Rab proteins (consensus alignment present common amino acid in the regions F1-F5 (red). When a position of another family is occupied by the same residue of Rab is highlighted in red as well. This figure shows also the SF regions of Rab, yellow highlighted. From Pereira-Leal and Seabra (25)

Moreover, Pereira-Leal and Seabra (25) have identified some conserved specific sequences motifs (RabSF) between some Rabs within the Rab family proteins. Therefore, this family have been grouped in 10 different Rab subfamilies each of them with similar sequences in the SF1-4 motifs (see Figure 2). It has been suggested that these SF motifs confer the specificity of interaction with their effector and regulators (25).

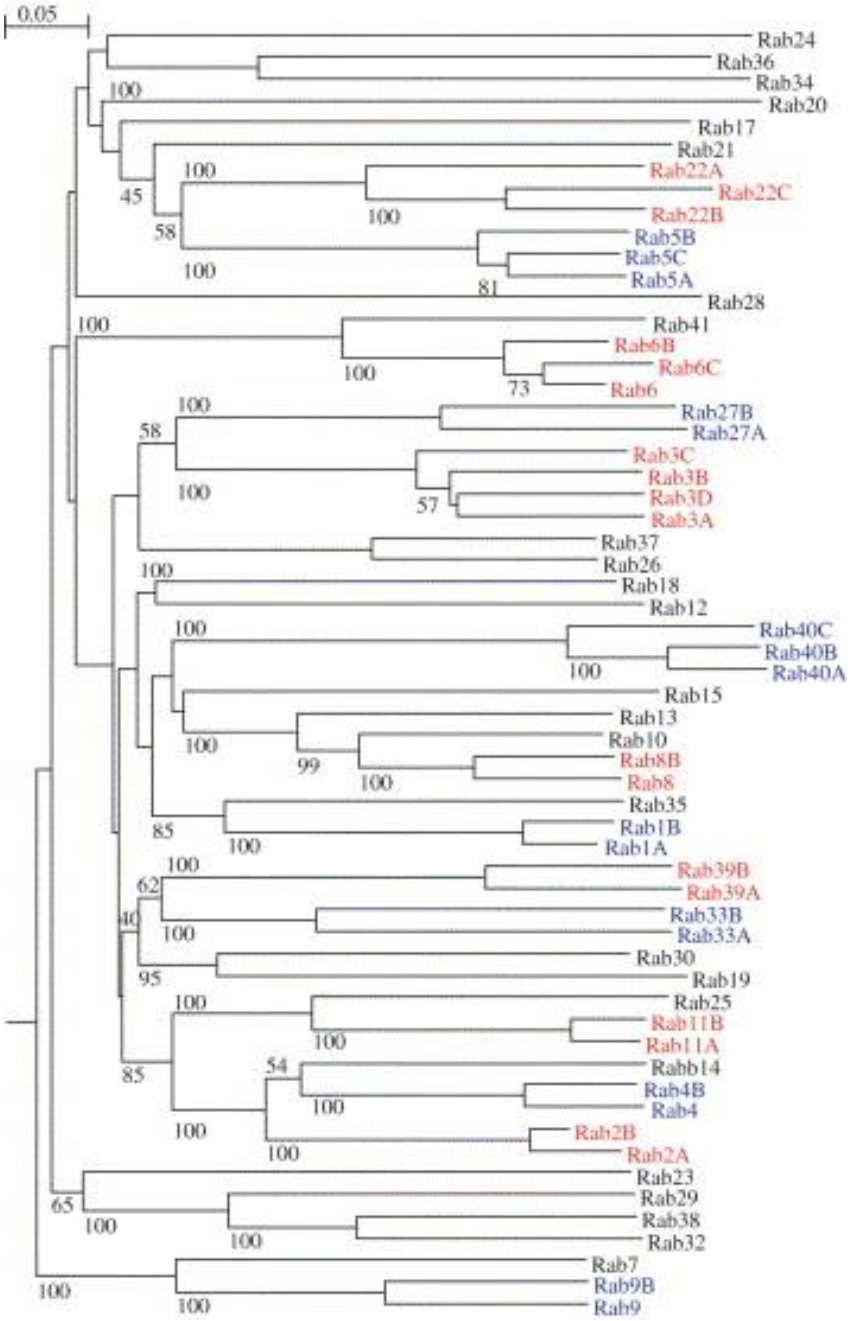


Figure 2 Human Rab family divided in subfamilies

The root is H-Ras (not shown), sequence branches are made on amino acids difference. Each subfamily within a branch is represented with the same colour (red or blue). From Pereira-Leal and Seabra (14)

Crystal structure of activated Rab3A bound to the effector domain of rabphilin-3A has revealed that RabSF1, RabSF3 and RabSF4 motifs forms interaction with its effector, although SF2 motif is on the opposite side of this binding (26). Moreover, studies on the Rab27 complexed with its effector Melanophilin have demonstrated that the RabF1, RabF2, RabF3, RabSF1 and RabSF4 motifs are important for the interaction with the effector (27).

Another feature that characterize Rab proteins is the prenylation motif. In fact, Ras and Rho proteins lipidation occurs in the tetrapeptide sequence CAAX, instead Rab proteins present at the C-terminus different sequences (CC, CXC, CCX, CCXX, or CCXXX). These sequences are used by the Rab geranylgeranyl transferase to attach isoprenoid to the cysteine present at the C-terminus, after recognising the complex Rab-REP.
Upstream of the box containing cysteine there is the hypervariable region. This sequence shows the greatest variability between Rab proteins (28). It has been suggested that the targeting of Rab proteins to their specific membranes is due to this region. Some examples of this understanding come out from the study executed with Rab5 and Rab7. In this study Rab5 was retargeted to late endosomes creating chimera in which hypervariable sequence of Rab5 was replaced with the hypervariable sequence of Rab7 (29). Nevertheless, recent studies have shown the central role of F and SF regions in targeting (30). In some cases, however, the targeting is controlled by GEF proteins such as the case of Rab1 in *Legionella pneumophila* which is targeted by DrrA GEF to the host plasma membrane (31).

1.2.2 **Rab proteins regulation**

As well as the other components of the Ras superfamily proteins, Rab proteins present high affinity for both GTP and GDP in the scale of low nanomolar to picomolar, as a consequence they release GDP with a slow rate, it has been estimated the half-life is of one or more hours. However, the GTP-bound is guarantee by the higher concentration of GTP compared to GDP in the cytosol. Additionally, the GTP hydrolysis in vitro (<0.03 min^{-1}) (32) is slow compared with the speed that occurs in the biological system (less than one minute). These observations have prompted to investigate the presence of enzymes able to increase the kinetic of releasing GDP and able to increase the kinetic of hydrolysis of GTP. Moreover, the cascade of cellular events that occurs upon Rab activation presupposes a tight regulation of the switching between the active and inactive state in order to activate cellular function and subsequently deactivate them when are not needed. Two different kind of proteins were found to be crucial in the cycle the inactive state to the active state and *vice versa* of the Rab proteins and more in general in the Ras superfamily proteins. These two class of enzymes are known as GEFs (*Guanine nucleotide Exchange Factors*) and GAPs proteins (*GTPase-activating proteins*). GEFs induce the release of GDP from Rab GDP-bound proteins and replace it with the more abundant GTP. The role of GAPs is to increase the intrinsic ability of Rab proteins to hydrolyse GTP, releasing the phosphate group and promoting the formation of the inactive GDP-bound state (4) (Figure 3).

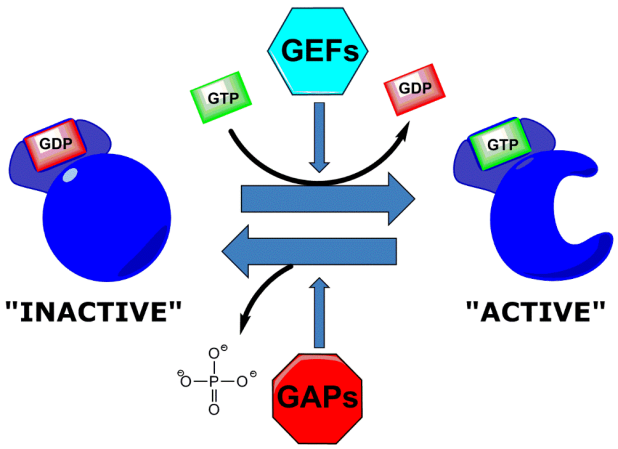


Figure 3 Rab activation and deactivation

Activation of Rab Proteins by GEFs and deactivation by GAPs which confer the active and inactive state

1.2.3 **Rab proteins cycle**

Newly synthesised Rab are suggested to interact with REP (*Rab escort protein*). This complex binds RGGT (*Rab-geranylgeranyl transferase*) which covalently attached one or two geranylgeranyl lipids to the cysteine amino acid(s) present at the C-terminus (33). The prenyl chains are crucial for the binding with the membranes because they increase the hydrophobicity of Rab proteins. It is thought that the complex GDP-Rab-REP is delivered to a specific membrane (34). The general assumption is that when Rab is associated with its target membrane, RabGEF is able to activate the Rab protein by switching GDP with GTP. However, the mechanism of targeting of Rab proteins to membrane is a subject of debate, and I will discuss it below. When Rab proteins are associated at the target membrane, in the active state, they are able to bind their effectors and perform their functions. Crucial for the correct function of Rab proteins is their inactivation performed by GAP proteins (35). Inactive GDP-bearing Rab proteins are then detached from the membranes by another family of proteins called Rab GDP-dissociation inhibitor proteins (GDI), which are able to disperse the inactive Rabs into the cytosol. RabGDI perform this action through two domains, one of them interacts with the GTPase and the other one interacts with the prenyl chains of the Rab proteins, this binding is important because it conceals the hydrophobic feature of the prenyl groups making Rabs soluble to the cytosol. Then, after reaching the target membrane (discussed below) Rabs are available to perform another cycle of activation by GEF and deactivation by GAP (Figure 4).

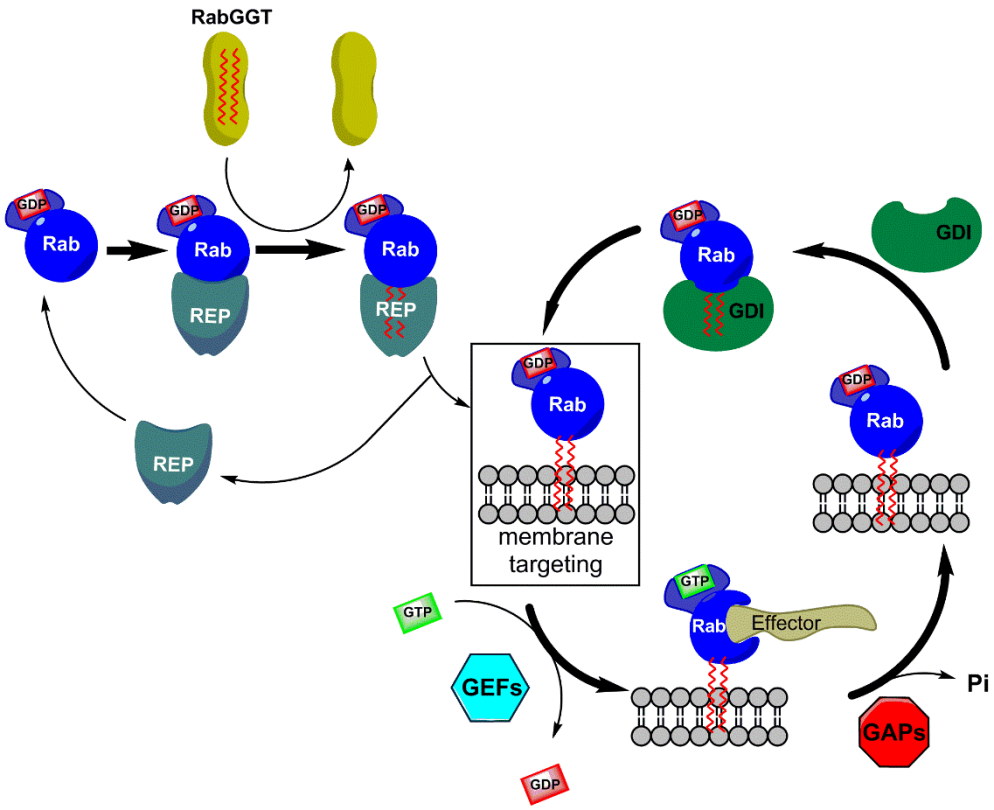


Figure 4 General Rab cycle

After translation, a GDP loaded Rab protein binds REP, this complex is recognized by RabGGT, which adds lipid chains to the Rab protein. Now Rab is structural ready to interact with the target membrane. Activation of Rab is catalyzed by GEF protein, then GDP is released and GTP is acquired. The active form of Rab now is able to interact with its effectors and to perform its downstream function. GAP proteins deactivate Rab. γ-phosphate is released and Rab remains GDP-loaded. At this point Rab GDP bound can be extracted from the membrane by GDI and the complex Rab-GDI can be targeted to the membrane for a new cycle.

The mechanism of Rab membrane targeting is still matter of debate, although several studies reported in the literature suggested possible mechanisms. Originally, it was thought that the hypervariable region of the Rab proteins was responsible for the membrane targeting (29). Then, Ali et al (36) challenged this model, in fact authors in order to investigate the targeting property of the hypervariable region swapped these regions between Rab1a, Rab2a, Rab5a, Rab7 and Rab27a and they did not see any mistargeting of those proteins. Instead they suggested the importance of the F and SF motifs of Rab proteins. Subsequently, an alternative model was proposed, based on the high affinity between the GDI and the GDP bound Rab it was thought that another protein should decrease this affinity directly to the membrane target. For this model was proposed the presence of GDI-

displacement factors (GDF) at each target membrane (37). However, only one GDF (Pra1) has been identified in humans. Instead, there is emerging evidence suggesting that GEFs may be the minimal machinery needed to target Rabs (38). A model that has been suggested proposes that the complex GDI-Rab deliver the Rab randomly and weakly with every membrane it encounters. If the membrane does not contain the GEF for the Rab, GDI is able to extract again the Rab. Instead, if the membrane contains the GEF, the Rab can be activated, therefore, GDI loses its ability to extract the Rab from the membrane, and the Rab-membrane interaction is stabilised (39). Moreover, the membrane binding of Rab proteins is stabilised by the recruitment of their effectors (28,40). This model does not need any other factors, however, a unique model of the targeting of Rab proteins seems uncertain and it is object of research.

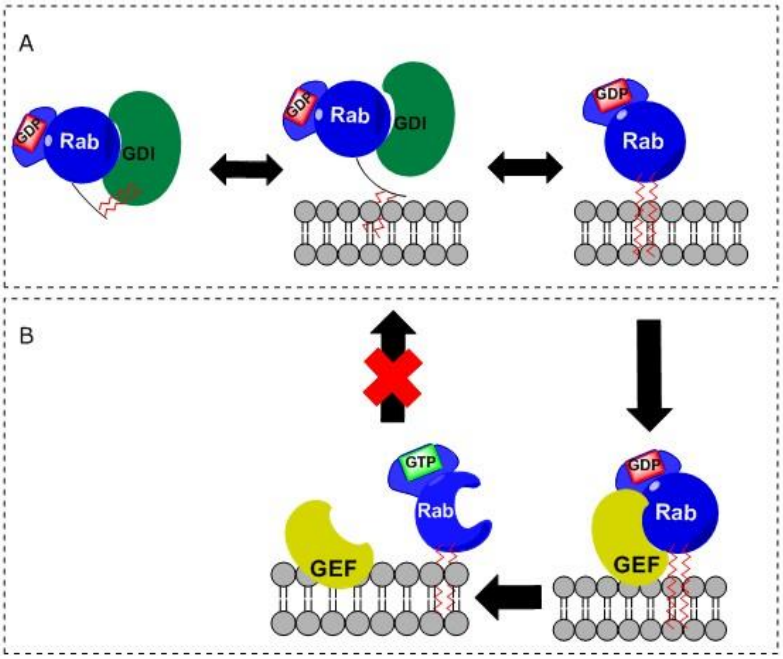


Figure 5 Models of Rab targeting to the membranes

A) Rab-GDI complex deliver Rab protein randomly to the membrane. B) If Rab finds its GEF it is activated and GDI is unable to extract it from the membrane

1.2.4 **Rab GEFs**

Crucial for the regulation of the Rab proteins is the activity of the RabGEF proteins, and about 36 Rab GEFs have been identified in human (41). Some of them present activity towards multiple Rabs such as Rab3GEP (Rab3 ad Rab27) (7,42). However, although the numerous RabGEFs identified, there are still Rabs which are missing their cognate.

The G domain of the Rab proteins, and more in general of the Ras superfamily proteins, can be seen as a sandwich model in which the two loops switch I and switch II, together with the phosphate-binding loop (P loop), create a meshwork of binding with the nucleotide and the magnesium ion. Both phosphates and the magnesium ion are essential for the high-affinity binding of the nucleotide with the G domain (16). In order to perform their function, the GEF proteins have to open this package structure and weaken the binding between the nucleotide and the G domain, as a consequence the GDP is released and the more abundant GTP is acquired.

A general mechanism of action of the GEF proteins can be viewed as a multistep reaction. Firstly, the GEF protein binds the GDP-Ras protein, the binding with GEF induces conformational changes in the switch regions and in the P loop, leaving the rest of the structure mostly unperturbed (43). Then this complex releases GDP, leaving GEF-Ras protein nucleotide free. Hence, the more abundant GTP is captured by this complex making the complex GTP-Ras protein-GEF. Now, GEF can be expelled from this complex (Figure 6).

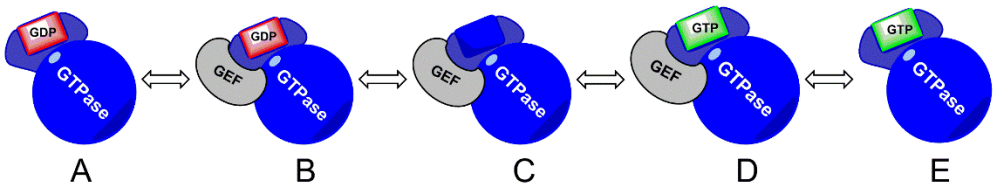


Figure 6 Multistep reactions of GEFs

Multistep reaction of GEFs performed to release GDP from GTPase making it available to add GTP. A) GTPase-GDP, B) GEF-GTPase-GDP, C) GEF-GTPase, D) GEF-GTPase-GTP, E) GTPase-GTP

Rab guanine nucleotide exchange factors are structurally different and they can contain many domains, although there are some conserved domains. RabGEFs have been classified in six different groups of based on the presence of the conserved domains. There are two classes of well-known RabGEFs which contain the DENN (Differentially Expressed in Normal versus Neoplastic), others that contain Vps9 (Vacuolar Protein Sorting 9), then other two classes of proteins containing the Sec2 domain and the multi-subunit TRAPP (Transport Protein Particle) complexes (44). Finally, others RabGEFs have been identified which are heterodimer GEFs complexes (45). Currently, some 3D structures have been resolved of GEFs in complex with their cognate Rab, such as Rab35-DENN1B, Ypt1p-TRAPP1, Sec4p-Sec2p and Rab21-Rabex5 (46-49) (see Figure 7).

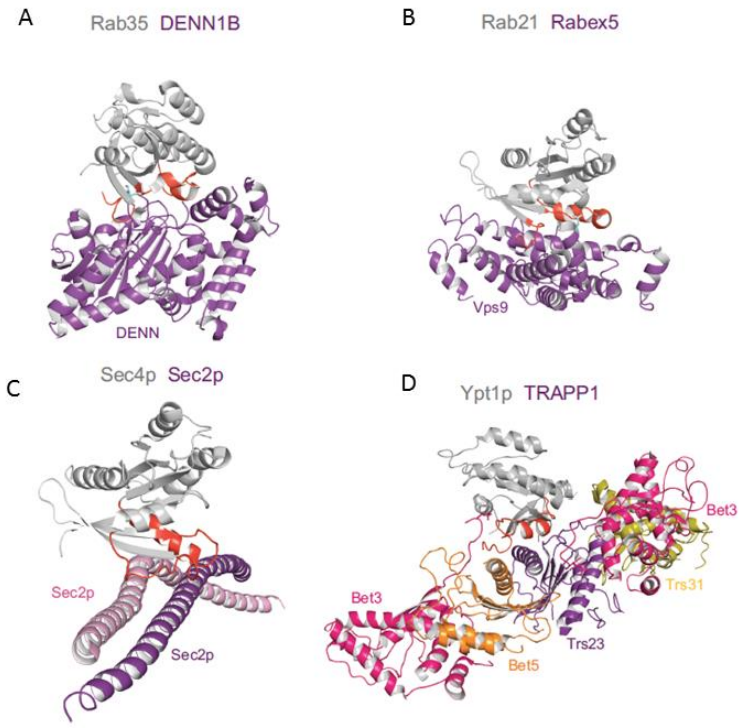


Figure 7 Structures of nucleotide-free Rab-GEF complex

This shows GEF in complex with Rab. Rab proteins are shown in gray. A) Rab35-DENN1B, B) Rab21-Rabex5, C) Sec4p-Sec2p, D) Ypt1p-TRAPP1. Modified from Cherfils and Zeghouf (44)

1.2.4.1 DENN domain proteins

Originally, the DENN (*differentially expressed in normal versus neoplastic*) domain contained in GEF proteins was sub-structured in three subdomain modules named central DENN, uDENN (*upstream DENN*) and dDENN (*downstream DENN*). In this way, it was possible to group 18 proteins containing the DENN domain into eight families based on the homology and on the domain organisation. All of them present the DENN domain at the N-terminus except for the DENND2 family in which it is present at the C-terminus (50) (Figure 14). The DENN domain core is about 180 residues, the size of the uDENN and dDENN is about 70 residues each, the linker region is variable between DENN proteins, it can range from 0 to 70 residues between uDENN-DENN, and 30 to 130 residues between DENN-dDENN.

After the 3D structure of the DENND1B with its cognate Rab35 (46), new elements have arisen about the structure of the DENN domain and other proteins have been considered as DENN-related. In fact, the three-dimensional structure indicates that the DENND1B consists of double lobes, the N-terminus, which contains the uDENN and the DENN core, has a structure that resembles the longin domain, instead the C-terminus lobe has no relatives known (51). The longin domain is characterised by a sandwich structure, where 5 β sheet are enclosed by 3 α helixes, 2 on one side and 1 on the other side. This domain is the binding side for GTPases (51).

Wu et al. (46) have shown that Rab35 engages contact with the C-terminus lobe and with one α helix and two β sheet of the N terminus lobe of the DENN domain. Authors suggested that this binding invokes a conformation change of the switch I and II regions of Rab35, resulting in a change in the 3D structure of the phenylalanine in position 33 which seems to be important for the binding with the GDP. However, authors indicate that it is not sufficient to displace the GDP from the G domain, suggesting that conformation changes in switch I region could open the nucleotide-binding facilitating the releasing of GDP and the acquisition of GTP.

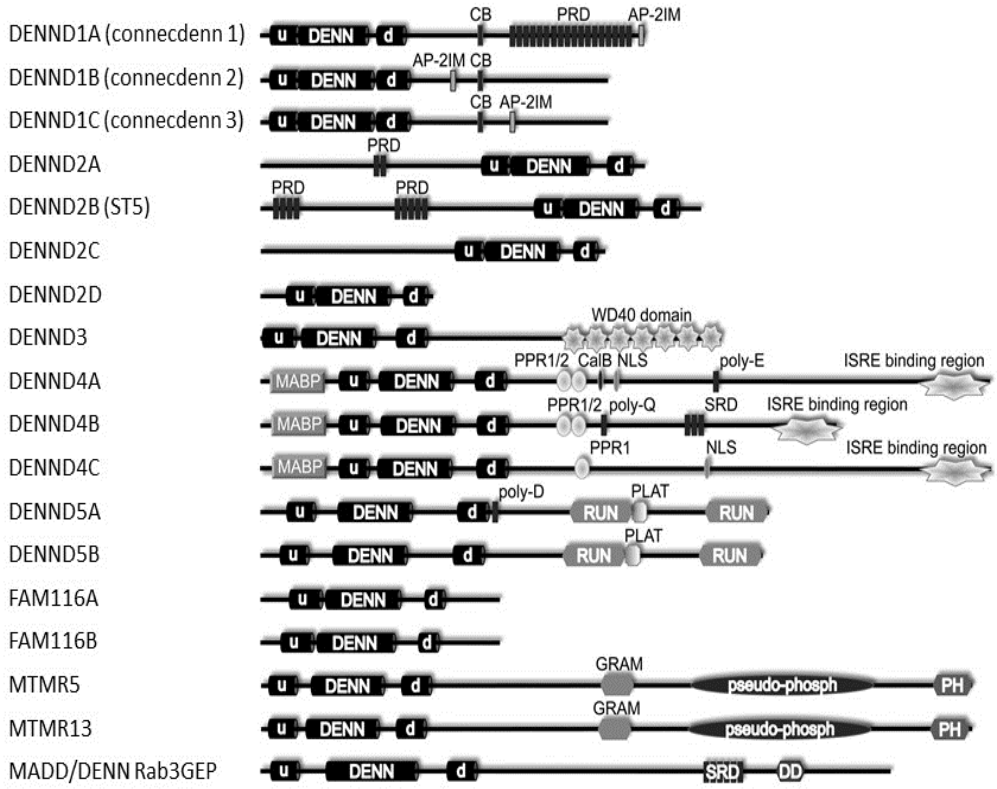


Figure 8 DENN domain protein families in human

Proteins containing the DENN domain. Modified from Marat et al. (50)

Within the 8 groups of proteins containing DENN domain there are the Connecdenns 1-3 named also DENND1A-1C. DENND1A contains in addition to the DENN domain, clathrin-binding motif for clathrin (CB), the clathrin adaptor AP-2 (AP-2IM), and multiple Src homology 3 (SH3) domain-binding motifs (proline rich) (52). DENND1B and DENND1C though contain same DENN domain, they have divergent C-termini, however, they can bind to clathrin and also clathrin adaptor AP-2. Connecdenns are all guanine-nucleotide exchange factors of Rab35 (53). However, Yoshimura et al. suggest that DENND1C has GEF activity towards Rab13 (54).

DENND2 family proteins are GEFs for Rab9a/b (54). Depletion either of DENND2A or Rab9 causes lysosome clustering in the perinuclear cytosol and the role of Rab9 in trafficking of mannose-6-phoshate receptor (MPR) between the late endosome and the *trans*-Golgi organelle is blocked (54). The best known of this family is DENN2B protein also called ST5 (suppressor of tumorigenicity 5), which present GEF activity even for Rab13 (55). There are three splice isoforms and the shortest seems to in cytoskeletal organisation and tumour suppressor in HeLa and fibroblast (56). However,

no link has been found between the GEF activity and the inhibition of the tumorigenicity yet (50).

DENND3 is the GEF of Rab12, in this case it is thought that the GEF activity depends on the DENN domain but it has not been tested (54,57).

DENND4 family has specific GEF activity towards Rab10 (54). Its role in mammalian cells is still unknown, although in *Drosophila* its ortholog Crag (calmodulin-binding protein related to a Rab3 GDP-GTP exchange protein) regulates secretion in order to polarize the distribution of the proteins in the basement membrane components (58).

DENND5 family has two isoforms 5A and 5B both are GEF for Rab39 (54). They contain in addition to the DENN domain two Run (RPIP8 (RaP2 interacting protein 8), UNC-14 and NESCA) domains. These domains are important to associate with other Rab GTPases, e.g. DENND5A binds Rab6 through the Run domain in a nucleotide-independent way (59). Furthermore, DENND5A can bind Rab11-GTP as an effector (60). The links between Rab39, Rab6 and Rab11 are still unknown.

Fam116A/B present GEF activity towards Rab14 (61).

MTMR5/13 (myotubularin-related proteins 5 and 13) are GEFs of Rab28, this protein is a distant member of the Rab family and has not been well characterised (54).

MADD/DENN/Rab3GEP has GEF activity for Rab3 and Rab27, and will be described in more detail in section 1.3.2.

In summary, based on the 3D structure of the nucleotide-free Rab35-DENND1B complex seems that DENN domain reduces the high affinity for GDP by repositioning the switch I region away in order to destabilise the GDP binding (44,46).

Table 1 Specificity GEF activity of the DENN Family

DENN Family	Substrate Rabs
DENND1A/B	Rab35
DENND1C	Rab35,Rab13
DENND2A/C/D	Rab9
DENND2B	Rab9, Rab13
DENND3	Rab12
DENND4A/B/C	Rab10
DENND5A/B	Rab39
Fam116A/B	Rab14
MTMR5/13	Rab28
MADD/DENN/Rab3GEP	Rab3,Rab27

Emerging evidence suggest that proteins containing the DENN domain can be regulated by phosphorylation. It has been suggested that DENND1C can be phosphorylated by Mst1 (Macrophage stimulating 1) *in vitro* (45). Moreover, Connecdenn 1 can be also phosphorylate and GTP loaded Rab35 increases in a Akt-dependent manner (62). Furthermore, it has been suggested that ULK (unc-51 like autophagy activating kinase 1) can phosphorylate DENND3 after starvation, and that the phosphorylation increase the GEF activity towards Rab12 (63). Moreover, it has been suggested that DENND3 can form an intramolecular interaction that cause the inhibition of its GEF activity, and that subsequently to the phosphorylation the protein can be released from the folded conformation and the GEF activity revealed (64).

1.2.4.2 Vps9 domain proteins

Another class of RabGEFs are the proteins containing the Vps9 domain, as for the DENN domain containing proteins these are often multidomain proteins. In fact, these proteins can contain along with the Vps9 domain additional domains such as coiled coil (CC), pleckstrin homology (PH), A20-like zinc finger (Z), Src-homology 2 (SH2), Ras Association (RA), RCC1-like (RCC1LD), Dbl Homology (DH), Membrane Occupation and Recognition Nexus (MORN, M), RasGAP and ankyrin (A) (65). Vps9 proteins are grouped in 5 types based on the domain organisation: Rabex-5, Gapex-5, VARP, ALS2 and RIN family. It has been shown that Vps9 domain proteins are GEFs for

Rab5, however, this activity is not specific for Rab5. In fact, they present activity even for other Rabs for example Rabex-5 can also activate Rab17, Rab21 and Rab22A (45), and GAPEX-5 and RIN3 can activate Rab22B and Rab31(66). VARP instead is an exception and has activity only versus Rab21 (66). The best studied of the proteins containing the Vps9 domain is Rabex-5. The GEF activity of this protein is modulated by Rabaptin-5 which is an effector of Rab5 (65). It has been found that Vps9 domain shows similarity with the Sec7 domain of ArfGEFs (67). GEFs act by using an aspartate residue, which corresponds to the glutamate finger in Sec7. This residue binds the invariant P-loop lysine of Rab, this causes repulsion of the GDP which can be expelled (49). A part the GEF activity for Rab5 and correlated, Vps9 domain containing proteins are able to interact with other GTPase such as Rho, Ran and Ras. This suggests that Vps9 proteins can interlink membrane vesicle trafficking mediated by Rab5 and other cellular events (45).

1.2.4.3 Sec2 domain proteins

Sec2 is the gene that was found in *S. cerevisiae*, subsequently it was established that this gene produced the protein Sec2p. In mammalian, this protein has two homologues: Rabin 8 and GRAB that are GEFs for Rab8 and Rab3, respectively (54,68). Rabin8 apart from being the GEF of Rab8 it is suggested to be an effector of Rab11, which in the active state recruits Rabin8 to the organelle where it is located and consequently activate Rab8. Sec2p performs its action of GEF by forming a dimeric coiled-coil (see Figure 13), in which two catalytic sites are located in the opposite side of the protein. It works by inducing a conformational change in the switch I and II of Rab proteins. Sec2 has a very efficient activity in vitro, even though it does not introduce any residue into the active site of Rabs (44,48,69). As well as the DENN domain containing proteins, Rabin 8 has been suggested to be regulated by phosphorylation which increase the GEF activity (70).

1.2.4.4 TRAPP domain proteins

TRAPPI is a GEF protein for the ER to Golgi Rab1/Ytp1 GTPases. It performs its action as pseudo-dimeric complex, in fact it is a multiprotein complex composed of Trs31, Bet5, Trs23, and two copies of Bet3. Other two TRAPPs

proteins have been identified which present the same subunits of TRAPPI with the addition of Trs65p, Trs120p, Trs130p and Tca17p in TRAPP II and Trs85p in TRAPP III (71). The exchange mechanism was provided by the structure of TRAPPI with Ypt1p (Figure 13). It has been suggested that TRAPPI stimulate GDP release by making conformational changes in the two switch domains and the P-loop of the GTPase. In this model Trs23, Bet5 and one Bet3 subunits interact with the GTPase in order to stabilize the GTPase nucleotide binding pocket in an open form, and the C terminus of Bet3 is inserted into the pocket and may allow the release of the GDP (47).

1.2.5 **Rab GAPs**

GAPs are crucial regulators of the Rab cycle, both temporally and spatially. Studies have shown that there are at least 42 different GAPs in human and mice (72). All of them, except for the Rab3GAP (73), contain TBC domain (Tre-2/Bub2/Cdc16). TBC containing proteins present specific activity toward specific Rab proteins, explaining the large number of TBC protein that has been found. However, some TBC-domain containing RabGAPs are able to inactive multiple Rabs (72).

The discovery that aluminium and beryllium fluorides (AlF_4^- and BeF_3) present structural similarity with phosphate group (PO_4^-), and that these molecules can mimic the γ-phosphate group when the GTPases is bound with GDP, so mimicking the transition state during the hydrolysis has permitted to study the mechanisms behind the GAPs (44).

Common in Rab proteins, and more in general in the Ras superfamily proteins, is the presence of a water molecule in their active site, which is able to react with the γ-phosphate group through a nucleophilic attack (16). The role of GAPs is to orientate the attacking of the water molecule and to increase the susceptibility of the γ-phosphate group to the nucleophilic attack (4).

TBC domain present an arginine amino acid able to increase the susceptibility of the γ–phosphate for the nucleophilic attack (74,75), and a glutamine that increases the reactivity of the water molecule (76).

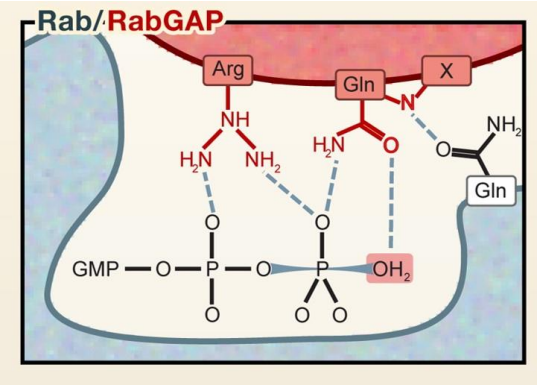


Figure 9 RabGAPs Mechanism

Molecular interaction between RabGAP and Rab GTPase to stimulate the GTP hydrolysis. Modified from Bos et al. (4)

1.3 Rab27 proteins

Rab27 is a subfamily of the Rab family and it is constituted by two isoforms Rab27a and Rab27b, which are crucial components of the regulation of the secretory vesicle traffic (77). Human Rab27 isoforms share 81% amino acid identity (78).

Rab27a subfamily is highly expressed in cells of hematopoietic lineage, as well as in eyes, lung, spleen and gastrointestinal tract. Its function is well characterised in melanocytes and cytotoxic T lymphocytes. Regarding these two cell lines a hereditary disease has been found caused by the dysfunction of Rab27a. This disease is named Griscelli syndrome type 2, which is characterised by silver hair and immunodeficiency. Most of the patients present stop codon mutations which results in C-terminal truncations, this produces Rab27a that cannot bind the prenyl chain, consequently cannot bind the membrane targeting for its function (79). Dysfunction in melanosome trafficking in melanocytes and defects in granule exocytosis in T-cells are the causes of the two features of this disease (80). Furthermore, Rab27a is considered as a general regulator of exocytosis in specialised secretory cell-types (endocrine, exocrine and immune cells) (81). Mature secretory vesicles and lysosome-related organelles are the sites where it is localised. Rab27b expression is restricted in stomach, pancreas, bladder, platelets, pituitary gland and large intestine (81). It has been proposed that Rab27 is involved in the regulation of organelle motility, in tethering and fusion of vesicles during the exocytosis process. Although Rab27a and Rab27b share a high level of homology their action could be either redundant or non-redundant, this depends on the cell type. For example, in Griscelli syndrome type 2 secretory cells except for cytotoxic T lymphocytes have not been found to be affected. This may be explained if Rab27b performs a redundant function in the other secretory cell types. By contrast, it has been suggested that Rab27a and Rab27b act with different roles in the same cell type by interacting with different effectors (82) e.g. in the exosome secretion in HeLa cell (83).

1.3.1 **Rab27 Cycle**

Rab27 needs to be activated to execute its action. Rab3GEP is the GEF which is able to activate Rab27 (7,84). Moreover, it has been suggested that Rab3GEP has an important role in targeting of Rab27a. In fact, in melanocytes, melanosome lack Rab27a protein after the downregulation of Rab3GEP (85). Therefore, it has been suggested a double role of targeting and activation of Rab3GEP towards Rab27. When Rab27 is in the membrane and in the GTP state can perform its action recruiting effectors (82). EPI64 (GAP) returns Rab27 to its inactive state enhancing the intrinsic hydrolytic activity. Once in the GDP-bound state, Rab27 is ready to recycle into the cytosol. However, it has not been identified a GDI for Rab27, only one research made on rat parotid acinar cells has shown that Rab27b is redistributed from the secretory granule to the cytosol in a time dependent manner. Therefore, authors suggest the extraction from the membrane to the cytosol is regulated by GDI (86). Now Rab27 can be reactivated by Rab3GEP to launch another cycle.

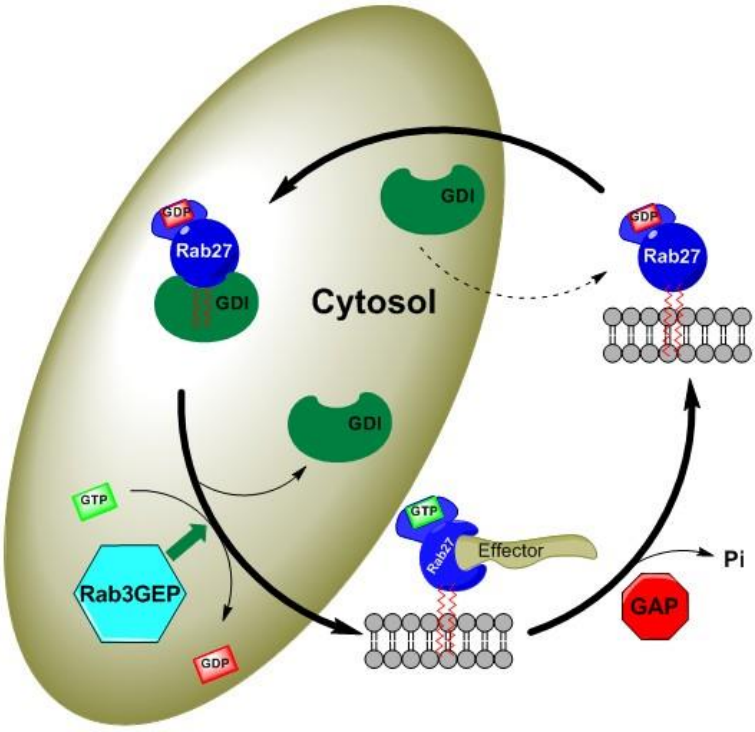


Figure 10 Model of Rab27 cycle

Rab27 in complex with GDI can be activated by Rab27GEF (Rab3GEP), then it can localise to the target organelle. Therefore, GTP bound Rab27 recruits its effectors and perform its function. Then Rab27 GAP inactivates Rab27 that can be extracted by GDI.

1.3.2 **Guanine nucleotide exchange factor of Rab27**

Rab3GEP is the only GEF so far discovered for Rab27 (7). It belongs to the family of DENN domain proteins and it is also called differentially expressed in normal versus neoplastic/MAP kinase-activating death domain (DENN/MADD). This protein conducts its GEF activity not only towards Rab27, but also towards Rab3 family proteins (7,42,84). Rab3 and Rab27 are considered belonging to the same sub-family, based on functional grouping and sequence similarity in different organisms (14). These two families of Rabs share about 40% of similarity of amino acid sequence and they are both involved in the regulation of exocytosis. Moreover, they have some effectors in common, such as Rabphilin and Slp-4a (*synaptotagmin-like proteins*).

Rab3GEP was firstly isolated from rat brain by Wada et al. (42). In this study, the authors indicated Rab3GEP as the guanine nucleotide exchange factor of Rab3 family, although they found differences in the GEF activity between the diverse components of this family. In fact, they suggested that it was active versus Rab3a, Rab3c, but inactive versus Rab3b and only partially active versus Rab3D. However, later Coppola et al. (87) showed no difference of the Rab3GEP GEF activity between the Rab3 family. In their screening, Wada et al. indicated the selectivity of its GEF activity towards Rab3 and not to the other Rabs tested (Rab2, Rab5a, Rab10 and Rab11). Lastly, they suggested the importance of the prenyl chain in RabGTPase for the GEF activity of Rab3GEP, in fact, absence of it induces lack of GEF activity for Rab3 (42).

Rab3GEP contains a DENN domain at the N-terminus and a Death domain at the C-terminus. The DENN domain contains 3 subdomain modules named central DENN, domain uDENN (*upstream DENN*) and dDENN (*downstream DENN*) (50).

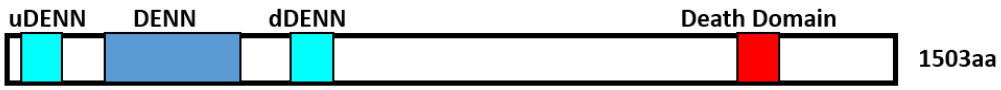


Figure 11 Structure of human Rab3GEP protein

This figure shows the DENN (differentially expressed in normal versus neoplastic) core (blue) surrounded by upstream DENN and downstream DENN (pale blue). At the C-terminus is shown the Death Domain (red)

Rab3GEP was the first protein discovered to possess the DENN domain. Subsequently, after the discovery that the DENN domain of Connecdenn has by itself the capacity to activate its cognate Rab, it was suggested that the DENN domain alone has the GEF activity (46). However, Coppola et al. (87) and previously Oishi (88) indicated that the integrity of Rab3GEP is essential for GEF activity towards Rab3, giving importance to the Death domain and other part of the protein. In fact, in their studies they found that the absence of the death domain reduces Rab3GEP GEF activity. Death domains instead are known to participate in homotypic protein: protein interactions which forms complexes able to promote apoptosis and inflammation (89), and there is no other evidence in the literature of link between the death domain and the GEF activity.

There is evidence that the Death domain of Rab3GEP (DENN/MADD) can dimerise with other Death domain of other proteins such as tumour necrosis factor receptor (TNRF)(90). TNRF is a membrane receptor, when it is active it promotes the recruitment of TNFR-associated death domain (TRADD) protein to the membrane, at a later stage of Fas-associated death domain (FADD) protein, and receptor interacting protein (RIP) or TNFR-associated factor 2 (TRAF2) protein to promote apoptosis. It has been suggested that Rab3GEP (DENN/MADD) binds TNRF preventing the interaction of TRADD and inhibiting the cell death (91). Subsequently, it has been suggested a crucial role of Rab3GEP in the signal pathway of TNRF, in fact it can promote resistance to the apoptosis induced by TNRα, by recruiting Grb2 (*Growth factor receptor-bound protein 2*) and Sos1/2 (*Son of sevenless homolog*) and activating indirectly the Ras signal which promote the cell survival (92). According with the anti-apoptotic function of Rab3GEP, it has been suggested that in Alzheimer's disease, neurons present lesser expression of Rab3GEP than normal neurons which is correlated with an higher neuronal cell death present in Alzheimer's disease (93).

Moreover, Oishi H. et al. suggested that in primary cultured hippocampal neurons Rab3 GEP is localised at the synaptic release sites that it is important in in the regulation of calcium-dependent exocytosis (88).

In order to explain the double role of Rab3GEP it has been suggested that in normal condition it acts as a normal GEF but when the cell is under stress it is able to bind TNRF performing the anti-apoptotic function (94). The presence of the DENN domain as well as of the DD domain is important for both roles (87).

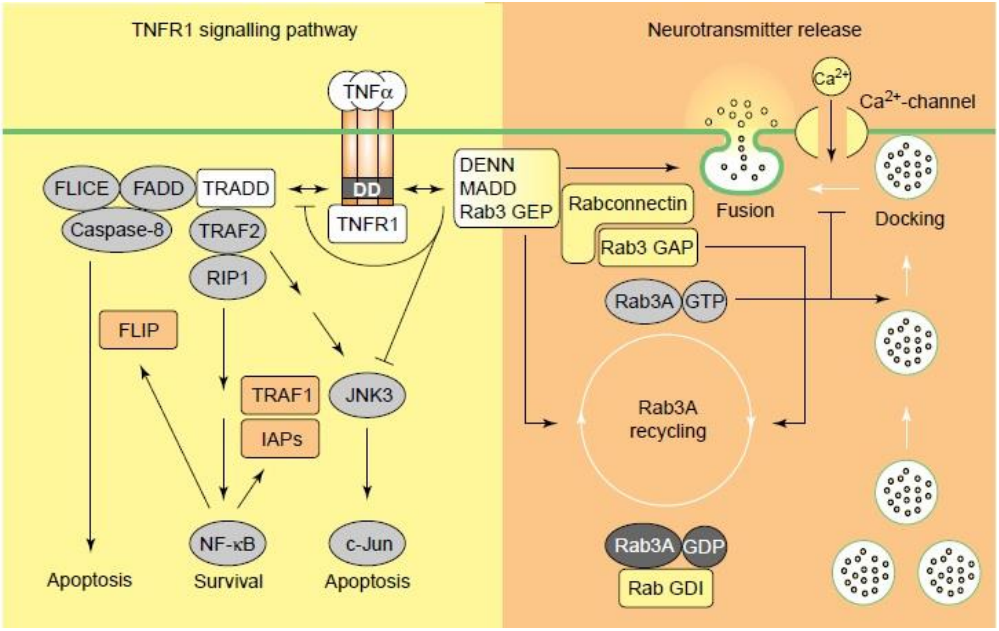


Figure 12 The double role of MADD/DENN/Rab3GEP

The double role of Rab3GEP under normal condition and under stress. During physiologic condition, Rab3GEP (DENN/MADD) acts a GEF showed in the right orange panel, instead, under stress condition it binds TNFR1 with its DD domain in impeded the binding between TNFR1 and TRADD. From Miyoshi and Takai (91)

Furthermore, in neuronal cells it has been suggested another role of Rab3GEP towards Rab3A not as GEF but as effector. In fact, Niwa et al. suggested that Rab3GEP binds KIF1Bβ (*Kinesin superfamily protein*) through the Death domain and GTP loaded Rab3A through the DENN domain acting as an effector (95). This complex they suggested is essential for transporting Rab3 positive vesicles along the microtubules in order to be release to the synapse.

Regarding Rab27, Rab3GEP has been recognised as its GEF, and this action seems to be combined with a crucial role of Rab3GEP in targeting Rab27a on melanosome membrane in melanocytes (85). Nonetheless, in this study authors have identified one mutant of Rab27a that can be activated by Rab3GEP but is not target to the membrane, suggesting that Rab3GEP action is in concert with other unknown factor(s) in order to target Rab27a to membranes in melanocytes (85).

1.3.3 **Rab27 GAPs**

Based on a screening of 40 TBC-domain containing proteins Itoh and Fukuda suggested two GAPs with activity for Rab27a, TBC1D10A (also known as EPI64) and FLJ13130 (8). These two GAPs are not specific for Rab27a and they have action on other Rabs (e.g. Rab35) (96). Subsequently, study in Pancreatic Acinar Cells made by Hou et al (97) suggested EPI64 and EPI64B as GAPs for Rab27b. Furthermore, it has been suggested that Rab27GAP activity can facilitate endocytosis by allowing coronin3 (the only effector of Rab27 who prefers the inactive state) to bind Rab27 (98).

1.3.4 **Rab27 Effectors**

As previously mentioned in section 3.1, Rab27 is involved in the regulation of the secretion of lysosome-related organelles (like melanosomes) and secretory granules in a variety of cell types. In order to execute its functions then this GTPase needs to bind its effectors, therefore, the different Rab27 functions in different cell types seems to be due to the binding of this protein towards different effectors.
Twelve effectors have been identified for Rab27 and all of them interact with the GTP-bound form of Rab27 (99), the only exception is coronin 3 which binds the inactive form (98). These effectors have been grouped in three classes based on their domain structure.

The first group is composed by synaptotagmin-like proteins (Slps) and rabphilin. This group is characterised by the presence of a Slp homology domain (SHD) at the N-terminus, this domain present two conserved structures SHD1 and SHD2 separated by two zinc-finger motifs. This part of the protein is able to bind Rab27, moreover at the C-terminus are present two C2 domains (C2A and C2B) which are able to bind phospholipids. This group is composed by Slp1 (Exophilin7/JFC1), Slp2-a (Exophilin4), Slp3-a (Exophilin3), Slp4-a (Granuphilin/Exophilin2), Slp5 (Exophilin9) and Rabphilin (Exophilin1). Slp1 and Slp2-a are the only two proteins belonging to this group that do not have the zinc-finger motif (82).

The second group of effectors is made up by the proteins Slac2-a (Melanophilin/Exophilin3) Slac2-b (Exophilin5), and Slac2-c (MyRIP

/Exophilin8) and Noc2. The common feature of this group is the lacking of the two C2 domains (82). They present the SHD domains separated by zinc-finger motif, with the only exception of Slac2-b. All the proteins contained in the first and second group are specific for Rab27 except Slp4-a, rabphilin and Noc2 which are able to bind also Rab3 and Rab8 (100,101).

The mechanism of binding of the SHD domain with Rab27 has been described as a direct interaction of the SHD domains with the switch II region of Rab27 (102).

Munc13-4 is the only component of the third group, this protein presents a peculiar structure compare to the other above listed (103). It presents the C2 domains, though separated and does not present the SHD domain. Between C2A and C2B there is an extended homologous region called the Mun domain. Although it lacks the SHD domain seems that the binding with Rab27 is between C2 domain and Mun domain and this region has been named RBD (Rab binding domain), though there is not any 3D structure at the moment. It has been found that Munc13-4 interacts also with Rab15, indicating no specificity for Rab27 (104).

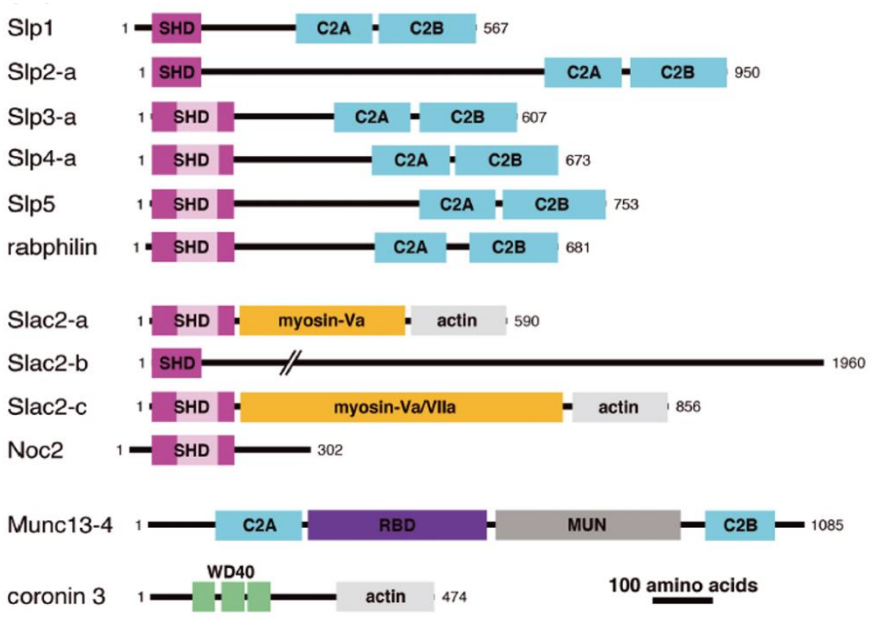


Figure 13 Rab27 effectors

Different domains and structures of the eleven effectors of Rab27 GTP bound and Coronin 3 Modified from Fukuda (85)

As already explained the functions of Rab27 in different cell lines or within the same cell line depend on its binding with the different effectors. It has

been suggested that in tumor derivates of adrenal chromaffin cell line called PC12 overexpression of rabphilin induce an increase of the number of vesicles close to the plasma membrane, suggesting role of Rab27-rabphilin complex in the vesicle docking to the plasma membrane in this cell line (105).

As well as for the Rab27-rabphilin complex, it has been suggested that Rab27 in complex with the effector Slp4 (Granuphilin) promotes in PC12 cell line the docking of dense granules to the plasma membrane (106). Furthermore, this complex seems to have a role in the plasma membrane docking of the insulin granule in pancreatic β cells (105).

However, in pancreatic β cells others Rab27 binding proteins have been suggested to have a role in the releasing of the insulin granule such as Slac2-c (MyRIP /Exophilin8) and Noc2 (107,108).
Another role suggested for Slac2-c effector is to link Rab27 and myosin VIIa in order to move melanosomes along the plus end of actin filament in retinal pigmented epithelial cells (109).

Kuroda and Fukuda suggested a role of Slp2 at the membrane level of melanocyte to anchor melanosome to the plasma membrane through interaction with phophatidylserine in the plasma membrane (110). These authors suggested that Rab27 uses melanophilin as effector to bind the motor protein in order to move along the plus end of actin filament (see section 1.3.6) and subsequently Slp2 to anchor melanosome at the plasma membrane. Moreover, Slp2 effector was found to be expressed in pancreatic endocrine α cells where it promotes the docking of glucagon vesicles to the plasma membrane (105).

The interaction of Rab27 with Slp1 is important in the regulation of azurophilic granule exocytosis (111) Moreover, Holt et al. suggested that Slp1 and Slp2 are important for the docking of secretory lysosomes in cytotoxic T lymphocytes (112).

Another critical downstream effector of Rab27 in cytotoxic T lymphocytes is Munch13-4. This protein has been suggested to be important for the docking of the lytic granules at the plasma membrane (113).

Table 2 Rab27 effectors and functions

Rab27 effector	Cell line	Role
Rabphilin	Adrenal chromaffin cell line PC12	docking
Slp4	PC12 (dense granule), Pancreatic β cells (insulin granule)	docking
Slac2-c	Pancreatic β cells (insulin granule), retinal pigmented epithelial cells	docking, melanosome transport
Noc2	Pancreatic β cells (insulin granule)	docking
Slp2	Melanocytes, Pancreatic endocrine α cells (glucagon vesicles), Cytotoxic T lymphocytes (secretory lysosomes)	docking
Mlph	Melanocytes	melanosome transport
Slp1	Cytotoxic T lymphocytes (secretory lysosomes), azurophilic granule	docking
Munc13-4	Cytotoxic T lymphocytes	docking

1.3.5 **Diseases correlated with Rab27**

Rab27 is a key component in the regulation of secretory granule transport and exocytosis (105). The importance of the secretory pathways is highlighted by the fact that dysfunction of it causes diseases. Griscelli syndrome is a disease caused by dysfunction of the releasing and trafficking of lysosome-related organelles.

There are three types of Griscelli Syndrome named I, II, and III.

The type I is characterised by albinism, which is caused by defect of melanosome trafficking in melanocytes due to mutation of the actin-based motor protein myosin-Va (114). Griscelli syndrome type II is due to mutation of Rab27a, which causes partial cutaneous albinism and immunodeficiency (115).

As well as for the type I, defects of melanosome trafficking in melanocytes are responsible for the albinism in Griscelli syndrome type II. In melanocytes, melanosomes are scattered through the cytoplasm in order to be delivered to the plasma membrane. Transport impairments caused by defect of the tricomplex Rab27-melanophilin-MyoV results in melanosome clustering in the perinuclear area of the melanocytes (see section 1.3.6), then vesicle content cannot be delivered to the neighbour cells. Therefore, keratinocytes present reduced pigmentation which results in albinism observed in Griscelli syndrome (116,117). The immunodeficiency observed in the Griscelli syndrome type II is due to malfunction of cytotoxic T lymphocytes. These cells are lymphocytes that kill other cells such as virus-infected cells, cells infected with intracellular bacterial, tumour cells. In order to do that they recognise the target cells by contact, and destroy them through secretion from lytic granules. The lytic granules move along microtubules in the cytoplasm towards the contact point with the target cell and then release their content by fusion with the plasma membrane (118,119). The docking of lytic granules with the plasma membrane is dependent on Rab27 in complex with Munc13-4 and it is impaired in Griscelli syndrome II (118).

Patients with Griscelli syndrome III present albinism due to mutation of melanophilin. Dysfunction of the Rab binding protein Munc13-4 causes type 3 familial hemophagocytic lymphohistiocytosis (113,120)

The integrity of Rab27 regulators is also crucial for the correct function of Rab27. In Choroideremia which is an X-linked recessive retinal degenerative

disease, it has been found that Rab27 is unprenylated so it cannot perform its action and it is due to dysfunction REP-1 (121).

Instead, little is known about dysfunctions of Rab3GEP. In *C.elegans* mutation of this protein causes defects of synaptic transmission and defecation (122). Moreover, mouse knock out for Rab3GEP die immediately after birth for failure of synaptic transmission that causes respiratory failure (123).

1.3.6 **Melanosome maturation and trafficking**

Melanocytes are cells that present the capacity to produce melanin within organelle called melanosome. Melanosomes are lysosome-related organelle which share with lysosomes some particular proteins such as acid-dependent hydrolases and lysosomal-associated membrane proteins (124). In skin, melanin contained in melanosome is released from the melanocytes and it is captured by the neighbour keratinocytes, resulting in the skin pigmentation (124). Melanosomes are synthesised via 4 stages of maturation, each of them with specific morphology. The first two stages are lacking melanin, which is synthetised in the other two stages. During stage I melanosomes are similar to endosomal structure and PMEL17 (*pre-melanosome protein*) a structural protein start to form intralumenal fibrils. These fibrils are completed in the stage II and the melanosomes acquire an elongated striated shape. Then, in stage III, the new synthesised melanin is deposited on the fibrils, and at the stage IV all the body of the melanosome organelle is full of melanin (125).

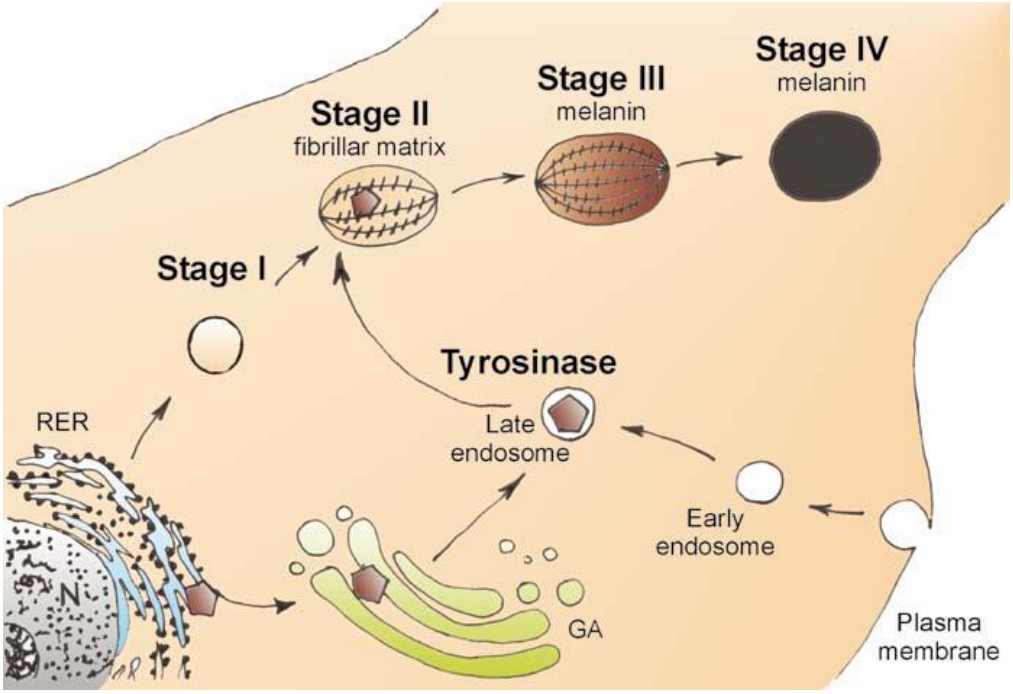


Figure 14 Melanosome stages I-IV

Stages of melanosome maturation. Stage I PMEL17 forms intralumenal fibrils. Stage II fibrils completed and recruitment tyrosinase. Stage III synthesis melanin, and Stage IV mature melanosome. Cichorek et al. (126)

Melanin pigments can be divided in eumelanin (black and dark brown) and pheomelanin (yellow, red). The description of melanosome maturation described above refer to melanosome containing eumelanin, melanosome containing pheomelanin are less well characterised (125). However, for the synthesis of both pigments different enzymes are necessary which are delivered to the pre-melanosome from the trans-Golgi. These include TYR (Tyrosinase), TYRP1(Tyrosinase related protein I) and DCT/TYRPII (Dopachrome tautomerase).

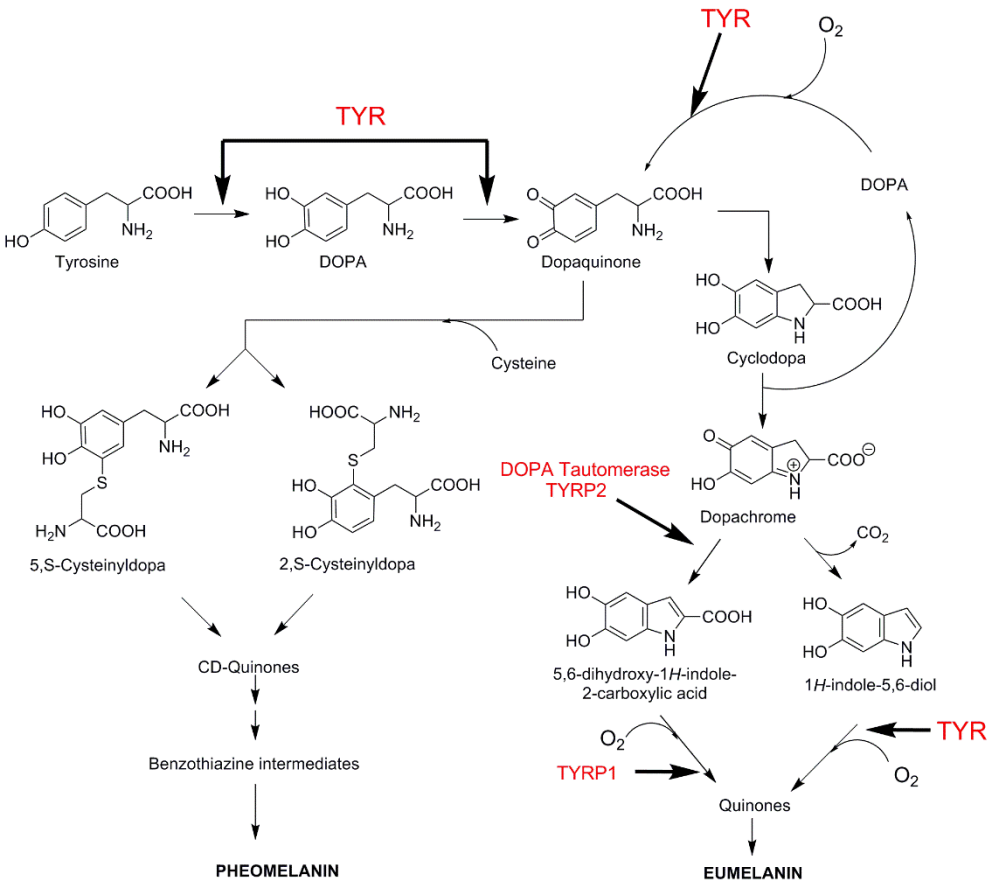


Figure 15 Eumelanin and pheomelanin biosynthetic pathways

Both pigments are synthetised from the amino acid L-tyrosine. tyrosinase (TYR) oxidases the tyrosine to DOPA and then to DOPAquinone. Hence, two ways are possible in relation of the pigment to synthesise (Eumelanin/Pheomelanin). Eumelanin= DOPAchrome is spontaneously formed. Then either the enzyme TYRP2 catalyze the formation of 5,6 dihydroxy-1H-indole-2-carboxylic acid or DOPAchrome lose spontaneously CO_2. Those two intermediates are converted in Quinones by TYRP1 or TYR and then the formation of the Eumelanin. Instead for the formation of the Pheomelanin the amino acid cysteine is added to DOPAquinone in order to form 5,S-Cysteinyldopa and 2,S-Cysteinyldopa. Then after few steps those molecules are converted in benzothiazine intermediates which are the precursor of the pheomelanin.

Crucial step to initiate the melanin synthesis is the conversion of the amino acid tyrosine to Dopaquinone, these oxidations are performed in a double step by Tyrosinase from DOPA. This intermediate is in common for both melanin pigments (Pheomelanin and Eumelanin). To synthetise eumelanin, Dopaquinone is converted in Dopachrome. This molecule can be a target of the enzyme TYRP2 (DOPA Tautomerase) and be converted in 5,6 dihydroxy-1H-indole-2-carboxylic acid, or Dopachrome can lose spontaneously CO_2 giving 1-*H*-indole-5,6-diol. Both molecules are converted in Quinones by TYR or TYRP1, and finally in Eumelanin (127).
The synthesis of the pheomelanin is from Dopaquinone as eumelanin, but one molecule of the amino acid cysteine is added forming the intermediates 5,S-Cysteinyldopa and 2,S-Cysteinyldopa. Then, benzothiazine intermediates as precursor of the pheomelanin (127).

Mature melanosomes containing melanin, can be transported from the perinuclear region to the cell periphery, in order to release their contents, which will be collected by the keratinocytes. However, melanosome can move in both direction towards the cell periphery and towards the perinuclear region. The mechanisms responsible for the melanosome transport are still object of study. Manuscripts in literature suggested that mature melanosomes are transported towards the cell periphery along the microtubules for long distances through kinesin motor proteins, then when they are close to the plasma membrane the role performed by the kinesin is taken by another motor protein MyosinVa which allow the movement along the actin filament. Then, the melanosome transport is performed by two motor proteins along the microtubules and actin filament (128). However, recent evidence supports the idea that although microtubules are responsible for the retrograde trafficking, the anterograde trafficking is performed only through the actin filaments by MyosinVa, therefore, given less importance to the microtubule trafficking (129). Figure 16 shown both the models proposed.

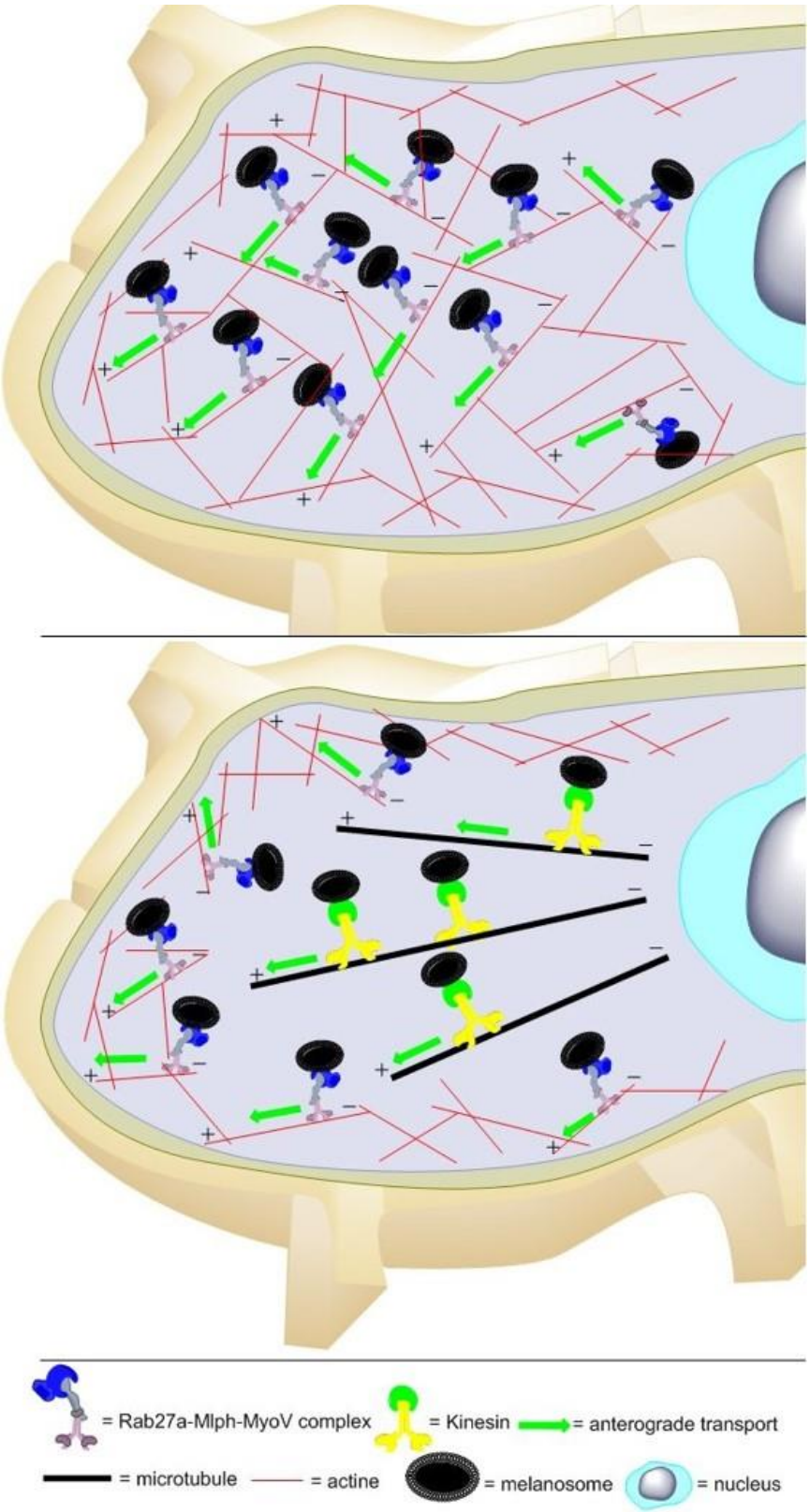


Figure 16 Melanosome anterograde trafficking models

This figure shows the two models of anterograde melanosome transport proposed. On the top, there is shown a transport along the actin filament preformed through the Rab27a-Mlph-MyoV complex. On the bottom, it is shown the model in which

the long distance is performed using the microtubules track through the kinesin motor protein and actin filament for short distance.

However, whatever is the mechanism behind the melanosome transport, switching between the two kinds of cytoskeletal filaments (microtubules and F-actin) is a crucial step of melanosome transport and Rab27a plays a pivotal role in this. It has been suggested that melanosomes are driven towards the nucleus along the microtubules, then inactive Rab27a free in the cytosol, could interact with Rab3GEP which would activate and target the Rab protein to the melanosome membrane, at this point Rab27a is anchored to the melanosome membrane through the geranylgeranyl groups contained at the C terminus. Then, Rab27a GTP-bound can be recognised by Melanophilin (Mlph/Slac2-a) one of the effectors of Rab27a, which in turn interacts with the motor protein MyosinVa. This final step, permit to the melanosome to move anterogradely along the actin filaments (116).

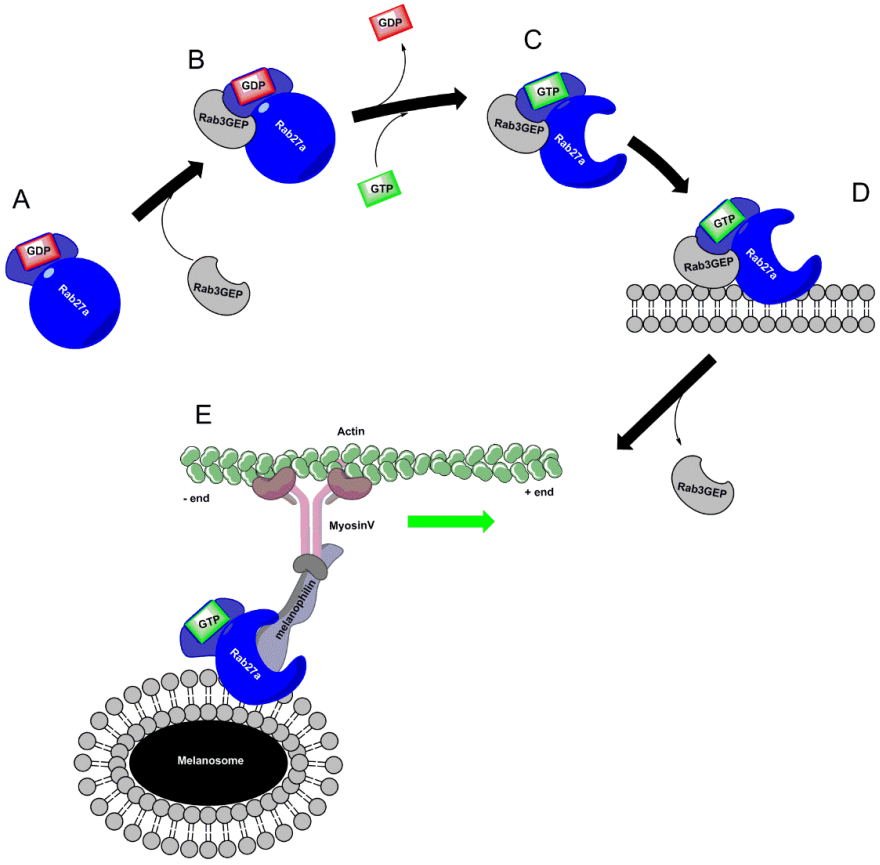


Figure 17 Model activation and targeting of Rab27a on melanosome membrane

A) Rab27a GDP-bound in the cytosol. B-C) Rab3GEP binds Rab27a and GDP is released to acquire GTP. D) Rab3GEP leads Rab27a to the melanosome membrane. E) active Rab27a binds its effector melanophilin, which interacts with the motor protein Myosin V. Then melanosome can move towards the plus end of the F-actin

Defects of any protein involved in this tripartite complex Rab27a (*ashen mouse*), Melanophilin (*leaden mouse*) or MyosinVa (*dilute mouse*), causes aggregation of the melanosomes at the perinuclear region (see Figure 18).

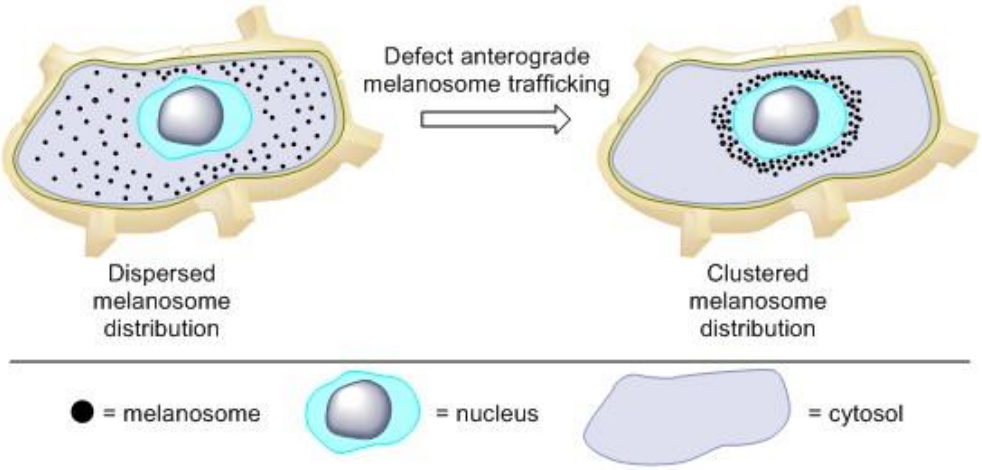


Figure 18 Melanosome redistribution due to defect of the anterograde trafficking

Melanosomes aggregation at the perinuclear cytosol after dysfunction of the anterograde trafficking.

Since melanocytes synthetise melanin within melanosomes, these organelles are pigmented (black/brown) and easily traceable using bright-field microscopy. Therefore, melanocytes are an excellent model to study organelle transport and the proteins involved in their trafficking.

However, mouse melanocytes are cells difficult to be transfected with liposomes transfection, and in order to get high efficiency of exogenous protein expression adenoviruses expressing required proteins have to be prepared.

1.3.7 **Aims**

In this thesis two main points were investigated, the mechanism and the domains of Rab3GEP responsible for the activation of Rab27a and the ability of Rab3GEP to target Rab27a to the membrane organelle.

Although it is known that Rab3GEP is a GEF of Rab27a, there is little knowledge regarding its mechanism of action. In order to investigate Rab3GEP protein and give insight of the domain/s important for the GEF activity, truncations and point mutations (within the DENN domain) were made. These mutants were tested in cell based assays using melanocytes knock out for Rab3GEP, then melanosomes localization was used as read out of the capacity of these mutants to activate Rab27a

On the other hand, to determine directly whether the mutants of Rab3GEP presented GEF activity towards Rab27a, in other words if they maintain the capacity to allow the switching of from GDP to GTP, pull-down assays were performed taking advantage of the ability of Rab27a to bind its effector Slp1 mainly in the GTP bearing form.

In order to investigate the targeting ability of Rab3GEP towards Rab27a, and the importance of the cytosolic localization of Rab3GEP for the activation of the melanosome trafficking two sets of experiments were performed: 1) mis-targeting of Rab3GEP to mitochondria through a 'knocksideways'-type approach follow by melanosome distribution investigation and 2) direct fusion of Rab3GEP to the mitochondria membrane follow by the investigation of melanosome distribution, and Rab27a localization.

Finally, in order to investigate the possible link between the GEF activity of Rab3GEP and its capacity of targeting Rab27a, mutants that lack the GEF activity were mis-targeted to mitochondria and Rab27a localization was investigated.

2 Materials and Methods

2.1 Cell culture

2.1.1 Murine Melanocytes

In order to obtain immortal Rab3GEP-deficient melanocytes (melan-Rab3GEP KO #1,#2,#3) mice heterozygous for a previously generated Rab3GEP loss of function allele (see below) were crossed with Ink4a-Arf mutant mice in order to generate embryos homozygous for the Rab3GEP mutant allele and heterozygous for Ink4a-Arf mutant allele. Genotyping of the embryos was as previously described Lavado et al. and Tanaka et al. (123,130) Melanocytes were then derived from the dorsal skin of mutant embryos as previously described Bennett et al. (131). melan-R3G KO #1,#2,#3 melanocytes were derived from 3 different embryos from the same litter. Knocking down of Rab3GEP was made with frame-shift mutation. The system adopted aimed to replace the 3' half of 1st exon and 5' half of the 2nd exon using MC1-neomycin resistance cassette as shown in Tanaka et al. (123), this work was done before the starting date of the project by Montoliu Lluis, and Sviderskada Elena. Immortal mouse melanocytes cell lines (melan-a wild type) and Rab3GEP-deficient melanocytes (melan-Rab3GEP KO #1,#2,#3) were maintained in RPMI-1640 (Sigma) supplemented with 10% (v/v) fetal calf serum (Gibco), 2mM L-glutamine, 100 units/ml penicillin and streptomycin 100 mg/L (Sigma), 40nM phorbol 12-myristate 13-acetate at 37 °C in a humidified atmosphere containing 10% CO_2.

2.1.2 Human Embryonic Kidney (HEK)-293a cell line

Cells were grown in Dulbecco's modified Eagle's medium (Sigma) with 10% fetal calf serum, 100 units/ml penicillin, and streptomycin 100 mg/L at 37 °C in a humidified atmosphere containing 10% CO_2.

2.1.3 Sub-culturing of cells

melan-a, melan-Rab3GEP KO melanocytes and HEK293a cell lines were passaged at 85-90% confluence, cells were split every 3-4 days for HEK293a and 5-6 days for melan-a and melan-Rab3GEP KO cells. Growth medium was aspirated and the cells were washed with phosphate-buffer saline solution (PBS 1X) (Lonza) then PBS was removed and the cells were incubated with Trypsin/EDTA 1X (Sigma) and incubated at 37°C for 3-5 mins till the cells were detached. Growth medium was used to quench the Trypsin, and the cells were collected in a 25ml sterile universal tube and centrifuged at 1500g using a Heraeus Biofuge Primo centrifuge (Thermo Scientific) fitted with a 45º fixed-angle rotor for 5 minutes, afterward the medium was aspirated and the pellet was re-suspended with the growth medium. One fifth of the total amount were re-seeded adding growth medium up to normal volume (10ml T-75 or 5ml T-25).

Table 3 Volume used for passaging tissue culture cells

Flask	1X Trypsin/EDTA	RPMI/DMEM to Quench
T-25 (Nunc)	1ml	2.5ml
T-75 (Nunc)	2.5ml	3.5ml

2.1.4 Cell cryopreservation

Cells with 80-90% confluency were removed from the flask as described in section 2.1.3. Supernatant was discarded, and the pellet was re-suspended with FBS supplemented with 10% (v/v) DMSO to obtain a final concentration of $1/10^6$ cells/ml (cell counting described in section 2.1.6). The cell suspension was aliquoted into cryogenic tubes (Thermo Scientific) and stored at -80° C for at least 72 hours. Afterward the cryovials were placed in liquid nitrogen for long-term storage.

To defrost the cell stock, the cryogenic tubes were placed at 37° C until all cells had thawed, then the suspension was transferred in a 25ml universal

tube containing 4 ml of growth medium. The suspension was centrifuged (as reported in the section 2.1.3). the supernatant was discarded, and the pellet was re-suspended with complete growth medium and transferred in a T25 flask (Nunc) at 37° C and 10% of $C0_2$ in incubator. After 24 hours, cells were washed with PBS 1X to remove all unattached cells and fresh complete medium was added.

2.1.5 Transfections

2.1.5.1 Plasmid DNA

DNA plasmids were obtained as shown in sections 2.2.1 and 2.2.2.
24 hours prior the transfection 50000 cells (see section for cell counting 2.1.6) were seeded in each well of a 6 well plate (Corning). Transfection per well was carried out by adding 5 µl of Fugene 6 (Promega) to 1 ml of serum-free OptiMEM medium (Gibco), mixed inverting the tube and left for 5 minutes at room temperature. Then 2.5 µg of DNA was added and incubated for 15 minutes to allow the formation of DNA/liposome complexes. Hence, the medium on the cells to be transfected was replaced with OptiMEM containing the DNA/liposome complexes and incubated at 37° C 10% CO_2 for 4/5 hours. Then the medium was replaced with normal cell growth medium.

2.1.5.2 siRNA Transfection

In a 6 well plate (Nunclon) 60000 cells per well were seeded 24 hours before transfection, and incubated at 37° C 10% CO_2. On the day of transfection 2 tubes were prepared, one with 165µl of OptiMEM (Gibco) and 10µl of siRNA (Sigma) 20µM, and the other one with 3µl of Oligofectamine (Invitrogen) and 15µl of OptiMEM. After 5 minutes at room temperature the 2 tubes were mixed and left for 15 minutes at room temperature. Hence, cells medium was replaced with 800 µl of OptiMEM added with the transfection mixed. Cells were incubated at 37° C 10% CO2 for 4 hours, then medium was replaced with normal growth medium. In order to allow the downregulation of the gene target the cells were incubated at 37° C 10% CO_2 for 72/96 hours.

Table 4 Table siRNA

siRNA	
Rab27a	5'-GGAGAGGUUUCGUAGCUUA-3'

2.1.6 **Counting cells**

Cells were detached using Trypsin/EDTA 1X for 3-5 mins at 37°C, then medium was used to quench the Trypsin (volume see Table 3). 10µl of cells in suspension were added to Neubauer Chamber and number of cells was manually determined. Cells contained in 3-5 squares of Neubauer Chamber (diagonals) were counted and average was calculated, then the number of cells contained in 1ml of solution was estimated multiplying the average for 10000.

2.2 DNA Techniques

2.2.1 **Transformations**

Escherichia coli (*E.coli*) DH5α competent cells (50µl) were defrosted on ice for 20 minutes and incubated with 200ng of DNA for 20 minutes. Afterwards cells were exposed to 60 seconds of heat shock at 42°C followed by 10 minutes of incubation on ice. Then 400µl Luria-Bertani (LB) medium (1% w/v tryptone, 0.5% w/v yeast extract, 1% w/v NaCl adjusted to pH 7.0 with 1M NaOH) was added and incubated for 60 minutes at 37°C with shaking (200rpm). Then 100µl of cells/LB medium was plated on a selective LB agar plate (10 g/L NaCl, 10 g/L Tryptone, 5 g/L yeast extract, 20 g/L agar) containing the appropriate antibiotic (ampicillin 100µg/ml or kanamycin 50µg/ml) and incubated for 16 hours at 37°C. Single colony was collected and inoculated with 5 ml of LB medium containing the appropriate antibiotic and incubated overnight at 37°C with shaking (200rpm).

2.2.2 **Small scale purification plasmid DNA**

In order to extract the plasmid contained in bacteria, *E.coli* derived from 2.2.1 were centrifuged at 3000 RPM for 10 minutes and plasmid DNA was extracted using a NucleoSpin plasmid kit (Macherey-Nagel). DNA concentration and purity were measured using a NanoDrop 2000 (Thermo Scientific).

2.2.3 **Polymerase chain reaction (PCR)**

PCR was performed using for each reaction 1µl of 50ng/µl of DNA template, 0.5µM of each primer forward and reverse designed to flank the gene sequence to amplify, 0.5µl 20mM dNTPs (Promega), 5µl 10x Pfu DNA polymerase reaction buffer (Promega), 1µl Pfu DNA polymerase (Promega), sterile H_2O up to a final volume of 50µl. PCR reaction controls were made in absence of the DNA template.

Table 5 Setting used for PCR reaction

Stage	Temperature (°C)	Time (min)	Cycles
Initial denaturation	95	3	1
Denaturation	95	1	30
Annealing	55	1	30
Extension	72	1/kb	30
Final Extension	72	10	1

2.2.4 Site-directed mutagenesis

Two complimentary oligonucleotides containing the desired mutation were designed using the unmodified nucleotide sequence. One/three nucleotides were modified in order to have the point mutation desired, 19-21bp in both side of the mutation were complementary of the original sequence in order to ensure the annealing of the primers with the DNA template.
The PCR reaction was made as seen in section 2.2.3.
Setting used for the site-directed mutagenesis is shown in Table 6.

Table 6 Setting used for site-directed mutagenesis

Stage	Temperature (°C)	Time (min)	Cycles
Initial denaturation	95	3	1
Denaturation	95	1	18
Annealing	55	1	18
Extension	72	1.5/kb	18
Final Extension	72	10	1

To eliminate the original plasmid template DNA, 16µl of PCR product was incubated with 1µl DpnI enzyme (NEB) and 2µl of Cutsmart buffer (NEB) for one hour at 37°C and then heat inactivation of DpnI for 20 mins at 80°C. Then the plasmid containing the point mutation was amplified following the steps in sections 2.2.1 and 2.2.2.

2.2.5 Agarose gel Electrophoresis

DNA separation was performed using 1-3% (w/v) TBE 1X (Tris/Borate/EDTA) agarose-gel depending on the DNA size to be analysed. Agarose was

dissolved in TBE using microwave. Afterwards, mixture was cooled down at about 50°C and ethidium bromide was added (1:100000). Then, mix was poured in a gel caster with appropriate comb, reaching approximately the thickness of 5 mm and left to solidify. DNA samples were prepared mixing the DNA template with 6X DNA loading buffer (40% sucrose, 0.25% bromophenol blue in sterile water) and sterile water. The samples were loaded to the gel wells along with 1kB or 100pb DNA ladder (Invitrogen) and run at 100V in TBE buffer until the end of the gel visualized by the dye front. Gel was images using a GelDoc system.

2.2.6 **Restriction endonuclease digestion**

1µg of DNA was digested using 1µl of each restriction enzyme (1 U/µl, New England Biolabs, Invitrogen) and 5µl of 10X buffer suggested by the manufacture for single and double digestions and sterile water till final volume of 50µl. The mix was incubated overnight at 37°C. Heat inactivation was performed as manufacture instructions when necessary. Agarose gel was used to investigate the efficiency of the digestion (see section 2.2.5).

2.2.7 **Ligation**

After the digestion insert, and open plasmid vector were ligated using T4 DNA ligase (Promega). Digestion products were cleaned using PCR clean-up kit (Macherey-Nagel) to remove small DNA pieces formed from the vector digestion, therefore, reducing the re-ligation. Digested insert and vector were in ratio 3:1, 2µl 10x DNA ligase buffer (Promega), 1µl of T4 DNA ligase were added and sterile water till the volume of 20µl. Then the mixture was left at 16°C overnight. Then, DNA was transformed to DH5α competent cells in order to amplified it (see sections 2.2.1 and 2.2.2).

2.2.8 **Plasmid constructs**

GFP-Rab3GEP-FKBP construct was prepared from the GFP-Rab3GEP plasmid and from the plasmid pEntr GFP-Myo5–FKBP both already in our possession. FKBP was amplified by PCR reaction (see section 2.2.3) using primers listed on the Table 7 from the plasmid pEntr GFP-Myo5–FKBP. GFP-Rab3GEP

plasmid and segment obtained by PCR reaction have been cut at the restriction sites using SacII and Xbal restriction site enzymes (see section 2.2.6), then ligation of vector and insert was performed (see section 2.2.7).

Tomm70-GFP-Rab3GEP construct was prepared from pEntr-GFP-Rab3GEP and pEntr-egfpn1 Tomm70 in our possession. PCR reaction (see section 2.2.3) was used to amplify Tomm70 segment. Primers for amplification segment are listed in Table 7. GFP-Rab3GEP plasmid was mutated in order to add a new restriction site HindIII (see section 2.2.4). Primers for point mutations are listed in Table 7. Then, Tomm70 segment and GFP-Rab3GEP with HindIII were cut using HindIII restriction site enzyme (see section 2.2.6). Then, ligation was performed (see section 2.2.7). The transformation and DNA purification were used to amplify and obtain plasmid DNA (see sections 2.2.1 and 2.2.2). Same approach was used to make the constructs Tomm70-GFP-ΔDD and Tomm70-GFP-I353V.

pEntr-GFP-ΔDD and pEntr-GFP-I353V were previously prepared by Deb Briggs and Alistair Hume.

Table 7 List of primers

Template	Primers
pEntr GFP-Myo5–FKBP	Fw= (5′-3′) GACTCCGCGGAATGGGAGTGCAGGTGGAAA Rv= (3′-5′) ACTATCTAGAGCGGTCATTCCAGTTTTAG
pEntr egfpn1-Tomm70	Fw= (5′-3′) GATCAAGCTTCGGACTCAGATCTCACCAT Rv= (3′-5′) GATCAAGCTTGCAGGCCGCTGGCGTCGCCCC
pEntr GFP-Rab3GEP plasmid mutation (HindIII)	Fw= (5′-3′) AAGCAGAGCTGGTTTAGTGAAGCTTCAGATCCGCTAGCGC RV = (3′-5′) GCGCTAGCGGATCTGAAGCTTCACTAAACCAGCTCTGCTT

2.2.9 **DNA sequencing**

DNA sequences of the newly made constructs was checked by sending 5µl of DNA plasmid (100ng/µl) with 5µl of primers (10µM) to Source Bioscience.

When was possible Source Bioscience primers were used instead of sending ours.

2.2.10 **Adenovirus generation**

Adenoviruses expressing GFP-Rab3GEP, GFP-DENN, GFP-ΔDENN, GFP-ΔDD, GFP-DD and point mutations of GFP-Rab3GEP (I353D, F350D P351K I353D, 6xHis Nterm GFP, R37A Y38A, P354A L355A L356A P356A, L366K, T371R P372R, R514A) were previously made by Deb Briggs and Alistair Hume as described in Hume et al (132). The same approach was used to produce the rest of the adenoviruses shown in this dissertation. Constructs were in pENTR entry vectors (Invitrogen, Cat #K2400-20) and they have been recombined into pAd destination vector through a recombination reaction using Gateway LR Clonase II (Invitrogen, Cat #11791020). For this purpose, 150ng pEntr vector was incubated with 150ng pAd destination vector, 2µl of LR Clonase (Invitrogen), and TE buffer pH 8.0 (1M Tris, 0.5M EDTA in sterile water) up to total volume of 20µl, overnight at 25^{o}C. Then, 1µl of Proteinase K (Invitrogen) was added and incubated at 37^{o}C for 10 mins. Then, DH5α competent cells were transformed with the plasmid and after antibiotic selection the plasmid was amplified and purified. Afterwards, a digestion with PacI restriction enzyme, the pAd vector was transfected in mammalian cells. HEK293a cells seeded in a 6 well plate were transfected with the pAd destination vector obtained using Fugene6 transfection reagent (Promega, Cat# E269) (see section 2.1.5.1). Cells were harvested and re-seeded in a 10cm dish (Corning) two days later. Then, cells were left for 15-20 days to express the adenovirus. Production of plaques indicated that cells were dying because they were producing adenovirus. Hence, cells were detached from the petri dish by agitation and medium containing cells in suspension and adenovirus were collected and exposed at three cycles of freezing and defrosting, performed at -80^{o}C for 30 mins and at 37^{o}C for 15 mins. At this point centrifugation at 3000 rpm, 15 min room temperature was performed using Eppendorf 5804 swinging-bucket centrifuge, and the supernatant containing the adenovirus was collected.

The new made adenovirus was amplified by infecting (10µl of the crude adenovirus obtained) other HEK293a cells seeded in 10 cm petri dish and repeating all the steps seen since the formation of the plaques. Then adenoviruses were aliquoted and stored at -80^{o}C.

2.3 Protein Techniques

2.3.1 **Western Blot analysis**

2.3.1.1 Preparation Sodium dodecyl sulphate polyacrylamide gel

Proteins were separated using sodium dodecyl sulphate polyacrylamide gels 10-6% (v/v).

Gels were made using the mixture suggested by Harlow and Lane (1988) pouring the mix between two glasses with distance 1.5mm BioRad Mini-PROTEAN Tetra Cell casting frames. Separating gels were prepared mixing 30% acrylamide mix, 1.5M Tris (pH 8.8) polymerised with ammonium persulphate (APS) and N,N,N',N'-Tetramethyethylene-diamine (TEMED) with H_2O as described in Harlow and Lane 1988 (see Table 9). Stacking gels were made with the same components with only exception of 1.0M Tris (pH 6.8) instead of 1.5M Tris (pH 8.8) (see Table 8).

Table 8 Components of Stacking Gel

Stacking Gel	
Solution components	Volume
H_2O	2.1 ml
30% Acrylamide	0.5 ml
1.0M Tris (pH 6.8)	0.38 ml
10% SDS	0.03 ml
10% APS	0.03 ml
TEMED	0.003 ml

Table 9 Components of Separating Gel

Separating Gel		
Solution components	6%	10%
H_2O	5.3 ml	4.0 ml
30% Acrylamide	2.0 ml	3.3 ml
1.5M Tris (pH 8.8)	2.5 ml	2.5 ml
10% SDS	0.1 ml	0.1 ml
10% APS	0.1 ml	0.1 ml
TEMED	0.008 ml	0.004 ml

2.3.1.2 Preparation of samples

Attached cells were collected using same approach used in section 2.1.3, then cells were washed with PBS and lysed using buffer A containing 50mM Tris pH7.5, 150mM NaCl, 5mM $MgCl_2$, 1mM dithiothreitol, 1% (w/v) CHAPS, and protease inhibitor (1 tablet each 10 ml (*Complete ULTRA Tablets, Mini, EASYpack)*) for 30 min on ice. Lysates were centrifugate at 13200rpm at 4°C using Eppendorf centrifuge 5415R, the supernatant containing the proteins was collected and the pellet was discarded. After, proteins quantification (see section 2.3.1.3) 25-30µg of samples were mixed Milli-Q water in order to have the same concentration and then 5 volume of it was mixed with 1 volume of 6X protein loading buffer (375mM Tris-HCl pH 6.8, 6% SDS, 48% glycerol, 9% β-mercaptoethanol, 0.03% bromophenol blue). Hence, samples were boiled at 95°C for 10 mins.

2.3.1.3 Protein quantification

Proteins contained in the lysates obtained as described in section 2.3.1.2 were quantified using Bradford assay. For this purpose, 5X Bradford reagent (Bio-Rad protein assay) was diluted with Milli-Q water in order to obtain 1X Bradford reagent. Then, it was added in a 96well plate to Bovine Serum Albumin (BSA) (10mg/ml) (NEB) to make the calibration curve. Therefore, a standard curve with 6 points was generated using concentration of BSA of 0, 0.2, 0.4, 0.6, 0.8 and 1µg. In order to determine the protein concentration 1µl of each sample was added to 199µl of 1X Bradford reagent and after 5 mins the absorbance was measured at 595nm using Thermo Scientific MultiSkan FC. Based on the results of the calibration curve, protein concentration of the samples was calculated.

2.3.1.4 Electrophoresis

Samples were loaded and run in gel using Mini-PROTEAN Tetra Cell tank containing running buffer (24mM Tris, 192mM Glycine, 0.1% (w/v) SDS) at 100-150V. One well, on the side of the gel was loaded with 2µl of molecular weight standard (Geneflow).

2.3.1.5 Transferring to membrane and immunoblotting

Protein samples separated on SDS-polyacrylamide gels were transferred to polyvinylidene difluoride membrane (PVDF) (Millipore, Cat.N. IPVH00010, Germany) using the Geneflow wet transfer system. PVDF membrane was previously activated with 100% methanol for 5mins. Transferring was performed using transfer buffer (25mM Tris, 192mM glycine, 10% methanol) for 3 hours at 300mA or overnight at 30V. Then, membrane contained transferred proteins was blocked with 5% (w/v) dried milk and 0.1% Tween-20 in PBS for 1 hour. Then it was incubated with primary antibody (see section 2.3.3) overnight at 4°C. The day after membrane was washed with 0.1% Tween-20 in PBS for 3 times 10 min each and incubated with the secondary antibody (see section 2.3.3) for 1 hour. Lastly, they were washed twice with 0.1% Tween-20 for 5 min each. Odyssey Li-cor system was used to image the signal.

2.3.2 **GST Pulldown Assay**

HEK293a cells were plated in 10cm petri dishes, the day after, infected with adenoviruses expressing the truncated mutations of Rab3GEP, point mutations of Rab3GEP, Rab3GEP full length wild type and GFP. The day after cells were washed twice with PBS and lysed using buffer A (see section 2.3.1.2) for 30 min on ice. Then the cell contents were obtained using cell scraper on cells attached on the plate in order to break cell integrity, these steps were carried out on ice. Cell lysates were clarified by centrifugation at 12,000 × RPM for 15 min at 4°C using Eppendorf centrifuge 5415R. Supernatant was collected, and proteins quantification was performed (see section 2.3.1.3). Then, 2mg of the total protein was pre-cleared by incubation with 20µl of glutathione-Sepharose 4 Fast Flow beads (GE Healthcare, Cat. N. 17-5132-01, U.K.) (to eliminate unspecific binding) for 2 hours on the wheel at 4°C. Then the beads were separated by centrifugation at 4000 RPM at 4°C. The supernatant was incubated with 200 pmol of GST or 200 pmol of GST-Slp1 (kindly made by Deb Briggs) and 25µl of glutathione-Sepharose 4B beads overnight at 4°C. The day after beads were separated by centrifugation and washed with buffer A 3 times 10min each. Proteins were separated from the beads by Laemmli buffer (100mM Tris-Cl (pH6.8), 4% (w/v) SDS, 0.2% (w/v) bromophenol blue, 20% (v/v) glycerol and 200mM β-mercaptoethanol) and boiled for 5 min at 95°C. Protein samples were separated on SDS-10% polyacrylamide gels and transferred to PVDF (Millipore), then immunoblotting. Steps and protocols adopted are described in *Western Blot Analysis* section 2.3.1. ImageJ software was used to measure the intensity of the bands.

2.3.3 Antibodies for Western Blot

The following antibodies listed in Table 10 were used for Western Blot identification:

Table 10 Antibodies used for Western Blot

Primary antibody	Dilution	Supplier
anti-Rab3GEP rabbit	1:1000	Yoshimi Takai, Kobe University
anti-GFP mouse	1:1000	Roche, Cat.N.11814460001
anti-Rab27a mouse	1:1000	Miguel Seabra, Imperial College London
anti-Calnexin goat	1:1000	Sicgen, Cat.N AB4100-500
anti-mCherry goat	1:1000	Sicgen, Cat.N AB0040-200
anti-Melanophilin goat	1:500	Everest biotech Cat.N. eb05444
anti-GAPDH goat	1:1000	Sicgen, Cat.N AB0049-200

Secondary antibody	Dilution	Supplier
Licor Donkey anti-Goat IR800	1:10000	Licor (P/N 926-32214)
Licor Donkey anti-Mouse IR680	1:10000	Licor (P/N 926-68072)
Licor Donkey anti-Rabbit IR680	1:10000	Licor (P/N 926-68073)

2.4 Microscopy

2.4.1 Cells seeding on coverslips

2.4.1.1 Free growing cells

Cells were detached from the original Flask T25 as described in section 2.1.3 and seeded on circular coverslips (VWR406/0189/12) with diameter of 13mm and No 1.5 thickness.

2.4.1.2 Micropattern

For experiments with the micropattern chip, melan-Rab3GEP KO #3 were seeded into wells of a 4-well plate, cells were maintained in RPMI-1640 (Sigma) supplemented with 10% (v/v) fetal calf serum (Gibco), 2mM L-glutamine, 100 units/ml penicillin and streptomycin 100 mg/L (Sigma), 80nM phorbol 12-myristate 13-acetate at 37°C in a humidified atmosphere containing 10% CO_2 overnight. The day after infections with adenoviruses was performed and cells were incubated for two days at the same condition said above. Then cells were detached with 1x trypsin-EDTA, cell number was adjusted in order to have 60000 cells per ml. CYTOOchip (micropattern chip coverslip) was placed into a CYTOOchamber located in a 6 well plate (CYTOOchips Mini DC-L-FN650 (Cytoo, 11-003-13-12, France)). 450µl of suspension cells were added on the top of the CYTOOchip and left 10mins at room temperature to sediment under the hood then 6 well plate containing the CYTOOchamber was moved into the incubator at 37°C 10% CO_2 for 20mins. Then 3 washes with growth medium were performed to remove unattached cells, hence cells were left overnight at 37°C under a humidified atmosphere containing 10% CO_2 to achieve full cell spreading.

2.4.2 Fixation and Immunostaining

Cells on coverslip were washed with phosphate-buffered saline (PBS) twice, fixed with 3% (w/v) paraformaldehyde (Sigma P6148) in PBS for 15 min, and rinsed with PBS. Fixed cells were then incubated with NH_4Cl (Sigma A9434) for 10 min. In order to perform the immunostaining cells were

permeabilized and blocked with 0.05% saponin (Sigma S7900) in PBS and with 0.5% bovine serum albumin (Fisher Scientific BP9700-100) for 15 min. The cells on coverslips were incubated with primary antibody (see table 11) for 30 minutes, washed 5 times and incubated with secondary antibody dilution 1:500 for 30 minutes, and washed again 3 times in the same buffer. Nucleus staining was performed incubating the cells with 300nM of DAPI (4',6-diamidino-2-phenylindole) for 10mins. Coverslips were mounted with Fluorogel mounting medium (GENE TEX, Cat.N GTX28214, U.S.A.).

Table 11 Antibodies used for immunostaining

Primary antibody	Dilution	Supplier
anti-Melanophilin goat	1:50	Everest biotech Cat.N. eb05444

Secondary antibody	Dilution	Supplier
alexa 568 donkey anti goat	1:500	ThermoFisher Cat.N. A-11057

2.4.3 **Mitotracker staining**

Mitochondria in live cells were stained using MitoTracker Red FM (Life Technologies). Cells seeded in a 4 well plate were incubated with normal grown medium containing 200nM of MitoTracker Red FM for 30mins at 37°C, the cells were washed with new medium twice and imaged.

2.4.4 **Microscopes used for imaging**

Axiovert S100 microscope fitted with 4x, 10x and 20x objective lens with DIC (Differential Interference Contrast) or with Ph (Phase contrast) was used to obtain bright field images of melanocytes, and phase contrast/fluorescence images of HEK293a. Free growing melanocytes phase contrast/fluorescence images were obtained using a Zeiss LSM710 confocal microscope fitted with 63× 1.4 NA oil-immersion Phase contrast objective lens. Micropattern cells images were obtained with Zeiss LSM 710 confocal

microscope fitted with 63× 1.4 NA oil-immersion Phase contrast objective lens. The microscope was set for semi-automated acquisition of images. Laser lines used 405nm, 488nm, 561nm, 594nm, and 633nm. All images are single sections in the *z*-plane. Time lapse images were obtained using Leica DMRE microscope fitted with 10x DIC objective lens.

2.4.5 **Cell phenotype analysis**

Four pictures of different areas of the well were imaged (see section 2.4.4) and cells phenotype was established counting manually the cells with melanosome clustered and cells with disperse melanosome distribution, using the plugin cell counter of ImageJ. Example is shown in Figure 19 with of one of four pictures and zoom in into a small section, where it is possible to see circle blue and cyan that represent respectively cells with clustered and dispersed melanosome distribution.

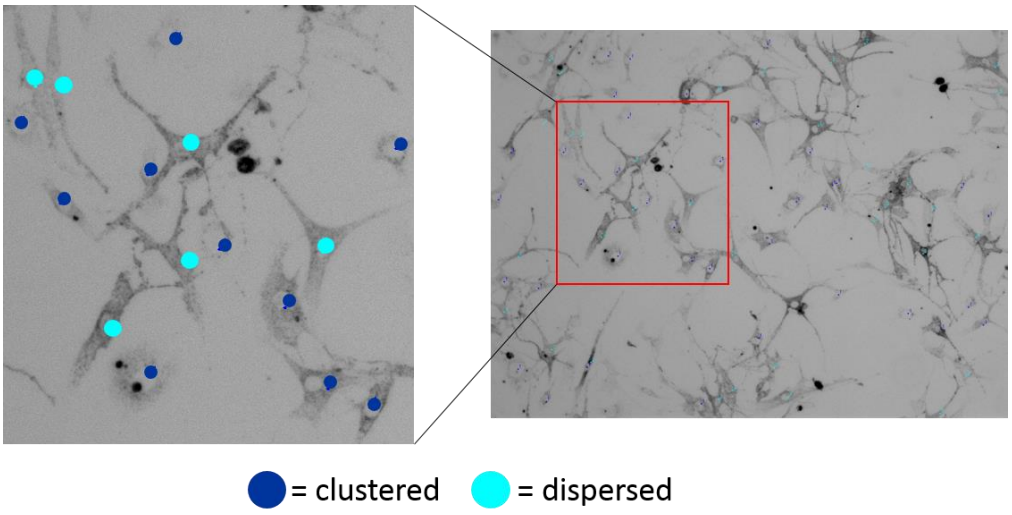


Figure 19 Example of cells with clustered and dispersed melanosome distribution counted with ImageJ

2.4.6 **Micropattern Cells analysis**

In order to analyse the cells in micropattern as a first step between 25 and 40 cells for experiment were manually located and then automatically acquired with autofocus on the micropatterns (excitation 633 nm; emission 650 nm) using Zeiss LSM710 confocal microscope as described in section 2.4.4. Selected cells were single occupying and completely spread on the fibronectin disk. Images were analysed with ImageJ software. Images were aligned in reference to the micropattern using a modified macro available from Cytoo (CellRefDemo). To measure the Pigment distribution phase images were inverted and threshold was applied in order to visualise dark-pigmented melanosomes, then binary images were created. Melanosome distribution was calculated by determining the radial profile of the binary images (Radial Profile Extended; http://rsbweb.nih.gov/ij/plugins/ radial-profile-ext.html). The PDD was defined as the radius of a circle with origin at the centre of the pattern that encompasses of the melanosomes. Statistical Bonferroni's multiple comparisons of data was carried out with GraphPad Prism 6 software.

3 Characterisation melan-Rab3GEP knockout cells

3.1 Introduction

As said in the introduction, melanocytes are an excellent model to study organelle transport. Previous studies have indicated that there are more than 50 genes in mouse that affect pigmentation of the coat (133), three of them do not affect the pigmented granule maturation but only their transport causing melanosomes aggregation at the perinuclear cytoplasm. One of these loci is the *ashen (ash)*, and it has been shown that Rab27a is the protein encoded (134), suggesting the importance of this GTPase in the melanosomes transport. Myosin Va, the actin based motor, is the protein encoded in the locus *dilute (d)* (135) which its mutation causes defects in melanosomes trafficking along the actin filaments. Third, but not for importance, *leaden (Ln)* encoded for Melanophilin (Mlph) protein (136), crucial protein for the interconnection between Rab27a and the motor protein Myosin-Va.
Melanocytes with mutation in these three loci (*ashen*, *leaden* and *dilute)* have been extensively used as model, and they have been extremely important to study the molecular mechanism of polarised melanosomes trafficking. In fact, re-introduction of wild type forms of respectively Rab27a into *ashen*, Melanophilin in *leaden* or Myosin-Va in *dilute* melanocytes cause rescue of the melanosome distribution with rearrangement from a perinuclear localisation to a disperse distribution.

Rab3GEP protein is a GEF protein, therefore, it stimulates the release of GDP and the acquisition of GTP, activating Rab27a in melanocytes. Moreover, it has been already suggested that Rab3GEP protein is important not only for the activation of Rab27a but even for its targeting to melanosomes membrane (85). Previous studies have suggested that down-regulation of Rab3GEP using siRNA causes defects at the melanosomes transport, featured by clustering at the perinuclear area (7).
In order to investigate in detail the role of Rab3GEP protein and the role of its domains in melanosome transport, melanocytes with null Rab3GEP were used as a model. The scope was to adopt the same approach used in the

previous work performed on *ashen*, *leaden* and *dilute*, therefore, reintroducing either Rab3GEP full-length or its domains and investigate whether the mutants were able to rescue melanosome transport.

Rab3GEP knockout mice were already generated by Tanaka et al (123) to investigate the role of this guanine nucleotide exchange factor in synaptic vesicle trafficking. However, homozygous Rab3GEP null mice died 30 min after birth for respiratory failure caused by constricted pulmonary tracts. Nevertheless, there were no differences in morphology between the wild type and the homozygous Rab3GEP null E18.5 embryos, suggesting that Rab3GEP is not essential for the development. Moreover, cells extracted from the embryos stage should present the deletion of the protein and might be used in culture.
Another crucial step to obtain Rab3GEP knockout melanocytes is the cell immortalisation. The fundamental requirement for the immortalization of melanocytes is the functional inactivation of retinoblastoma (Rb) and p53 tumour-suppressor.

Retinoblastoma (Rb) plays a pivotal role in the negative control of the cell cycle, it is considered a gatekeeper of the access from the G1 to S phase (137). When Rb is in the hypophosphorylated active state it blocks the cell cycle in G1 phase. To perform this function, it binds E2F (*Transcription factor*) causing repression of gene transcription, which is required to access to S phase. After the activation of the cell duplication, the cell cycle proteins Cyclin Dependent Kinase (CDK) phosphorylates Rb, and the hyperphosphorylated Rb is unable to bind E2F anymore so the cell can have access to the S phase (138).

p53 is a transcription factor that promotes the transcription of genes that cause growth arrest or apoptosis in response to a plethora of different cell stress signals (139). The protein expression level of p53 is low and has a short life in normal cells, instead, in cells with damaged DNA there is accumulation of this protein. One of the target gene transcript by p53 is p21, which is a CDK inhibitor that causes arrest of the cell cycle. Activity of p53 is highly controlled by MDM2 protein, which its binding inhibits p53 activity, and catalyse its degradation. In response of various signals such as DNA damage or hyperproliferative signals caused by activation of RAS, MDM2

releases p53 and then it can perform its functions arresting the cell cycle in G1 phase through p21 or causing apoptosis through Bax protein.

Therefore, a crucial point for the immortalisation of melanocytes is the deletion of the gene Ink4a-Arf tumour suppressor, this locus encoded for two powerful inhibitors of the cell growth: $p16^{Ink4a}$ and Arf, which are directly linked with Rb and p53.

$p16^{Ink4a}$ inhibits the hyperphosphorylation of Rb performed by CDK4/6, arresting the cell cycle to the G1 phase. Meanwhile, Arf interacts with MDM2 restricting its action on p53, then the transcription factor is free and able to block the cell cycle or to cause apoptosis. Hence, the immortalisation of melanocytes required the knockout of the Ink4a-Arf gene (Figure 20).

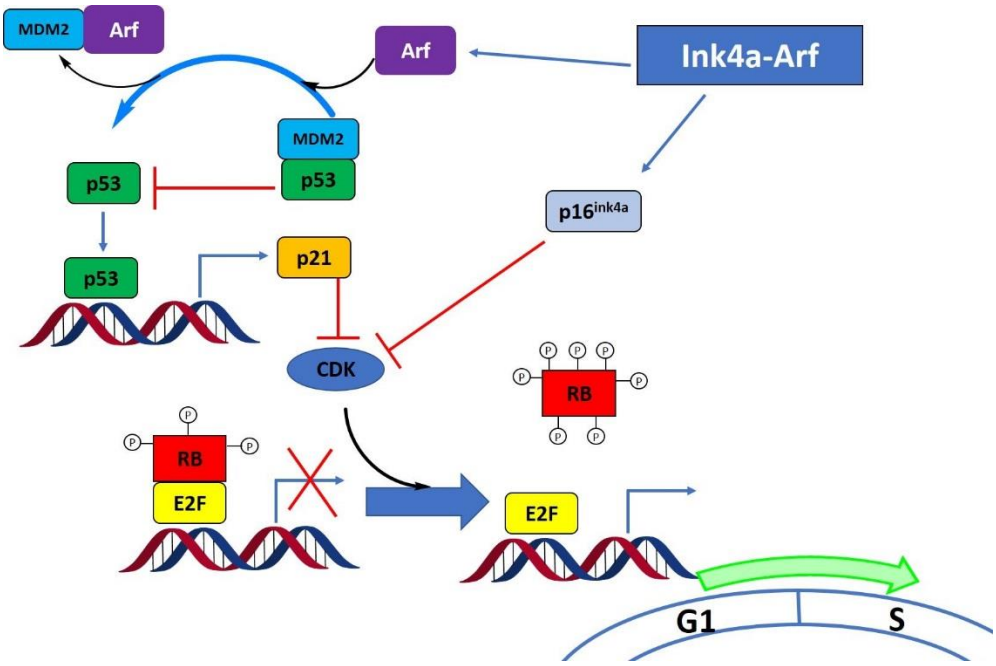


Figure 20 Cell cycle regulation by Retinoblastoma and p53

E2F activates the expression of genes for the passage from G1 to S phase. Retinoblastoma (Rb) binds E2F and inhibits its activity blocking the cell cycle to G1 phase. CDK phosphorylates Rb, and hyperphosphorylated Rb cannot binds then inhibits E2F. CDK activity is inhibited by $p16^{ink4a}$ and p21. $p16^{ink4a}$ is product by the gene Ink4a-Arf, p21 is product after activation of p53.MDM2 binds p53 and inhibits its action. Arf binds MDM2 freeing p53. Arf is product by the gene Ink4a-Arf as $p16^{ink4a}$.

In order to investigate the function of Rab3GEP protein were necessary cells immortalised and null for Rab3GEP (Ink4a-$Arf^{-/-}$ and $Rab3GEP^{-/-}$). Therefore, these cells could be used as a model to test the ability of the mutants of

Rab3GEP protein to rescue melanosome trafficking. As previously mentioned, Rab3GEP null mice died after birth so to obtain cells with the double knockout it was necessary to inter-cross mice heterozygotes (Ink4a-Arf$^{+/-}$ and Rab3GEP$^{+/-}$) to produce mice homozygotes (Ink4a-Arf$^{-/-}$ and Rab3GEP$^{-/-}$). Considering that the mice cannot live after birth, it was necessary to get the cells from the embryo, and analyse the genetic mutation by PCR, to confirm the double knock out genes.

At the end of this screening three melan-Rab3GEP KO cell lines derived from three different pups were obtained, then these cells were used in this study. Double knockout cells were obtained by Montoliu Lluis, Sviderskaya Elena before starting the project (details in M&M).

3.2 Active Rab27a in melan-Rab3GEP KO cells with disperse melanosome distribution

The importance of Rab3GEP protein in melanosome transport has been firstly suggested by Figueiredo et al. (7), who found that this protein can function as a guanine nucleotide exchange factor of Rab27a. Therefore, crucial for the activation of this Rab protein and consequently for the anterograde melanosome trafficking. In that study, the authors showed that depletion of Rab3GEP cause melanosomes re-distribution with accumulation at the perinuclear area, similarly to *ashen* cells. Moreover, authors showed that down regulation Rab3GEP decreases the ability of endogenous Rab27a to bind its effector Slp1, detected through pull-down assay using GST-Slp1 and GST recombinant proteins. Furthermore, authors showed through immunostaining that there was down regulation of Melanophilin effector in cells depleted for Rab3GEP, which indicates that Rab27a was not in the GTP-bound form. Figure 21 shows the silencing of Rab3GEP protein in melan-INK4 ko cells.

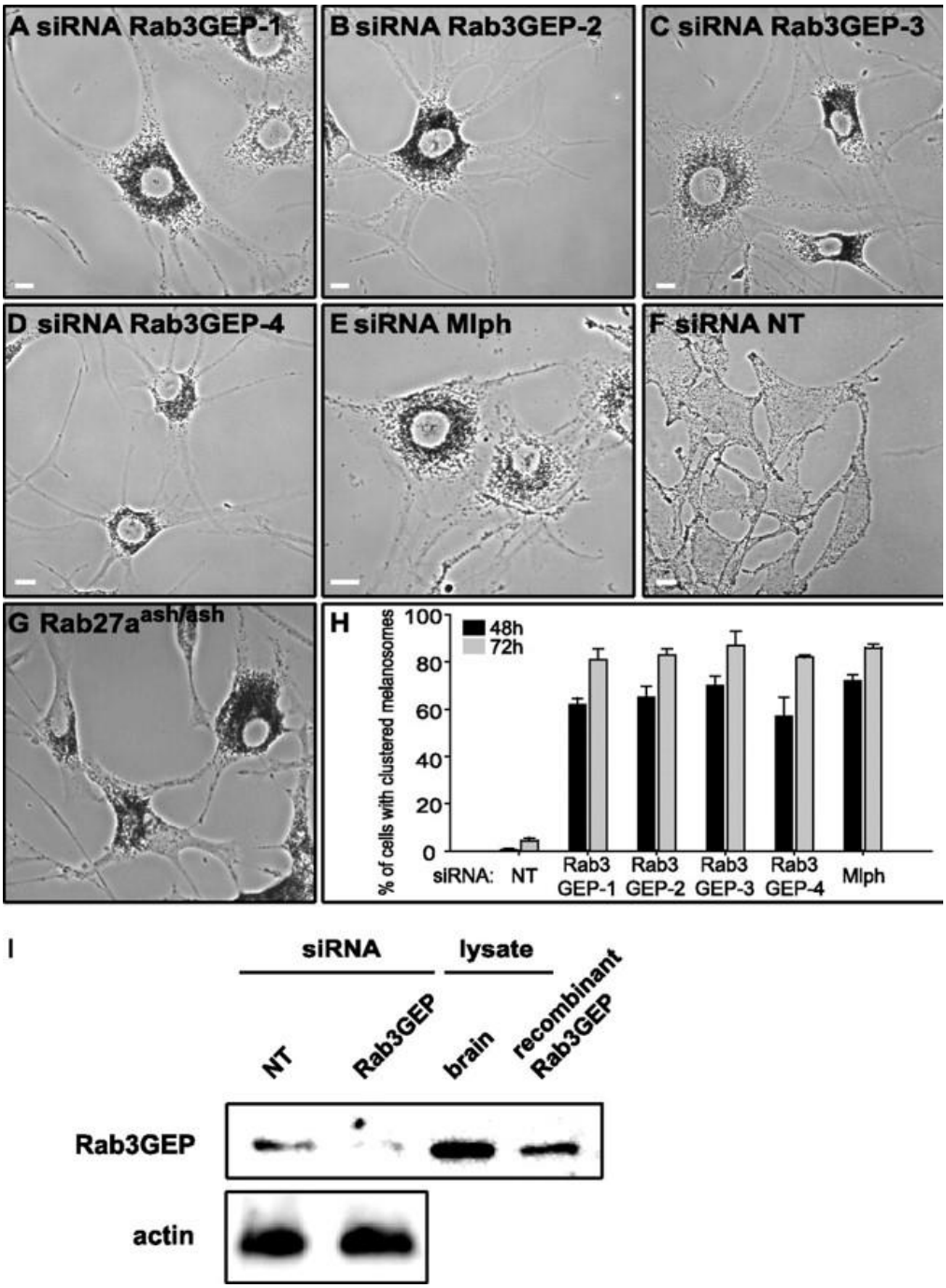


Figure 21 Rab3GEP knockdown in melan-ink4 melanocytes induces perinuclear distribution of melanosomes

Downregulation of Rab3GEP was performed in melan-ink4 melanocytes using 4 oligonucleotides 1-4 (A-D). siRNA positive and negative control were the depletion of Mlph, and not targeting respectively (E-F). G shows melan-ash cells. Quantification cells with clustered melanosome was performed 48-72hrs after the silencing (H). I) shows the protein expression level of Rab3GEP after after silencing through WB. Taken from Figueiredo et al. (6)

In Figure 21 it is possible to notice that the depletion of Rab3GEP in wild type melanocytes causes clustering of the melanosomes similarly to the

downregulation of the effector Mlph. The graph H shows the quantification of cells with melanosome clustering, indicating that the GEF down regulation induces an increase in the proportion of cells with melanosome clustering of about 60% of the total population after 48hrs, and about 80% after 72hrs likewise melanophilin downregulation.

As previously mentioned, in order to investigate in detail the role of Rab3GEP protein, cells with deletion of this protein were produced. Based on the previous studies on Rab3GEP protein in melanocytes, in which its silencing induces melanosomes aggregation at the perinuclear area, an obvious expectation was to see cells phenotypically similar to the *ashen* cells. However, melan-Rab3GEP knockout melanocytes manifest mixed phenotypes with different proportions of cells with clustered and dispersed distribution of melanosomes Figure 22.

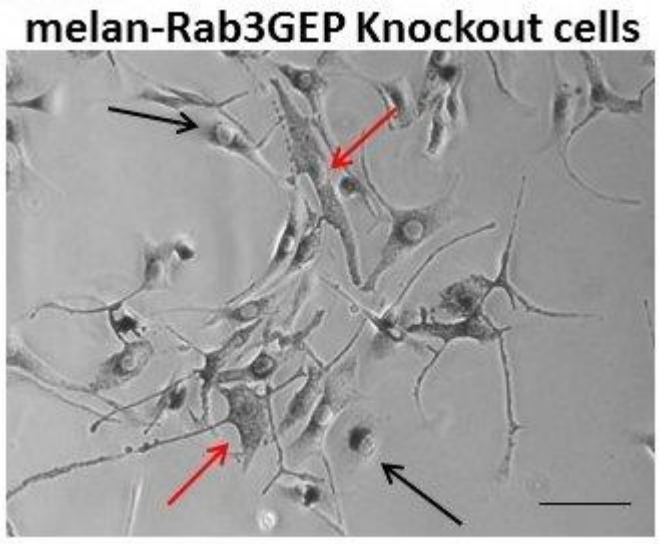


Figure 22 Representative image of melan-Rab3GEP KO cells show a mixed population of cells with different melanosome distribution

Cells were grown on glass coverslips, fixed and imaged using phase contrast as described in M&M. Red arrows indicate cells with disperse distribution of the melanosomes throughout the cell body. Black arrows point out cells with clustered melanosome distribution at the perinuclear cytosol. Scale bar 100μm

In Figure 22 it is possible to see one particular behaviour of the melan-Rab3GEP knockout cells regarding the melanosome distribution. In fact, some cells present dispersed melanosome distribution throughout the cell body (pointed by the red arrows), while, others exhibit a clustered melanosomes phenotype indicated by the black arrows. This suggests that

surprisingly in some cells the melanosome trafficking machinery is working even in absence of Rab3GEP protein.

Since three melan-Rab3GEP KO cell lines derived from three different pups were obtained (#1, #2, #3), the obvious, first step was to investigate whether the same behaviour was repeated in all them. It was observed that all the three cell lines show the same mixed phenotype (Figure 23).

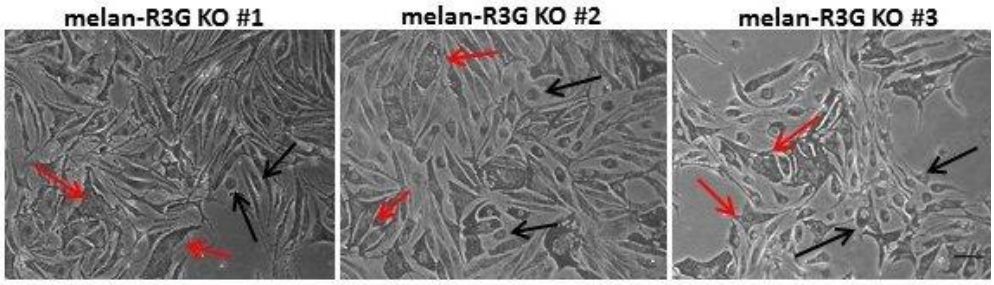


Figure 23 Images showing the mixed phenotype of the #1, #2 and 3# melan-Rab3GEP cell lines

Cells were grown on glass coverslips, fixed and imaged using phase contrast optics. On the left melan-Rab3GEP #1, in the middle melan-Rab3GEP #2 and on the right melan-Rab3GEP #3. Red arrows indicate cells with dispersed melanosomes, black arrows indicate cells with clustered phenotype. Scale bar 100μm

Several questions arise from the observation of this particular behaviour of melan-Rab3GEP KO cells: 1) are the melan-Rab3GEP KO cells truly knockout for Rab3GEP? 2) Is Rab27a protein involved in melanosome trafficking even in absence of Rab3GEP? Or there are other Rabs involved? 3) If Rab27a is responsible for the pigmented granule trafficking, is it active? 4) If so, what is the mechanism of Rab27a activation?

PCR results screening performed previously by Montoliu Lluis, Sviderskaya Elena has indicated that the three cell lines are homozygous knockout for Rab3GEP. To determine whether the knockout induce lack of Rab3GEP protein in these cell lines, answering to the first question, western blot assay was performed, immunoblotting against Rab3GEP protein (Figure 24).

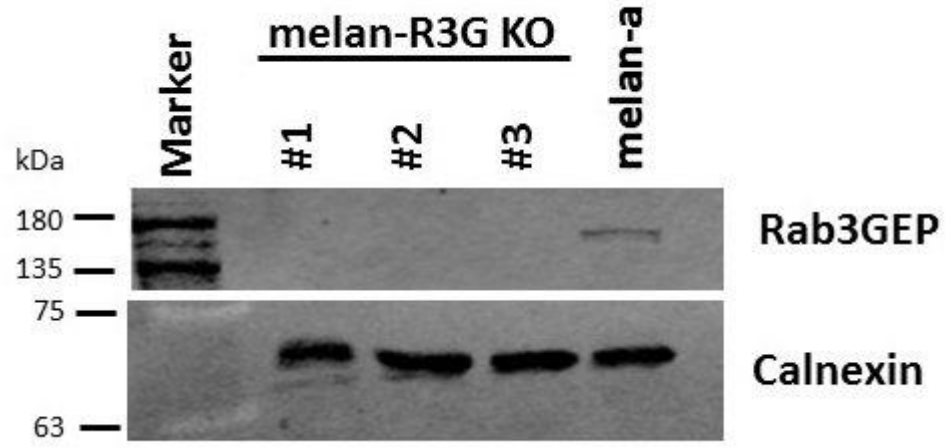


Figure 24 melan-Rab3GEP KO cells do not express Rab3GEP protein

melan-Rab3GEP KO cells were seeded on 6 well plate, harvested, and lysed (see M&M), melan-a wild type cell line was used as a positive control. Lysates (25µg) were loaded on 6% SDS-PAGE gel, immunoblotting was performed with anti-Rab3GEP antibody. This image shows the expression level of Rab3GEP in 3 cell lines with Rab3GEP KO. and in melan-a wild type. On the top Rab3GEP detection at about 170 kDa. On the bottom loading control Calnexin at 67 kDa

The Figure 24 shows clearly that there is a band at about 170 kDa which correspond to the predicted molecular weight of Rab3GEP protein in the positive control melan-a wild type cell line. Instead this band is absent in all three of the melan-Rab3GEP KO cell lines. Suggesting that the three cell lines lack Rab3GEP protein. The lower panel show the loading control Calnexin and it is possible to define them equal loaded.

However, the question regarding the role of Rab27a in melanosome transport in cells with dispersed distribution of these organelles remains unanswered. One hypothesis would be that in these cells other Rab proteins drive the melanosomes trafficking. Although the importance of Rab27a has been extensively accepted, there are papers in which are suggested other Rabs such as Rab8 (140) or Rab1 (141) able to regulate the anterograde movement of melanosome.

To establish whether Rab27a is the main actor in melanosome transport in melan-Rab3GEP KO cells with dispersed distribution of pigmentate granules, downregulation of this Rab protein was performed. If Rab27a is crucial for the anterograde transport of melanosomes in melan-Rab3GEP KO cells, its silencing should increase the retrograde transport, leading to melanosome

clustering. melan-Rab3GEP KO cells were transfected with siRab27a; to establish if the silencing was working correctly melan-a wild type cells were

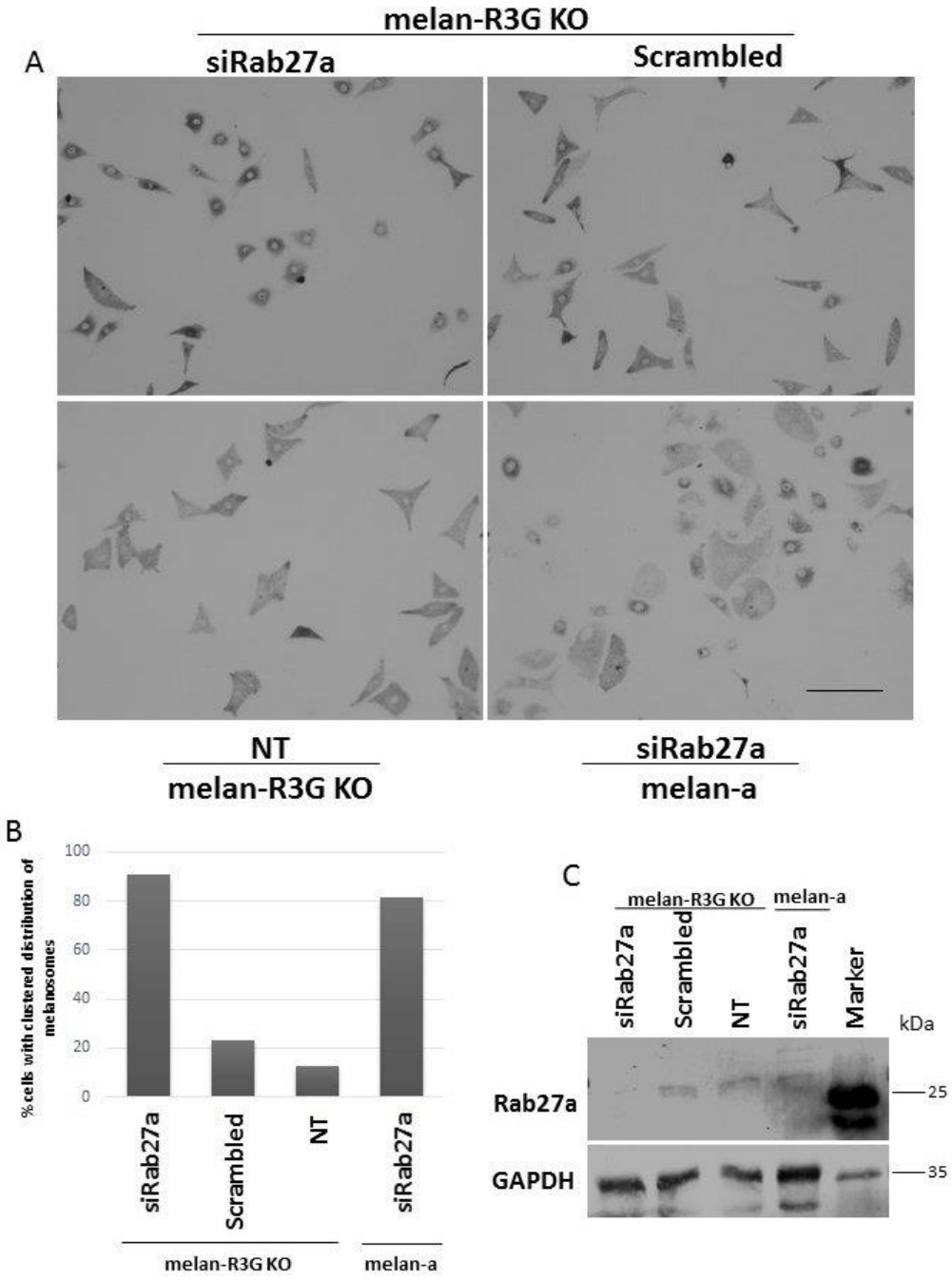


Figure 25 Disperse melanosome distribution in melan-Rab3GEP KO cell is driven by Rab27a

melan-Rab3GEP KO #1 cells and melan-a cells were seeded in a 6 well plates and maintained in medium without PMA. When melan-Rab3GEP KO cells presented disperse melanosome distribution were transfected with siRab27a. After 48hrs cells were imaged (4 images per condition) and harvested. Lysates were loaded in a 10% SDS-PAGE gel and immunoblotting was performed against Rab27a and GAPDH. A) Images of the cells 48hrs after transfection and before harvesting. Top left shows melan-Rab3GEP KO #1 with siRab27a. Top right shows melan-Rab3GEP KO #1

treated with siRNA scrambled. Bottom left melan-Rab3GEP KO #1 Not Treated. Bottom right shows melan-a wild type treated with siRab27a as a positive control. This experiment was done 3 times B) Graph shows the percentage of cells with melanosome clustering at the perinuclear area. Bars are the mean of number of cells counted in 4 frames per condition. C) Immunoblotting using Rab27a and GAPDH antibodies for all the lysates. The left three columns are melan-Rab3GEP KO #1 cells with siRab27a, Scrambled and No Treated respectively. The fourth column is the lysate of melan-a treated with siRab27a

used as positive control. Moreover, to establish the specificity of the siRab27a, scrambled siRNA and no transfected cells were used in parallel.

In Figure 25 it is possible to notice a high proportion of melan-Rab3GEP KO cells with dispersed melanosome distribution in cells not treated or treated with siRNA Scrambled (88% and 73% respectively), these high percentages were obtained because all the cells in this experiment were maintained without PMA. In fact, investigation of this particular behaviour of melan-Rab3GEP KO cells indicates cell maintained without PMA grow slower and present higher percentage of cells with dispersed melanosome distribution (see Appendix 7.1-7.2).

melan-Rab3GEP KO cells transfected with siRab27a present defects of the anterograde melanosomes transport causing accumulation of these organelles at the perinuclear cytoplasm. On the other side, Scrambled and Not Treated maintained melanosomes dispersed throughout the cell body indicating that the clustering is caused specifically by Rab27a downregulation (Figure 25). In melan-a used as a positive control for the siRab27a, melanosome clustering was observed like in melan-Rab3GEP KO cells. This suggested that in melan-Rab3GEP KO cells the melanosomes trafficking towards the cell periphery is driven by Rab27a.
Quantification of the percentage of cells with clustered melanosome shown in the bar graph indicates clearly that the silencing of Rab27a causes defects in the melanosomes anterograde trafficking for 90.6% of the cells imaged, with percentage very similar to the silencing of Rab27a in melan-a. Instead, Scrambled and NT show percentages of 23.2 and 12.6% respectively. This indicates an increase of cells with melanosome clustering of about 80-70%. Furthermore, the immunoblotting in Figure 25C shows that the downregulation of Rab27a had occurred in melan-Rab3GEP KO cells and in melan-a cells clarifying that the siRNA worked on Rab27a and that the effect of melanosome distribution is likely to be due to the downregulation of the level of Rab27a protein.

The results of the last experiment indicate that Rab27a does appear crucial for the anterograde transport in melan-Rab3GEP KO cells with dispersed melanosome distribution, since its silencing induced granule cluster in the perinuclear cytoplasm. Nevertheless, this experiment does not answer to the question whether Rab27a is in the active state in those cells with disperse melanosome.

It has been recently proposed that Coronin 3 effector binds Rab27a in the GDP state in pancreatic β cell line MIN6 (98), which suggested that Rab27a is able to bind effector even in the inactive state. Hence, it could be possible that the melanosome anterograde trafficking in melan-Rab3GEP KO cells is driven by Rab27a in the GDP state in complex with other effectors excluding melanophilin. Therefore, in order to define the state of Rab27a in melan-Rab3GEP KO cells with dispersed melanosomes, melanophilin effector protein expression was determined by Western Blot in the three melan-Rab3GEP KO cell lines, and it was used as read out of Rab27a state. As a positive control was used melan-a wild type cell line.

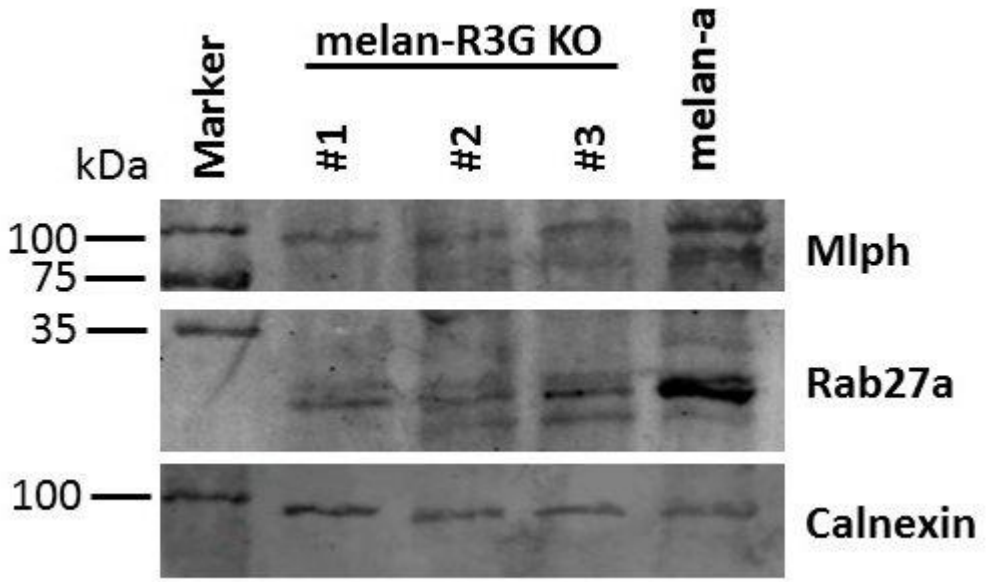
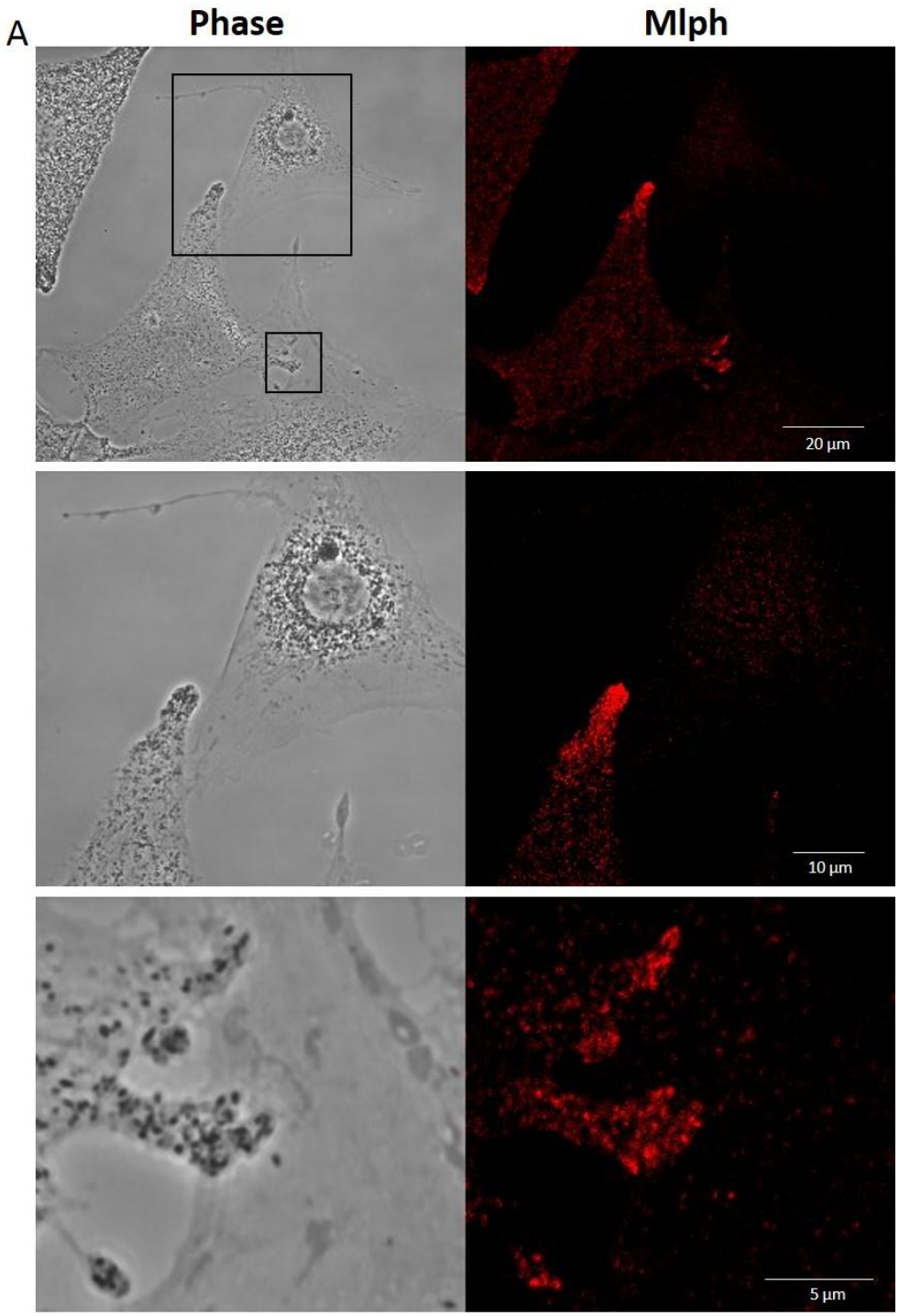


Figure 26 Lower expression of endogenous melanophilin and Rab27a in melan-Rab3GEP KO cell lines compared to melan-a cell line

Cells were lysed and loaded on 10% SDS-PAGE gel, immunoblotting was performed with anti-Rab27a and melanophilin antibodies. This image shows the expression level of Rab27a and melanophilin in 3 cell lines with Rab3GEP K.O. and in melan-a wild type. On the top melanophilin (Mlph) was detected at about 100kDa. The middle panel shows the protein expression level of Rab27a detected at 27kDa and on the bottom loading control Calnexin at approximately at 90kDa.

Figure 26 shows the level of Rab27a and Mlph proteins in the three cell lines with Rab3GEP knocked out and in melan-a used as a control. The immunoblotting against Mlph indicates that the protein level of the effector of Rab27a is decreased in the three melan-Rab3GEP KO cell lines compared with the control. A similar effect is visible in the lower panel for Rab27a. This suggests that melan-Rab3GEP KO cells having lost the guanine nucleotide exchange factor Rab3GEP could have less stabilised Rab27a active form so it is susceptible of degradation. It could be possible that stabilization of melanophilin effector protein is dependent on the level of Rab27a.

Protein levels of Rab27a and melanophilin are decreased in melan-Rab3GEP KO cells compared to melan-a wild type (Figure 26). Nevertheless, melanosome anterograde trafficking is driven by Rab27a, as evidenced by the fact that its downregulation causes increased frequency of clustering (Figure 25). Hence, further investigation was necessary to establish the subcellular localisation of melanophilin in cells with dispersed and clustered melanosome distribution (Figure 27).


A
Phase
Mlph
20 µm
10 µm
5 µm

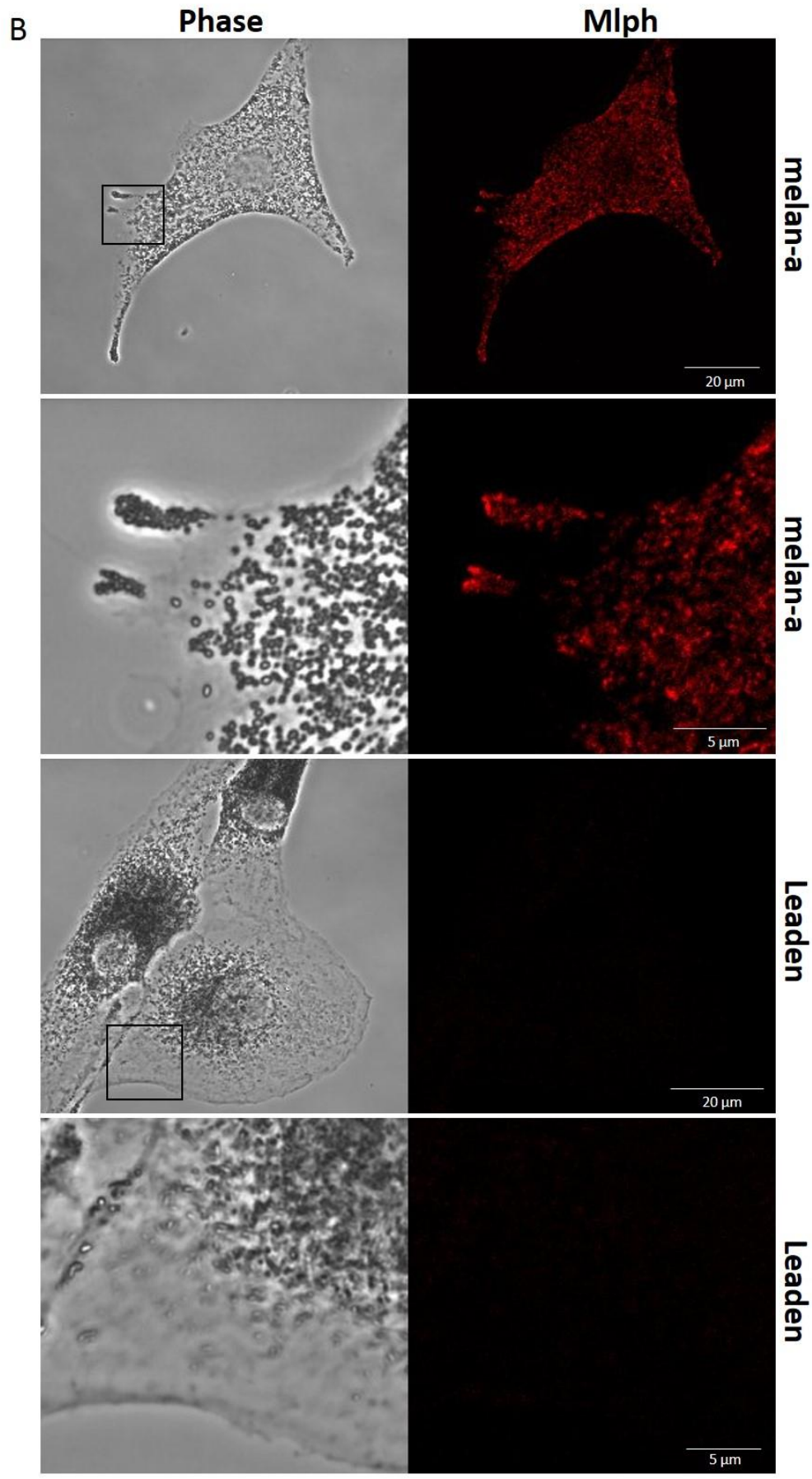

B
Phase
Mlph
melan-a
20 µm
melan-a
5 µm
Leaden
20 µm
Leaden
5 µm

Figure 27 Endogenous localisation and expression of melanophilin in melan-Rab3GEP KO, melan-a and Leaden cell lines

melan-Rab3GEP KO cells, melan-a wild type and leaden cells were seeded on glass coverslip, fixed and stained with anti-melanophilin antibody (see M&M). These images show the endogenous localisation of melanophilin in melan-Rab3GEP KO cells, in the positive control melan-a and in the negative control leaden cell lines. The right panels show the bright field images indicating the melanosome distribution. The left panels show the melanophilin signal.

Immunostaining of melanophilin was performed in melan-Rab3GEP KO cell, melan-a cells (positive control), and leaden cells (negative control). This experiment allows to establish the localisation of the effector, and to establish whether the melanosomes at the periphery are transported by Rab27a and melanophilin, and consequently the GTP state of Rab27a.

Right panels in Figure 27A show the distribution of melanophilin in melan-Rab3GEP KO cells, the top panel shows the different expression of this effector between two cells, one with dispersed melanosome throughout the cytoplasm, and another cell with melanosome clustering at the perinuclear area. The melan-Rab3GEP KO cell with normal melanosome trafficking has a higher level of melanophilin staining compared to that with defect in melanosomes trafficking. Moreover, from the middle and bottom panels of the Figure 32A is possible to notice the high expression of melanophilin at the cell periphery which is colocalised with the melanosomes position. In Figure 32B are shown the controls of this immunostaining which are melan-a wild type cells (top panels) and leaden cells (bottom panels). In melan-a wild type cells is evident the localisation of melanophilin with the melanosomes (second panel) and the melanophilin signal is dispersed throughout the cell body. Instead, in leaden where melanophilin is absence there is no signal, confirming the specificity of the staining.

In conclusion, melan-Rab3GEP KO cells show the same pattern of melan-a wild type cells when melanosome trafficking towards the cell periphery is active, with co-localisation of melanophilin and melanosomes, while in cells with defect of the melanosomes trafficking there is less expression of melanophilin. These results suggest that in melan-Rab3GEP KO cells with dispersed distribution of melanosomes the trafficking is mediated by Rab27a (its downregulation causes melanosome clustering) and co-localisation of melanophilin with melanosome suggest active state of Rab27a.

3.3 Discussion

This chapter has investigated the behaviours of melan-Rab3GEP KO cell lines. Although the downregulation of Rab3GEP induces melanosome clustering, melan-Rab3GEP KO cell lines present mixed population of cells with dispersed and clustered melanosomes. Therefore, the knockout has a different effect compared to the knockdown, and in some cells the pigmented granules move towards the periphery even without the GEF of Rab27a. To understand this phenomenon, it is necessary to focus on the main difference between the short interference RNA and the deletion of the gene through knock out. One crucial difference between the two processes is the time of the annulment of the function of the target gene. During the silencing, the cell undergoes a quick and strong ablation of the target protein, causing "shock" and misbalance of a normal basal conditions. Instead, in knock out cells there is a permanent absence of the protein target. This raises the question whether the phenotypes derivate from the permanent ablation mirror the phenotypes derivate from a short-term silencing. It might be possible that during the prolonged absence of the target gene there is genetic compensation which confer normal phenotype.

In agreement with this theory, it has been recently suggested that the loss of DOCK6 GEF cause a different phenotype between the acute silencing and the prolonged lack of gene (142). In this work, the authors suggested that during long deletion of the gene, cells are able to compensate the lack of the gene. DOCK6 GEF is the guanine nucleotide exchange factor of Rac1 and Cdc42 proteins. Hence, this protein activates two Rho proteins important for the cell cycle and the cytoskeleton structure. During the acute depletion Rac1 and Cdc42 cannot be activated then there is a predominance of the GDP forms. This increase the activity of RhoA causing collapse of F-actin, microtubules, and intermediate filaments, driving toward cell rounding shape. Instead, during sustained depletion or KO of DOCK6 there is higher level of G-actin compared to WT which blocks the translocation of the MRTF-A/SRF transcription factor (promote cytoskeleton organisation) to the nucleus. This causes the lack of synthesis of ISG15 (Ubiquitin-like protein), which performs the ISGylation of IQGAP1 effector of CDC42 and Rac1causing its degradation. Hence, during the sustained depletion or KO of DOCK6, IQGAP1, one effector of CDC42 and Rac1, is not degraded. The presence of

the effector stabilises CDC42 and Rac1 in the active form, therefore the cells present the same features of the wild type. Hence, possible effect of the deletion of Rab3GEP in melanocytes could be a stabilization of Rab27a active form due to a not degradation of its effector melanophilin.

Another possibility of the anterograde melanosomes trafficking in some cells may be due to the redundancy between Rabs. It has been suggested that Rab27b compensates the absence of Rab27a in ashen platelets but not in melanocytes in which Rab27b is absent (143). Following this idea, it could be possible that deletion of Rab3GEP causes the overexpression of another Rab which substitutes Rab27a in the complex with melanophilin and Myosin V. It has been suggested that Rab8 is associate to the melanosome and can regulates its trafficking along the actin filament (140). Nevertheless, in this chapter it has been demonstrated that the melanosomes trafficking is driven by Rab27a in the active state, in fact its downregulation invokes melanosomes aggregation, and in cells with dispersed melanosomes the effector melanophilin localises to the membrane of these organelles, which indicate the presence of Rab27a GTP loaded. Another possibility could be the compensation by another Rab GEF that would activate Rab27a when Rab3GEP is knockout.

4 Integrity of Rab3GEP protein is crucial for the GEF activity

4.1 Introduction

The previous chapter focused on the characterisation of melan-Rab3GEP KO cells. The aim of that chapter was to optimize the conditions to provide a clear background for functional studies of Rab3GEP protein. In other words, the best condition to use in order to have melan-Rab3GEP KO cells with the highest proportion of cells with melanosome clustered in the perinuclear cytoplasm. Based on the results displayed in chapter 3 and in Appendix 7.1, 7.2, hereafter all the experiments are conducted using melan-Rab3GEP KO #3 cell line maintained with 80nM of PMA. The reason of this choice is based on the higher percentage of cells with melanosome clustering in this cell line compared to the other two cell lines. This characteristic offers a clearer background on which to investigate the ability of Rab3GEP wild type protein and its mutants to reactivate the anterograde melanosome trafficking (see below).

Hence, this chapter is focused on Rab3GEP protein and on the investigation of its function as guanine exchange factor of Rab27a and subsequently promoter of the anterograde melanosome transport.
Parallel approaches were adopted to characterize the GEF activity of Rab3GEP. On one hand to better understand the role of the different domains present in this protein, truncations of the full-length protein were made, in order to isolate or delete domain from the wild type protein. On the other hand, based on the suggestions that isolated DENN domain of Connecdenn presents GEF activity for Rab35 (144), and point mutations within this domain impair the exchange activity (46), corresponding point mutations in Rab3GEP were made. This approach permits to investigate similarities of working mechanisms between DENN domains.

In order to establish which contribution these changes give to the guanine exchange activity of Rab3GEP a cell based assay and a biochemical approach were used.

melan-Rab3GEP KO cells were used in the cell based assay, these cells present perinuclear clustered melanosomes, due to the absence of the GEF of Rab27a. Re-introduction of a functioning guanine nucleotide exchange factor would activate Rab27a leading to the formation of the Rab27a-Mlph-MyoV complex and subsequently redistribution of melanosomes toward the cells periphery.

Hence, the cell based assay uses restoration of dispersed melanosome distribution in melan-Rab3GEP KO melanocytes as a read-out of the functionality of Rab3GEP truncations or point mutations (Figure 28).

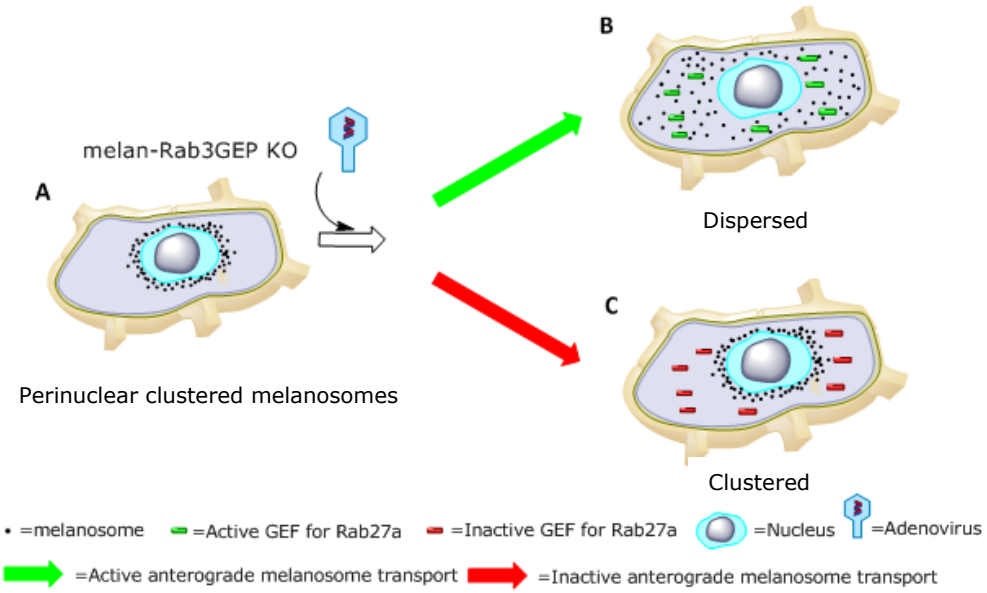
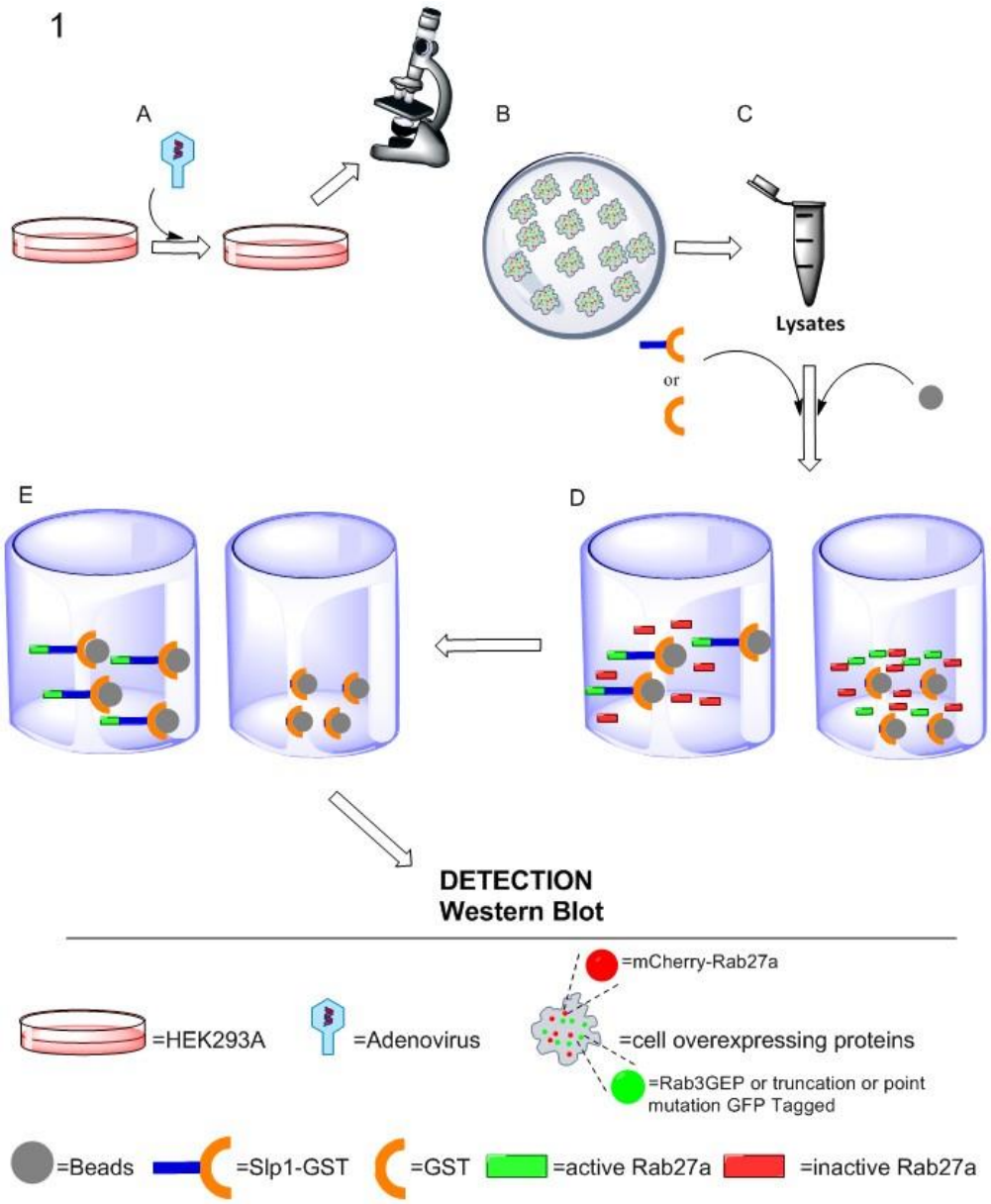


Figure 28 Schematic representation of the cell based assay of Rab3GEP function

melan-Rab3GEP KO in A) with melanosome clustering at the perinuclear cytoplasm, are infected with adenovirus expressing Rab3GEP truncations or point mutations. B) a cell overexpressing protein with active GEF activity for Rab27a and rescued melanosome distribution. C) a cell overexpressing inactive protein with no GEF activity, therefore melanosomes remain at the perinuclear area.

The biochemical approach was based on the ability of Rab27a to bind its effector Slp1 mainly in the active GTP-bound state (116,145). Based on this ability mCherry-Rab27a and either truncations or point mutations were overexpressed in HEK293a and measurement of the proportion of active Rab27a in lysates was determined using pull-down assay (Figure 29).


1
A
B
C
Lysates
or
E
D
DETECTION
Western Blot
=mCherry-Rab27a
=HEK293A
=Adenovirus
=cell overexpressing proteins
=Rab3GEP or truncation or point mutation GFP Tagged
=Beads
=Slp1-GST
=GST
=active Rab27a
=inactive Rab27a

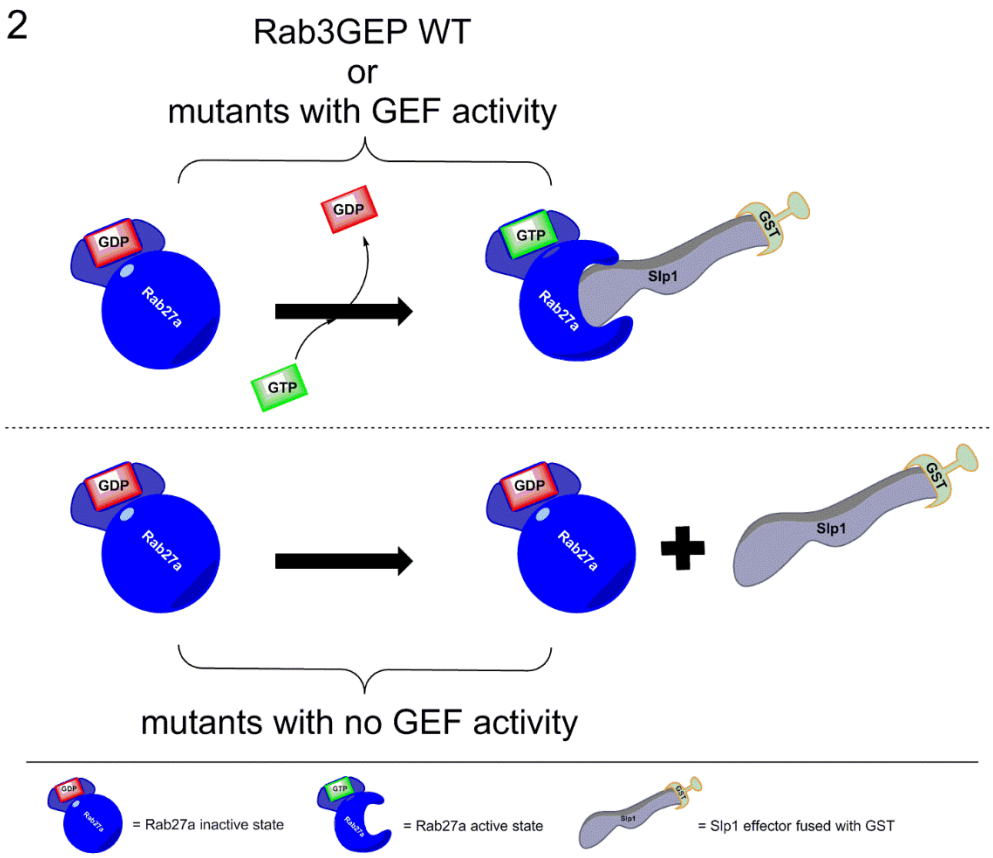


Figure 29 Schematic representation of the GST-Slp1 pull-down assay

1) Schematic representation of the steps performed for the pull-down assay. HEK293a cells were A) double infected with adenoviruses expressing mCherry-Rab27a and GFP tagged Rab3GEP mutants. B) proteins expression was estimate using mCherry and GFP emission. C- D) cells were lysed and 2 mg of lysates were incubated overnight with beads and either Slp1-GST or GST. After washing E) the bound fraction of Rab27a was determine with Western Blot. 2) Representation of the pull-down assay based on the ability of the mutants to activate Rab27a.

4.2 Truncated Rab3GEP mutant expression in HEK293a

As mentioned in the introduction Rab3GEP (DENN/MADD) is a protein containing DENN domain at the N terminus and a Death Domain at the C-terminus, and a long intervening region of 681 aa (see Figure 59). To establish the crucial parts of Rab3GEP protein for the Rab guanine nucleotide exchange activity the full-length protein was truncated. For this purpose, plasmids contained the full-length or the truncation mutant were prepared, and lastly adenoviruses expressing these proteins were produced (Materials and Methods).

Evidence on DENND1B domain of Connecdenn proteins suggests that the DENN domain is crucial and sufficient for the GEF activity (144), therefore, one of the truncation was made at the C-terminus of the DENN domain and it was fused with GFP at the N-terminus. On the other hand, another truncation protein was made by removing the DENN domain from Rab3GEP full-length (ΔDENN). Similarly, to better understand the role of the Death Domain in the GEF activity of Rab3GEP, this domain was removed (ΔDD) and a reciprocal truncation containing the death domain and the extreme C-terminus was made (DD). Similarly, to DENN truncation, all these truncation proteins presented GFP fused at the N-terminus. These adenoviruses were previously prepared by D. Briggs and A. Hume (University of Nottingham).

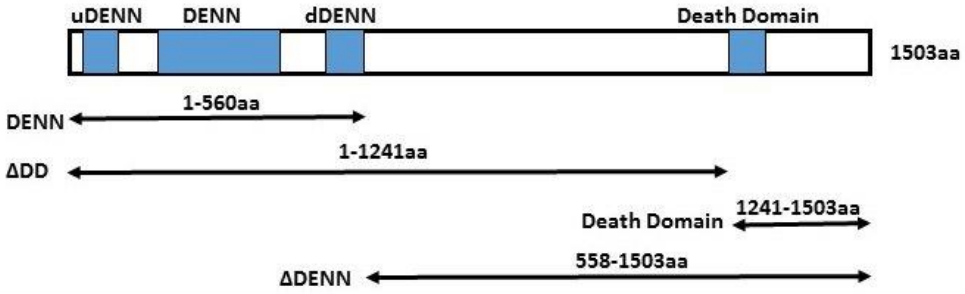


Figure 30 Schematic representation of truncated mutations of Rab3GEP

This picture shows the different truncated mutations of the human Rab3GEP. Indicated are the DENN domain containing upstream DENN (uDENN), core (DENN) and downstream (dDENN) (146), and the Death Domain (DD) at the C-terminus (90). Δ indicate deletion. Arrows indicate the regions that have been truncated of the full length.

Having obtained the different viruses expressing the different truncated fragment of Rab3GEP, the first step was to titer the viruses. The reason of the titering was to control the number of adenoviral particles introduced to the cells, in order to establish the amount to use for each virus to ensure similar expression levels of protein between the different truncation mutants so that the comparison between their effect was not complicated by differences in expression.

For this purpose, serial dilution of the viruses was performed (10^{-3}, 10^{-4}, 10^{-5}, 10^{-6}, 10^{-7}, 10^{-8}) mixing the viruses with the DMEM medium, then, virus particles were tested in HEK293a cells. Cells were infected with the same volume of viruses (20µl) and after overnight incubation, light microscopy was used to look at the different dilutions for each virus in order to determine which dilution for each gave equivalent levels of expression (Figure 31).

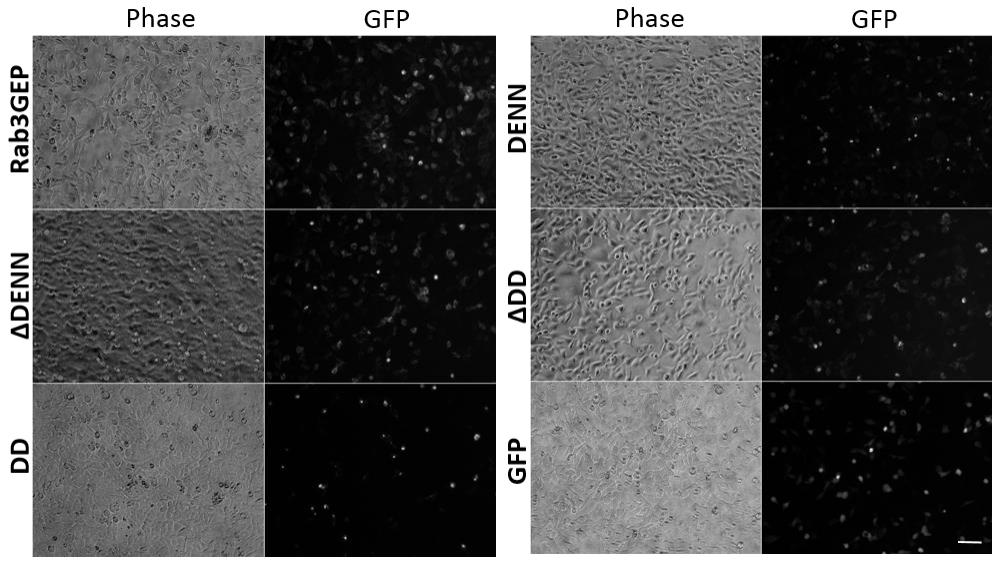


Figure 31 Similar GFP signal between the different truncation of Rab3GEP protein in HEK293a

Serial dilution of the original crude viruses was performed by mixing 20 µl virus with 980 µl of DMEM and subsequently dilution 10^{-3}, 10^{-4}, 10^{-5}, 10^{-6}, 10^{-7}, 10^{-8} was performed. Then, HEK293a cells were seeded in a 24 well plate and treated with 20 µl virus of each dilution. The day after, phase contrast images and GFP emission pictures were taken. The picture shows the expression of the different truncation mutant with the dilution of 10^{-5} which was the limit between the expression of GFP and the no expression (10^{-6}). Left images show the Phase Contrast, right images display the GFP expression. Scale bar 100µm

Images gained after overnight incubation with virus are shown in Figure 31 where phase contrast (on right) and GFP expression (on left) of the adenoviruses expressing the full-length of Rab3GEP protein, and the truncated mutation (DENN, ΔDENN, ΔDD, DD) and GFP protein used as control are displayed. In this figure, only the dilution 10^{-5} is shown, because it is the dilution limit, further dilution did not present GFP expression. Phase contrast pictures showed that similar confluence of cells were present in the different conditions, with no empty spaces and no death cells. Moreover, visual inspection of GFP expression indicates that all the viruses prepared were able to infect HEK293A cells and to express GFP tagged proteins. Furthermore, considering that the dilution 10^{-5} was the lowest dilution able to express GFP tagged proteins for all the truncation mutants it is was assumed that there was similar number of adenoviral particles between the truncations. However, the expression of the GFP tagged proteins was investigated through western blot in 4.3.

4.3 Expression of truncated Rab3GEP mutants in melan-Rab3GEP K.O. cells

Having established that the different truncated forms of Rab3GEP adenoviruses were expressing similar level of GFP fluorescence in HEK293a, expression of these proteins was investigated in melan-Rab3GEP KO cells.

In order to determine whether the cells infected with the adenoviruses were expressing the predicted proteins, western blot assay was performed. This allowed to detect the molecular weight of the truncation mutants and used that as a read-out of the protein stability based on comparison with the predicted molecular weight. As a control were used lysate from cells not infected (Figure 32).

Results indicate that all the truncated proteins were expressed in the cells. The molecular weights of the bands detected correspond with the prediction. In fact, Rab3GEP sample shows a band between 245-170kDa and its prediction is 194.4 kDa, DENN should present a band at 90.3kDa and in the western blot there is a band between 100-75kDa. Moreover, band between 130-170kDa was detected in ΔDENN sample and its prediction is 131.8kDa, DD sample shows a lower molecular weight band close to 63kDa which is close with the predicted at 58.6KDa, and finally, ΔDD sample present a band close to 170kDa and the predicted is 163.7kDa. Hence, these results correspond to the predicted GFP fusion proteins of Rab3GEP, DENN, ΔDENN, ΔDD and DD molecular weight and are marked with a single asterisk (Figure 32). However, based on the intensity of the bands seems that there are variations in the level of expression among the samples, where ΔDENN truncation isoform seems to be the highest expressed and the Death Domain (DD) is the lowest. Samples with overexpression of Rab3GEP full length and ΔDeath Domain (ΔDD) display lower bands at 135kDa (marked with double asterisks). Considering that GFP is located at the N-terminus, these secondary bands might be products of the cleavage at the C-terminus of the full-length and of the ΔDD proteins. The molecular weights of these secondary bands suggest that Rab3GEP full-length can be cleaved at the linker regions between the DENN domain and the Death domain. Absence of band in the negative control indicates the specificity of the antibody used. Moreover, immunoblotting of the loading control protein Calnexin shows

similar intensity of the bands amongst the samples indicating similar amount of proteins loaded, except for the NT where the band intensity seems to be slightly lower than the others.

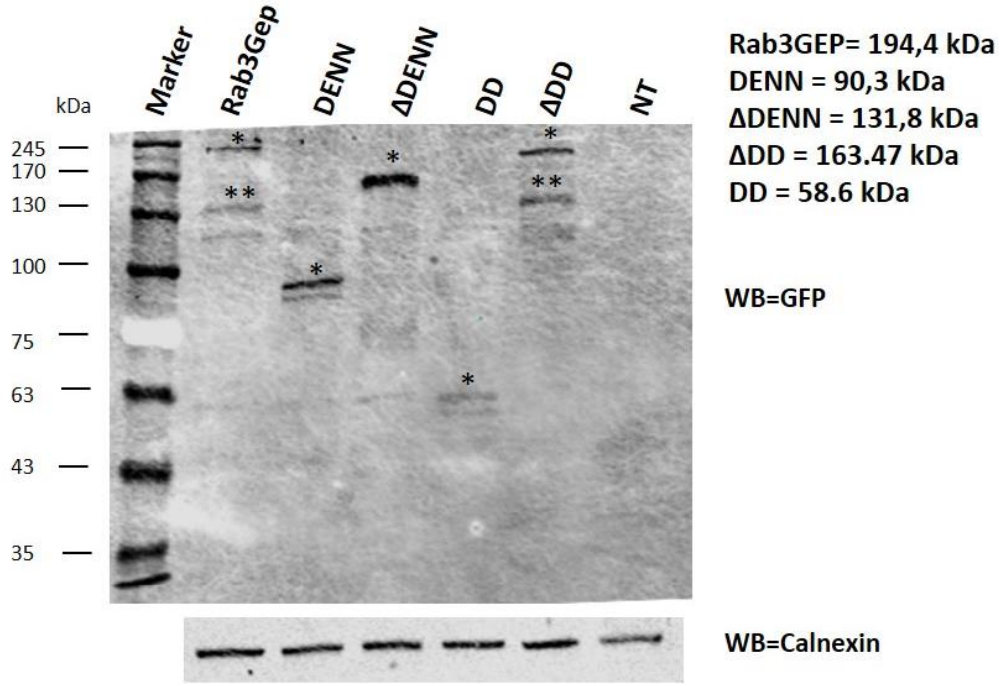
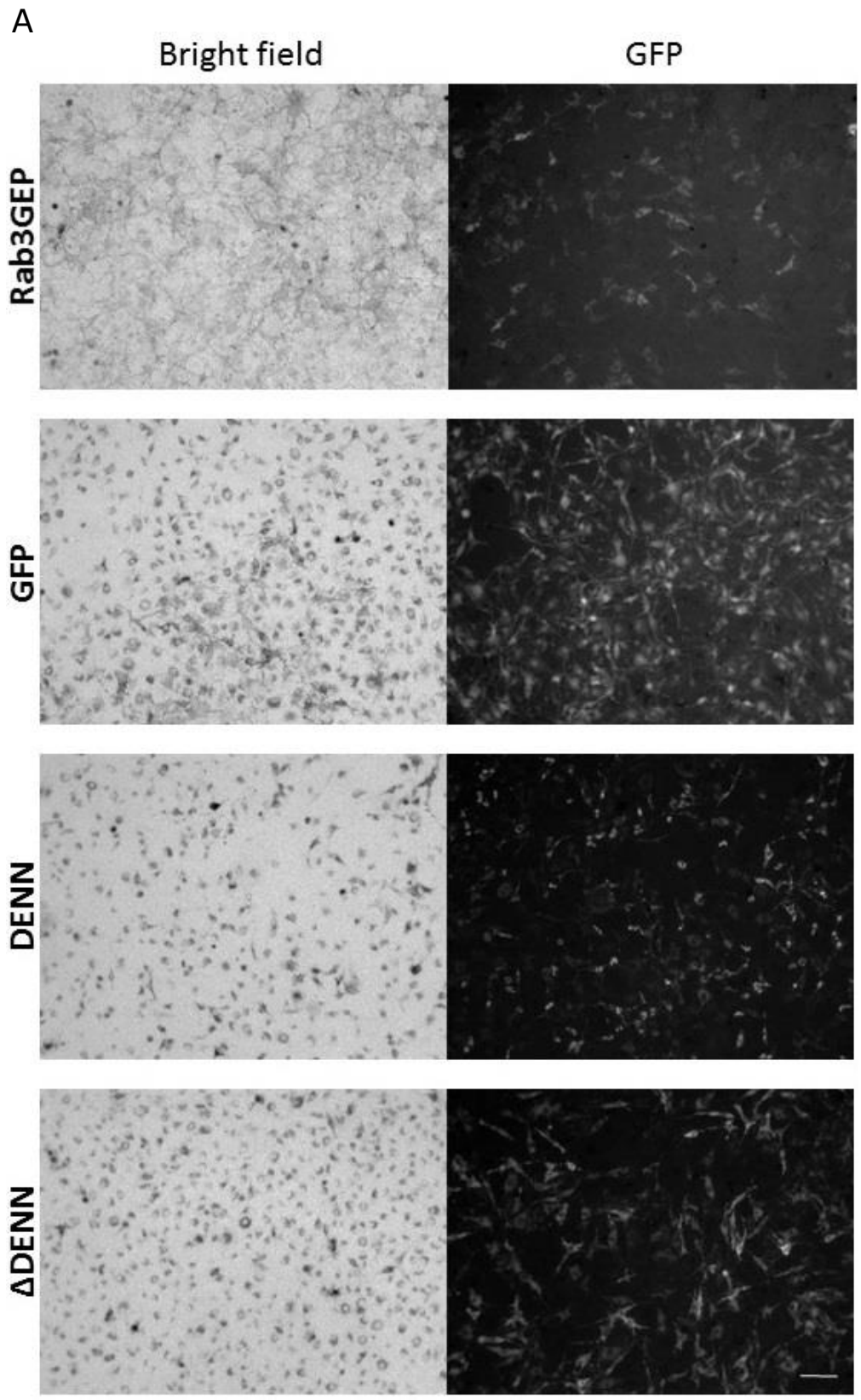
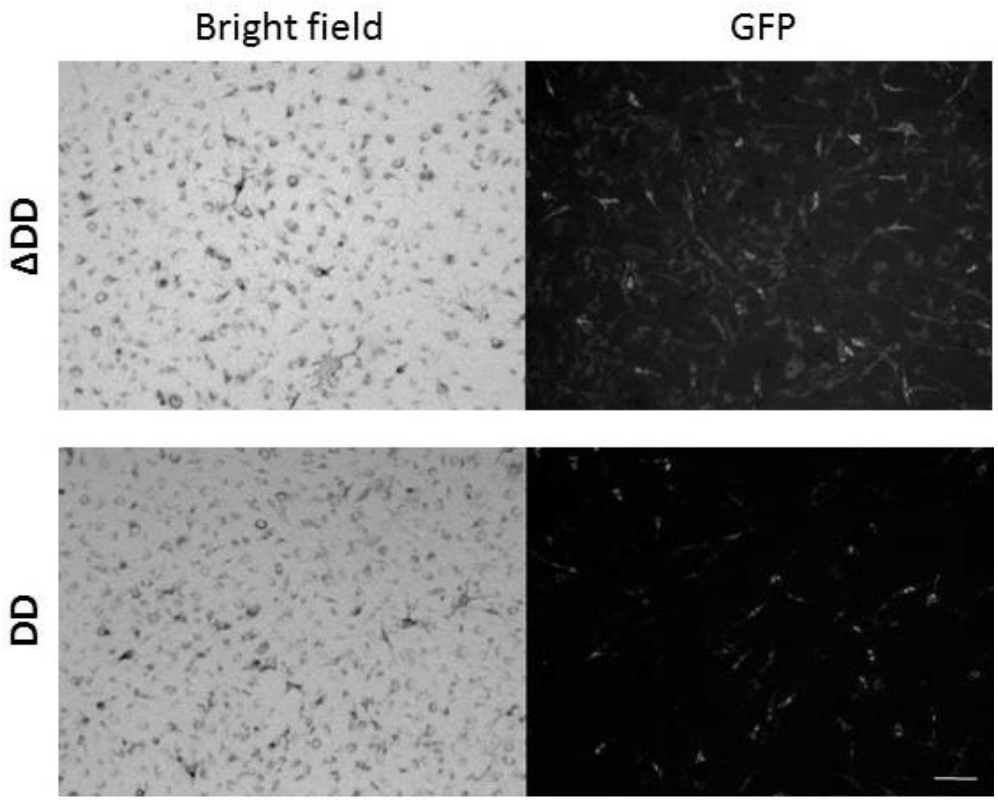


Figure 32 Truncated mutations of Rab3GEP present the predicted molecular weight in melan-Rab3GEP KO cells

melan-Rab3GEP KO cells were infected with adenoviruses expressing the different truncated mutations of Rab3GEP-GFP, 72 hrs later homogenates were loaded on 6%SDS-PAGE gel. Upper panel, immunoblotting performed using anti-GFP antibody. This image shows the expression of the truncated mutants of Rab3GEP. The single asterisk indicates the bands corresponding with the predict molecular weight for each truncated protein. The double asterisk marks the lower bands with the same molecular weight between Rab3GEP and ΔDD. On the top right, predicted molecular weight of the GFP fused proteins. Lower panel loading control immunoblotting with anti-Calnexin (predicted MW= 67kDa)

The Western Blot (Figure 32) indicates that Rab3GEP and the truncation mutants were expressed in melan-Rab3GEP KO cells, nevertheless, no indication was given of their ability to activate Rab27a, or to rescue melanosome distribution in this cell line. To investigate this capacity of the truncation isoforms, melan-Rab3GEP KO cells were imaged after the overexpression of these proteins, and melanosome distribution was investigated (Figure 33).


A
Bright field
GFP
Rab3GEP
GFP
DENN
ΔDENN


Bright field
GFP
ΔDD
DD

B

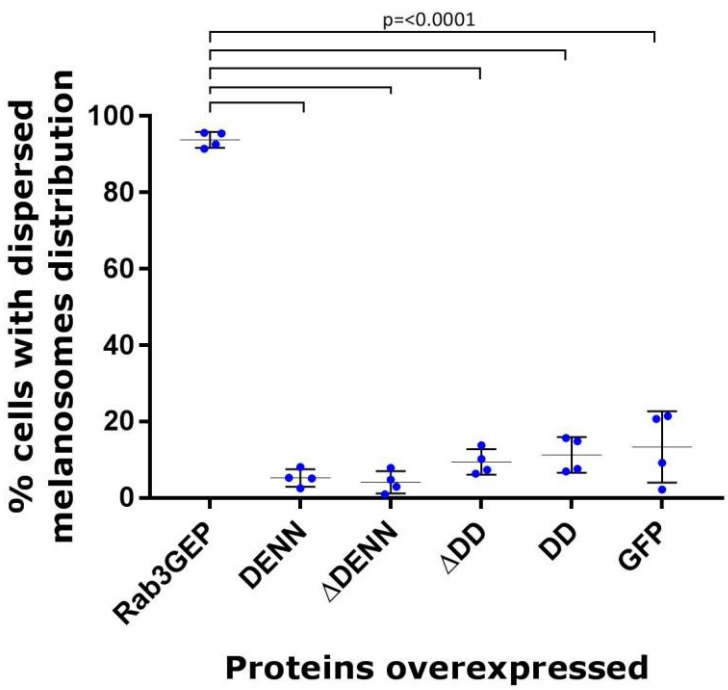


Figure 33 Overexpression of the truncation mutant of Rab3GEP in melan-Rab3GEP KO cells do not rescue melanosome distribution

melan-Rab3GEP KO cells were seeded in a 24 well plate and infected with viruses expressing GFP-Rab3GEP wild type, GFP-DENN, GFP-ΔDENN, GFP-ΔDD, GFP-DD and GFP. A) After two days, cells were fixed and imaged with bright field optics, and GFP emission was detected in the same field. The left panels show bright field images, the right panels show the GFP expression. Scale bar 100 μm. B) 4 pictures were obtained per condition with about 100 cells per picture so with a total of 400 cells. Cells with clustered, dispersed melanosome distribution, and total number of cells were counted, and percentage was obtained

The results indicate that fluorescence intensity of GFP, shown in the right column, is similar for all the truncated mutations and that it is comparable with Rab3GEP full-length protein GFP emission. Only exception is given by the truncation mutant Death domain (DD) were fluorescence intensity of GFP seems to be lower than the other samples, confirming results obtained from the Western blot (Figure 32). Furthermore, overview of the melanosome distribution obtained with the bright-field optics indicate that only Rab3GEP full-length was able to redistribute the melanosome peripherally, while the truncation mutants and GFP alone did not.

In order to quantify the effect of the overexpressed proteins on the melanosome distribution, counting of the number of cells with melanosomes dispersed was performed (Figure 33B).

Results obtained from the quantification of the population of cells with melanosomes dispersed throughout the cell body indicated clearly that the overexpression of the full-length protein rescues the melanosome distribution of 98% of the cells. Instead, the truncation mutants of Rab3GEP do not affect the melanosome distribution given a percentage of cells with disperse melanosomes similar to the GFP negative control.

Summarising, the results of these experiments suggest that although all the adenoviruses produced are able to infect and induce the translation of Rab3GEP full-length or the truncation mutants, with similar level of expression, only Rab3GEP full -length is able to re-distribute melanosomes peripherally.

4.3.1 Visualization of Rab3GEP truncations in melan-Rab3GEP KO cells with high magnification

In the previous section, it has been established that overexpression of the truncation mutants of Rab3GEP proteins did not rescue melan-Rab3GEP KO cells, and melanosomes remained perinuclear. However, this result was gained from images with low magnification obtained with a 4X objective, which allowed to analyse a consistent number of cells, but on the other hand, it gives back a poor accuracy on the determination of the cells effectively expressing the GFP labelled proteins. Hence, in order to look for subtle effects of expression of the protein, more sensitive methods were used. As a first step, same experiment with the truncation mutants performed in section 4.3 was repeated, and confocal microscopy was used to acquire images of melanosome and GFP distribution of Rab3GEP and its truncation mutants (Figure 34).

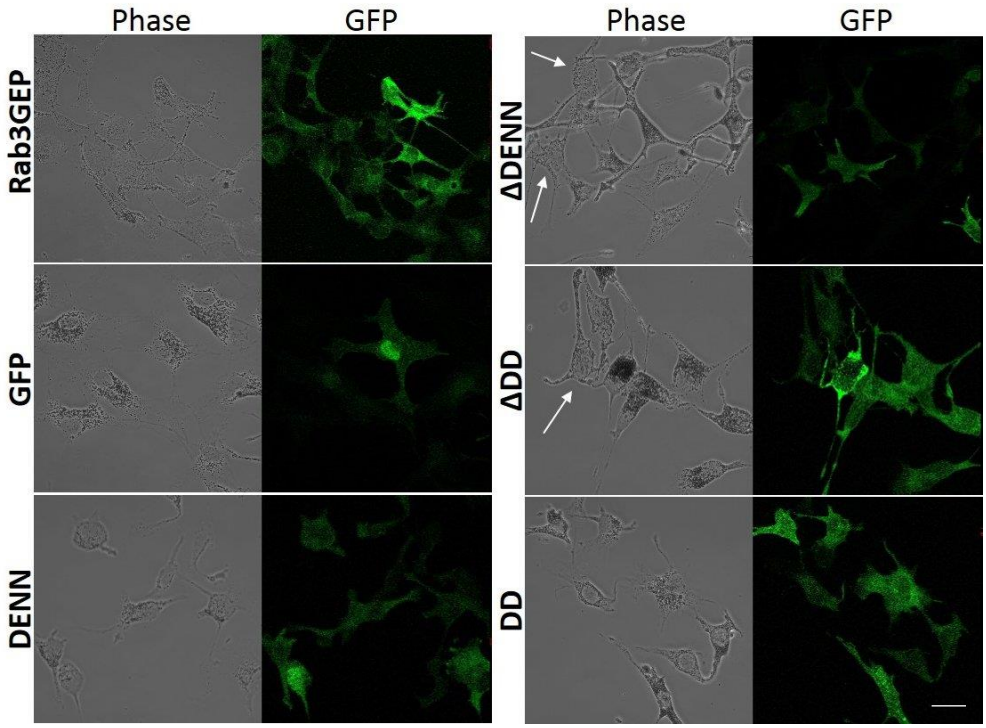


Figure 34 High magnification images of in melan-Rab3GEP KO cells expressing GFP-labelled truncated mutants of Rab3GEP

melan-Rab3GEP KO cells were seeded on glass coverslips and infected with adenoviruses expressing the different truncated mutants of GFP-Rab3GEP. After 72 hrs, cells were fixed and imaged using confocal microscopy. This picture shows the expression of the Rab3GEP full length, GFP alone as controls and the different truncated isoforms of Rab3GEP.White arrows indicate cells with dispersed melanosome distribution. All these images are in scale 20μm

The images obtained from the confocal microscopy (see Figure 34) reveal that Rab3GEP full-length restores the dispersed melanosome distribution, and that cells expressing GFP alone maintain the clustered distribution of melanosomes at the perinuclear region as predicted. The truncation mutants of Rab3GEP were expressed in cells as indicated by the GFP signal. Phase images showed that these proteins were not able to re-distribute the melanosomes toward the cell periphery. Nonetheless, there were inconsistencies in the outcomes such as some cells presented rounded shape like in the sample overexpressing DENN truncation mutant, or in the samples overexpressing ΔDENN and ΔDD there were few cells with dispersed melanosome distribution as shown by arrows.

As seen in chapter 3 and in data shown in Appendix 7.1, 7.2, melan-Rab3GEP KO cells show a mixed phenotype, therefore, the disperse melanosome distribution displayed in some cells might be due to the constitutive presence

of cells with this phenotype rather than the rescue activity of the truncation mutants ΔDENN and ΔDD.

The ambiguity of the results obtained did not help us to clarify which mutants of Rab3GEP protein were able to rescue melanosome distribution. In fact, the presence of outlier results and the lack of quantification to support the findings did not allow the comparison of the outcomes. Therefore, micropattern chip was used to assess melanosome distribution (see section 4.3.2).

4.3.2 Analysis of the function of truncated Rab3GEP proteins using micropattern chip

In the previous experiment (sections 4.3.1), the variability of the cell shape makes difficult to establish the distance travelled by the melanosomes from the perinuclear cytoplasm. Therefore, it makes difficult to obtain statistical quantification and comparison between group of cells treated with different truncation mutants. For this purpose, micropatterns chip has been used, this system permits to standardize the cell shape in the x/y plane, in fact it is made by circular fibronectin patterns with area of 1600 μm^2 printed on cytophobic glass coverslip. Melanocytes seeded on the micropattern are able to adhere to the fibronectin but their shape is limited by the area occupied by this glycoprotein, which is circular. Hence, melanocytes body cover the same area with circular shape, the nucleus is located near the center and the melanosomes are spread around it.
The use of micropattern chip has allowed more precise quantification of the melanosome distribution in each cell compared to the free growing cells. Also, image acquisition and quantification could be carried out in an automated manner, facilitating stringent analysis of organelle distribution in large number of cells.

Figure 35 shows examples of two melan-Rab3GEP KO cells overexpressing Rab3GEP or GFP proteins. The right panels show the GFP fluorescence expression, which allow to discriminate cells expressing the exogenous proteins from cells not infected by the viruses, and the level of expression. In phase contrast images, it is possible to see melanosome distribution. These are dispersed throughout the cell body, reaching the cell periphery in the cell overexpressing Rab3GEP protein. Instead the cell overexpressing GFP presented the pigmented granules mainly clustered around the nucleus. Therefore, these two overexpressed proteins have different outcomes which lead to two different melanosome distributions, which can be measured by the distance travelled by the melanosomes from the cell center to the periphery throughout micropattern chip.

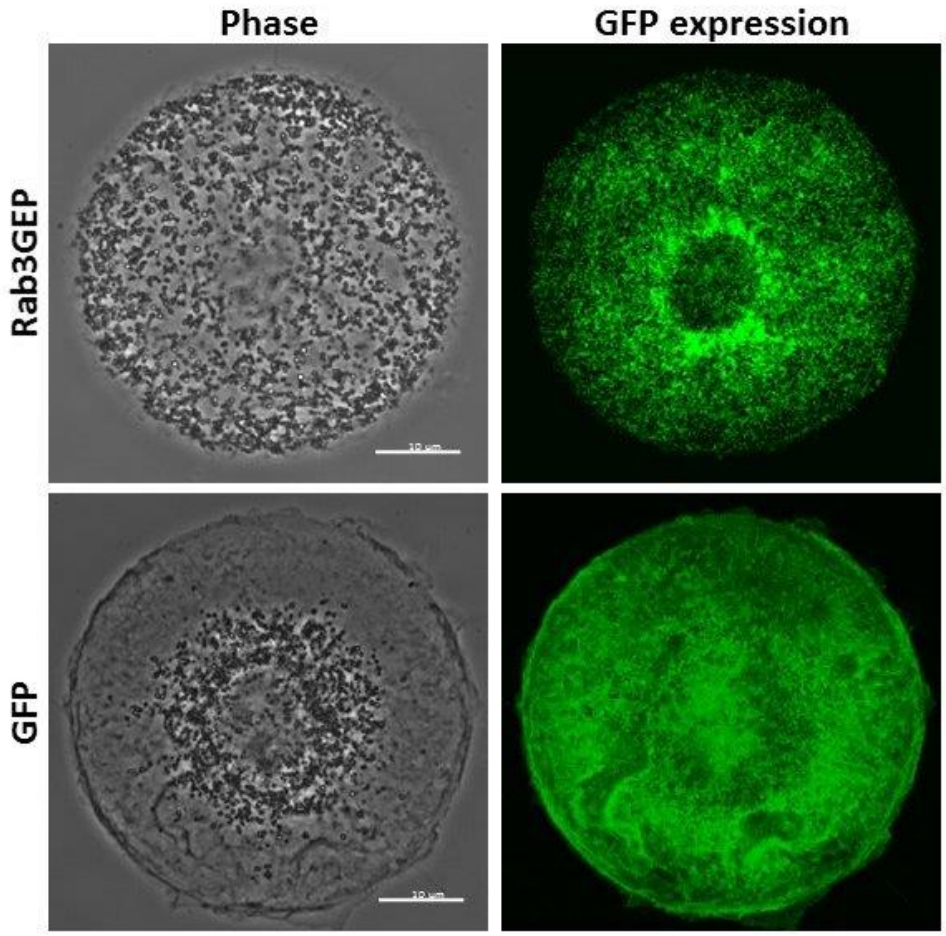


Figure 35 Melanosome distribution in GFP-Rab3GEP and GFP expressing melan-Rab3GEP KO cells grown on micropattern substrates

melan-Rab3GEP KO cells were infected for 48hrs with adenoviruses expressing GFP-Rab3GEP and GFP, then cells were harvested and seeded on micropattern chip and left overnight before fixation. The left column shows the phase contrast images in which is possible to see the melanosome distribution. The second column shows the GFP expression. Scale bar 10μm

Hence, efficiency of the truncation mutants of Rab3GEP on activating the melanosome trafficking could be determined overexpressing these proteins in melan-Rab3GEP KO cells, seeding them on micropattern chip, and defining the average of the distance covered by the melanosomes from the perinuclear cytoplasm. Two methods were used to describe the melanosome distribution in cells overexpressing the truncation mutants of Rab3GEP and seeded on micropattern chip: 1) Average pigment distribution map displays the probability of finding melanosomes in a given localisation in each cell within a test population and 2) Pigment dispersion distance (PDD) for each cell within a population, which indicates numerically the melanosome distribution permitting comparison between the different conditions (Figure 36).

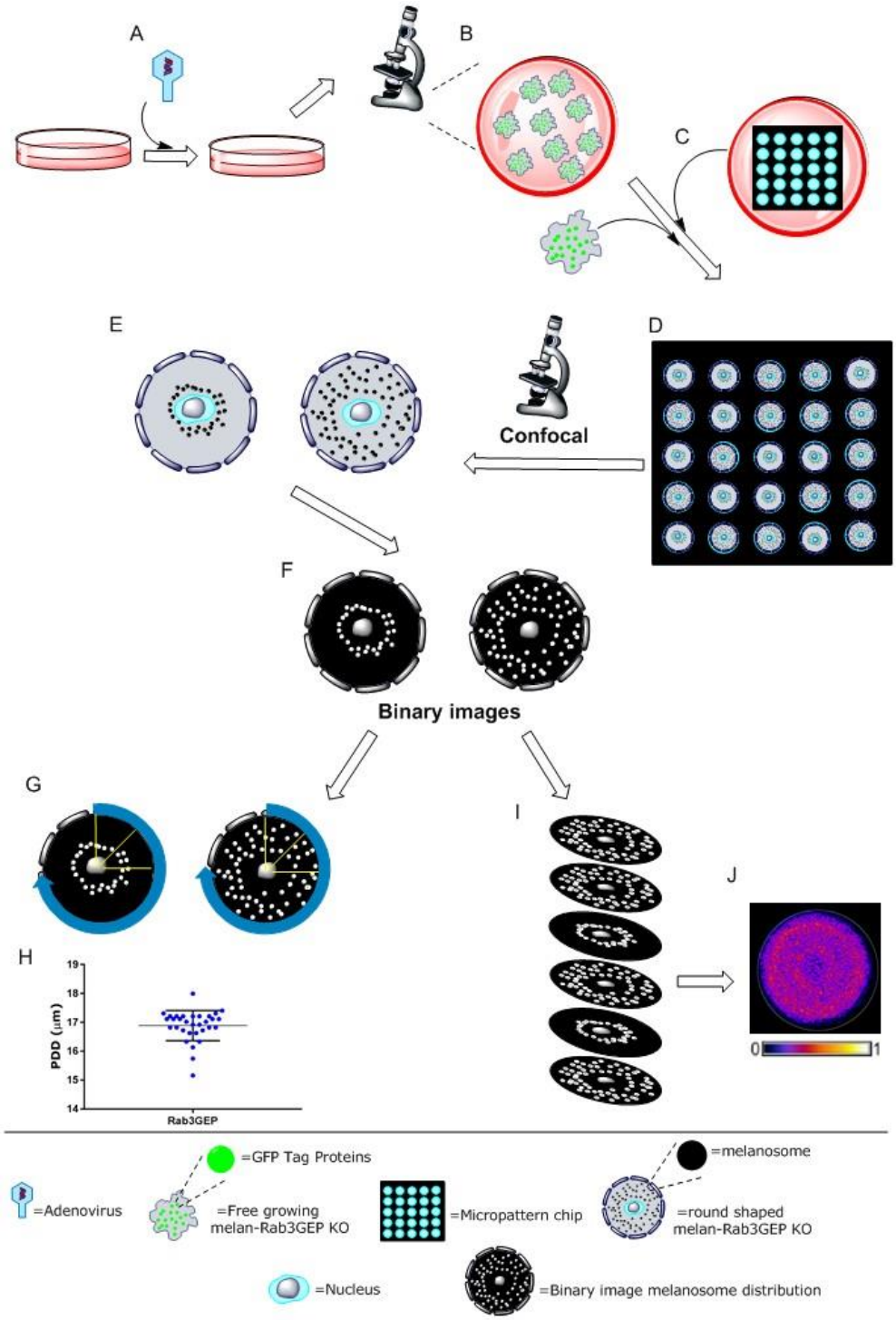


Figure 36 Schematic representation of micropattern chip analysis

A) Free growing cells were infected with adenoviruses. B) detection of GFP emission. C) cells harvested and re-seeded on micropattern chip. D) cells on micropattern. E) schematic representation of cells on disk with clustered or dispersed melanosome distribution as seen by confocal microscopy F) images of pigment inverted and binary images of melanosome distribution. G) Pigment dispersion distance (PDD) for each cell (distance travelled by melanosomes from the cell center to cell periphery) H) PDD for each cell within a population. I) Overlapping of melanosomes map of each cell. J) Probability map showing melanosome distribution in population of cells see M&M.

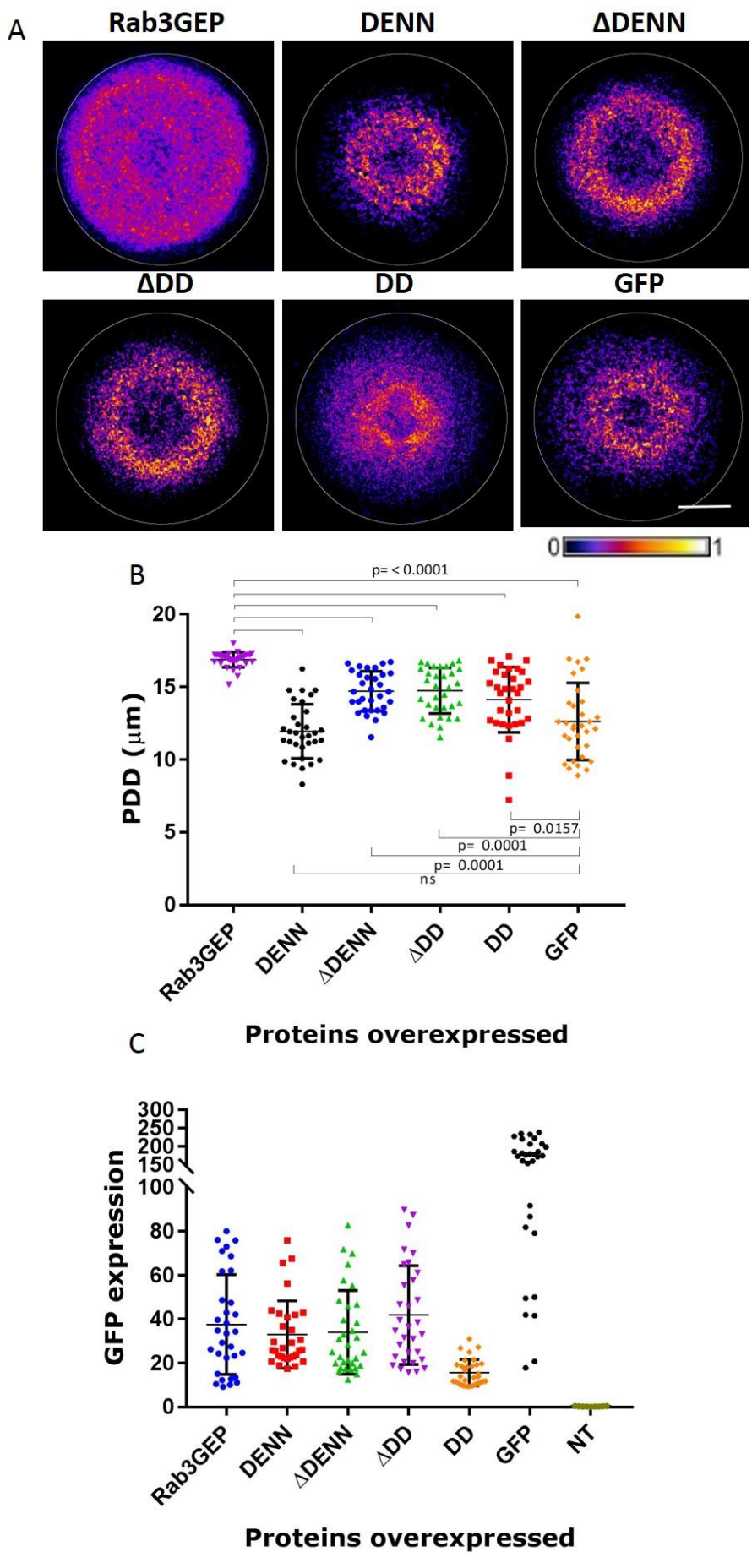

A
Rab3GEP
DENN
ΔDENN
ΔDD
DD
GFP
0
1
B
p= < 0.0001
PDD (μm)
20
15
10
5
0
p= 0.0157
p= 0.0001
p= 0.0001
ns
Rab3GEP
DENN
ΔDENN
ΔDD
DD
GFP
Proteins overexpressed
C
GFP expression
300
250
200
150
100
80
60
40
20
0
Rab3GEP
DENN
ΔDENN
ΔDD
DD
GFP
NT
Proteins overexpressed

Figure 37 Truncation of Rab3GEP lose the ability to disperse melanosomes toward the cell periphery

melan-Rab3GEP KO cells were infected with adenoviruses expressing GFP-Rab3GEP, GFP-DENN, GFP-ΔDENN, GFP-ΔDD, GFP-DD and GFP, after 48hrs harvested and seeded on micropattern chip and allowed to spread overnight before fixing. Thirty-five cells for each condition were imaged using confocal microscope. Therefore, images were analyzed using ImageJ. A) Look up table [LUT] images show the melanosome distribution where black=0% and white=100% probability of finding melanosomes. These images have been obtained creating a binary mask of the melanosomes for each cell and then overlaying these images in order to obtain the average pigment map. The white circle indicates the border of the micropattern (diameter =46μm). Scale bar 10μm B) Scatterplots showing the PDD (pigment dispersion distance) for each cell (dot) within a population overexpressing adenoviruses. One way ANOVA multiple comparisons was used to determine p value. C) Scatterplots showing the fluorescence intensity obtained from GFP tag for each cell within each condition examined, Arbitrary unit was assigned to *y* axis.

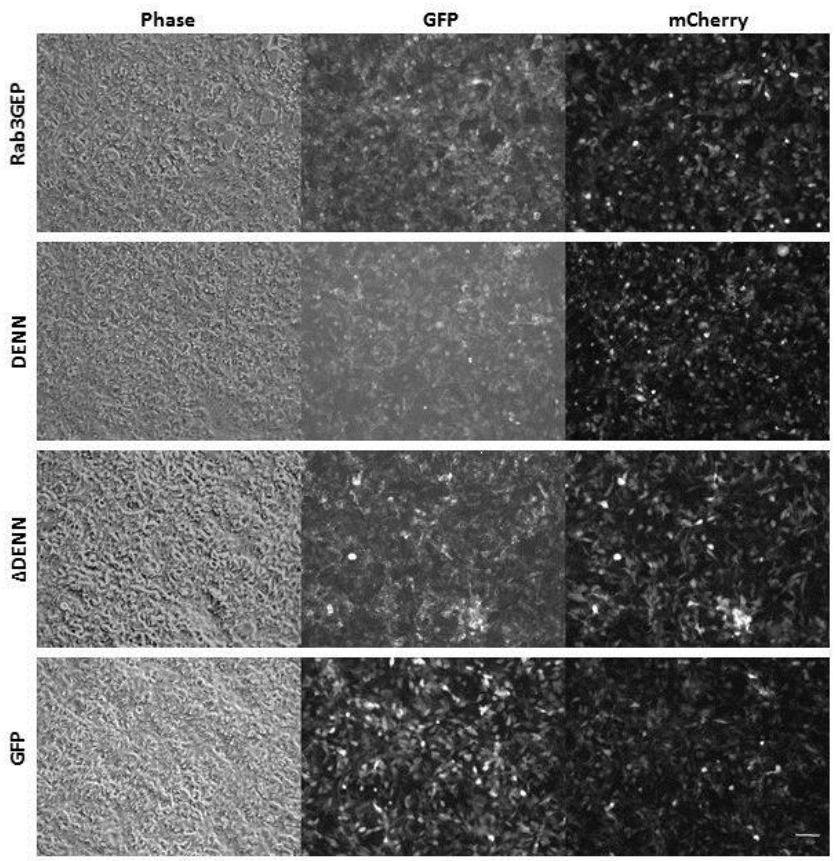
Images obtained from the micropattern were processed using ImageJ software (see Materials and Methods) and the results are shown in Figure 37. Comparison between the different truncation mutants with the Rab3GEP full length indicates clearly that none of the truncations has the same ability of Rab3GEP to rescue melanosome distribution (Figure 37A-B) Pigment dispersion distance (PDD) (Figure 37 B) confirmed what was observed in the previous sections of these chapters (4.3 and 4.3.1), namely that overexpression of Rab3GEP increase the mobility of the pigmented granules in cells examined (mean PDD = 16.89 ± 0.5225 μm), instead the truncation mutants are not functional as Rab3GEP full-length. Although the DENN domain has been considered as a GEF domain, it has no effect on the PDD with mean similar to GFP (DENN mean PDD = 11.94 ± 1.859 μm; GFP mean PDD = 12.63 ± 2.648 μm). The other three truncation mutants examined are all statistically significant different from Rab3GEP full-length ($p=<0.0001$). Nevertheless, comparison between these truncations and GFP might have partial function based on PDD data. Their mean is higher than GFP (ΔDENN mean PDD = 14.71 ± 1.369 μm, ΔDD mean PDD = 14.74 ± 1.573 μm, DD mean PDD = 14.13 ± 2.257 μm), and statistical analysis *versus* GFP indicate a P value=0.0001 for ΔDENN and ΔDD, and P value=0.0157 for DD. The scatter blot in the graph C shows that the cells examined had all a level of expression of GFP signal higher than the cells not treated. Micropattern chip assay has confirmed the original observations, pointing out that although Rab3GEP protein is able to rescue the melanosome distribution in melan-Rab3GEP KO cells, its truncation mutants do not have the same ability of Rab3GEP full length and melanosomes remain mainly at the perinuclear area.

4.3.3 Truncated mutants of Rab3GEP are not able to activate Rab27a

Truncation mutants of Rab3GEP protein are not able to rescue the melanosome distribution, consequently clustering around the nucleus is observed after their overexpression in melan-Rab3GEP KO cells. Nevertheless, previous experiments (see sections 4.3, 4.3.1 and 4.3.2) do not explain the reason of the failure of activity of these truncation mutants. Rab3GEP has been identified as crucial protein for melanosome distribution because it is recognised as the GEF of Rab27a protein and is required for Rab27a targeting to melanosome membrane.

To investigate in more detail the GEF activity of the truncation mutants a biochemical approach was used. GST-pull-down assay was performed to determine the capacity of the Rab3GEP and truncations to catalyse GDP/GTP exchange on Rab27a. Reasoning that Rab27a in the active state binds Slp1 effector, the bound fraction of Rab27a incubated with GST-Slp1 in the pull-down assay was used as a read out of the functionality as a GEF of the truncation mutants. This approach has allowed comparison of the GEF activity of Rab3GEP with DENN domain and ΔDENN domain and in parallel with ΔDD and DD.

HEK293a cells were co-infected with adenoviruses expressing mCherry-Rab27a and either GFP-Rab3GEP (wild type or mutant) or GFP alone. The day after GFP and mCherry expression was confirmed by fluorescence microscopy (Figure 38).


Phase
GFP
mCherry
Rab3GEP
DENN
ΔDENN
GFP

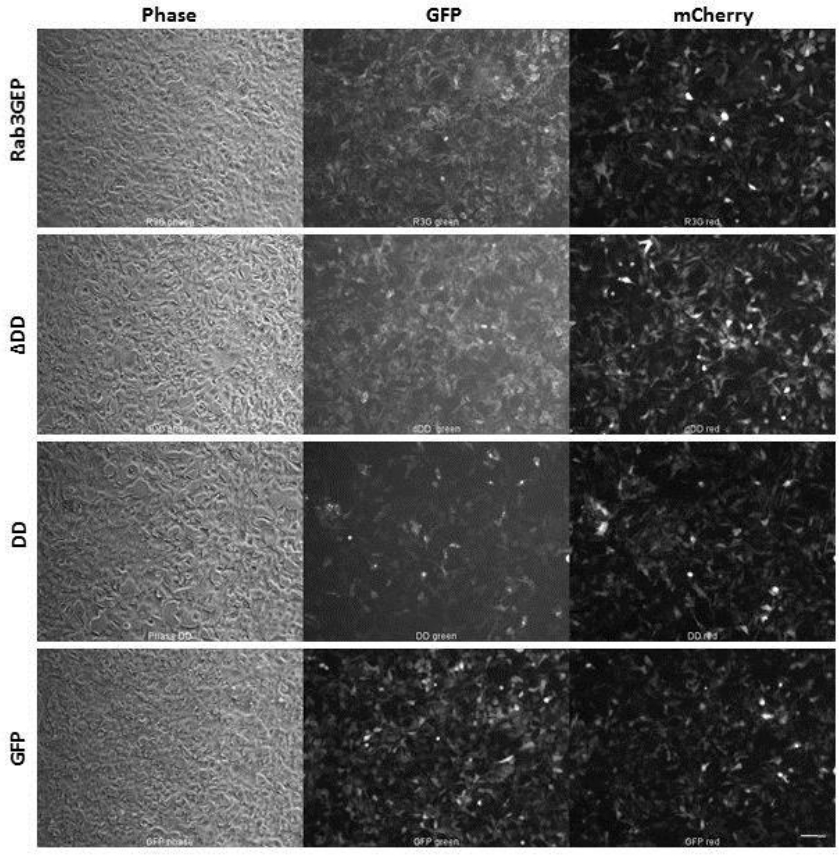
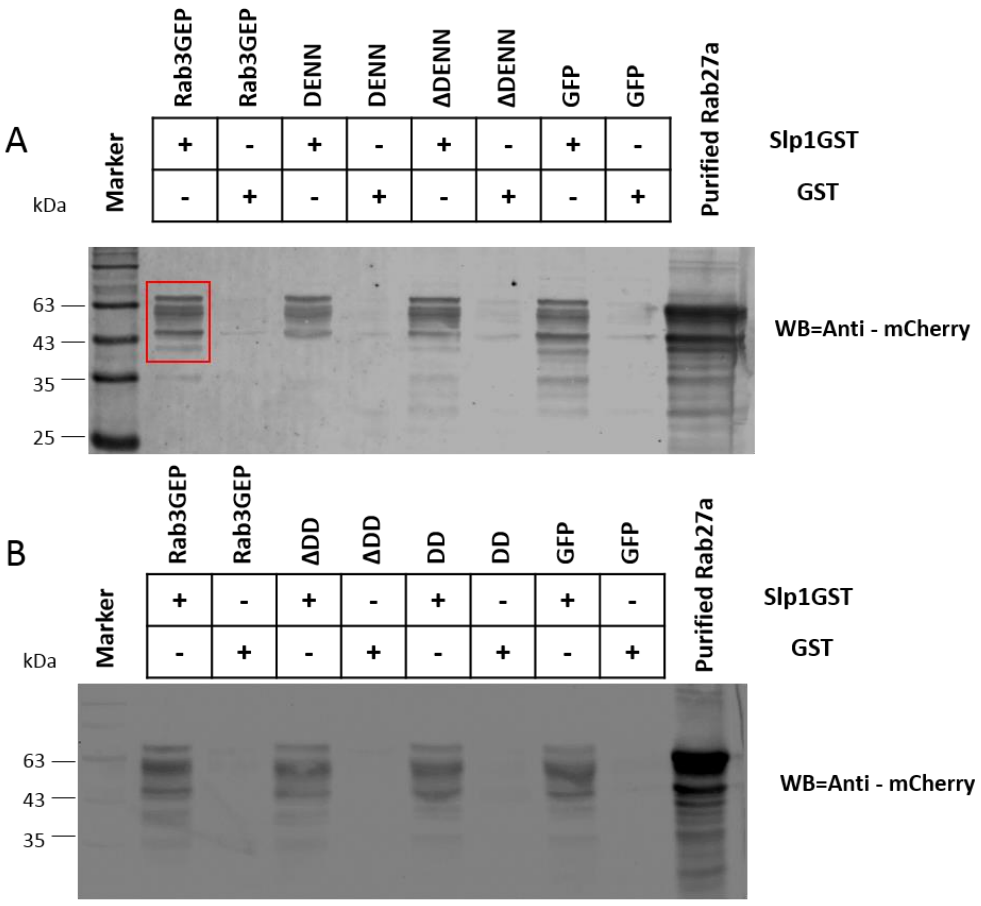

Phase
GFP
mCherry
Rab3GEP
ΔDD
DD
GFP

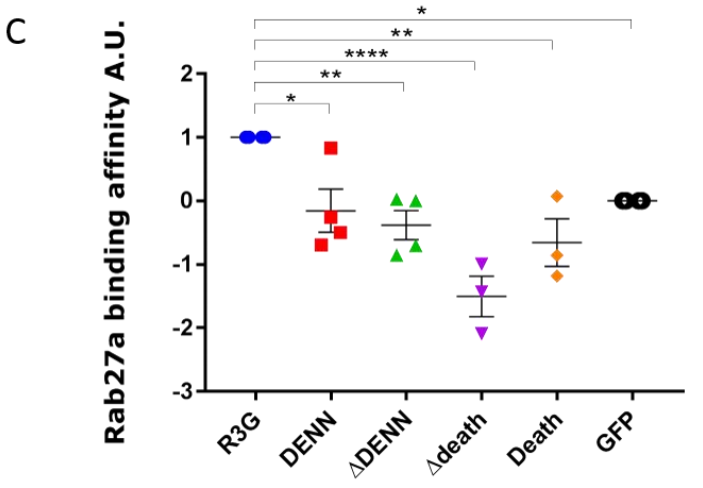
Figure 38 GFP expression truncation isoforms of Rab3GEP and their controls full-length and GFP, and expression level of Rab27a between all the samples

HEK293a cells were seeded in 10cm Petri dishes, when cells were confluent, were co-infected with mCherry-Rab27a and either one of the truncation isoforms of Rab3GEP, Rab3GEP full-length or GFP. Then left overnight to express the proteins. The day after cells were imaged with phase contrast, and fluorescence of mCherry and GFP Tags was detected. Scale bar 100 μm

In Figure 38 it is shown that HEK293a cells were expressing GFP and mCherry tagged proteins in all the combination used. Then, pull-down of Rab27a was performed (schematic representation in Figure 29) (Materials and Methods).

The Western blot shows that GST-Slp1 protein, but not GST, was specifically able to bind Rab27a (Figure 39 A and B). In all the samples incubated with GST-Slp1 it was possible to notice bands at 63kDa which matched with the purified protein mCherry-Rab27a used as positive control. Moreover, in each sample, it was possible to see bands with lower molecular weight between 63-43kDa, which I hypothesised that are products of the cleavage of Rab27a, in fact they are present even in the purified Rab27a. Nevertheless, it is possible to see that sample with Rab3GEP full-length shows more intense band of mCherry-Rab27a, compared to DENN and ΔDENN in A and ΔDD and DD in B and that it is more intense than GFP alone. This suggests a higher GEF activity in the sample with the full-length and lower activity for the others.
This experiment was performed 4 times and in order to quantify the results obtained measuring the intensity for each band was performed using ImageJ and normalization was performed (Figure 39C).


A
Rab3GEP
Rab3GEP
DENN
DENN
ΔDENN
ΔDENN
GFP
GFP
Purified Rab27a
Marker
kDa
Slp1GST
GST
63
43
35
25
WB=Anti - mCherry
B
Rab3GEP
Rab3GEP
ΔDD
ΔDD
DD
DD
GFP
GFP
Purified Rab27a
Marker
kDa
Slp1GST
GST
63
43
35
WB=Anti - mCherry


C
Rab27a binding affinity A.U.
2
1
0
-1
-2
-3
*
**
****
**
*
R3G
DENN
ΔDENN
Δdeath
Death
GFP

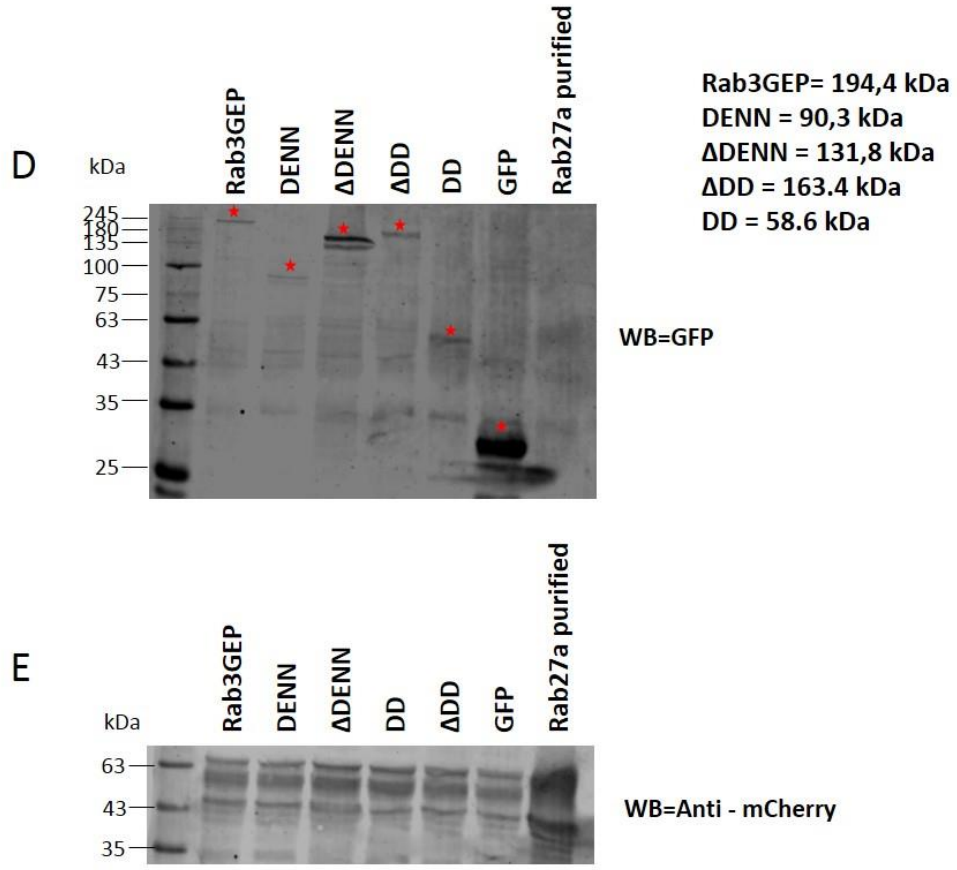


Figure 39 Truncation isoforms of Rab3GEP are not able to activate Rab27a

HEK293a cells were infected with adenoviruses expressing mCherry-Rab27a and either truncated GFP-Rab3GEP proteins, GFP-Rab3GEP, or GFP. Then left overnight to express the proteins. A-B) Cell lysates were incubated with either GST-Slp1 or GST in presence of glutathione-beads and left overnight. Therefore, supernatant was washed out and bound fraction was loaded in a 10% SDS-Page gel, transferred in membrane, and mCherry-Rab27a was detected by with anti-mCherry antibody. C) Quantification Rab27a binding affinity after 4 independent experiments, quantification bands performed with ImageJ and normalized. Red box indicates the area that was quantified, same field for all the samples, statistical analysis asterisk indicate significance (*<****) D-E) Immunoblotting of 25 µg of the crude lysates using anti-GFP and anti-mCherry antibodies.

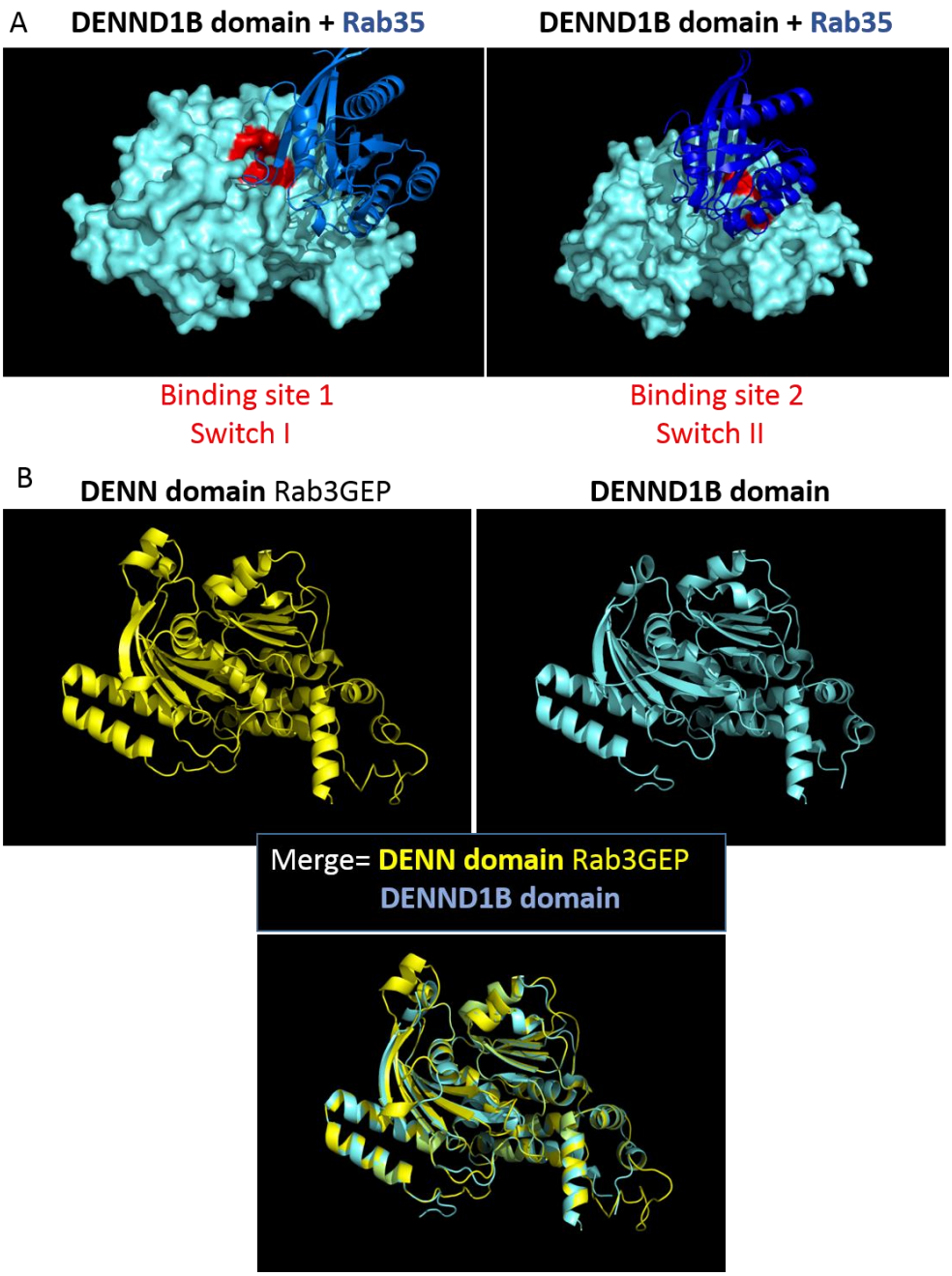
Quantification of results obtained indicate that none of the truncation mutant of Rab3GEP full-length was able to activate Rab27a. In fact, the mean of Rab3GEP was 1, instead the mean of DENN, ΔDENN, ΔDD and DD were lower respectively -0.1552, -0.3805, -1.504, -0.6557, hence, with results similar to the control GFP (mean=0) (Figure 39C). Furthermore, statistical analysis indicate that all the truncation mutants are statistical different than Rab3GEP full length. In one experiment the sample with overexpression of DENN truncation has higher level compared to the other set of experiments, nevertheless it did not reach Rab3GEP level. Instead, the samples overexpressing ΔDD truncation presented lower levels of active Rab27a than

GFP, indicating that they inhibit endogenous Rab3GEP activity. Western blot in D shows Rab3GEP full-length, GFP and the truncation mutant expression proteins in 25µg of the lysates. Band intensity indicates that they were all expressed with similar level, except for ΔDENN which band seems to be more intense than the other truncation mutants. Finally, Rab27a level is shown in E and it seems to be expressed equally between the samples.

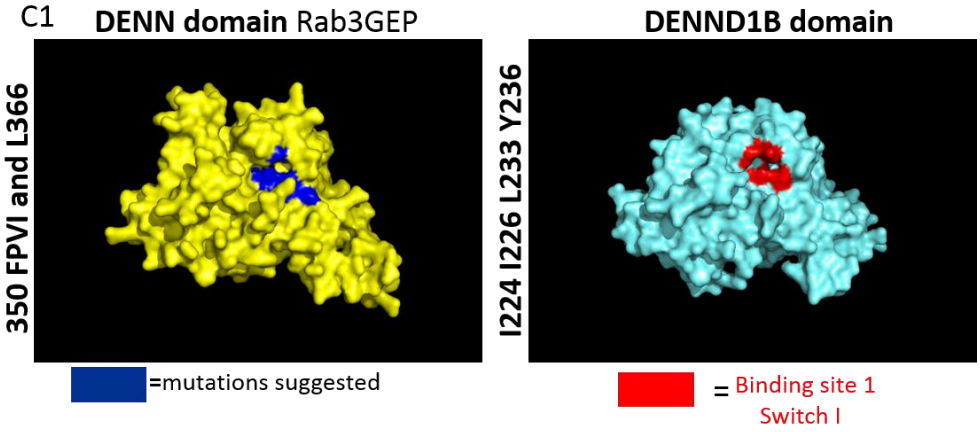
Although the DENN domain of Connecdenn-2 has been suggested to have GEF activity towards Rab35, our results do not support this for Rab27a. Based on the data obtained in our experiments is possible to conclude that Rab3GEP protein full-length is able to function as a GEF and rescue melanosome distribution, but none of the truncation mutants tested were able to do so.

4.4 Expression of point Rab3GEP mutant in melan-Rab3GEP KO cells

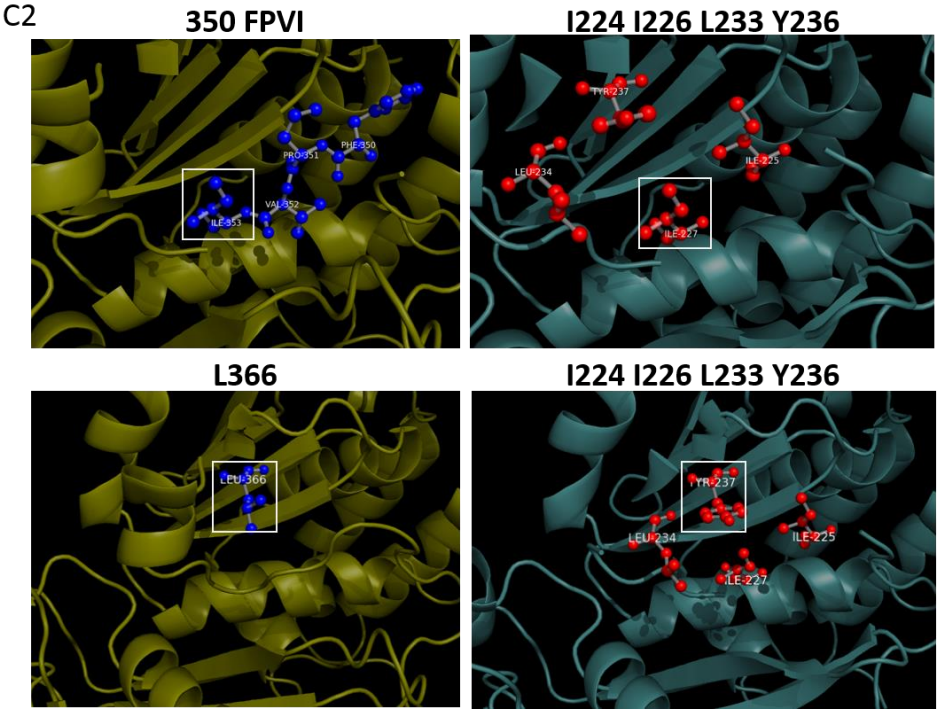
Considering that it has been suggested that DENN domains are crucial for the GEF activity, and its importance in the Rab3GEP activation, another aim of this project was to investigate the mechanism of action of the DENN domain of Rab3GEP and to determine whether this domain works with a similar mechanism of DENND1B. Xudong Wu et al. (2011) (46) after structuring the DENN domain of Connecdenn-2 in complex with Rab35 have identified some crucial amino acids within the DENN domain that allow interaction with its cognate. The authors of this research suggest that DENND1B binds the switch regions I and II of Rab35. Moreover, they suggest that the GEF activity of DENND1B requires these interactions, in fact replacement of crucial residues within the binding sites of the DENN domain causes the loss of the GEF activity. Based on this study, our collaborator Dr. Aymelt Itzen (Technical University of Munich, Germany) has modelled the DENN domain of Rab3GEP, and point mutations in Rab3GEP (DENN domain) were suggested that matched in the 3D model with the binding sites of DENND1B for the Rab35. Hence, these point mutations were made in Rab3GEP, in positions corresponding to the essential residues in DENND1B (Figures 40-41). The suggested mutations included the binding sites I and II, which interacts respectively with the switch I and II of Rab35. The amino acids F350 P351 I353 (350 FPVI) and L366 in the DENN domain of Rab3GEP correspond to I224 I226 L233 Y236 in DENND1B and are present in the binding site I. Instead, the amino acids T371 P372 in Rab3GEP are directly correspondent to M241 P242 in DENND1B, which in combination with the amino acid Q360 represent the binding site II (Figure 40).


A
DENND1B domain + Rab35
DENND1B domain + Rab35
Binding site 1
Switch I
Binding site 2
Switch II
B
DENN domain Rab3GEP
DENND1B domain
Merge= DENN domain Rab3GEP
DENND1B domain

C1


DENN domain Rab3GEP
DENND1B domain
350 FPVI and L366
I224 I226 L233 Y236
=mutations suggested
= Binding site 1
Switch I

C2


350 FPVI
I224 I226 L233 Y236
PHE-350
PRO-351
VAL-352
ILE-353
TYR-237
LEU-234
ILE-225
ILE-227
L366
I224 I226 L233 Y236
LEU-366
TYR-237
LEU-234
ILE-225
ILE-227

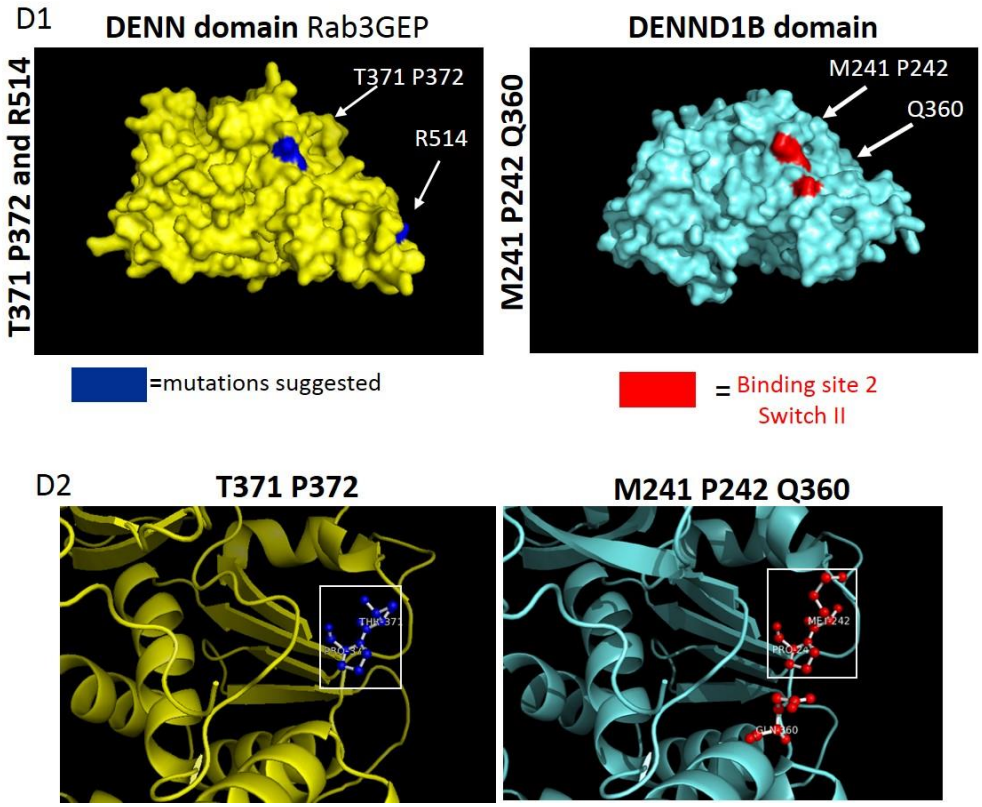


Figure 40 3D model of DENN domain of Rab3GEP based on DENND1B and point mutations

A) Representation of DENND1B (cyan surface structure) and Rab35 (blue cartoon structure) and the binding sites 1 and 2 of DENND1B (red) (Wu et al (46) 3TW8.pdb). B) DENN domain of Rab3GEP (yellow) modelled as DENND1B (cyan) and merge (bottom). C1) 350 FPVI and L366 (blue) suggested amino acids with equivalent 3D position of DENND1B binding site I (red). C2) Magnification amino acids position in the 3D structure, white box indicates exactly same position in DENN of Rab3GEP and in DENND1B. D1) T371 P372 (blue) suggested amino acids with equivalent 3D position of DENND1B binding site II (red), and R514 ((blue) one more change in DENN domain. D2) Magnification T371 P372 amino acids position in the 3D structure, white box indicates exactly same position in DENN of Rab3GEP and in DENND1B

Reasoning that DENN domains present highly conserved amino acids within the family (146), and that the conserved residues are assumed to have important function, mutation of them could help to test the importance of the DENN domain in Rab3GEP function. For this purpose, it was chosen the amino acids R37 Y38 and P354 L355 L356 P357 (354 PLLP) which are highly conserved. Moreover, a mutation in the downstream DENN domain in the position R514 was made with the aim of having a negative control. Schematic representation of the location of the mutation and changed performed are shown in Figure 41. GFP-tag was added at the N-terminus of these mutants of Rab3GEP. Moreover, another positive control of the

Rab3GEP activity was made using GFP-Rab3GEP full-length with a 6xHis tag at the N-terminus of GFP.

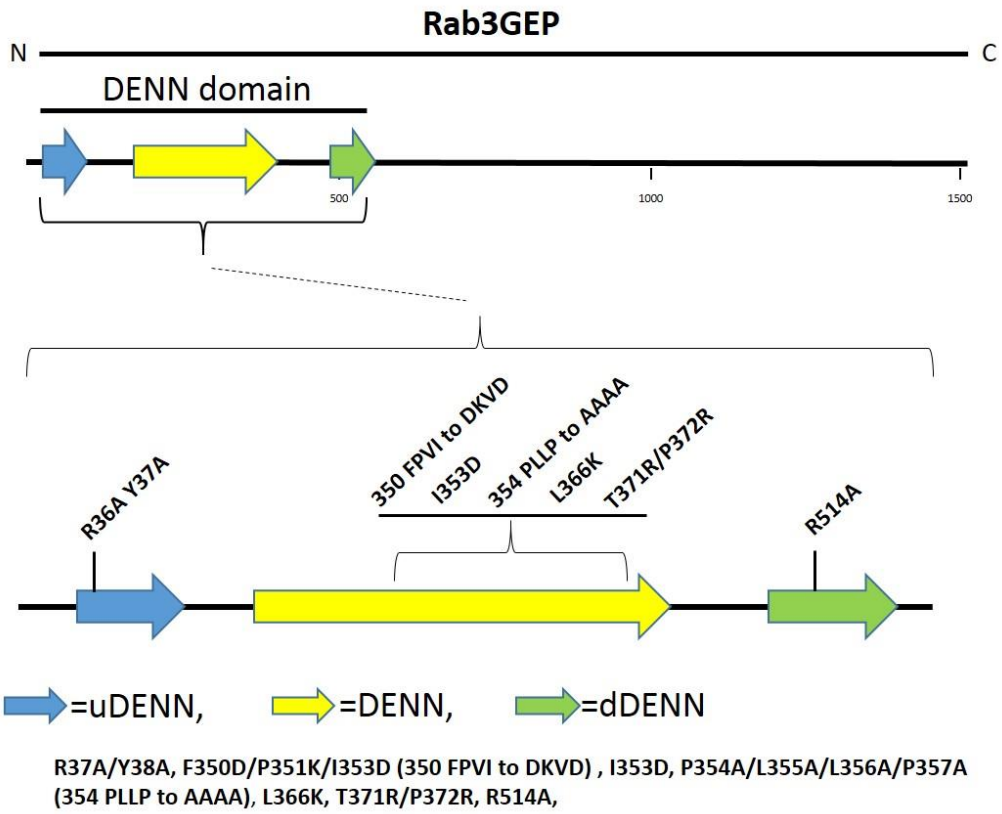


Figure 41 The location of point mutations in Rab3GEP protein

This schema shows the location of the point mutations made in Rab3GEP protein. Mutations are in the DENN domain. All the mutations have been made in the core of DENN domain, except for R37A Y38A and R514A which are in upstream DENN (uDENN) and downstream DENN (dDENN) respectively.

Firstly, in order to determine the integrity of the new made point mutation proteins, HEK293a cells were infected with adenoviruses encoding the point mutations protein and the expression was detected by immunoblotting using antibody raise against GFP (Figure 42).

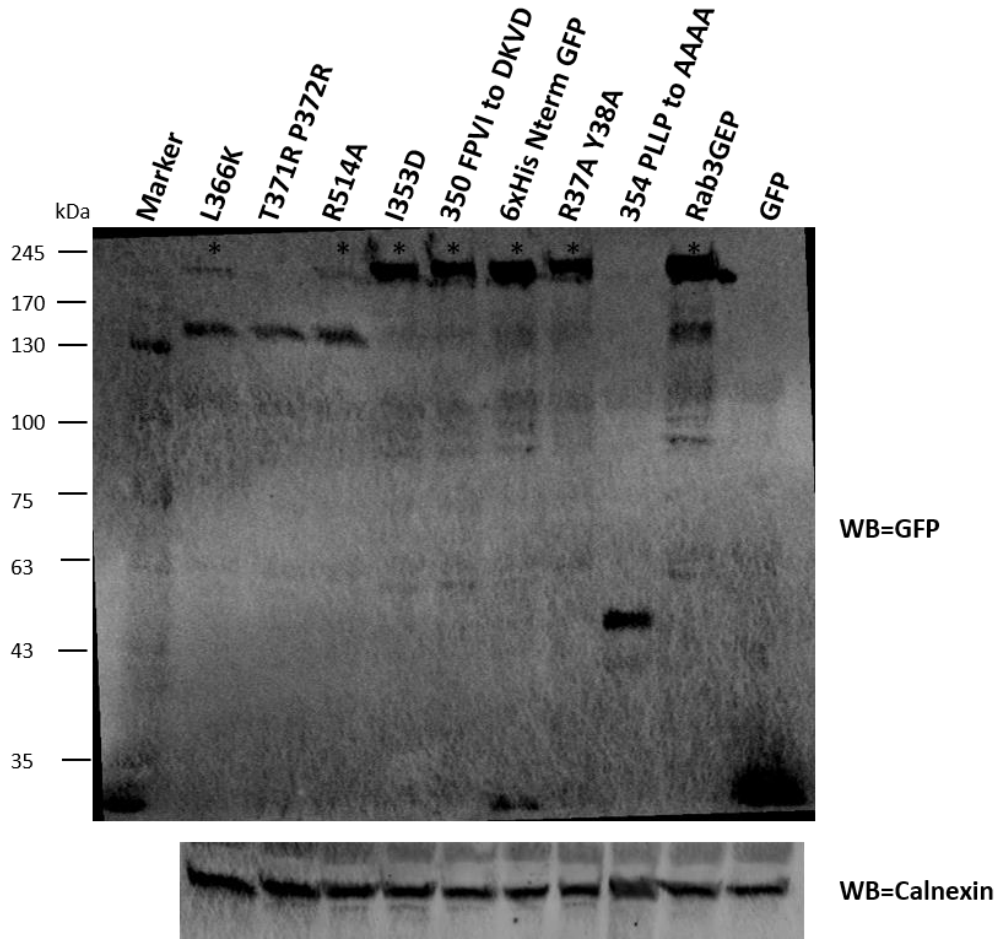


Figure 42 Expression of Rab3GEP point mutants in HEK293a

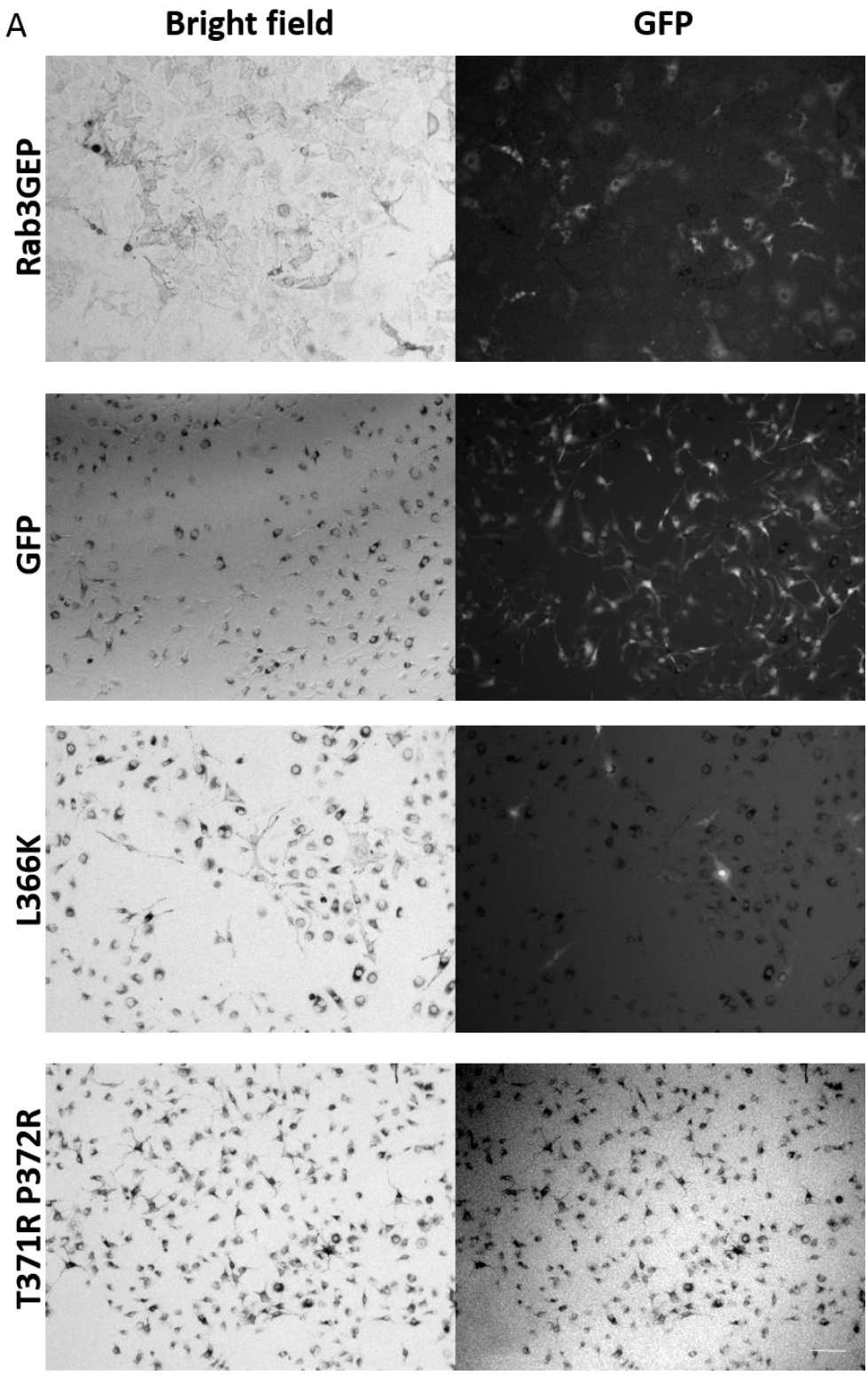
HEK293a cells were infected with adenoviruses expressing the different point mutations of Rab3GEP, 72 hrs later homogenates were loaded on 6%SDS-PAGE gel. on the top, immunoblotting for performed with anti-GFP antibody. Asterisks show the bands with the same molecular weight as Rab3GEP. The Western blot shows that all the isoforms were expressed. It is possible to see cleaved bands of the L366K and R514A, the mutant T371R P372R shows single band at the same level as the 2 cleaved isoforms above mentioned. The 354 PLLP to AAAA shows single band at lower molecular weight. Below Calnexin as loading control

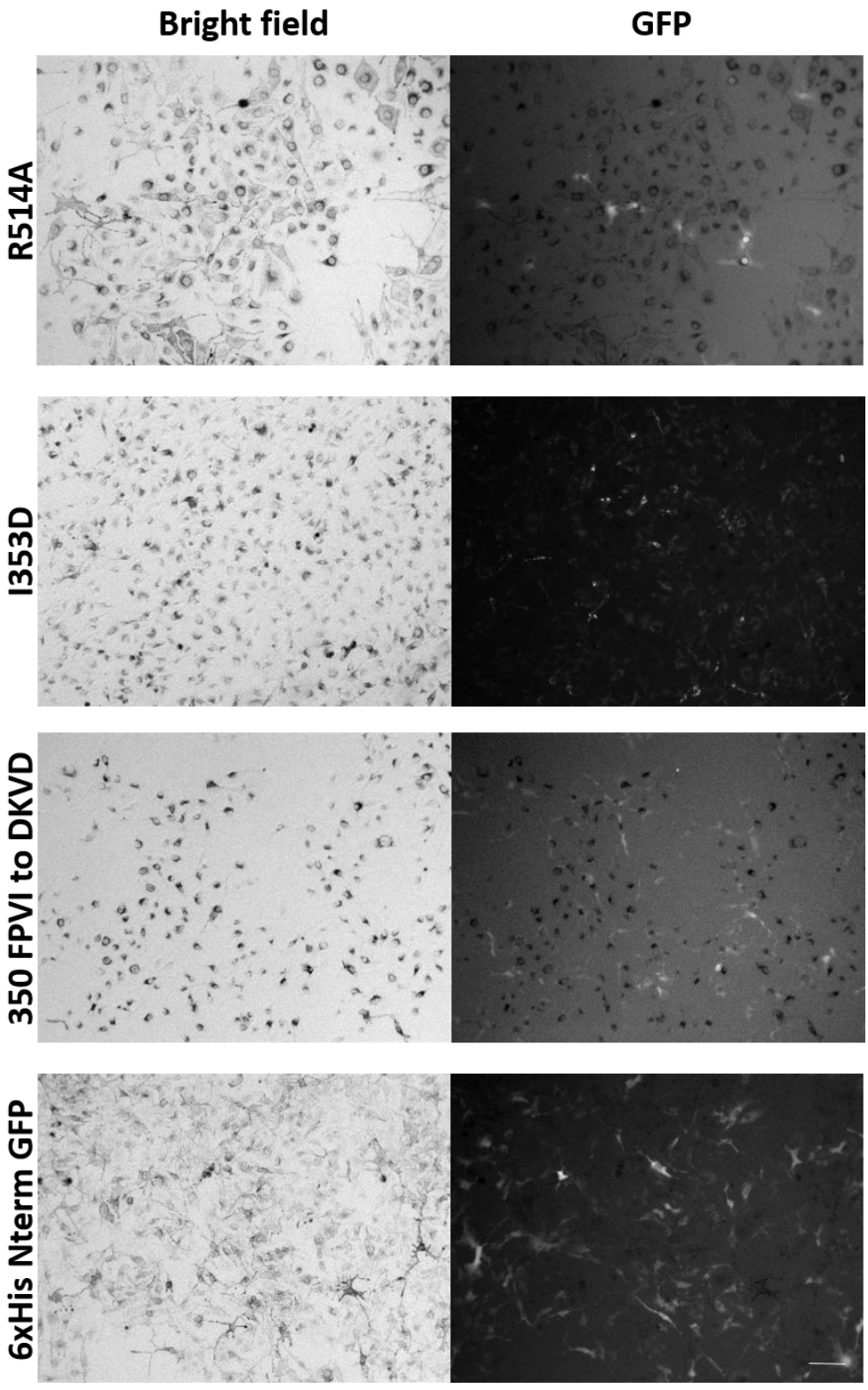
The outcome of the Western blot shows that all the mutants were expressed. The mutants Rab3GEP^{L366K}, and Rab3GEP^{R514A} present a band between 170-245kDa, which is the predicted molecular weight, in fact, it corresponds to the molecular weight of the positive controls (Rab3GEP wild type-6xHis Nterm GFP), and a more intense band between 130-170kDa. Interestingly, Rab3GEP full length has a band at the same molecular weight 130-170kDa, which is at the same molecular weight of the band seen with ΔDD seen in Figure 32, suggesting that these mutations affect the stability/structure of the protein. Despite that in Rab3GEP^{L366K}, and Rab3GEP^{R514A} mutants is

possible to see the bands related with the full length. Instead the point mutant Rab3GEP$^{T371R-P372R}$ shows only the band between 130-170kDa, and not the band at between 170-245kDa. The mutant Rab3GEP$^{P354A-L355A-L356A-P356A}$ displays a single band a low molecular weight which does not appear in any of the other mutant, which could be due to a non-correct translation of the mRNA or a product of cleavage.

Rab3GEP^{I353D}, Rab3GEP$^{F350D-P351K-I353D}$, Rab3GEP$^{R37A-Y38A}$ present a band between 170-245kDa like the positive controls, suggesting no lack of stability after modification.

Having determined the expression of the point mutation in HEK293a, the other step was to investigate their effect on melanosome distribution in melan-Rab3GEP KO cells (Figure 43).


A
Bright field
GFP
Rab3GEP
GFP
L366K
T371R P372R


Bright field
GFP
R514A
I353D
350 FPVI to DKVD
6xHis Nterm GFP

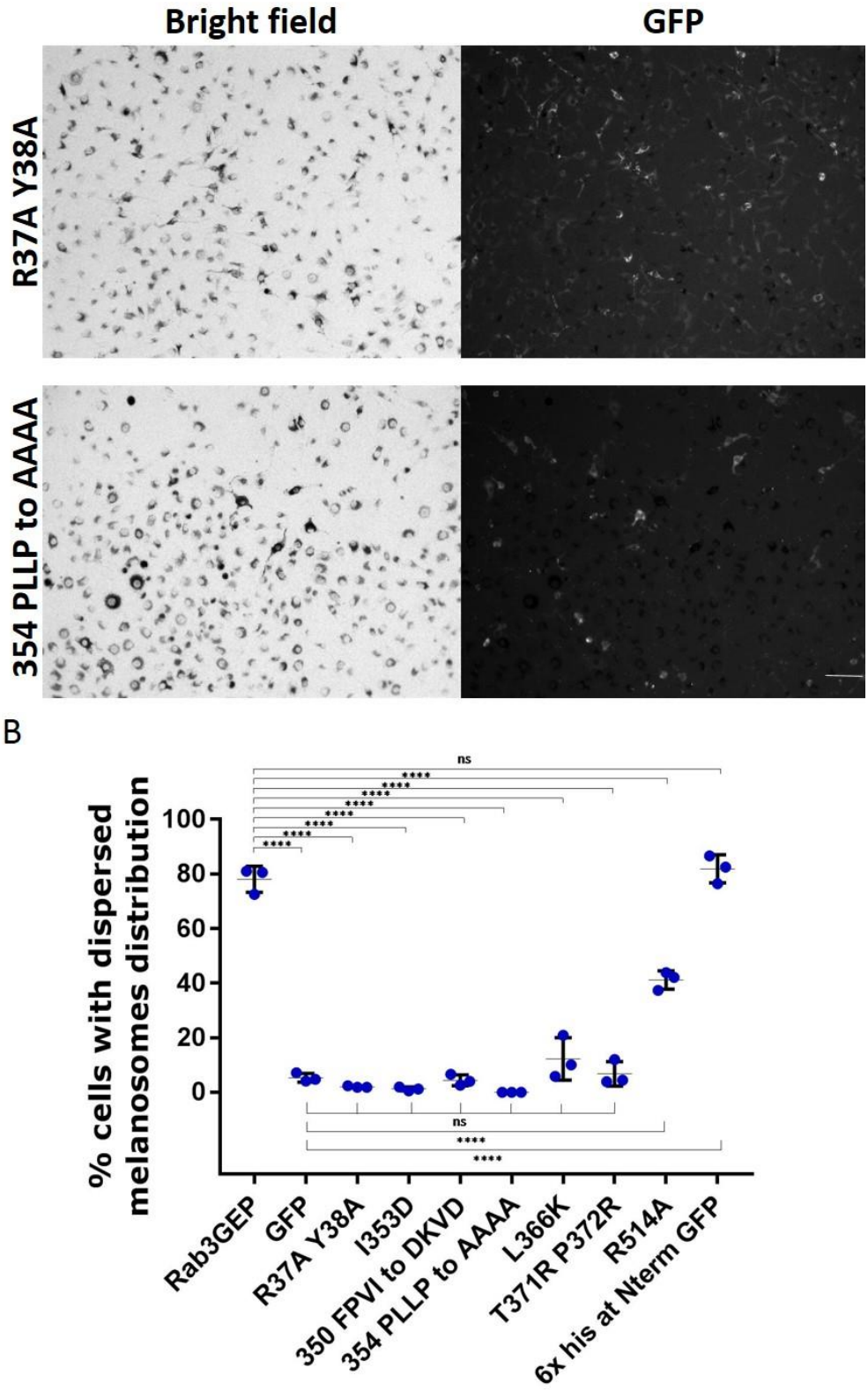


Figure 43 Expression of the point mutation of Rab3GEP in melan-Rab3GEP KO cells do not restore the dispersed distribution of melanosomes

melan-Rab3GEP KO cells were seeded in a 24 well plate and infected with viruses expressing Rab3GEP, L366K, T371R P372R, R514A, I353D, 350 FPVI to DKVD, 6xHis Nterm GFP, R37A Y38A, 354 PLLP to AAAA and GFP. A) After two days,

cells were fixed and imaged with bright field optics. The left panels show bright field images, the right panels show the GFP expression. Scale bar 100μm. B) Three pictures were obtained per condition with about 100 cells per pictures so with a total of 300 cells. Cells with clustered, dispersed melanosome distribution, and total number of cells were counted and the percentage was obtained

Bright field and GFP emission fluorescence of melan-Rab3GEP KO cells infected with the adenoviruses expressing Rab3GEP point mutants is shown in Figure 43A. Investigation of the melanosome distribution indicate that overexpression of the positive controls (Rab3GEP full-length and 6xHis Nterm GFP), restores the melanosomes trafficking as predicted. Instead, the point mutants Rab3GEP^{L366K}, Rab3GEP$^{T371R-P372R}$, Rab3GEP^{I353D}, Rab3GEP$^{F350D-P351K-I353D}$, Rab3GEP$^{R37A-Y38A}$, Rab3GEP$^{P354A-L355A-L356A-P356A}$ seem not to restore the melanosome distribution. Cells overexpressing the mutant Rab3GEP^{R514A} present 41,1% percent of cells with dispersed melanosomes, higher population compared to the other mutants which are between 1,2% and 12.2% (Figure 43B). Level of the exogenous proteins seems to be different between the samples, in fact Rab3GEP, GFP, Rab3GEP^{I353D}, Rab3GEP$^{F350D-P351K-I353D}$, 6xHis Nterm GFP, Rab3GEP$^{R37A-Y38A}$ seem to be well expressed in the cells based on GFP emission fluorescence, instead Rab3GEP^{L366K}, Rab3GEP$^{T371R-P372R}$, Rab3GEP^{R514A} and Rab3GEP$^{P354A-L355A-L356A-P356A}$ are poorly expressed, especially the point mutant Rab3GEP$^{T371R-P372R}$. This suggest that the partial activity of the mutant Rab3GEP^{R514A} or the lack of detectable activity of the other mutants might be due to the poor stability of these proteins or to a lack of infection from the adenoviruses.

Quantification of the rescued cells after adenoviruses infections indicate clearly that between all the overexpressed proteins only Rab3GEP was able to re-distribute the melanosome in 78% of the cells, instead, point mutations cause lack of this ability. The only exception to this was the point mutant Rab3GEP^{R514A} which increase the percentage of rescued cells, although do not reach the level of Rab3GEP wild type. This might be due to the lower level of expression of this protein compared to Rab3GEP, then more accurate analysis was necessary.

4.4.1 **Visualization of point mutants Rab3GEP in melan-Rab3GEP KO cells with high magnification**

In order to assess in a more sensitive way the possible function/distribution of each point mutant of Rab3GEP, melan-Rab3GEP KO cells were infected with adenoviruses expressing the point mutants and confocal microscopy was used to detect subtle effects as in section 4.3.1 (Figure 44).

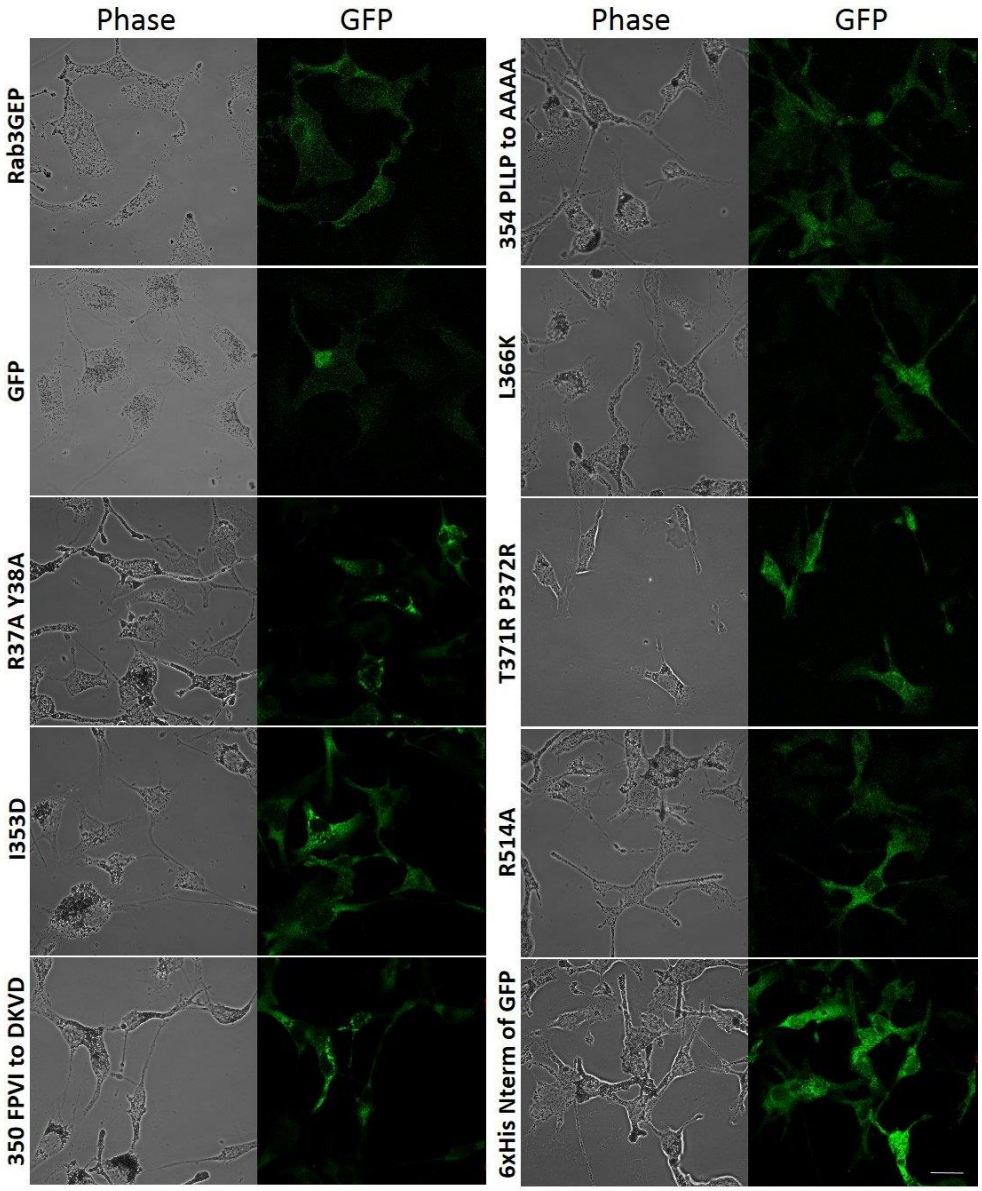


Figure 44 Expression of Rab3GEP point mutants and melanosome distribution in free growing melan-Rab3GEP KO cells

melan-Rab3GEP KO cells were seeded on glass coverslips and infected with adenoviruses expressing the different point mutations of GFP-Rab3GEP. Two days later cells were fixed. This picture shows the expression of the Rab3GEP full length, GFP alone as a control and the different point mutants of Rab3GEP. Scale bar 20μm

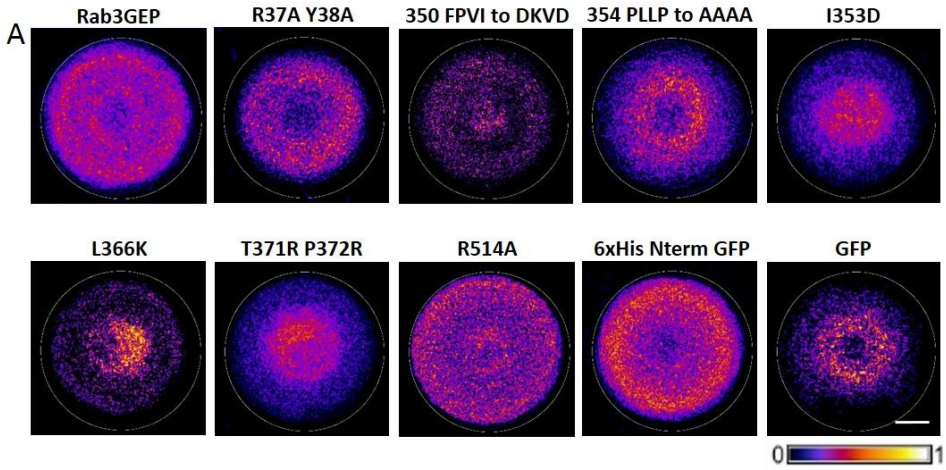
As predicted both positive controls (Rab3GEP and 6xHis N-Term of GFP) were able to rescue the melanosome distribution as well as the cells overexpressing GFP maintained the clustered distribution of melanosomes. Point mutants of Rab3GEP presented different outcomes. GFP expression shows clearly that the cells are expressing the point mutation proteins, moreover, analysis of the phase contrast images indicate that except for and Rab3GEP^{R514A} all the others point mutations were unable to restore the dispersed distribution of the melanosomes. This finding suggests that the point mutant Rab3GEP^{R514A} might be functional, the low percentage of 41% of cells with dispersed melanosomes in Figure 43 could be due to the low proportion of cells expressing this point mutant of Rab3GEP, although this percentage was higher than the other point mutants, suggesting that only partial number of cells were expressing the protein. Furthermore, seems that mutations on conserved amino acids between the DENN domains (Rab3GEP$^{R37A-Y38A}$, Rab3GEP$^{P354A-L355A-L356A-P356A}$) causes impairment of the Rab3GEP activity, as well as the mutation of amino acids corresponding to essential residues in DENND1B (Rab3GEP^{I353D}, Rab3GEP$^{F350D-P351K-I353D}$, Rab3GEP^{L366K}, Rab3GEP$^{T371R-P372R}$), in fact all these mutations did not change melanosome distribution. Instead the only mutation that seems to rescue melanosome distribution was that in position R514A.

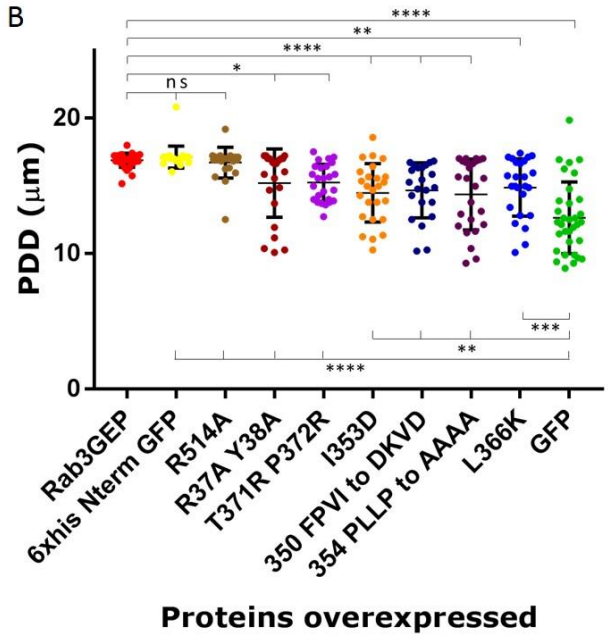
4.4.2 Analysis of the function of Rab3GEP DENN domain point mutants using micropattern chip transport assay

As well as for the truncation mutants of Rab3GEP (section 4.3.2), micropattern chip was used to have cell shape standardised in order to measure the distance travelled by the melanosomes after expression of the point mutants into the cells, and in order to have high resolution images of the cells, which permits to discriminate cells infected and overexpressing the point mutants from cells not infected. Moreover, in order to analyse consistent number of cells which allow to obtain statistical quantifications and comparison between the effects invoked by the point mutants on melanosome transport.

This method, would clarify whether the point mutant Rab3GEP^{R514A} is functional, considering that in low magnification analysis only 41% of total cells rescued the melanosome distribution (Figure 43B), instead the cells expressing this mutant in section 4.4.1 imaged with high magnification presented dispersed melanosome distribution.

Then, melan-Rab3GEP KO cells expressing Rab3GEP point mutants were seeded on micropattern following the same steps seen in Figure 36.


A
Rab3GEP
R37A Y38A
350 FPVI to DKVD
354 PLLP to AAAA
I353D
L366K
T371R P372R
R514A
6xHis Nterm GFP
GFP
0
1


B
PDD (µm)
20
10
0
ns
*
****
**
****
****
**
***
Rab3GEP
6xhis Nterm GFP
R514A
R37A Y38A
T371R P372R
I353D
350 FPVI to DKVD
354 PLLP to AAAA
L366K
GFP
Proteins overexpressed

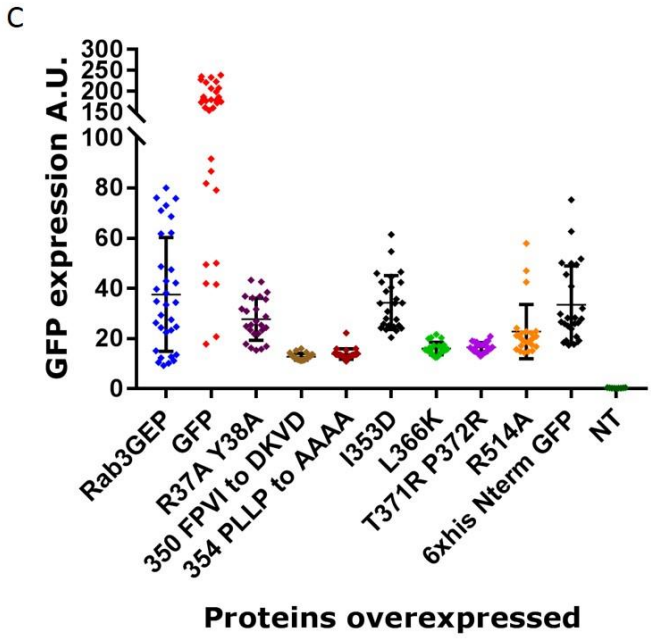

C
GFP expression A.U.
300
250
200
150
100
80
60
40
20
0
Rab3GEP
GFP
R37A Y38A
350 FPVI to DKVD
354 PLLP to AAAA
I353D
L366K
T371R P372R
R514A
6xhis Nterm GFP
NT
Proteins overexpressed

Figure 45 Point mutations of Rab3GEP expressed in cells visualised in Micro Pattern

melan-Rab3GEP KO cells were infected with adenoviruses expressing different point mutations of Rab3GEP. After 48hrs, cells were harvested and re-seeded on micropattern chip. Cells were fixed 24hrs later, and then imaged. A) Look up table [LUT] images show the melanosome distribution where black=0% and white=100% probability of finding melanosomes. Scale bar 10μm. B) Scatterplot shows the PDD (pigment dispersion distance) for each cell (dot) in each of the populations overexpressing Rab3GEP point mutants. One way ANOVA multiple comparisons was used to determine p value statistical significance showed with dots (4 dots highest -1 dot lowest), ns No significance. C) GFP expression per cell indicated by arbitrary unit measured.

Melanosome distribution maps shown in Figure 45A indicates that the positive controls (Rab3GEP wild type, 6xHis N-term of GFP) and Rab3GEP^{R514A} were able to restore melanosome trafficking. Instead, cells overexpressing the other point mutants present low probability to find melanosomes at the periphery, suggesting that the mutation of the Arginine (R) in position 514 leave unaltered the ability of Rab3GEP to activate the melanosome transport in melan-Rab3GEP KO cells, on the other hand the other mutations made on Rab3GEP reduce the ability to scatter the melanosome from the perinuclear cytoplasm.

Statistical comparison between the PDD of the different Rab3GEP point mutants with Rab3GEP indicates that 6xHis N-term of GFP, and Rab3GEP^{R514A} were equal with no significant difference between them (Rab3GEP mean= 16.89, standard deviation 0.5225; 6xHis 17.12, standard deviation 0.8148; Rab3GEP^{R514A} 16.71 standard deviation 1.138). Instead, the other point mutants presented lower PDD, although with different statistical significance, represented by different P Values compared to Rab3GEP wild type (Rab3GEP^{L366K} P value = 0.0048, Rab3GEP$^{T371R-P372R}$ P Value =0.0488, Rab3GEP^{I353D} P Value = 0.0002, Rab3GEP$^{F350D-P351K-I353D}$ (350 FPVI to DKVD) P Value = 0.0018, Rab3GEP$^{R37A-Y38A}$ P Value = 0.0450, Rab3GEP$^{P354A-L355A-L356A-P356A}$ (354 PLLP to AAAA) P Value = <0.0001). Moreover, statistical comparison between the point mutants and the negative control indicates high significant difference between the mutant Rab3GEP^{R514A} and GFP as well as between the positive controls (Rab3GEP wild type, 6xHis N-term of GFP) and GFP confirming once more that the mutant Rab3GEP^{R514A} activate the melanosome transport. However, high significant difference is present also between the negative control and the mutants Rab3GEP$^{R37A-Y38A}$ (P Value = 0.0001) Rab3GEP$^{T371R-P372R}$ (P Value = 0.0001), although comparison with the positive control shows also significant differences. Interestingly, the

other mutants are not equal to GFP but display differences, more noticeable with Rab3GEP^{L366K} P value = 0.0002, and less pronounced with Rab3GEP^{I353D} (P Value = 0.0033), Rab3GEP$^{F350D-P351K-I353D}$ ((350 FPVI to DKVD) P value = 0.0015) and Rab3GEP$^{P354A-L355A-L356A-P356A}$ (354 PLLP to AAAA) P Value = 0.0071). Noteworthy, in this experiment a higher standard deviation was estimated for these point mutants (Rab3GEP^{L366K} Std. Deviation 2.121, Rab3GEP$^{T371R-P372R}$ Std. Deviation 1.36; Rab3GEP^{I353D} Std. Deviation 2.156; 350 Rab3GEP$^{F350D-P351K-I353D}$ (350 FPVI to DKVD) Std. Deviation 2.033, Rab3GEP$^{P354A-L355A-L356A-P356A}$ (354 PLLP to AAAA) Std. Deviation 2.614 Rab3GEP$^{R37A-Y38A}$ Std. Deviation 2.513) compared to 6xHis and Rab3GEP^{R514A}. This suggests that all the cells infected with Rab3GEP wild type and Rab3GEP^{R514A} rescue the melanosome distribution, on the other hand cells infected with the other point mutants of Rab3GEP presented a mixed population, indicating that these mutants are unable to activate the melanosome trafficking like Rab3GEP wild type, and suggesting that they presenting partial activity considering that they are different from GFP as well. Finally, the graph C in Figure 45 shows the GFP expression of the cells analysed, and it clearly indicates that the cells presented all a higher expression compared to cells no treated (NT).

Summarising, the results of these experiments suggest that although all the melan-Rab3GEP KO cells were expressing the GFP tagged proteins, only Rab3GEP full-length and the mutant Rab3GEP^{R514A} were able to reactivate the anterograde melanosome trafficking, instead the other mutants were not able to rescue melanosome distribution. This suggests that Rab3GEP proteins uses its DENN domain to activate its cognate Rab in a similar way of Connecdenn-2.

4.4.3 I353D point mutation of Rab3GEP causes impairment of the GEF activity of Rab3GEP

In the previous sections of 4.4 it has been suggested that point mutation within the DENN domain blocks function of Rab3GEP, with the only exception of R514A point mutation. While, the experiments performed give information on the directly link between the point mutation and the melanosome distribution, they give no indication of the GEF activity of these point mutation. Therefore, Rab27 effector pull-down assay was used as a measure of GEF activity of the point mutants.

For this assay were chosen the point mutants Rab3GEP^{I353D} and Rab3GEP^{R514A}, reasoning on the fact that in the case of Rab3GEP^{I353D} a single mutation was generated, which correspond in the 3D structure to the isoleucine in position 226 in the DENND1B which is part of the binding site I for Rab35. Instead, in the case of Rab3GEP^{R514A} this amino acid is located in another area of the DENN structure, far from the binding site I and II, so it was chosen to confirm its activity (Figure 46).

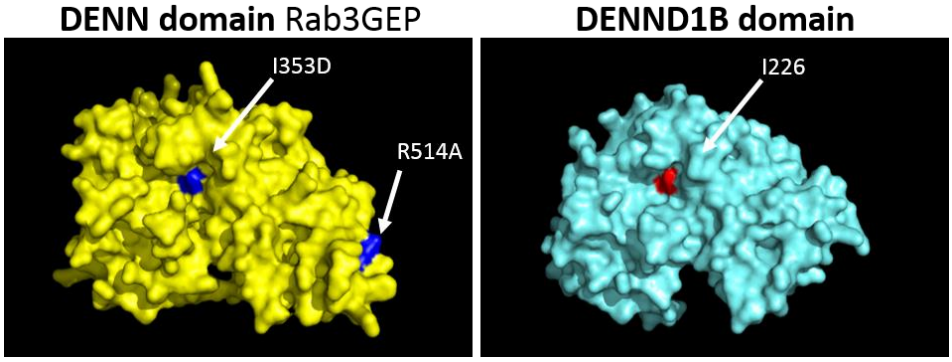


Figure 46 I353D of DENN domain of Rab3GEP and correspond to I226 of DENND1B

3D models of the DENN domain of Rab3GEP (yellow) and the DENND1B of Connecdenn (cyan). Blue areas in DENN domain of Rab3GEP indicate position mutations, and Red area highlight the isoleucine 226 in DENND1B

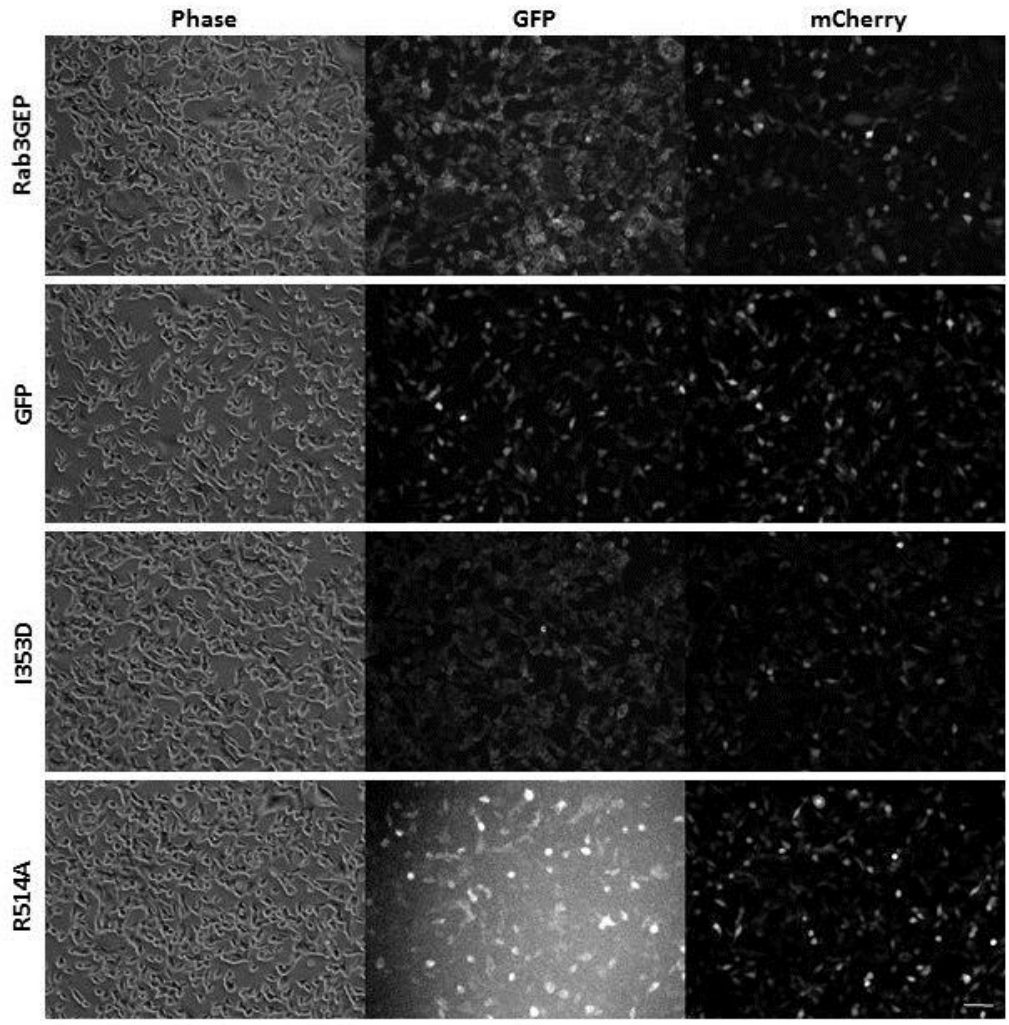


Figure 47 GFP and mCherry expression in HEK293a before protein collection

HEK293a were seeded in 10cm Petri dishes, when the confluence was of 98% cells were co-infected with mCherry-Rab27a and either I353D, R514A, Rab3GEP wild type or GFP. Then left overnight to express the proteins. The day after cells were imaged with phase contrast, and fluorescence of mCherry and GFP Tags was detected. Scale bar 100µm

Point mutants of Rab3GEP, Rab3GEP wild type and GFP expression proteins in HEK293a cells was determined through the GFP emission (Figure 47). GFP expression indicates that cells were expressing the GFP labelled proteins as well as for the mCherry tagged Rab27a.

Having established that the proteins of interest were expressed in HEK293a, Slp1-GST pull down assay was performed and immunoblotting against mCherry was performed to determine the bounded fraction of Rab27a (Figure 48).

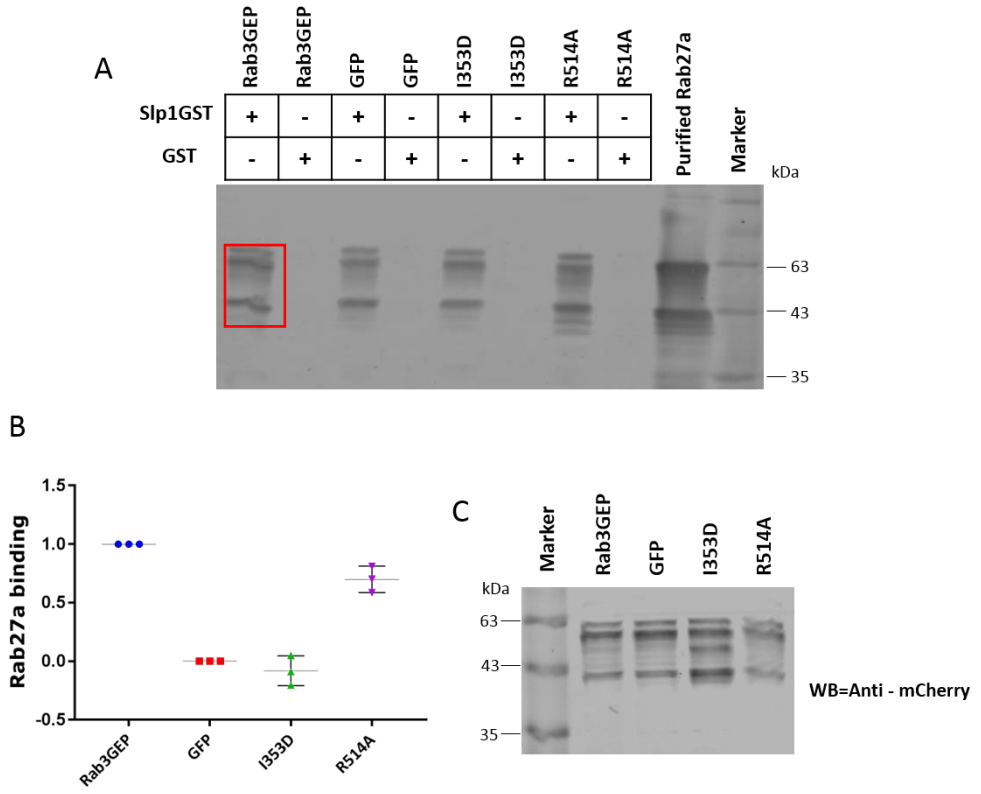


Figure 48 Pull-down assays indicate lack of GEF activity of the point mutation I353D and activity of R514A

HEK293a cells were infected with adenoviruses expressing Rab27a-mCherry and either Rab3GEP, GFP, I353D, or R514A and left overnight for protein expression. The day after cell were lyses and 2 mg of lysate was incubated overnight with either GST-Slp1 or GST in presence of glutathione-beads the supernatant was washed out and A) Rab27a pulled down by Slp1 was detected by Western blot using anti-mCherry antibody. Red box shows area quantified, same area all samples B) this experiment was repeated 3 times and this scatter plot shows the quantification of the three experiments normalizing Rab3GEP equal to 1 and GFP equal to 0. C) Immunoblotting against mCherry-Rab27a of 25µg of crude cell lysates.

Figure 48A shows that mCherry-Rab27a was retained by the beads only when incubated Slp1-GST, in fact, samples incubated with GST do not show bands at the mCherrry-Rab27a level. Purified mCherry-Rab27a was used as a positive control. Moreover, intensity of the bands examined indicate more intense bands for Rab3GEP and Rab3GEP^{R514A} and lesser intense bands for GFP and Rab3GEP^{I353D}. Quantification of the bands intensity after three independent experiments indicates that Rab3GEP^{I353D} mutant has the same activity as GFP, instead the mutant Rab3GEP^{R514A} has a GEF activity similar to Rab3GEP, although do not reach its level. This could be due to the lower expression of the point mutation in the cells as seen in Figure 47. Finally, the Figure 48C shows the level of mCherry-Rab27a in the crude extracts,

and it indicates similar expression protein level except for Rab3GEP^{R514A} which bands seem to be less intense suggesting lower expression.

In conclusion, this experiment suggests that the point mutation I353D of Rab3GEP loses the GEF activity, therefore, it is unable to activate Rab27a. This effect is mirrored in the defect of the melanosome re-distribution as seen in the previous section 4.4.1 and 4.4.2. Instead, the mutation at the dDENN R514A do not change the GEF activity of Rab3GEP and this mutant is able to activate Rab27a which in turn is able to bind Slp1. Confirming the results obtained with the micropattern chip assay.

4.5 Discussion

In this study, the mechanism by which Rab3GEP regulates the activity of Rab27a was investigated. To do this, truncations and point mutations of Rab3GEP were generated with the scope to characterize the domains and amino acids important for the GEF activity.
Firstly, having already made the truncation mutants adenoviruses, the protein expression was investigated in mammalian cells, and molecular weights were detected to determine correct translation experimental Rab3GEP proteins. Immunoblotting results indicate that all the truncated isoforms of Rab3GEP were expressed in the cells even though there is a different level of expression between them. Furthermore, bands with lower molecular weight were detected suggesting that there is some cleavage of the Rab3GEP as well as for the truncation mutation ΔDD, which have the same molecular weight (Figure 32).

Different methods of analysis were used to investigate the capacity of the truncation mutants to rescue melanosome distribution such as low/high magnification microscopy and micropattern chip. The results obtained present the same trend and indicate that the truncation mutants of Rab3GEP protein lose the ability to rescue melanosome distribution. Moreover, measurement of the PDD (Pigment dispersion distance) for cell population through the micropattern chip assay indicate clearly significant different with a P value lower than 0.0001 ($p=<0.0001$) between Rab3GEP full-length and the truncation isoforms (DENN, ΔDENN, ΔDD, DD) (Figure 37).
As a confirm of the results obtained with the microscopy approach, the biochemical results obtained with the pull-down assay of Rab27a GTP bound indicate loss of GEF activity of the truncation mutant compared to Rab3GEP full-length (Figure 39). Hence, evidence obtained in this chapter indicate clearly that truncation of the full length of Rab3GEP protein induce the loss of the GEF activity towards Rab27a, consequently this Rab cannot be activated, therefore, melanosomes are maintained in the perinuclear cytoplasm. Data obtained in this chapter confirmed the results gained in a previous study based on Rab3GEP, in fact it has been suggested that truncation of Rab3GEP lose the GEF activity versus Rab3 (88). In this study, the authors used a human growth (GH) co-expression assay system to identify the importance of the Rab3GEF and Rab3GAP on the release of

vesicle in PC12 cells. In this study it was observed that overexpression of active Rab3A Q81L inhibits the K^+ induced GH release, similarly of a precedent study which indicate Rab3A as an inhibitor of Ca^{2+}-dependent vesicle release in chromaffin cells (147), then authors tested with the same approach the effect of some truncation of Rab3GEP. They made truncation of the Rab3GEP full length at the N-terminus and at the C-terminus. One of these truncation mutants was lacking 108 amino acids at the C-terminus and it was still able to inhibit about 32% of K^+ induced GH release. However, further deletion at the C-terminal of Rab3GEP like 242 and 392 amino acids as well as deletion at the N-terminus were unable to inhibit K^+ induced GH release. Suggesting that they were not able to activate Rab3A. The truncation isoform that was able to induce inhibition of the GH vesicle release was called ΔC1, and this truncated mutant still contain the Death domain.

In another study performed by Coppola et al. it was confirmed the importance of the death domain for the GEF activity of Rab3GEP towards Rab3 (87). In this study authors performed two truncations of Rab3GEP ΔC1 and ΔC2, missing respectively 127 and 229 amino acids at the C-terminus. The first still contained the death domain and was found to preserve the GEF activity, the second lacked the death domain and lacked the GEF activity. Moreover, they created another truncation in which only the death domain was deleted and not the C-terminus part, once more they found that this ΔDeath domain was unable to activate Rab3, suggesting the importance of this domain for the GEF activity.

These results highlight a difference between Rab3GEP and other protein containing the DENN domain. In fact, although it has been suggested that the DENN domain of Connecdenn is sufficient to perform the GEF activity towards Rab35 (144), the truncated DENN domain of Rab3GEP does not retain GEF activity towards Rab27a. This could be due to a different structure conformation conferred by the other part of the protein, in other words the DENN domain 3D conformation is preserved only when the other part of the protein is present, deletion of them would induce a not correct folding of the protein and Rab3GEP lose the GEF activity. Another interpretation would be related to the characteristic of the death domain of forming dimer, in this case it is possible that Rab3GEP dimerise in order to perform the GEF activity and that deletion of the death domain decrease or cancel this capacity.

Nevertheless, the DENN domain of Rab3GEP is crucial for its activity as a GEF for Rab27a, in fact deletion or changes within this domain cause lack of activity as seen for the point mutations.

Overexpression of point mutants in free growing melan-Rab3GEP KO cells indicate that mutation in uDENN and DENN domain cause the lack of the ability of Rab3GEP to disperse melanosomes. These outcomes were confirmed using the micropattern chip assay. Moreover, the results obtained in this chapter indicate that it could work similarly to the DENN domain of Connecdenn (see below). The only mutation that conserved the GEF activity toward Rab27a was R514A. However, this mutation was not on the binding site predicted based on the DENND1B structure.

As said the results obtained from studies using Rab3GEP DENN point mutants suggest similar mechanism of action between the DENN domain of Rab3GEP and the DENND1B. In fact, based on a possible 3D structure of the DENN domain of Rab3GEP made by our collaborator Dr Aymelt Itzen, the substitution of amino acid in Rab3GEP located in position directly correlated to key amino acids in the binding site I and II of the DENND1B, cause the lack of the activity of Rab3GEP towards Rab27a. In fact, isoleucine in position 353 (I353) in Rab3GEP mirrors the position of the isoleucine 226 (I226) in the DENND1B (binding site I) (Figure 40), and its change with aspartic acid (D) block the GEF activity as seen in the micropattern assay (Figure 45) and in the pull-down assay (Figure 48). This effect was seen both with the point mutants Rab3GEP^{I353D}, Rab3GEP$^{F350D\text{-}P351K\text{-}I353D}$, moreover, always referring to the binding site I the leucine in position 366 mirrors the tyrosine in 236 of DENN1DB, and its mutation in lysine (K) block the GEF activity of Rab3GEP as well (Figures 43-45). Referring to the binding site II of the DENND1B the methionine and proline in position 241 and 242 respectively are mirrored by the threonine in position 371 and the proline in position 372, and their changed in arginine T371R P372R block once more the GEF activity of Rab3GEP (Figures 43-45). As a confirm of these conclusions the mutation of an amino acid distant from the binding site I and II such as R514A do not block the GEF activity of Rab3GEP (Figures 45-48). Furthermore, mutation of the conserved amino acids between the DENN family proteins, like R37A Y38A block the GEF activity as well. The same cannot be said about the mutant Rab3GEP$^{P354A\text{-}L355A\text{-}L356A\text{-}P356A}$ because although the results indicate block of the GEF activity, the western block in Figure 42 shows instability of

the protein, which may due to the change of the two Proline known to be important for this function.

Summarizing our results indicate that Rab3GEP could use the DENN domain to perform the GEF activity toward Rab27a, with similar mechanism of the DENND1B of Connecdenn. Nevertheless, the integrity of the full-length protein is crucial for the GEF activity.

5 Rab3GEP distribution and its activity

5.1 Introduction

Rab3GEP protein has been recognised as the guanine nucleotide exchange factor for Rab27a in melanocytes and in rat parotid acinar cells (7,84). Moreover, Tarafder et al. indicated Rab3GEP important for the targeting of Rab27a to the melanosome membrane (85). In chapter 4 our attention was focused on the understanding of the role of the domains contained in Rab3GEP protein and on the possible mechanism responsible for the GEF activity towards Rab27a. Evidence presented there indicated that the truncations of Rab3GEP protein causes loss of GEF activity towards Rab27a. Moreover, point mutations of full-length protein suggested that Rab3GEP might bind Rab27a similarly to the DENND1B domain towards Rab35. The aim of this chapter will be to investigate the role of Rab3GEP in re-targeting Rab27a to different organelle than melanosome membrane, and to examine whether the mis-targeting of Rab27a is able to rescue melanosome distribution in melan-Rab3GEP KO cells.

Members of the Rab family localise to specific intracellular membranes. The proteins involved, and the mechanism of the targeting of Rabs is still unknown. Recent data suggest that GEF proteins are candidates to perform the targeting function. Studies on *Legionella pneumophila* have revealed that recruitment of Rab1 to the LCV (*Legionella-containing vacuole*) is due to DrrA (*Defect in Rab1 recruitment A*)(148). Moreover, it has been demonstrated that DrrA is a guanine nucleotide exchange factor of Rab1, and that it is able to displace GDI from Rab1 (148,149). The peculiar localisation and its GEF activity demonstrate the role of this GEF on membrane recruitment and activation of Rab1. Furthermore, it has been demonstrated that eukaryotic GEFs control the correct localisation of their cognate Rab. Blumer et al. (38) were able to redirect Rab5 to mitochondria by mis-targeting of Rabex-5 (Rab5 GEF) to the same organelle. Moreover, in that study authors have shown that the Rab5 localisation is directly correlated with the Rabex5 GEF activity.

To fulfil its action, active Rab27a protein needs to localise to melanosome membrane. Previous observation suggested that both activation and targeting of Rab27a are performed by Rab3GEP. Tarafder et al. (85) show that Rab27a is not localised in the melanosome membrane when Rab3GEP has been depleted by small interfering RNA. However, it is noteworthy that one of the mutants used Rab27a^{SF2} was able to bind the effectors indicating that it was activated by Rab3GEP but was not localised to melanosomes in WT melanocytes. This indicates that Rab3GEP is important but not sufficient to target Rab27a to melanosome membrane. Therefore, Rab3GEP and Rabax5 may differ in their targeting activity. Consistent with this Rabex5 is located on the target organelle while Rab3GEP is not melanosome resident (7). In order to understand the mechanism of Rab3GEP in targeting of Rab27a, plasmid constructs of Rab3GEP able to target this protein to the mitochondria were created, with the aim of following similar approach used by Blumer et al. for Rabex-5 (38). Then Rab27a localisation and capacity of rescuing melanosome distribution was investigated.

5.2 The cytoplasmic distribution of Rab3GEP is essential for its function in melanosome transport

Recent studies suggested that RabGEF localisation is crucial for the proper activity of the cognate Rab (148). In this section, normal localisation of Rab3GEP was defined and the protein was mis-located to a different compartment to test the relationship between Rab3GEP localisation and its function.

Rab3GEP endogenous localisation in primary cultured rat hippocampal neurons detected by Oishi et al. (88) suggested punctate staining pattern along neuritic processes. Nevertheless, overexpression of Rab3GEP in melanocytes performed by Figueiredo et al. (7) and as shown in this dissertation in section 4.3.1 Figure 34 and in section 4.4.1 Figure 44 display a cytosolic localisation of this protein. Unfortunately, I was not able to detect endogenous Rab3GEP because low antibody binding efficiency through immunostaining.
To remind the reader the localisation of the guanine nucleotide exchange factor of Rab27a, melan-Rab3GEP knockout cells were infected with adenovirus expressing Rab3GEP tagged with GFP at the N-terminus. As a negative control cells were infected with adenovirus expressing only GFP which is not able to rescue the cells (Figure 49).

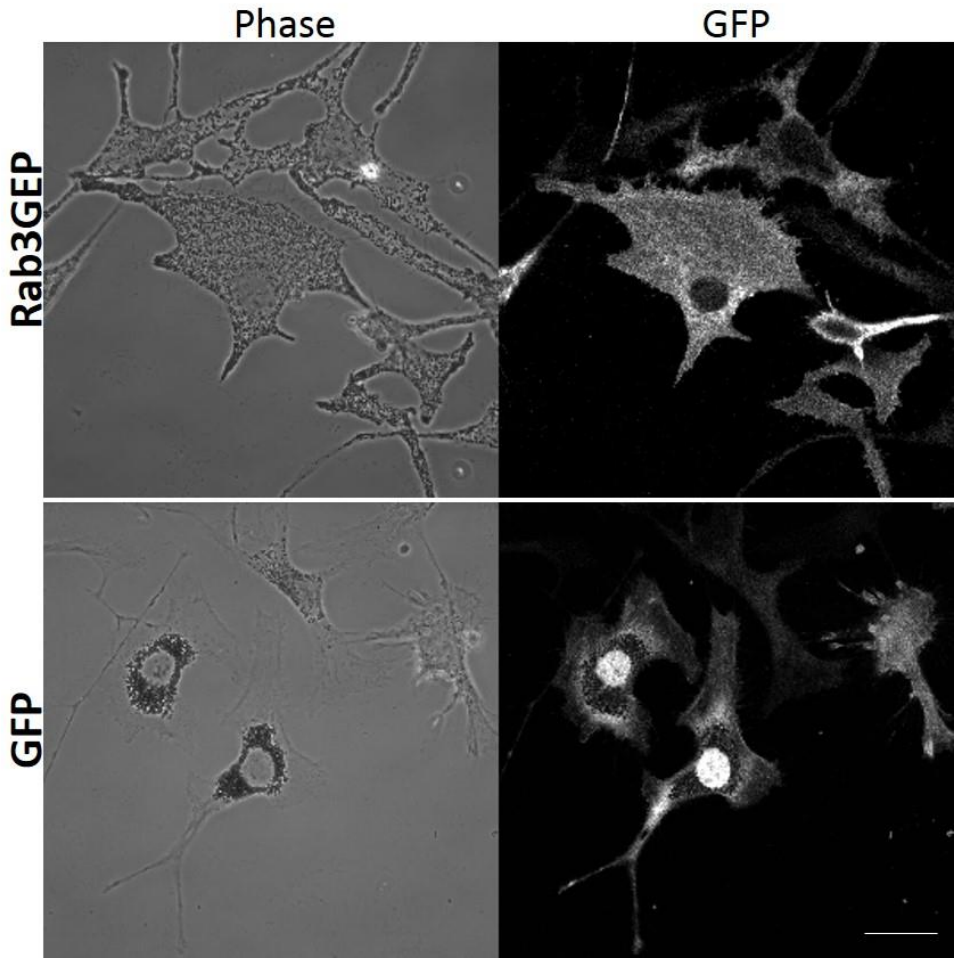


Figure 49 The intracellular distribution of GFP-Rab3GEP in melan-Rab3GEP KO melanocytes

melan-Rab3GEP knockout cells were seeded on coverslips and infected with adenovirus expressing GFP-Rab3GEP or GFP. Distribution of GFP signal was detected by confocal imaging. Upper panel shows cells expressing GFP-Rab3GEP, Lower panel shows cells expressing GFP. On the left are phase contrast images, on the right GFP expression. Scale bar 20μm

Phase contrast images show a dispersed distribution of melanosomes in cells expressing Rab3GEP, instead cells expressing GFP maintained perinuclear clustering indicating that Rab3GEP is able to rescue the melanosome disperse distribution. This result has been viewed in several experiments with 77% and 98% of cells that rescued the disperse melanosome distribution when infected with adenovirus expressing Rab3GEP protein (see Figures 33 and 43). Furthermore, GFP signal indicates that Rab3GEP is uniformly scattered in the cytosol matching the previous observations (7).

To investigate the role of the localisation of Rab3GEP protein in the targeting of Rab27a a similar approach used by Blumer et al. (38) was adopted, using the Rapamycin-based heterodimerisation system to relocate Rab3GEP to a

non-physiological cellular membrane. This system uses the ability of FKBP (*FK506-binding protein domain*) and FRB (*FKBP-rapamycin-binding domain*) proteins to form dimer when A/C heterodimeriser (*Rapamycin-related molecule/Rapalog*) is present. To explore the influence of the cytosolic distribution of Rab3GEP in targeting of Rab27a, this GEF was relocated to mitochondria and melanosome dispersion in melan-Rab3GEP KO cells was used as read-out of Rab27a and Rab3GEP function. For this purpose, two fusion proteins were made; GFP tagged Rab3GEP fused to FKBP, and FRB fused to Tomm70 and mCherry. Tomm70 is a protein which is known to be located at the mitochondria membrane (150). This system has allowed us to study the role of the distribution of Rab3GEP in the activation and targeting of Rab27a. Schematic representation of FKBP-FRB system is shown Figure 50.

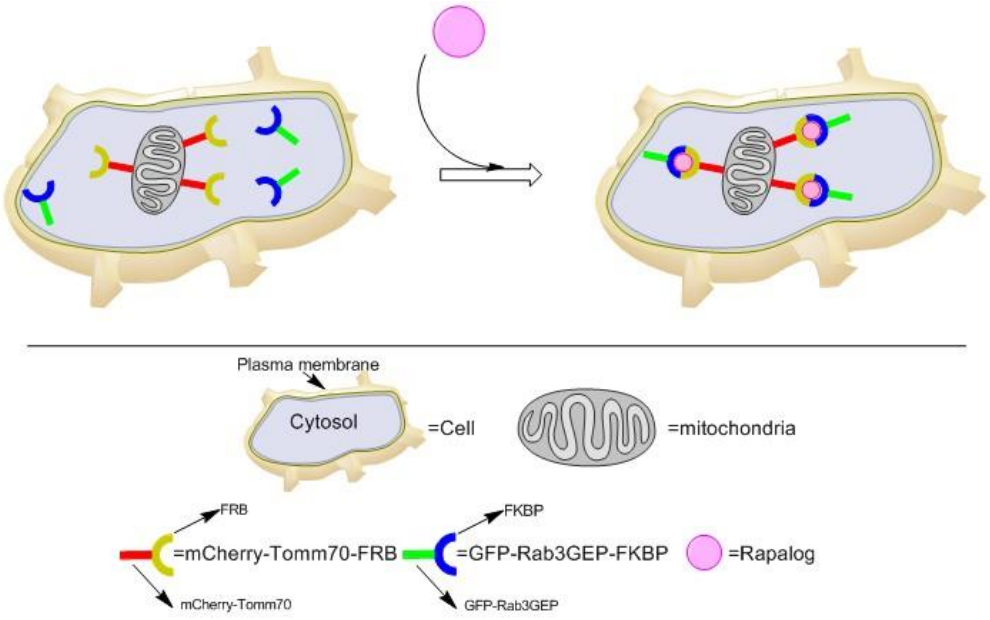


Figure 50 Schematic representation of Rab3GEP-FKBP/FRB-Tomm70 system

Schematic representation of the Rab3GEP-FKBP- FRB Tomm70 system, Tomm70 binds to the mitochondria through the transmembrane domains and present a link with the FRB protein which is co-localised with it. Rab3GEP- FKBP is free in the cytosol. When Rapamycin-related molecule is added to the medium the FKBP and FRB are able to form a dimer, therefore Rab3GEP is driven to the mitochondria.

It was predicted that the double introduction of Rab3GEP-FKBP and Tomm70-FRB would be able to restore the disperse distribution of melanosomes in the cell, because Rab3GEP was predicted to be free in the cytosol to perform its function of Rab27a activation. Then the treatment with

Rapalog would be predicted to relocate Rab3GEP to the mitochondria losing its normal localisation and leading to melanosome clustering at the perinuclear cytosol due to the lack of activation of Rab27a or its re-targeting to mitochondria. Schematic representation is shown in Figure 51.

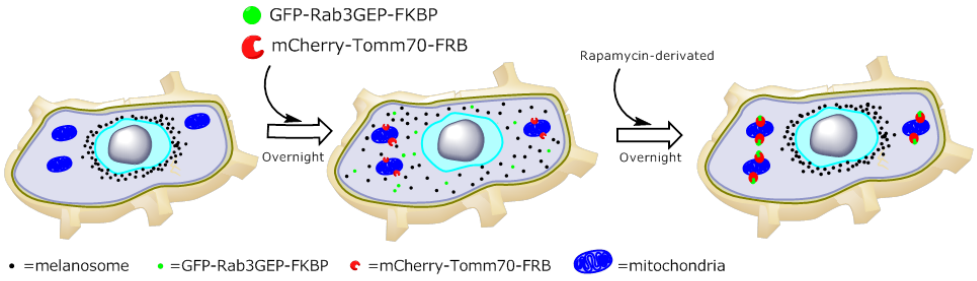


Figure 51 Schematic representation of predicted results using GFP-Rab3GEP-FKBP

Representation of GFP-Rab3GEP-FKBP function in its cytosolic free distribution and in mitochondria localisation using melanosome distribution as read-out. On the left melan-Rab3GEP KO with clustered melanosomes, middle cartoon, after the infection with adenoviruses expressing GFP-Rab3GEP-FKBP and Tomm70-mCherry-FRB, Rab3GEP (green dots) free in the cytosol and Tomm70 (red dots) associated with mitochondria (blue) melanosomes (black dots) disperse throughout the cytosol. On the right, the day after treatment with the drug Rab3GEP co-localise with Tomm70 and reoccurrence melanosome clustering

melan-Rab3GEP knockout cells were infected with adenoviruses expressing GFP-Rab3GEP-FKBP (Rab3GEP-FKBP) and Tomm70-mCherry-FRB (Tomm70-FRB), individually or together and left until fluorescence protein expression was detectible. Then, overnight drug treatment was performed in order to allow recruitment of Rab3GEP to the outer mitochondrial membrane. As a positive control of the melanosome distribution was used Rab3GEP wild type fused with GFP which is able to restore the disperse distribution (see Figure 49).

In order to investigate whether the Rapalog has an effect on melanosome distribution the two controls GFP-Rab3GEP and Tomm70-FRB individually were treated with the drug as well.

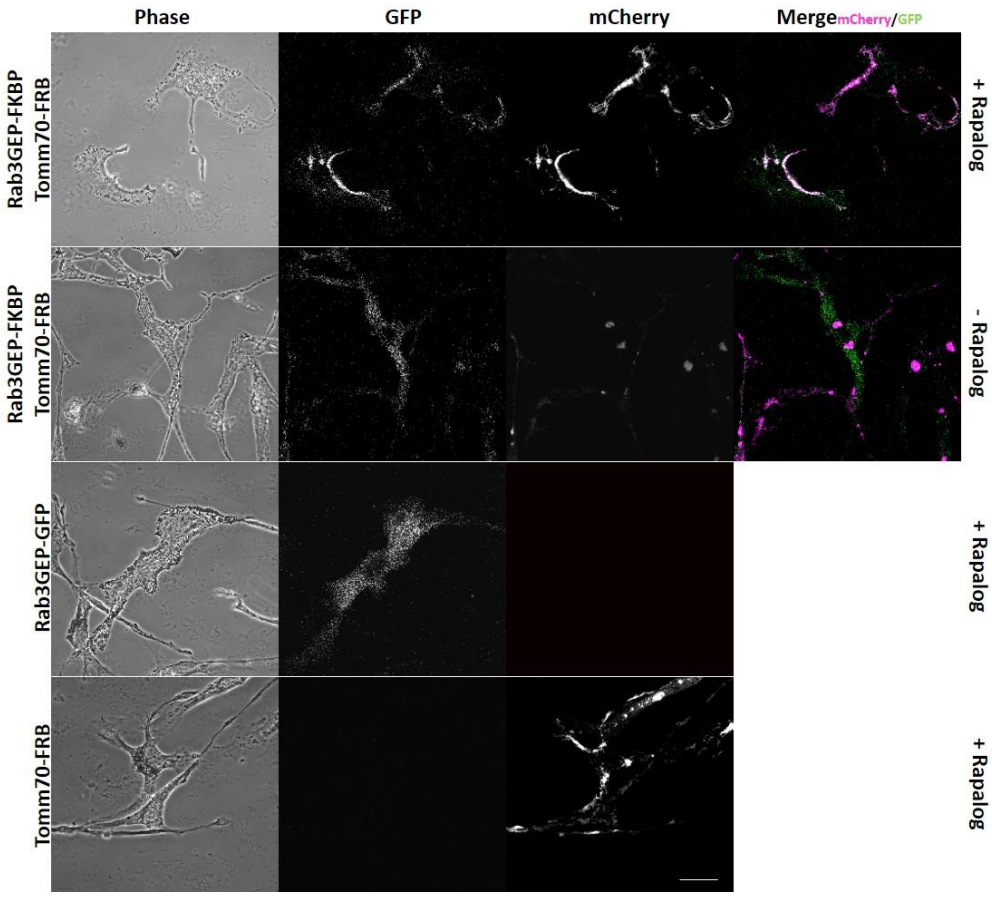


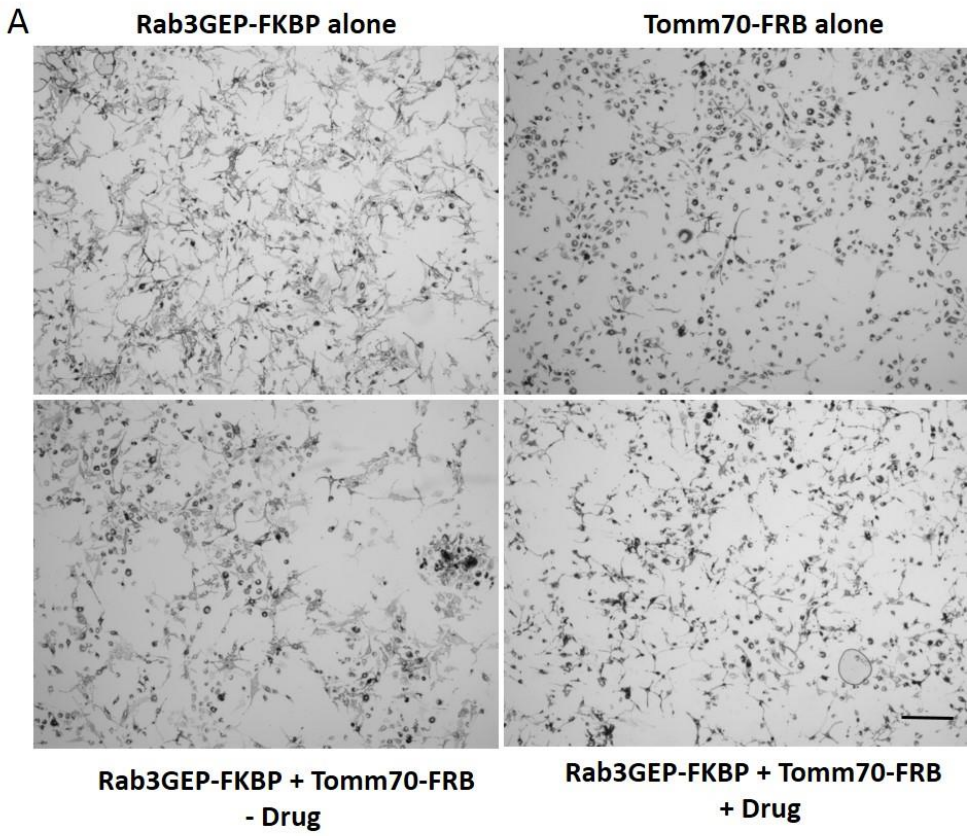
Figure 52 Drug treatment allows the formation of the heterodimer FKBP-FRB and co-localisation of Rab3GEP with Tomm70

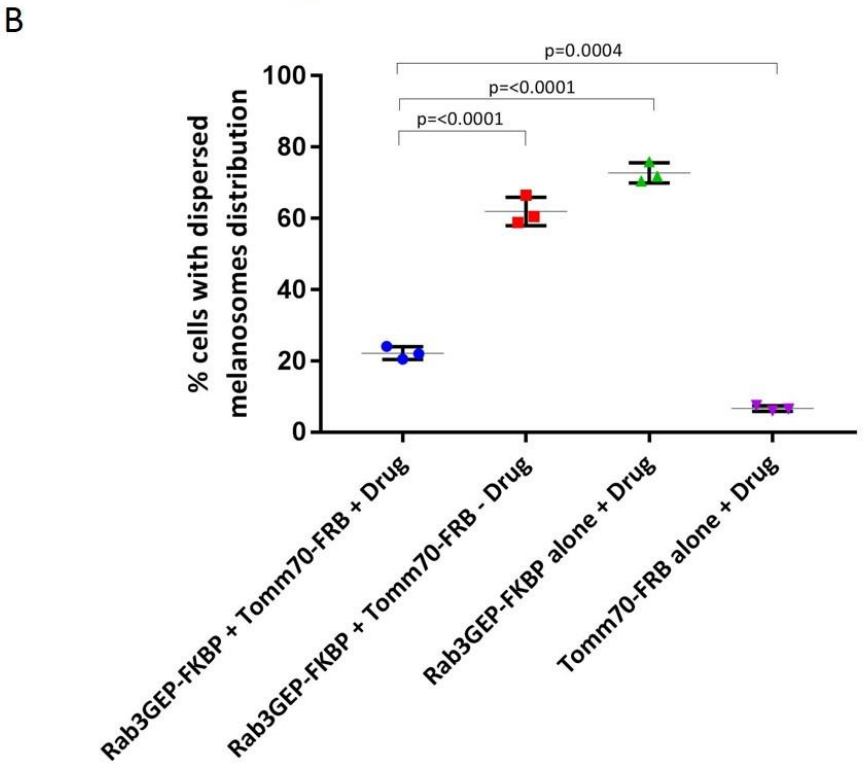
melan- Rab3GEP knockout cells were seeded on coverslips and infected with adenoviruses expressing GFP-Rab3GEP-FKBP (Rab3GEP-FKBP) and Tomm70-mCherry-FRB (Tomm70-FRB). After 48hrs, Rapamycin-related small molecule was added to the medium. Cells were fixed the day after. Top row shows cells expressing Rab3GEP-FKBP, Tomm70-FRB and treated with Rapalog. Second row shows cells infected with Rab3GEP-FKBP, Tomm70-FRB and not treated with Rapalog. Third row shows cells expressing Rab3GEP and treated with drug. The last panel shows cells expressing only Tomm70-FRB and treated with Rapalog. Left column shows Phase contrast images, next to it, the second column shows GFP signal, the third column shows mCherry signal and the last column on the right shows the merge signal between GFP and mCherry. Scale bar 20µm

Cells co-infected with adenoviruses expressing GFP-Rab3GEP-FKBP, Tomm70-mCherry-FRB and not treated with Rapalog (second panel Figure 52) show disperse distribution of GFP signal, and on the other hand restricted distribution of Tomm70-mCherry-FRB representative of mitochondrial distribution. This indicates that the two parts of the heterodimer FKBP-FRB cannot bind together in absence of the Rapalog drug, and that GFP-Rab3GEP-FKBP preserved the cytoplasmic localisation like GFP-Rab3GEP (third panel). Moreover, rescue of melanosome distribution was observed in

phase contrast images, demonstrating the ability of GFP-Rab3GEP-FKBP to rescue melanosome distribution when is localised in the cytosol (Figure 52). In cells, co-expressing GFP-Rab3GEP-FKBP, Tomm70-mCherry-FRB and treated with A/C heterodimeriser, mCherry and GFP signals were co-localised as shown in the merge, indicating that the dimer FKBP-FRB was formed (Figure 52). Nevertheless, phase contrast image shows only a partial clustering melanosome distribution. One possible explanation for this may be that before adding the drug Rab3GEP was in the cytosol and its activity could have allowed the rescue of the melanosome distribution. Therefore, addition of the drug with consequent re-targeting of Rab3GEP could not overcome the earlier activation of the melanosome trafficking machinery. Positive control Rab3GEP-GFP is able to rescue the wild type phenotype melanosome distribution even if treated with the drug as can be seen in the phase contrast, suggesting no influence of the Rapamycin-related drug on melanosome distribution. Cells infected with only Tomm70-mCherry-FRB and treated with the drug maintain the clustering (phase contrast) and Tomm70 is localised to mitochondria, indicating that Tomm70-FRB alone has no activity in melanosome distribution.
This experiment suggests that the FKBP-FRB system is working and that Rab3GEP can be re-located to the mitochondria. Nevertheless, the re-distribution of Rab3GEP does not cause melanosome clustering in these conditions. This may be due to the activity of the free Rab3GEP-FKBP which could be able to target and activate Rab27a causing the activation of the melanosome trafficking, and only subsequently, it is mis-located to the mitochondria by the Rapalog.

In order to prevent the cytosolic free localisation of the new translated GFP-Rab3GEP-FKBP, melan-Rab3GEP KO cells were incubated with the Rapalog at the same moment of adenoviruses infection, so that Rab3GEP was immediately targeted to mitochondria thereby diminishing the chance for Rab3GEP-FKBP to act in the cytosol. This *modus operandi* allowed us to establish whether the disperse distribution of melanosomes seen in the previous experiment in cells expressing GFP-Rab3GEP-FKBP and Tomm70-mCherry-FRB was due to activity of the free Rab3GEP (Figure 53).


A
Rab3GEP-FKBP alone
Tomm70-FRB alone
Rab3GEP-FKBP + Tomm70-FRB
- Drug
Rab3GEP-FKBP + Tomm70-FRB
+ Drug


B
p=0.0004
p=<0.0001
p=<0.0001
% cells with dispersed melanosomes distribution
100
80
60
40
20
0
Rab3GEP-FKBP + Tomm70-FRB + Drug
Rab3GEP-FKBP + Tomm70-FRB - Drug
Rab3GEP-FKBP alone + Drug
Tomm70-FRB alone + Drug

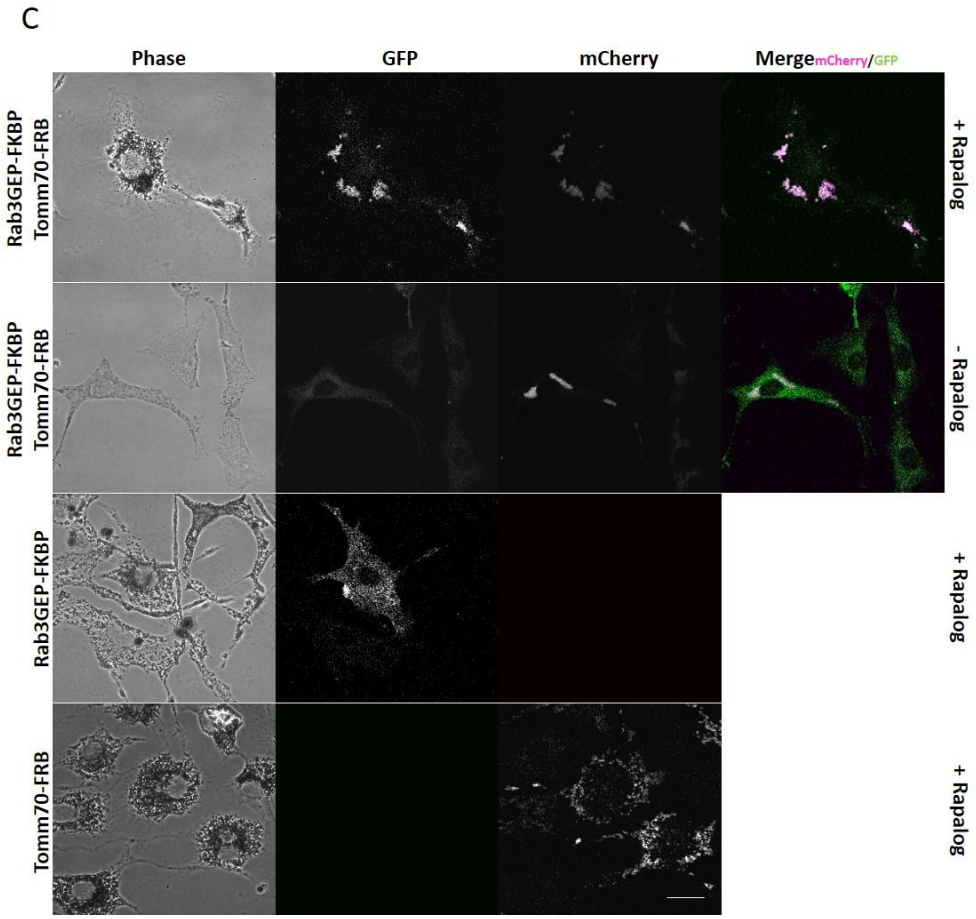


Figure 53 Formation of the heterodimer Rab3GEP-FKBP-FRB-Tomm70 reduces the percentage of cells with disperse melanosome distribution

melan-Rab3GEP KO cells were seeded onto coverslips, infected with adenoviruses as annotated in the figure, and 20nM Rapalog drug was added to the medium at the same time, except one sample co-infected with adenovirus expressing GFP-Rab3GEP-FKBP (Rab3GEP-FKBP) and Tomm70-mCherry-FRB (Tomm70-FRB). The day after, A) bright-field images were taken for each condition. Scale bar 200μm. B) Quantification of the percentage of cells with rescued melanosome distribution C) Confocal images of cells infected with the indicated adenoviruses in the presence/absence of Rapalog. Scale bar 20μm.

Low magnification images (using 4X objective) shown in Figure 53A indicate that GFP-Rab3GEP-FKBP rescued melanosome distribution better than Tomm70-mCherry-FRB as predicted. In fact, 72.7% of cells presented dispersed melanosome distribution when express GFP-Rab3GEP-FKBP, while only 6.7% when express Tomm70-mCherry-FRB (Figure 53B). This indicates that Rab3GEP fused with FKBP is able to rescue melanosome distribution, instead Tomm70-mCherry-FRB has no effect on melanosome distribution. Moreover, although the co-expression of GFP-Rab3GEP-FKBP and Tomm70-mCherry-FRB increase the percentage of rescued cells to 61.9% (Figure

53B), incubation with Rapalog inhibits the augmentation of this percentage maintaining it at 22.2%.
High magnification images obtained with confocal microscopy indicate clearly that Rab3GEP-FKBP is expressed and present a dispersed distribution throughout the cytosol in cells singularly infected with this adenovirus (Figure 53C third panel). Moreover, dispersed melanosome distribution seen in phase contrast image indicates clearly that cytoplasmic Rab3GEP-FKBP is functional, and it is able to restore the wild type phenotype.

Cells co-expressing both GFP-Rab3GEP-FKBP and Tomm70-mCherry-FRB in the absence of Rapalog (Figure 53C second panel) presented dispersed melanosome distribution. Moreover, GFP and mCherry detected signals indicate clearly that GFP-Rab3GEP-FKBP and Tomm70-mCherry-FRB presented a different distribution in the cell, localised in mitochondria organelles in the case of Tomm70-mCherry-FRB and dispersed throughout the cytosol in the case of GFP-Rab3GEP-FKBP. On the other hand, incubation with Rapalog induce co-localisation of GFP-Rab3GEP-FKBP and Tomm70-mCherry-FRB as it possible to see in the merge image (Figure 53C first row). This confirms once more that Rapalog is able to form the heterodimer GFP-Rab3GEP-FKBP-FRB-mCherry-Tomm70, therefore, GFP-Rab3GEP-FKBP is subtract from the cytosol and re-located to the mitochondria where Tomm70-mCherry-FRB is based. Interestingly, these cells maintained the clustered distribution of melanosomes around the nucleus, indicating that although GFP-Rab3GEP-FKBP is functional (as seen in Figure 53C second and third panels) its re-location from cytosol to mitochondria inhibits its function in melanosome trafficking. This suggests that the rescue of transport seen in the previous experiment (Figure 52) was due to the presence of Rab3GEP in the cytosol prior to the addiction of Rapalog. The last panel of Figure 53C shows that although Tomm70-mCherry-FRB was expressed in cells, melanosome clustering was maintained, indicating no effect of this construct on melanosome trafficking.

These experiments suggest that re-location of Rab3GEP to the mitochondria in not able to restore the wild type phenotype and that the cytosolic distribution of Rab3GEP is important for the its function in melanosome trafficking. However, temporary localisation of Rab3GEP in the cytosol is able to activate the melanosome trafficking as shown by the difference between the first and second experiment, indicating that Rab27a in the active state remains in the melanosome membrane for more than sixteen hours.

5.3 Rab27a follows Rab3GEP to mitochondrial localisation

In the previous section, evidence suggest that the mitochondrial relocation of GFP-Rab3GEP-FKBP upon Rapalog treatment is unable to restore the disperse melanosome distribution in melan-Rab3GEP KO cells. Hence, the role of Rab3GEP localisation in its function was tested directly by targeting it away from the cytosol. Moreover, in order to determine more directly whether Rab3GEP is a Rab27a targeting factor, localisation of the RabGTPase was investigated when Rab3GEP is re-targeted to mitochondria. For this purpose, adenovirus expressing GFP-Rab3GEP directly fused with Tomm70 at the N terminus was made and an adenovirus expressing mCherry-Rab27a was used in order to relocate Rab3GEP to the mitochondria and to visualise Rab27a localisation through the mCherry signal.

In order to establish whether the chimeric protein Tomm70-GFP-Rab3GEP was targeted to mitochondria, co-localisation with Mito-tracker was investigated. As a control was used GFP instead of Tomm70-GFP-Rab3GEP (Figure 54).

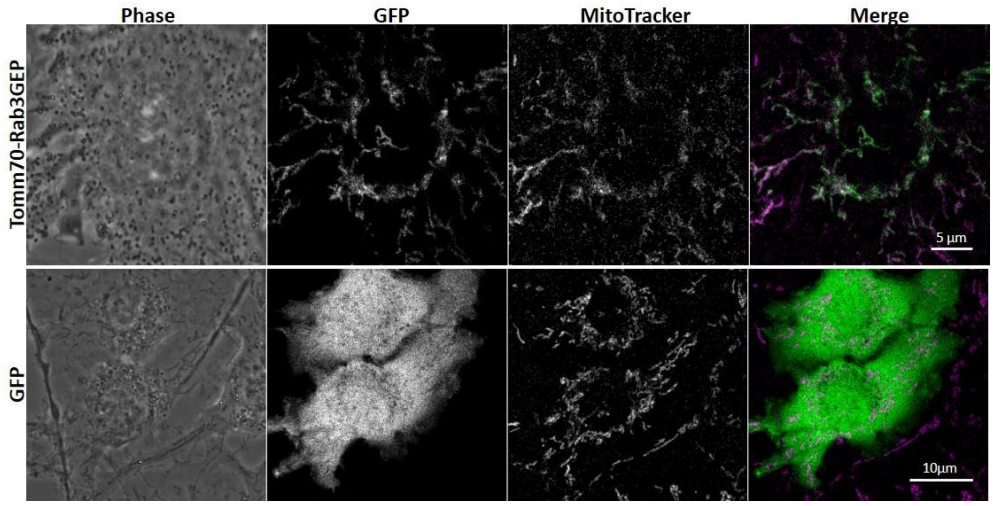


Figure 54 Tomm70-GFP-Rab3GEP is localised to mitochondria

melan-Rab3GEP KO cells were seeded in 4 well plate and infected either with Tomm70-GFP-Rab3GEP (Tomm70- Rab3GEP) or GFP. Two days after, when GFP emission was detected, the medium was replaced with new medium containing 400nM of Red MitoTracker. Cells were left in the incubator for 20 mins. Then confocal live images were taken using phase contrast, green and red channels.

Results of the experiment shown in Figure 54 indicates clearly that the Tomm70-GFP-Rab3GEP chimeric protein was localised to the mitochondria. The merge image of the top panel shows that GFP signal of the fused protein Tomm70-GFP-Rab3GEP is colocalised with the red signal emitted by the MitoTracker. Instead in the cells expressing GFP control there is no colocalisation between the GFP and the MitoTracker signals.

In order to determine whether the chimeric protein Tomm70-GFP-Rab3GEP was unable to restore the melanosome distribution, comparison of the percentage of rescued cells was done between melan-Rab3GEP KO cells expressing either Tomm70-GFP-Rab3GEP or GFP-Rab3GEP wild type, the second used as positive control for the dispersion (Figure 55).

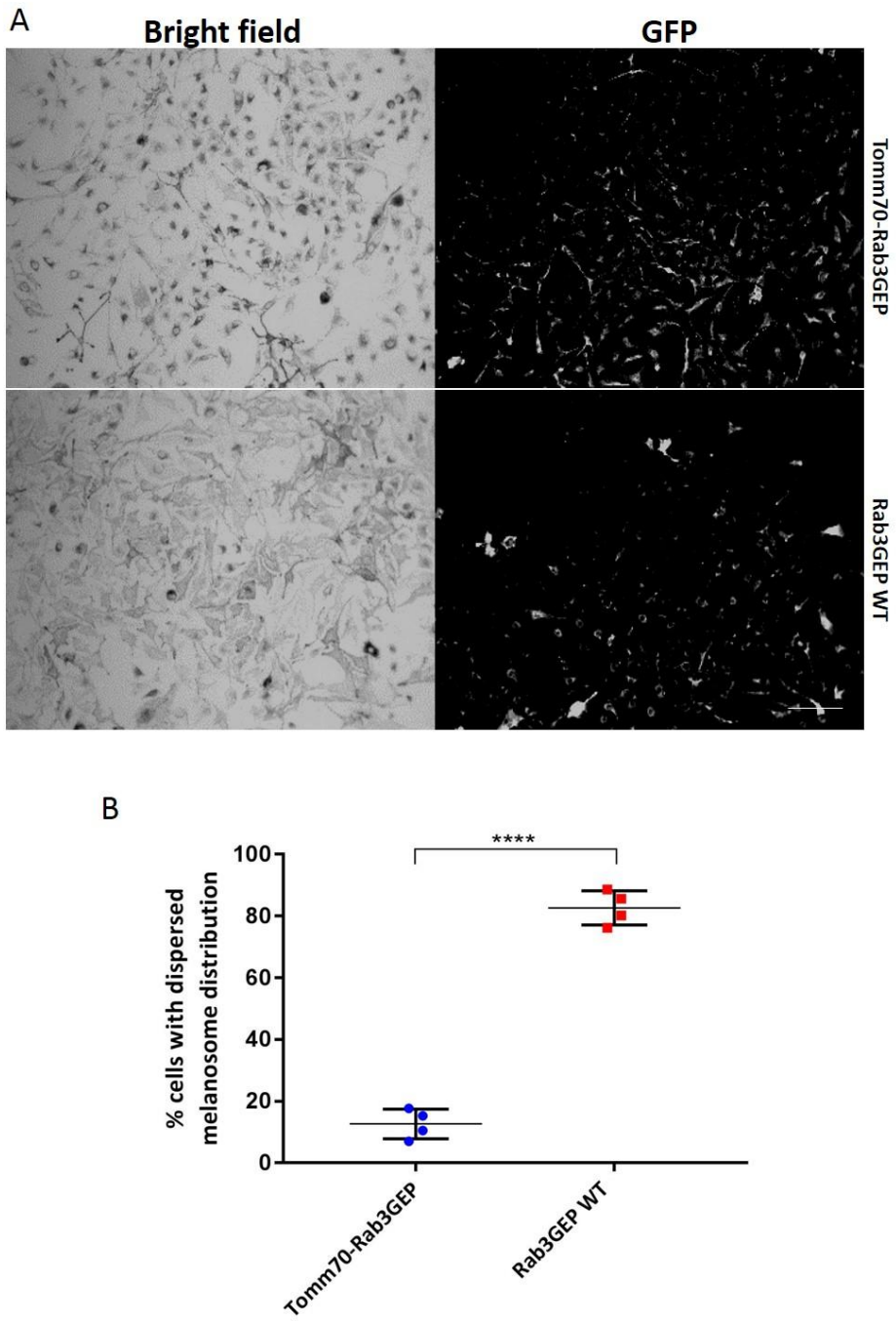
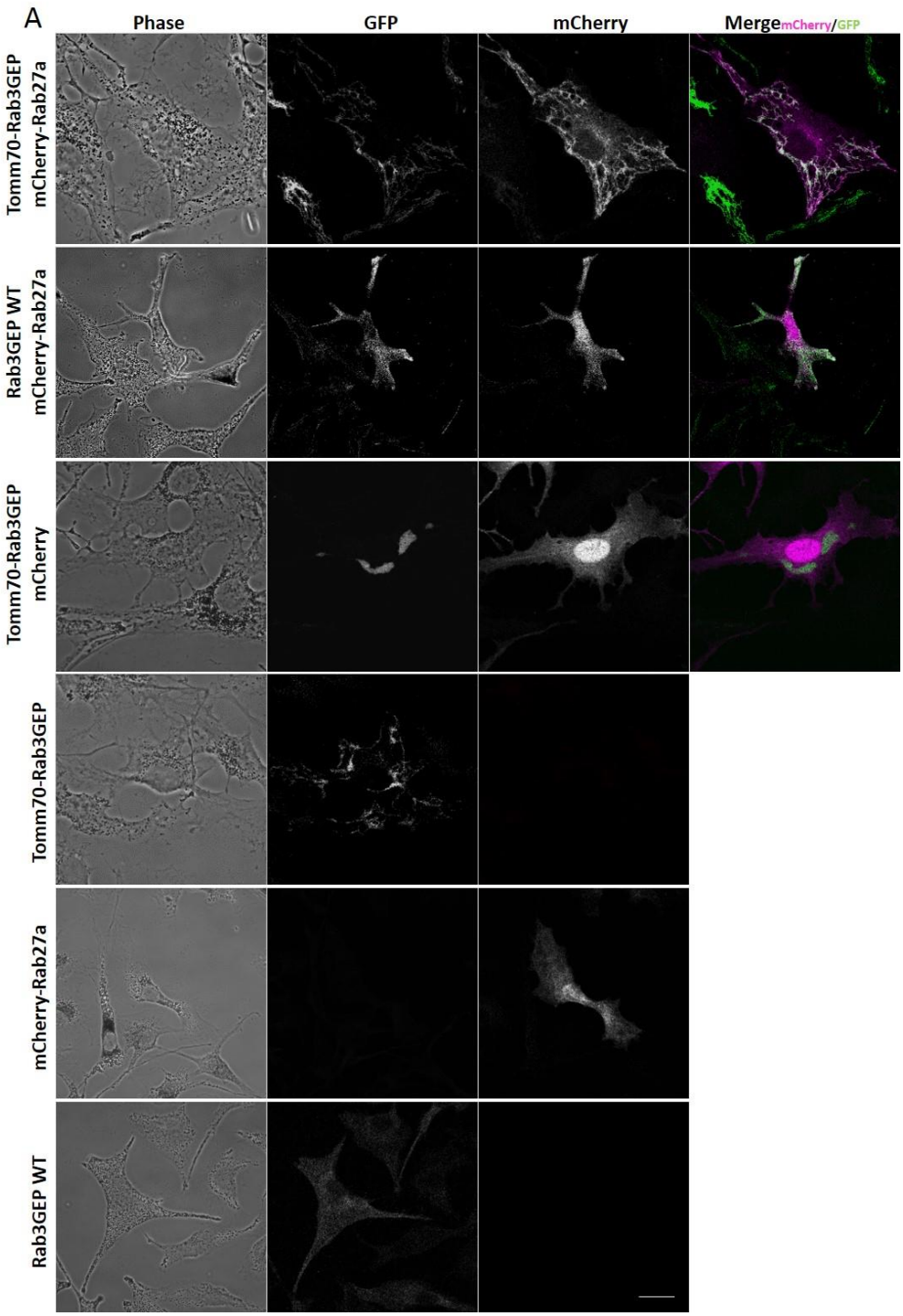


Figure 55 Expression of Tomm70-GFP-Rab3GEP protein does not restore melanosome distribution in melan-Rab3GEP KO cells

melan-Rab3GEP knockout cells were seeded on a 4 well plate and infected with adenovirus expressing Tomm70-GFP-Rab3GEP (Tomm-Rab3GEP) or GFP-Rab3GEP (Rab3GEP). Images were taken 48 hours after the infection. A) On the left bright field images of cells expressing either Tomm70-GFP-Rab3GEP (top) or GFP-Rab3GEP (bottom) proteins. On the right GFP expression of these proteins as indicated. Scale bar 150µm. B) Quantification of percentage of cells with dispersed melanosome distribution p value = <0.0001.

The bright field images in Figure 55A indicate that cells expressing GFP-Rab3GEP wild type present a higher population of cells with dispersed melanosome distribution than cells expressing Tomm70-GFP-Rab3GEP. In fact, quantification of the cell phenotype (Figure 55B) indicate that 80.6% of melan-Rab3GEP knockout cells infected with GFP-Rab3GEP show wild type phenotype with melanosomes disperse throughout the cell cytoplasm, suggesting that the endogenous Rab27a and the anterograde melanosome trafficking has been activated. Instead, only 13.4% of cells expressing the Tomm70-GFP-Rab3GEP present dispersed melanosome distribution. This can be due either to the lack of activation of Rab27a as consequence of the absence of its GEF in the cytosol, or to a mis-targeting of the endogenous Rab27a, which is unable to target melanosome membrane anymore, or to both inactive Rab27a targeted to another organelle rather than melanosome.

To better understand whether the mitochondrial localisation of Rab3GEP induces mis-targeting of Rab27a with possible colocalisation of the two proteins at the mitochondria membrane, melan-Rab3GEP knockout cells were co-infected with adenoviruses expressing Tomm70-GFP-Rab3GEP and mCherry-Rab27a. As negative control for the mitochondrial localisation of Tomm70-GFP-R3G was used GFP-Rab3GEP wild type which is scattered throughout the cytosol. Moreover, as negative control for the binding/localisation of mCherry-Rab27a was used mCherry which does not bind with Rab3GEP and it is dispersed in the cytosol. Combinations used are indicated in the Figure 56.


A
Phase
GFP
mCherry
Merge mCherry/GFP
Tomm70-Rab3GEP mCherry-Rab27a
Rab3GEP WT mCherry-Rab27a
Tomm70-Rab3GEP mCherry
Tomm70-Rab3GEP
mCherry-Rab27a
Rab3GEP WT

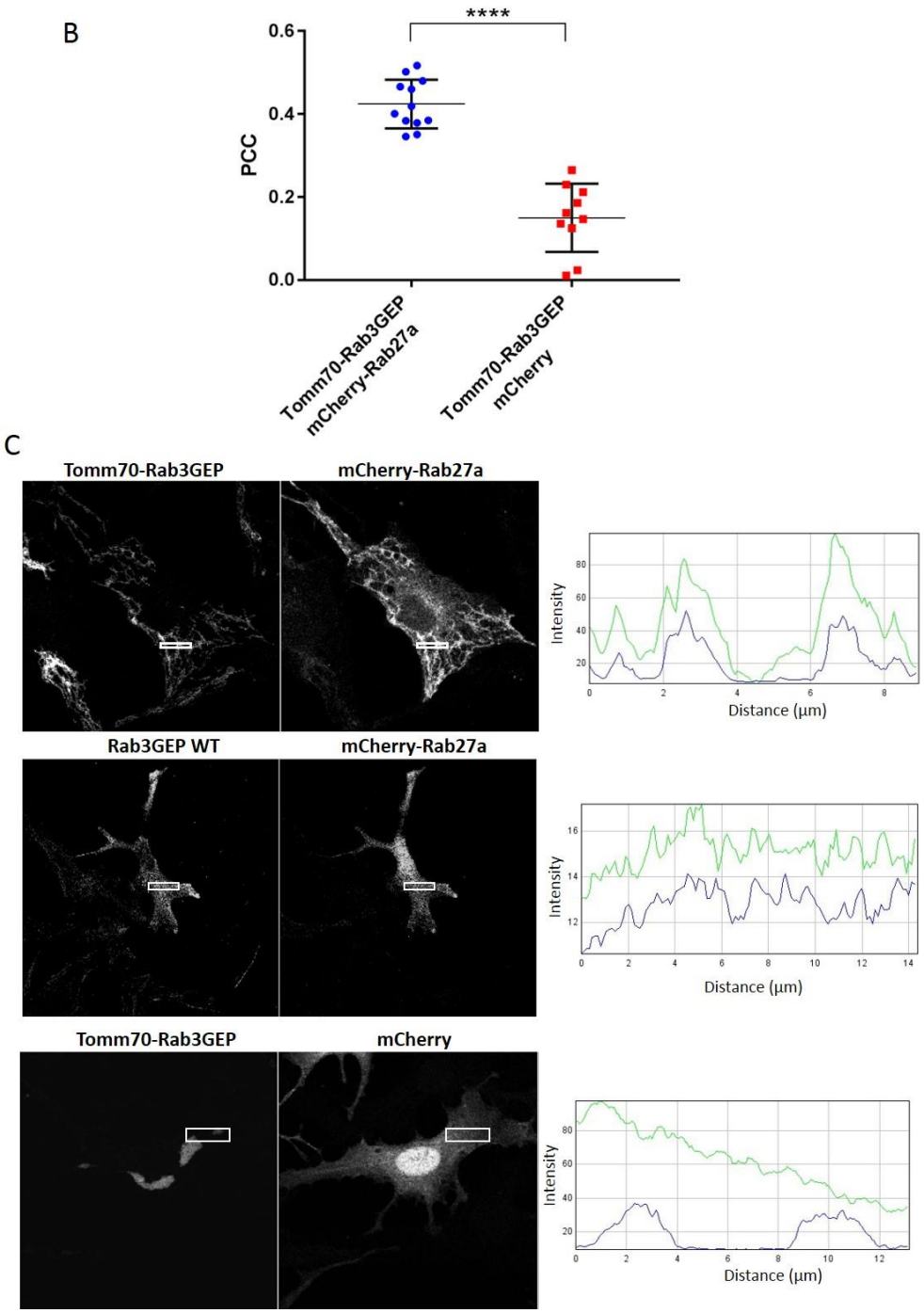


Figure 56 Expression of Tomm70-GFP-Rab3GEP in melan-Rab3GEP KO cells results in mis-targeting of Rab27a to mitochondria

A) melan-Rab3GEP KO cells were grown on coverslips and infected with adenoviruses as indicated on the left. Cells were fixed after 48hrs. Columns show Phase contrast, GFP signal, mCherry signal and Merge GFP/mCherry as indicated on the top. Scale bar 20µm. B) Scatter plot shows quantification colocalisation Rab3GEP-Tomm70 and mCherry-Rab27a *versus* negative control Rab3GEP-Tomm70 and mCherry using Peason's coefficient for a population of cells (10-12 cells quantified) (****) p=<0.0001. C) GFP and mCherry signal intensity in a defined area (white boxes). On the left and in the middle respectively GFP and mCherry emissions in the cell. On the right graphs show the change of intensity of

GFP (green line) and mCherry (blue line) within the selected area (white box in cell images).

Results obtained in this experiment indicate once more that Tomm70-GFP-Rab3GEP is not able to rescue the disperse melanosome distribution, in fact in phase contrast images (Figure 56A) cells overexpressing this fusion protein preserve the melanosome clustering. Instead, cells overexpressing Rab3GEP wild type restore the dispersed melanosome distribution. Cells expressing only mCherry-Rab27a maintained the melanosome clustered distribution, consistent with importance of the GEF to activate Rab27a and therefore the anterograde melanosome trafficking.

GFP images indicate that Tomm70-GFP-Rab3GEP is not dispersed throughout the cytosol as Rab3GEP wild type but it is distributed in a cytoplasmic tubular network consistent with its being targeted to mitochondria. Furthermore, GFP signal of this fusion protein co-localise with MitoTracker as seen in Figure 54 which indicate mitochondria localisation. mCherry signal present partial localisation in a restricted area in cell co-expressing Tomm70-GFP-Rab3GEP and mCherryRab27a. Moreover, merge image shows that similar pattern distribution is present between GFP and mCherry signals suggesting partial co-localisation between Tomm70-GFP-Rab3GEP and mCherryRab27a (Figure 56A first row). Instead, cells overexpressing mCherryRab27a in the presence of Rab3GEP wild type (second row) or alone (fifth panel) display scattered emission of mCherry signal throughout the cell body. Further confirmation of the specificity of the colocalisation between Tomm70-GFP-Rab3GEP and mCherryRab27a can be seen in the third panel (Figure 56A) in which Tomm70-GFP-Rab3GEP is localised in particular areas of the cell while mCherry appears to be dispersed throughout the cytoplasm.

Level of colocalisation between GFP and mCherry signals in population of cells shown in Figure 56B indicates that there is a significant difference in the PCC (Peason's correlation coefficient) with a P value=<0.0001 between cells overexpressing Tomm70-GFP-Rab3GEP/mCherryRab27a and cells overexpressing Tomm70-GFP-Rab3GEP/mCherry.
Furthermore, analysis of the signal intensity in a defined area of the cell (Figure 56C) indicates that there is positive correlation between GFP and mCherry intensity in cell co-expressing Tomm70-GFP-Rab3GEP and

mCherryRab27a as seen in the intensity plot. In fact, increase of signal between 2-4 and 6-8 μm of the selected area of the GFP (blue line) is mirrored by the increase of the mCherry (green line) signal. Instead in cells co-expressing Tomm70-GFP-Rab3GEP and mCherry there is no evident correlation between the two signals, in fact although the GFP (blue line) signal increase twice between 1-3 and 8.5-12 μm of the selected box there is no concomitant increase of the mCherry signal (green line). In the cell overexpressing GFP-Rab3GEP and mCherry-Rab27a there is no evidence of correlation but this could be due to the uniformly dispersion of the two signals throughout the cell body.

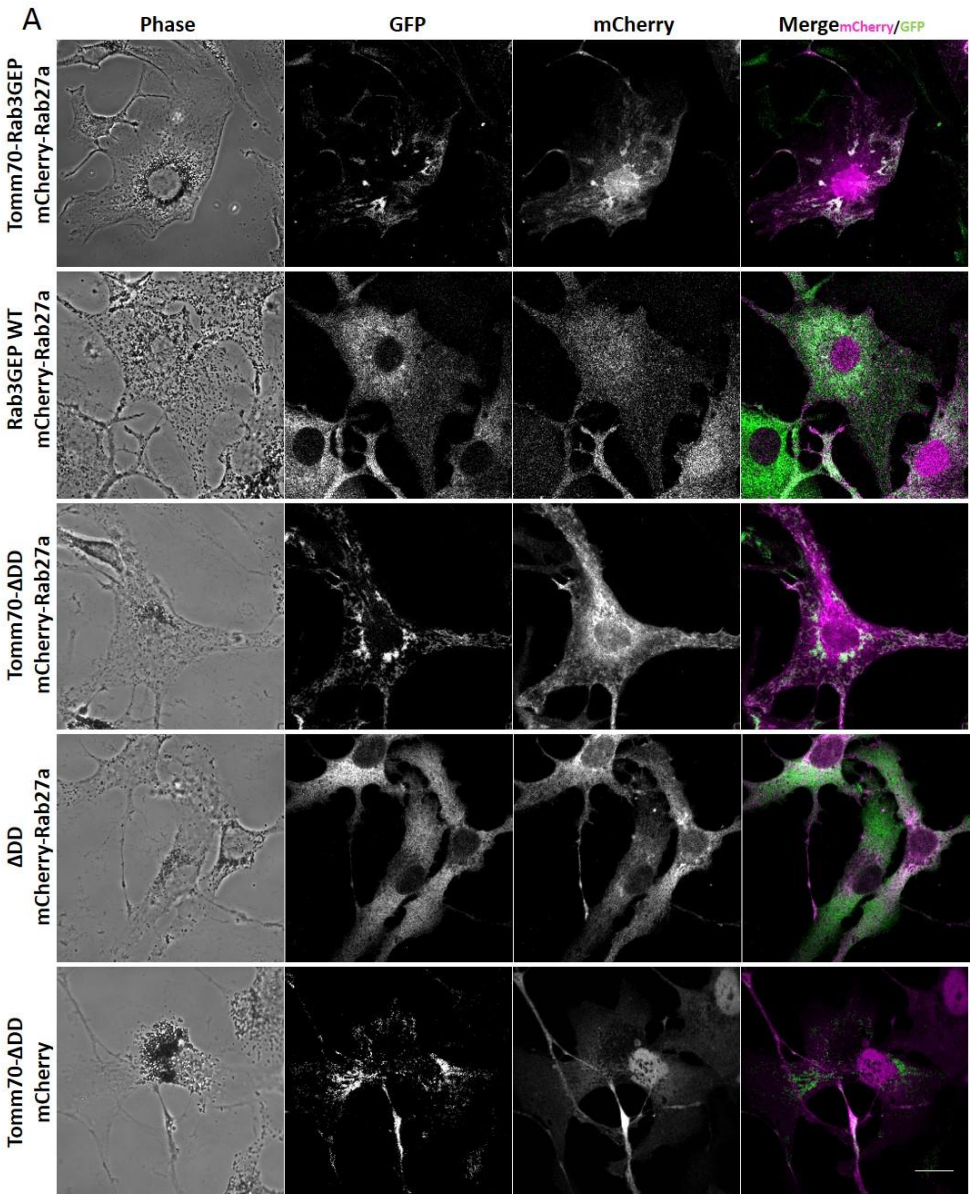
This experiment confirms the suggestion that Rab3GEP localisation is crucial for the proper functioning of the melanosome trafficking. Furthermore, mis-localisation of Rab3GEP leads to mis-localisation of Rab27a, which follows the guanine exchange factor localisation. Hence, Rab27a follows Rab3GEP to mitochondria but in this localisation cannot function normally.

5.4 Deletion of the Death Domain of Rab3GEP abolish its capacity to target Rab27a

Results obtained in section 5.3 indicate that the re-targeting of Rab3GEP causes a mis-target of Rab27a which follows its GEF to the mitochondria. Moreover, data shown in chapter 4 indicate that truncations of Rab3GEP full length block its GEF activity for Rab27a. In this section, it will be explored whether the truncations still are able to re-target Rab27a in a different organelle as the full length, although they have lost the GEF activity as seen in chapter 4. In other words, the link between GEF activity and targeting behaviour of Rab3GEP will be investigated.

Considering that the deletion of the Death domain impairs the GEF activity of Rab3GEP for Rab3 as suggested by Coppola et al. (87) as well as towards Rab27a as shown in chapter 4, the truncation mutant ΔDD was used to investigate the link between the GEF activity and the role in targeting of Rab3GEP for Rab27a. This mutant protein still contains the DENN domain, and the linker region between the DENN domain and the Death domain. Therefore, this mutant allows to explore possible role of the Death domain and its importance in targeting of Rab27a.

For this purpose, an adenovirus that is able to express the chimeric protein Tomm70-GFP-ΔDD was made and its role in Rab27a targeting and on melanosome distribution was investigated, with similar approach used in the previous section 5.3.


A
Phase
GFP
mCherry
Merge mCherry/GFP
Tomm70-Rab3GEP mCherry-Rab27a
Rab3GEP WT mCherry-Rab27a
Tomm70-ΔDD mCherry-Rab27a
ΔDD mCherry-Rab27a
Tomm70-ΔDD mCherry

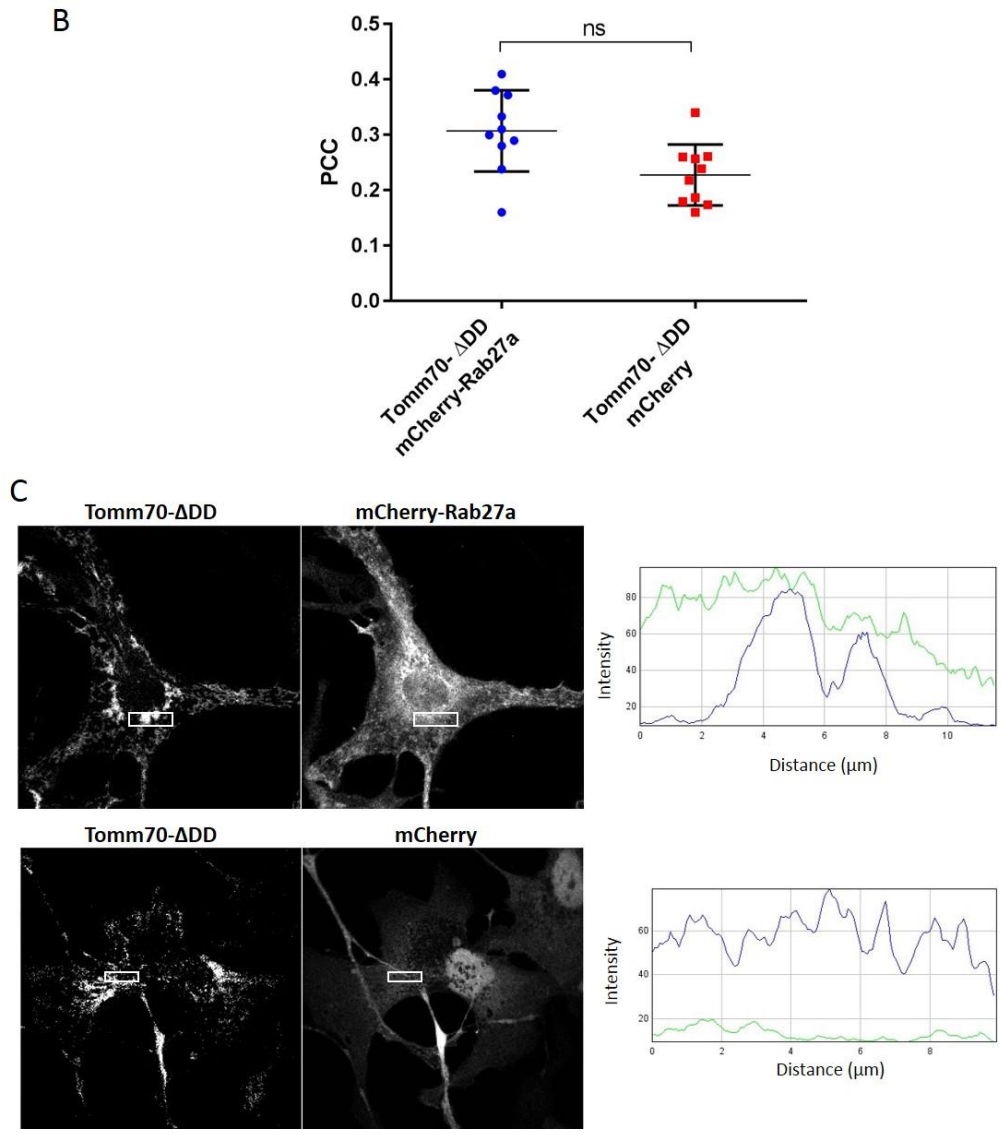


Figure 57 ΔDD truncation loss the capacity to re-target Rab27a to mitochondria

melan-Rab3GEP KO cells were grown on coverslips and infected with adenoviruses expressing Tomm70-GFP-Rab3GEP (Tomm70-Rab3GEP), mCherry-Rab27a, GFP-Rab3GEP wild type (Rab3GEP WT), Tomm70-GFP-ΔDD (Tomm70-ΔDD), ΔDD, mCherry as indicated on the left side of A. Cells were fixed after 48hrs. Columns show Phase contrast, GFP signal, mCherry signal and Merge GFP/mCherry as indicated on the top. Scale bar 20μm. B) Scatter plot shows quantification colocalisation Tomm70-ΔDD/mCherry-Rab27a *versus* negative control Tomm70-ΔDD/mCherry using Pearson's correlation coefficient for a population of cells (10-12 cells quantified) (****) p=<0.0001 ns=non-significance. C) GFP and mCherry signal intensity in a defined area (white boxes). On the left and in the middle respectively GFP and mCherry emissions in the cell. On the right graphs show the change of intensity of GFP (green line) and mCherry (blue line) within the selected area (white box in cell images).

Phase contrast images shown in Figure 57A indicate that neither Tomm70-GFP-Rab3GEP, Tomm70-GFP-ΔDD nor ΔDD were able to restore the disperse melanosome distribution, confirming that the free cytosolic localisation of Rab3GEP is essential for its activity and that the ΔDD truncation mutant is non-functional. The only construct that was able to rescue the melanosome distribution was Rab3GEP wild type.

Cells expressing Rab3GEP wild type and ΔDD presented scattered GFP signal showing no specific localisation in the cytoplasm, while in cells expressing either Tomm70-GFP-Rab3GEP or Tomm70-GFP-ΔDD the GFP signal was filamentous and located to specific areas of the cytoplasm suggesting the mitochondria localisation.

mCherry signal presented in the cell co-expressing Tomm70-GFP-Rab3GEP and mCherryRab27a is localised and partially overlap the GFP signal indicating co-localisation between Tomm70-GFP-Rab3GEP and mCherryRab27a and confirming the previous results obtained in section 5.3. Instead, in the cell co-expressing Tomm70-GFP-ΔDD and mCherryRab27a the mCherry signal is scattered throughout the cytoplasm while the GFP signal is in restricted areas suggesting no colocalisation between Tomm70-GFP-ΔDD and mCherryRab27a. These observations suggest that Tomm70-GFP-ΔDD loses the ability of Rab3GEP full length to re-target Rab27a, therefore, the Death domain of Rab3GEP is important for Rab27a targeting. Consistent with this observation the cell co-expressing Tomm70-GFP-ΔDD and mCherry presented a mCherry signal dispersed throughout the cytoplasm like the mCherry signal of the cell expressing Tomm70-GFP-ΔDD and mCherryRab27a confirming the lack of activity in retargeting of ΔDD for the RabGTPase protein.

Statistical comparison of the results obtained are shown in Figure 57B where PCC was measured in a population of cells co-expressing either Tomm70-GFP-ΔDD/mCherryRab27a or Tomm70-GFP-ΔDD/mCherry. Scatter plot displays that there is no significant difference between Tomm70-GFP-ΔDD/mCherryRab27a and its negative control Tomm70-GFP-ΔDD/mCherry, confirming that Tomm70-GFP-ΔDD is not able to retarget Rab27a.
However, the mean of the PCC of the samples co-expressing Tomm70-GFP-ΔDD/mCherry is 0.227, which is higher than the mean of Tomm70-GFP-Rab3GEP/mCherry which is 0.149 shown in Figure 56. Nevertheless, the PCC

of Tomm70-GFP-Rab3GEP/mCherry-Rab27a is 0.424 (Figure 56) is higher than Tomm70-GFP-ΔDD/mCherryRab27a which is 0.307. This may be due to a higher proportion of the chimeric protein Tomm70-GFP-ΔDD free in the cytosol compared to Tomm70-GFP-Rab3GEP, which would increase the colocalisation coefficient considering that Rab27a and mCherry are free in the cytosol as well. This hypothesis would suggest that the Tomm70-GFP-ΔDD protein is less able to bind the mitochondria than the full length Tomm70-GFP-Rab3GEP.

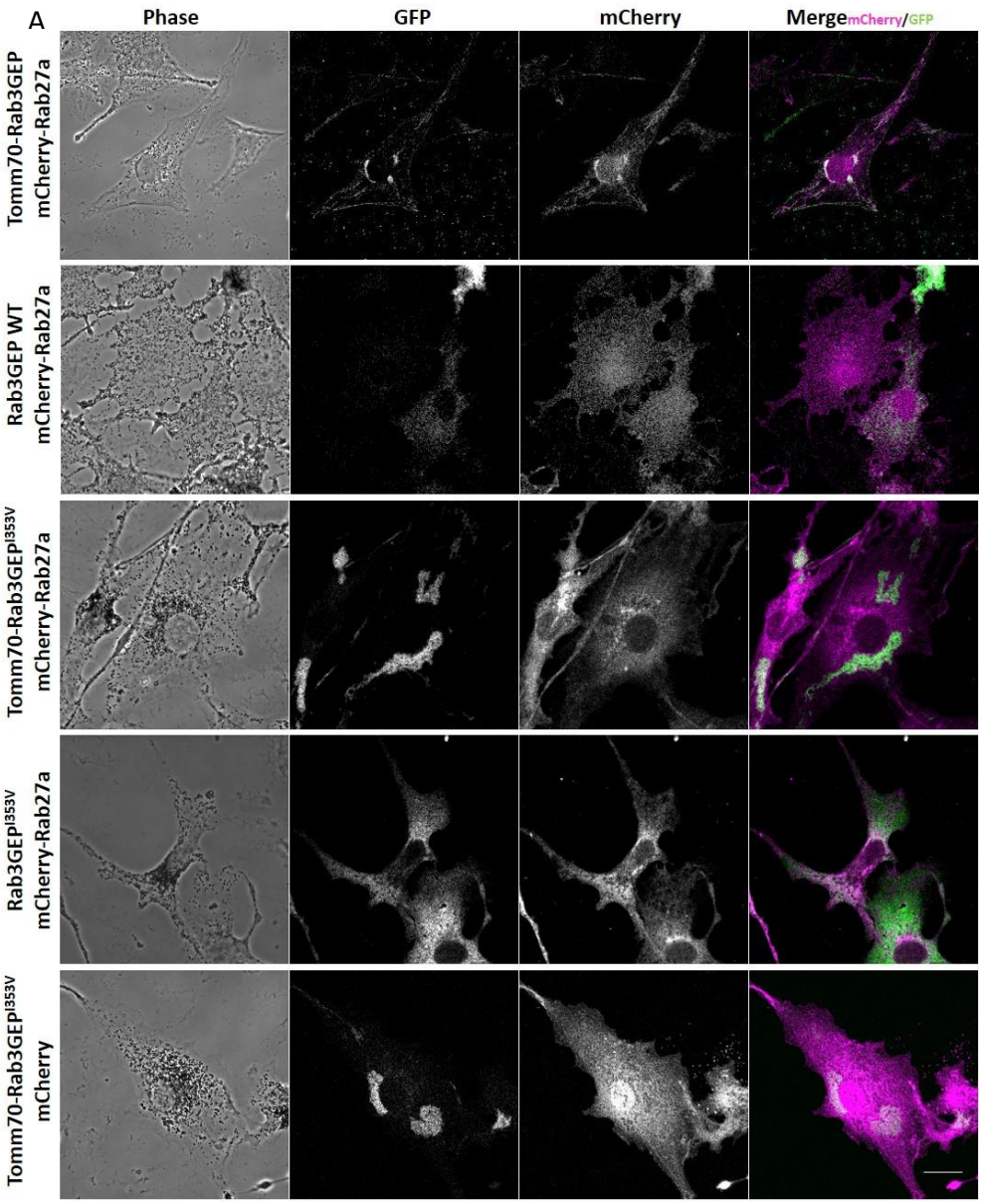
GFP/mCherry profile plot of the intensity measured in a defined area is shown in Figure 57C. In this case, the graph indicates clearly that although there is an increase of the GFP intensity (blue line) it is not correlated with an increase of mCherry signal. Hence, Rab27a and Tomm70-GFP-ΔDD are not strongly colocalised. This analysis revealed similar lack of colocalisation between Tomm70-GFP-ΔDD and mCherry (Figure 57C).

Overall these results indicate that the deletion of the Death domain in Rab3GEP not only lack its GEF activity but also lose the capacity to target Rab27a.

5.5 I353V point mutation reduce the capacity to re-target Rab27a to mitochondria

This section will investigate the targeting ability of a point mutant of the Rab3GEP full-length which lack the GEF activity. This experiment would allow to understand more directly whether the GEF activity of Rab3GEP is linked with its capacity to target Rab27a. The use of the full-length protein reduces the chance of an incorrect folding of the protein that truncation can promote, conferring a more accurate understanding of the behaviour of Rab3GEP in targeting and activation of Rab27a.
For this purpose, it was chosen the point mutant Rab3GEP^{I353V} because 1) a single mutation is present, reducing mis-folding probability of the protein, 2) this mutation correspond with the Isoleucine in position 226 of the DENND1B domain of Connecdenn protein that is present in the binding site I, 3) Western blot in Figure 42 shows no degradation of the protein, therefore, single band at the same molecular weight of Rab3GEP wild type, 4) results from cell based assays indicate that this mutant do not rescue the melanosome disperse distribution (section 4), 5) pull down assay indicates that this mutant has lost the GEF activity towards Rab27a (section 4.4.3).

Hence, adenovirus expressing the chimeric protein Tomm70-GFP-Rab3GEP^{I353V} was made, and it was tested in melan-Rab3GEP KO cells using same approach used for the truncation mutant Tomm70-GFP-ΔDD (Figure 58).


A
Phase
GFP
mCherry
Merge mCherry/GFP
Tomm70-Rab3GEP mCherry-Rab27a
Rab3GEP WT mCherry-Rab27a
Tomm70-Rab3GEP I353V mCherry-Rab27a
Rab3GEP I353V mCherry-Rab27a
Tomm70-Rab3GEP I353V mCherry

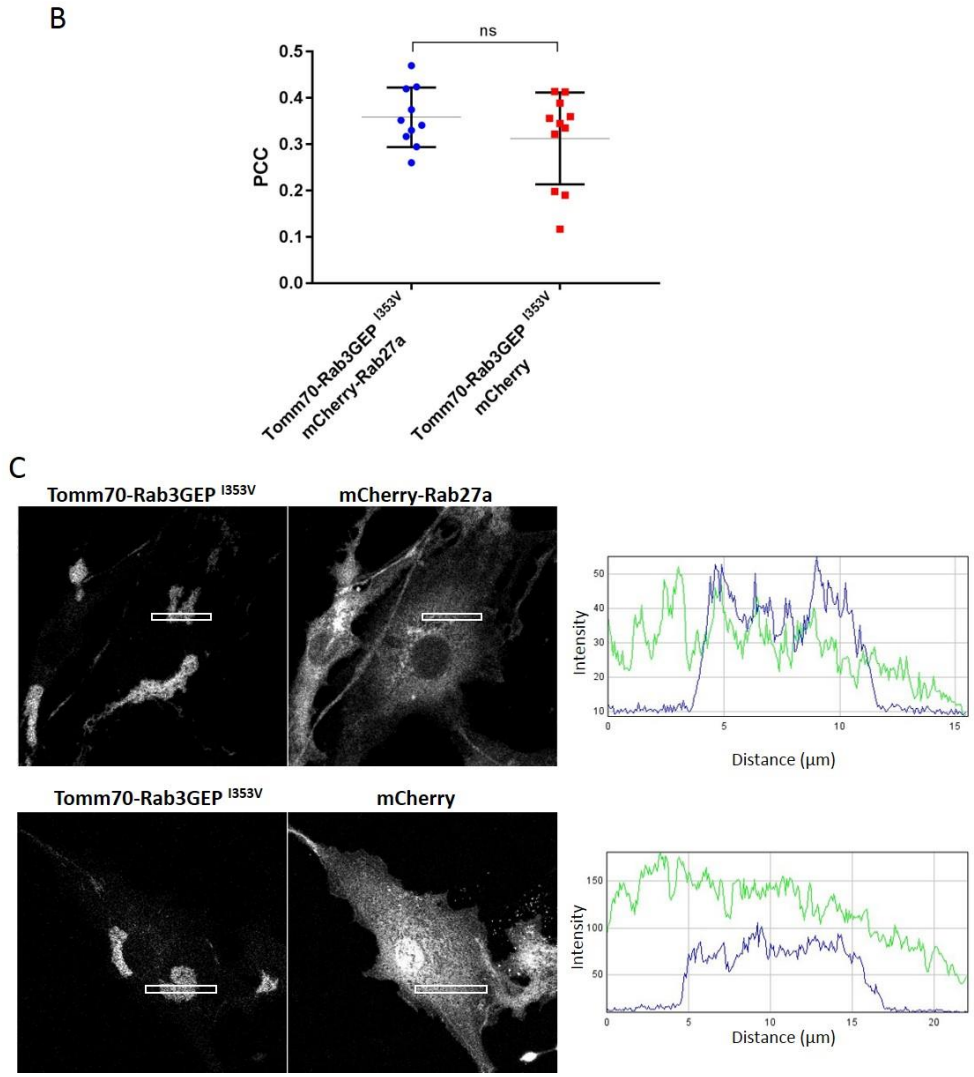


Figure 58 Point mutant Rab3GEP^{I353V} loss the capacity to re-target Rab27a to mitochondria

A) melan-Rab3GEP KO cells were grown onto coverslips and infected with adenoviruses expressing Tomm70-GFP-Rab3GEP (Tomm70-Rab3GEP), mCherry-Rab27a, GFP-Rab3GEP wild type (Rab3GEP WT), Tomm70-GFP- Rab3GEP^{I353V} (Tomm70- Rab3GEP^{I353V}), GFP-Rab3GEP^{I353V} (Rab3GEP^{I353V}) and mCherry as indicated on the left side. Columns show Phase contrast, GFP signal, mCherry signal and Merge GFP/mCherry as indicated on the top. Scale bar 20µm. B) Scatter plot shows quantification of the colocalisation between Tomm70-Rab3GEP^{I353V} /mCherry-Rab27a *versus* negative control Tomm70-Rab3GEP^{I353V}/mCherry using Pearson's correlation coefficient (PCC) for a population of cells (10-12 cells quantified) (****) p value=<0.0001, ns=no significant. C) GFP and mCherry signal intensity in a defined area (white boxes). On the left and in the middle respectively GFP and mCherry emissions in the cell. On the right graphs show the change of intensity of GFP (green line) and mCherry (blue line) within the selected area (white box in cell images).

melan-Rab3GEP KO cells expressing Rab3GEP wild type as predicted presented dispersed melanosome distribution as shown in the phase contrast image in Figure 58A. Furthermore, the cytosolic free mutant Rab3GEP^{I353V} was unable to rescue the dispersed melanosome distribution in melan-Rab3GEP KO cells, confirming the results displayed in section 4.4. Therefore, also the cells expressing Tomm70-GFP-Rab3GEP^{I353V} presented clustered melanosome distribution, suggesting no activation of the melanosome anterograde traffic.

GFP signal indicate that GFP-Rab3GEP wild type and GFP-Rab3GEP^{I353V} proteins are scattered throughout the cytosol, while Tomm70-GFP-Rab3GEP and Tomm70-GFP-Rab3GEP^{I353V} proteins are localised in restricted area of the cells. In the case of the fusion protein Tomm70-GFP-Rab3GEP wild type GFP signal present tubular network shape instead in the case of Tomm70-GFP-Rab3GEP^{I353V} it has clumpy shape.

The mCherry signal in the cell co-expressing Tomm70-GFP-Rab3GEP and mCherry-Rab27a is localised in defined areas that matched with the GFP signal as shown in the merge (white pixels). This result confirms the co-localisation between Rab3GEP wild type and Rab27a. Instead in the cell expressing the chimeric protein Tomm70-GFP-Rab3GEP^{I353V} the mCherry signal is scattered throughout the cytoplasm, although the GFP signal is localised in restricted areas. This indicates that Rab27a is not localised with the point mutant Rab3GEP^{I353V}. Moreover, the negative control mCherry is dispersed like mCherry-Rab27a.

Comparison between the PCC obtained from a population of cells shown in Figure 58B indicates that there is no significance difference between Tomm70-GFP-Rab3GEP^{I353V}/mCherryRab27a and the negative control Tomm70-GFP-Rab3GEP^{I353V}/mCherry. In other words, mutant Tomm70-GFP-Rab3GEP^{I353V} is not able to retarget Rab27a to the mitochondria.

GFP and mCherry signal intensity shown in Figure 58C indicate that although GFP intensity increases between 5 and 10 μm in the area selected in the cell overexpressing Tomm70-GFP-Rab3GEP^{I353V} and mCherryRab27a there is no augmentation of mCherry signal, similarly to the test done in the cell overexpressing Tomm70-GFP-Rab3GEP^{I353V} and mCherry used as a negative

control. This confirm once more that the mutant Rab3GEP^{I353V} has lost the Rab3GEP wild type ability to retarget Rab27a.

5.6 Discussion

In this study, it was investigated the subcellular localisation of Rab3GEP, and evidence indicate that its cytoplasmic localisation is essential for the melanosome trafficking machinery. In order to identify Rab3GEP localisation melan-Rab3GEP knockout cells have been infected with adenovirus able to express Rab3GEP GFP tagged construct. Melanosome dispersion was rescued after infection and GFP signal was scattered throughout the cytosol, this result is in harmony with the previous findings of cytoplasmic distribution of Rab3GEP. In that study overexpression of Rab3GEP was able to restore the dispersed melanosome distribution in wild type melan-a depleted for this GEF, and it presented cytoplasmic localisation (7). To define whether the cytosolic distribution of Rab3GEP is important for its activity this GEF was re-located to mitochondria using the FKBP-FRB system. This system has allowed to establish that Rab3GEP re-targeted to mitochondria is unable to rescue melanosome distribution, suggesting that cytoplasmic localisation is crucial for its activity. Moreover, our results show that temporally presence of Rab3GEP in the cytosol is able to activate the melanosome transport towards the cell periphery as seen in the first attempt when Rapalog drug was added after the visualization of Rab3GEP-FKBP overexpression. Instead cells incubated with the drug since the infection with the adenovirus maintained the clustering phenotype. Therefore, direct subtraction of Rab3GEP from the cytosol inhibits the activation of the melanosome transport. Previous studies (7,85) suggested that Rab3GEP is the guanine nucleotide exchange factor of Rab27a and it is important for its targeting to the melanosome membrane. Having determined that Rab3GEP localisation is important, it was explored whether the relocation of Rab3GEP to a different organelle (ex. mitochondria) influence Rab27a distribution and redirect it to mitochondria. For this purpose, as a first step a new chimeric protein Tomm70-GFP-Rab3GEP was made and its overexpression in melan-Rab3GEP KO cells was unable to restore melanosome distribution, confirming the necessity of having Rab3GEP in the cytosol to activate the melanosome transport (Figure 55). Hence, co-expression of Tomm70-GFP-Rab3GEP and mCherry-Rab27a was performed and cellular localisation of the two proteins was investigated. Our results indicate that Rab27a was redirected to the mitochondria when co-expressed with Tomm70-GFP-Rab3GEP, instead Rab27a was distributed equally throughout the cytoplasm when it is co-expressed with cytoplasmic

Rab3GEP wild type. Moreover, cells co-expressing Tomm70-GFP-Rab3GEP and mCherry presented a scattered distribution of mCherry, although GFP signal was located in restricted areas of the cytoplasm. This observation has confirmed the specific ability of Tomm70-GFP-Rab3GEP to target Rab27a to the mitochondria and its incapacity to target the negative control mCherry. These results were in accordance with the previous suggestion of the ability of Rab3GEP to target Rab27a made by Tarafder et al. (85). In this study authors found that in cells depleted for Rab3GEP Rab27a was not present in melanosome membrane, which suggests that Rab3GEP is important for the Rab27a targeting. Our results confirm this suggestion indicating that if Rab3GEP is artificially redirected to a different organelle such us mitochondria Rab27a follows its cognate.

In order to determine the link between the Rab3GEP GEF activity and its capacity to target Rab27a, mutants with no GEF activity where re-directed to mitochondria and Rab27a distribution was investigated.

For this purpose, a truncation mutant ΔDD and a point mutant Rab3GEP^{I353V} were used. Both these mutants have lost the GEF activity of Rab3GEP wild type and they were unable to rescue melanosome distribution in melan-Rab3GEP KO cells as can be seen chapter 4. Our results indicate that neither ΔDD nor Rab3GEP^{I353V} are able to retarget Rab27a to the mitochondria (sections 5.4 and 5.5) suggesting that the GEF activity of Rab3GEP is directly correlated with the capacity of targeting its cognate Rab27a. Another guanine nucleotide exchange factor has been recently suggested to have the same behaviour (38). In fact, in this study authors have pointed out that point mutations of Rabex-5 which decrease its GEF activity for Rab5, induce diminutions of its ability to re-direct Rab5 to mitochondria, suggesting direct link between GEF activity and targeting ability. Moreover, similar behaviour seems to be present in Rab3GAP, which although it is the GAP of Rab3, has been suggested that it is a GEF for Rab18 (151). In this study authors suggest that the complex Rab3GAP is important to target Rab18 and that point mutation knowing as disease-causing induce the lack not only of the GEF activity but even its ability to target Rab18 (151).

Summarizing, evidence contained in our results confirm that Rab3GEP is the guanine nucleotide exchange factor of Rab27a and that it is able to target Rab27a to organelle membrane, and this activity is dependent on the GEF activity.

6 Conclusion

In this thesis I have investigated the role of Rab3GEP in the activation and targeting of Rab27a using melanocytes with Rab3GEP gene knockout (melan-Rab3GEP KO cells) as a model.

In this work it has been observed that melan-Rab3GEP KO cells presented mixed phenotypes with different proportion of cells presenting disperse melanosomes distribution and cells with clustered melanosomes distribution. This behaviour indicates that although Rab3GEP is important for the activation of Rab27a and consequently for the initiation of the anterograde melanosome trafficking, it is not essential for the targeting and activation of Rab27a. In fact, in this thesis it has been shown that in cells with melanosome disperse distribution the trafficking is driven by Rab27a (silencing of Rab27a causes clustering), which suggested that Rab27a reaches the melanosome membrane, furthermore, localization of Mlph in melanosome membrane indicates that it is in the active form. Nevertheless, part of melan-Rab3GEP KO cells present clustering melanosome distribution, and re-introduction of Rab3GEP protein in melan-Rab3GEP KO cells increase the percentage of cells with scattered melanosome distribution to almost 100%, suggesting that Rab3GEP has a crucial role in increasing the kinetic of targeting and activation of Rab27a. Possible explanations of the presence of active Rab27a in the melanosome membrane in absence of Rab3GEP might be due to the nucleotide exchange activity of other RabGEFs, who would compensate the lack of Rab3GEP. Consistent with this, it has been shown previously that DENN4B and GRAB are able to activate Rab27a *in vitro*, though at a lower level than their common substrates, Rab10 and Rab3a respectively (7,54). Another explanation could be the intrinsic ability of Rab27a to switch its nucleotide from GDP to GTP, therefore, its own ability to activate and target itself.

Moreover, consistent with previous reports (87,88) in this thesis it has been shown that truncation of the full-length of Rab3GEP causes defects in its GEF activity and loss of the ability to rescue melanosome clustering. Nevertheless, results in this thesis show that the DENN domain of Rab3GEP is essential although not alone sufficient for the GEF activity and targeting towards Rab27a. In fact, truncations containing the DENN domain were not

able to activate Rab27a (as determined by Slp1 pull-down) in vitro, or target Rab27a to mitochondria, however, point mutations within the DENN domain (predicted to disrupt interaction of the DENN with Rab27a) interrupted the GEF activity of Rab3GEP suggesting crucial role of the DENN domain for the binding/activation of Rab27a. These results indicate once more that although Rab3GEP contains a DENN domain its activity is peculiar compared to other proteins containing DENN domain. In fact, data from studies on other DENN containing Rab GEFs suggested that the DENN domain alone is able to activate its cognate Rab (46,55,144). These suggested that other elements present in Rab3GEP protein are important for its function.

Another finding in this thesis is the link between the GEF activity and the ability to target. In fact, here it has been shown that the GEF activity of Rab3GEP is necessary for its function of Rab27a targeting to the membrane. In chapter 5 it is shown that although Rab3GEP full-length is able to re-target Rab27a to mitochondria, mutants that loss the GEF activity (ΔDD and Rab3GEP^{I353V}) are unable to mis-target Rab27a, suggesting that the GEF activity and the targeting activity are directly connected. These results are consistent with previous work on Rabex5, DrrA and Rabin8 (38).

In conclusion, results in this thesis displayed broadly agreement with the model of the important role of the GEF proteins on Rab targeting. However, considering that Rab27a can be melanosome resident even in cells with Rab3GEP KO, seems unlikely that this GEF is the sole determinant of Rab27a targeting.

7 Appendix

7.1 The proportion of cells with melanosomes clustered mirrors the rate of cell proliferation

Evidence in section 3.2 suggest that melan-Rab3GEP KO cells present mixed population of cells with dispersed and clustered distribution of melanosomes. Moreover, that in cells with dispersed melanosome distribution, melanophilin co-localise with melanosome at the periphery therefore, Rab27a is in the active state.

Monitoring of the three melan-Rab3GEP KO cell lines (#1, #2, #3), indicates that there are some variabilities between the three cell lines.
In fact, Figure 59A shows the different phenotypes of the three melan-Rab3GEP KO cell lines. The top panel shows the cells at Day 1 after passage and it is possible to see cells with dispersed melanosome distribution (red arrows) and cells with clustered melanosome distribution (black arrows). The bottom panel shows the same cell lines after five days, in which melan-Rab3GEP KO #3 cell line shows high percentage of cells with clustered melanosomes. Instead, melan-Rab3GEP KO #1 show high percentage of cells with disperse melanosome. Moreover, time course quantification analysis revealed that cell line #3 has the highest proportion of cells with clustered melanosome reaching 95% after 4 days as indicate by the graph C, and that this cell line grew faster than the others cell lines as indicate by the graph B. On the other hand, the cell line 1# grew slower (graph B) presenting the lowest number of total cells after five days and exhibits the lowest proportion of cells with clustered melanosomes (graph C).

These results suggest that there is a positive correlation between melanosome clustering and cell proliferation.

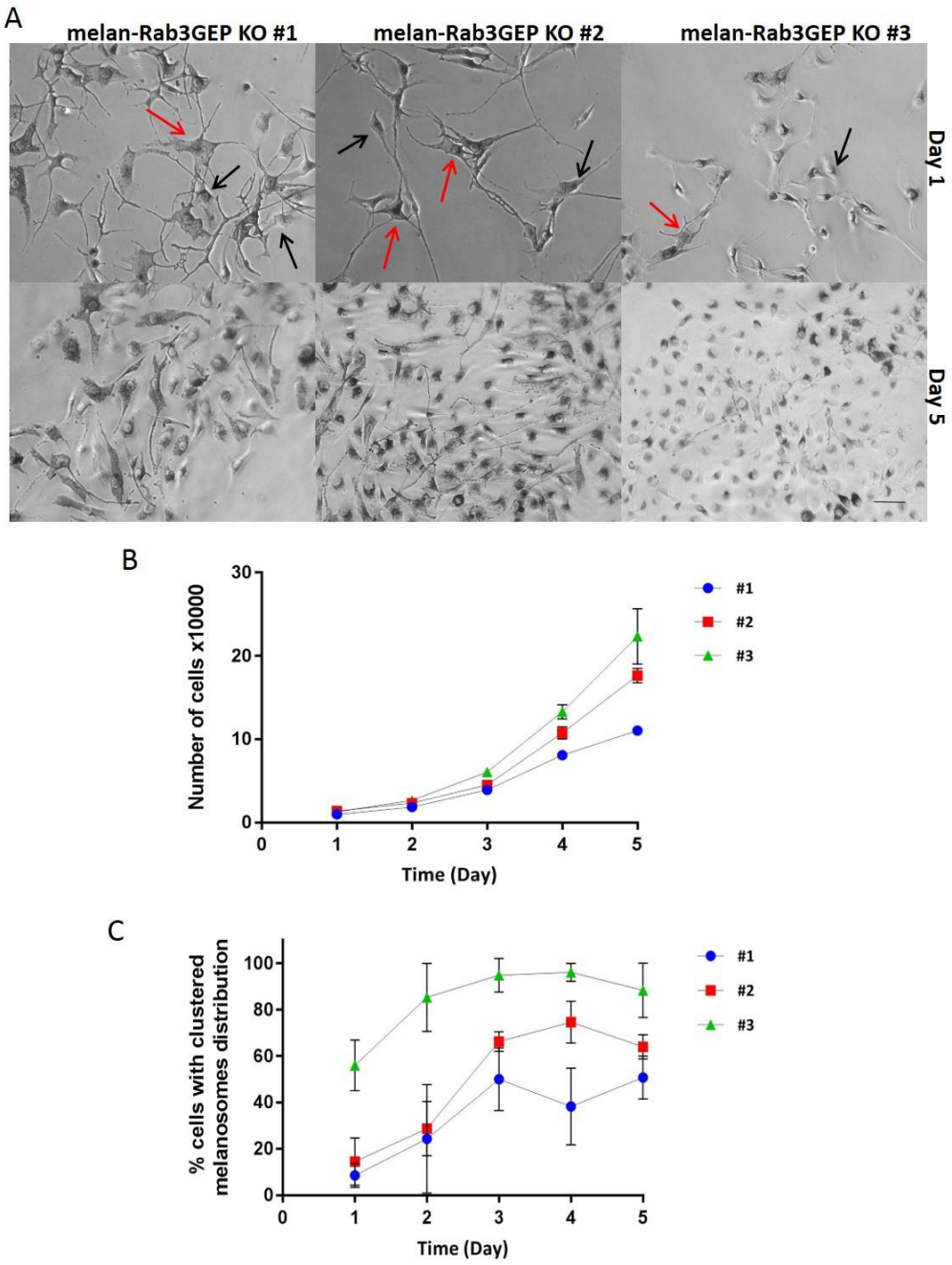


Figure 59 Relationship between total number of melan-Rab3GEP ko cells and cells with clustered melanosomes

A) Cells were seeded in a 24 well plates and pictures have been taken every day for 5 days using phase contrast. Three different cell lines melan-Rab3GEP #1,2,3 were imaged for 5 days, the top panels show the first day, black dots indicated phase-dark intracellular structures (melanosomes), red arrows specify cells with dispersed melanosome distribution, black arrows point to cells with clustered melanosome distribution at the perinuclear area. Bottom panels show picture at day 5. Scale bar 100µm B) Line plot shows the total number of cells day by day obtained from the average of 3 wells C) Line plot shows the percentage of cells with clustered melanosomes day by day obtained from 4 pictures of different areas

.

7.2 Defect of anterograde melanosomes trafficking during cell growth

Based on the results indicated in the Appendix 7.1 regarding the positive correlation between the number of cells with clustered melanosomes and the rate of growth, it was decided to test whether it is possible to increase the number of cells with melanosomes clustered by accelerating the rate of cell growth. For this purpose, melan-Rab3GEP cells were grown in presence and absence of growth stimulatory factors. In general, melan-Rab3GEP knockout cells are grown in RPMI supplemented with 10% fetal calf serum, 2mm l-glutamine, 100 units/ml penicillin and streptomycin, 40nm of a tumour promoter compound phorbol 12-myristate 13-acetate (PMA).
Tumour promoter compounds are not directly carcinogen or mutagenic, but if administrated chronically promote a later stage of the carcinogenesis, they do not alter the structure of DNA but change the expression of the genetic information, after exposure of carcinogen this can lead to tumour (152). It has been suggested that PMA can activate Protein Kinase C (PKC) a serine/threonine kinase (153). Normally, PKC is activated by diacylglycerol which is the product of the hydrolysis of PtdIns(4,5)P_2 performed by phospholipase C (PLC). PMA mimics diacylglycerol in the activation of PKC.

For our experiment, melan-Rab3GEP KO cells were incubated with different doses of PMA, then cell growth and melanosome distribution was monitored for 5 days. melan-Rab3GEP KO #1 cell line was chosen for this experiment, reasoning that it grows relatively slowly (see Figure 59), and that increasing the dose of growth factors might increase the proliferation and the percentage of clustering thereby allowing us to directly test the hypothesis that clustering occurs in rapid growth phase. Cells were grown in medium containing 0nM, 10nM, 20nM, 40nM and 80nM of PMA, imaged (Figure 60) and counted every day (see M&M) as previously.

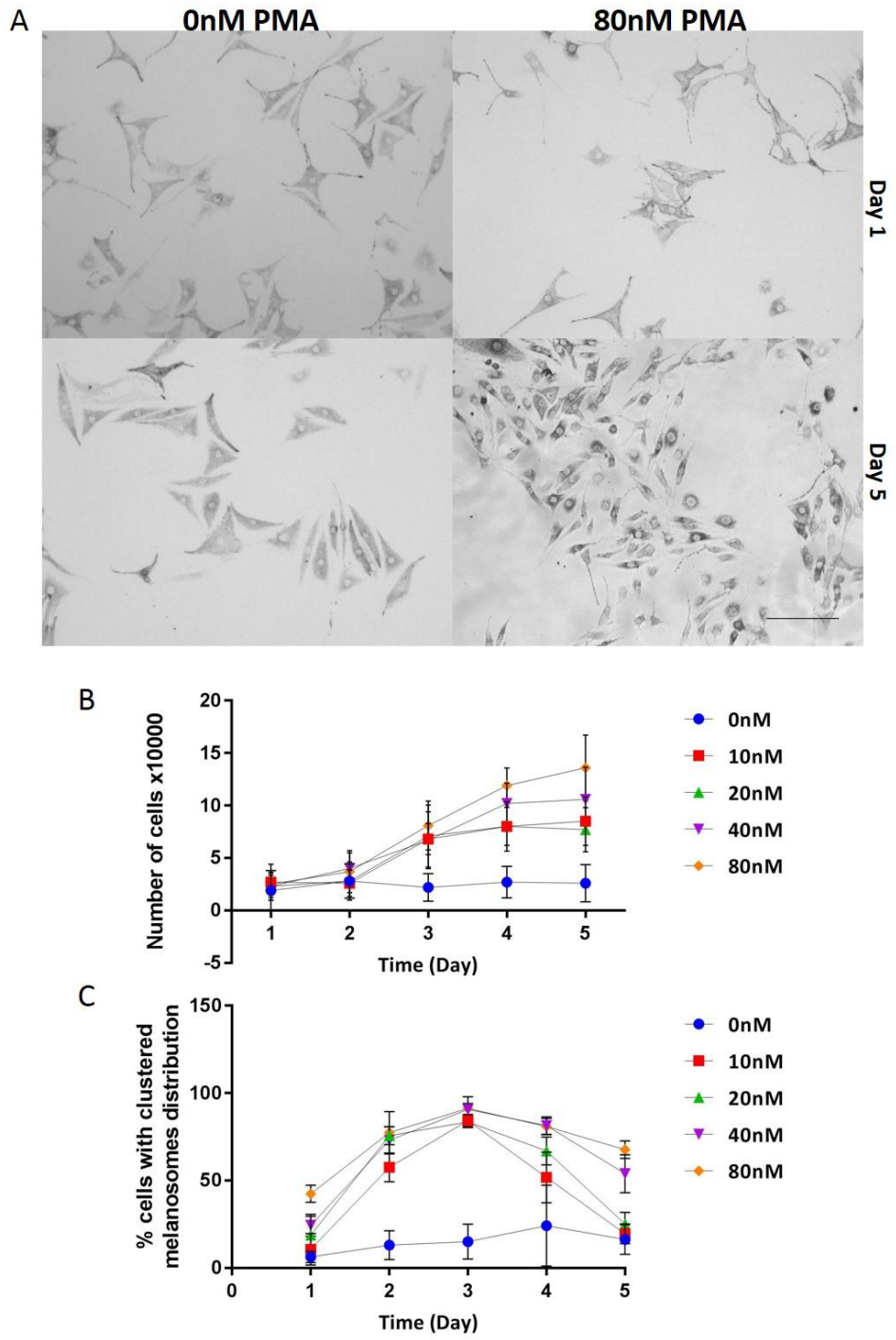


Figure 60 PMA increases cell number and proportion of cells with clustered melanosome distribution in melan-Rab3GEP KO #1

Cells were grown on glass coverslips with different concentration of PMA (0,10,20,40,80nM) and monitored for 5 days, fixed and imaged using bright-field optics A) Upper panel shows melan-Rab3GEP KO #1 cells at day 1. Lower panel shows same cell line after 5 Days. These pictures show the change in phenotype (melanosome distribution) in cells treated with the highest and the lowest dose of PMA during the time course. Scale bar 100µm. B-C) Line plots show the quantification of the total number of cells and the percentage of cells with clustered melanosome during the time course

Figure 60 shows clear evidence that cells maintained with the highest and the lowest concentration of PMA presented different melanosome distribution after 5 days. Cells grown with 0nM of PMA conserved the dispersed distribution of pigmented granules, instead cells incubated with 80nM of PMA showed mainly melanosome clustering at the perinuclear region. This suggests that PMA influences the melanosome distribution, causing phenotype change from a disperse melanosome distribution to a clustered distribution.
Moreover, cells maintained with 80nM of PMA grew faster and reached the peak of almost $1.4x10^5$ cells, instead cells maintained without PMA did not proliferate. Cells maintained with 40nM PMA grew faster than cells maintained with lower concentration of PMA. Cells incubated with the other two concentrations 10 and 20nM presented similar grow rates. All the concentrations show the same trend and the peak of cells with melanosomes clustered is reached at day 3, except for the cells without PMA. Possible explanation of these peaks at day 3 could be relate to the cell confluence, in fact, melanosome clustering is observed with high frequency when the cells have space to grow, instead when they become more confluent the growth is inhibited and melanosomes redistribute throughout the cell body.

Taking together these data, we are able to conclude that there is positive correlation between the number of cells with melanosomes accumulation at the perinuclear cytoplasm and rate of cell growth. Moreover, in cells with slow or absent proliferation that present disperse melanosome the trafficking is led by Rab27a, in fact its downregulation induces melanosome clustering (section 3.2). It is possible to conclude that Rab27a is the actor of this process, it might be activated by another RabGEF or it may be intrinsically activated.

References

1. Lodish H, B. A., Zipursky SL, et al. (2000) *Molecular Cell Biology*,

2. Rojas, A. M., Fuentes, G., Rausell, A., and Valencia, A. (2012) The Ras protein superfamily: evolutionary tree and role of conserved amino acids. *The Journal of cell biology* **196**, 189-201

3. Wennerberg, K., Rossman, K. L., and Der, C. J. (2005) The Ras superfamily at a glance. *Journal of cell science* **118**, 843-846

4. Bos, J. L., Rehmann, H., and Wittinghofer, A. (2007) GEFs and GAPs: critical elements in the control of small G proteins. *Cell* **129**, 865-877

5. Wasmeier, C., Hume, A. N., Bolasco, G., and Seabra, M. C. (2008) Melanosomes at a glance. *Journal of cell science* **121**, 3995-3999

6. Hume, A. N., Collinson, L. M., Rapak, A., Gomes, A. Q., Hopkins, C. R., and Seabra, M. C. (2001) Rab27a regulates the peripheral distribution of melanosomes in melanocytes. *The Journal of cell biology* **152**, 795-808

7. Figueiredo, A. C., Wasmeier, C., Tarafder, A. K., Ramalho, J. S., Baron, R. A., and Seabra, M. C. (2008) Rab3GEP is the non-redundant guanine nucleotide exchange factor for Rab27a in melanocytes. *The Journal of biological chemistry* **283**, 23209-23216

8. Itoh, T., and Fukuda, M. (2006) Identification of EPI64 as a GTPase-activating protein specific for Rab27A. *The Journal of biological chemistry* **281**, 31823-31831

9. Downward, J. (1998) Ras signalling and apoptosis. *Current opinion in genetics & development* **8**, 49-54

10. Etienne-Manneville, S., and Hall, A. (2002) Rho GTPases in cell biology. *Nature* **420**, 629-635

11. Ridley, A. J. (2001) Rho family proteins: coordinating cell responses. *Trends in cell biology* **11**, 471-477

12. Weis, K. (2003) Regulating access to the genome: nucleocytoplasmic transport throughout the cell cycle. *Cell* **112**, 441-451

13. Li, H. Y., Cao, K., and Zheng, Y. (2003) Ran in the spindle checkpoint: a new function for a versatile GTPase. *Trends in cell biology* **13**, 553-557

14. Pereira-Leal, J. B., and Seabra, M. C. (2001) Evolution of the Rab family of small GTP-binding proteins. *Journal of molecular biology* **313**, 889-901

15. Bhuin, T., and Roy, J. K. (2014) Rab proteins: The key regulators of intracellular vesicle transport. *Experimental cell research* **328**, 1-19

16. Vetter, I. R., and Wittinghofer, A. (2001) The guanine nucleotide-binding switch in three dimensions. *Science* **294**, 1299-1304

17. Schmitt, H. D., Wagner, P., Pfaff, E., and Gallwitz, D. (1986) The ras-related YPT1 gene product in yeast: a GTP-binding protein that might be involved in microtubule organization. *Cell* **47**, 401-412

18. Salminen, A., and Novick, P. J. (1987) A ras-like protein is required for a post-Golgi event in yeast secretion. *Cell* **49**, 527-538

19. Schwartz, S. L., Cao, C., Pylypenko, O., Rak, A., and Wandinger-Ness, A. (2008) Rab GTPases at a glance. *Journal of cell science* **121**, 246-246

20. Fischer von Mollard, G., Mignery, G. A., Baumert, M., Perin, M. S., Hanson, T. J., Burger, P. M., Jahn, R., and Sudhof, T. C. (1990) rab3 is a small GTP-binding protein exclusively localized to synaptic vesicles. *Proceedings of the National Academy of Sciences of the United States of America* **87**, 1988-1992

21. Lutcke, A., Jansson, S., Parton, R. G., Chavrier, P., Valencia, A., Huber, L. A., Lehtonen, E., and Zerial, M. (1993) Rab17, a novel small GTPase, is specific for epithelial cells and is induced during cell polarization. *The Journal of cell biology* **121**, 553-564

22. Zahraoui, A., Joberty, G., Arpin, M., Fontaine, J. J., Hellio, R., Tavitian, A., and Louvard, D. (1994) A small rab GTPase is distributed in cytoplasmic vesicles in non polarized cells but colocalizes with the tight junction marker ZO-1 in polarized epithelial cells. *The Journal of cell biology* **124**, 101-115

23. Goitre, L., Trapani, E., Trabalzini, L., and Retta, S. F. (2014) The Ras superfamily of small GTPases: the unlocked secrets. *Methods in molecular biology* **1120**, 1-18

24. Vetter, I. R. (2014) The Structure of the G Domain of the Ras Superfamily. in *Ras Superfamily Small G Proteins: Biology and Mechanisms 1: General Features, Signaling* (Wittinghofer, A. ed.), Springer Vienna, Vienna. pp 25-50

25. Pereira-Leal, J. B., and Seabra, M. C. (2000) The mammalian Rab family of small GTPases: definition of family and subfamily sequence motifs suggests a mechanism for functional specificity in the Ras superfamily. *Journal of molecular biology* **301**, 1077-1087

26. Ostermeier, C., and Brunger, A. T. (1999) Structural basis of Rab effector specificity: crystal structure of the small G protein Rab3A complexed with the effector domain of rabphilin-3A. *Cell* **96**, 363-374

27. Chavas, L. M., Ihara, K., Kawasaki, M., Torii, S., Uejima, T., Kato, R., Izumi, T., and Wakatsuki, S. (2008) Elucidation of Rab27 recruitment by its effectors: structure of Rab27a bound to Exophilin4/Slp2-a. *Structure* **16**, 1468-1477

28. Hutagalung, A. H., and Novick, P. J. (2011) Role of Rab GTPases in membrane traffic and cell physiology. *Physiological reviews* **91**, 119-149

29. Chavrier, P., Gorvel, J. P., Stelzer, E., Simons, K., Gruenberg, J., and Zerial, M. (1991) Hypervariable C-terminal domain of rab proteins acts as a targeting signal. *Nature* **353**, 769-772

30. Ali, B. R., and Seabra, M. C. (2005) Targeting of Rab GTPases to cellular membranes. *Biochemical Society transactions* **33**, 652-656

31. Arasaki, K., Toomre, D. K., and Roy, C. R. (2012) The Legionella pneumophila effector DrrA is sufficient to stimulate SNARE-dependent membrane fusion. *Cell host & microbe* **11**, 46-57

32. Bourne, H. R., Sanders, D. A., and McCormick, F. (1990) The GTPase superfamily: a conserved switch for diverse cell functions. *Nature* **348**, 125-132

33. Alexandrov, K., Horiuchi, H., Steele-Mortimer, O., Seabra, M. C., and Zerial, M. (1994) Rab escort protein-1 is a multifunctional protein that accompanies newly prenylated rab proteins to their target membranes. *The EMBO journal* **13**, 5262-5273

34. Goody, R. S., Rak, A., and Alexandrov, K. (2005) The structural and mechanistic basis for recycling of Rab proteins between membrane compartments. *Cellular and molecular life sciences : CMLS* **62**, 1657-1670

35. Barr, F., and Lambright, D. G. (2010) Rab GEFs and GAPs. *Current opinion in cell biology* **22**, 461-470

36. Ali, B. R., Wasmeier, C., Lamoreux, L., Strom, M., and Seabra, M. C. (2004) Multiple regions contribute to membrane targeting of Rab GTPases. *Journal of cell science* **117**, 6401-6412

37. Sivars, U., Aivazian, D., and Pfeffer, S. R. (2003) Yip3 catalyses the dissociation of endosomal Rab-GDI complexes. *Nature* **425**, 856-859

38. Blumer, J., Rey, J., Dehmelt, L., Mazel, T., Wu, Y. W., Bastiaens, P., Goody, R. S., and Itzen, A. (2013) RabGEFs are a major determinant for specific Rab membrane targeting. *The Journal of cell biology* **200**, 287-300

39. Barr, F. A. (2013) Review series: Rab GTPases and membrane identity: causal or inconsequential? *The Journal of cell biology* **202**, 191-199

40. Pfeffer, S. R. (2001) Rab GTPases: specifying and deciphering organelle identity and function. *Trends in cell biology* **11**, 487-491

41. Muller, M. P., and Goody, R. S. (2017) Molecular control of Rab activity by GEFs, GAPs and GDI. *Small GTPases*, 1-17

42. Wada, M., Nakanishi, H., Satoh, A., Hirano, H., Obaishi, H., Matsuura, Y., and Takai, Y. (1997) Isolation and Characterization of a GDP/GTP Exchange Protein Specific for the Rab3 Subfamily Small G Proteins. *Journal of Biological Chemistry* **272**, 3875-3878

43. Cherfils, J., and Chardin, P. (1999) GEFs: structural basis for their activation of small GTP-binding proteins. *Trends in biochemical sciences* **24**, 306-311

44. Cherfils, J., and Zeghouf, M. (2013) Regulation of small GTPases by GEFs, GAPs, and GDIs. *Physiological reviews* **93**, 269-309

45. Ishida, M., M, E. O., and Fukuda, M. (2016) Multiple Types of Guanine Nucleotide Exchange Factors (GEFs) for Rab Small GTPases. *Cell structure and function* **41**, 61-79

46. Wu, X., Bradley, M. J., Cai, Y., Kummel, D., De La Cruz, E. M., Barr, F. A., and Reinisch, K. M. (2011) Insights regarding guanine nucleotide exchange from the structure of a DENN-domain protein complexed with its Rab GTPase substrate. *Proceedings of the National Academy of Sciences of the United States of America* **108**, 18672-18677

47. Cai, Y., Chin, H. F., Lazarova, D., Menon, S., Fu, C., Cai, H., Sclafani, A., Rodgers, D. W., De La Cruz, E. M., Ferro-Novick, S., and Reinisch, K. M. (2008) The structural basis for activation of the Rab Ypt1p by the TRAPP membrane-tethering complexes. *Cell* **133**, 1202-1213

48. Dong, G., Medkova, M., Novick, P., and Reinisch, K. M. (2007) A catalytic coiled coil: structural insights into the activation of the Rab GTPase Sec4p by Sec2p. *Molecular cell* **25**, 455-462

49. Delprato, A., and Lambright, D. G. (2007) Structural basis for Rab GTPase activation by VPS9 domain exchange factors. *Nature structural & molecular biology* **14**, 406-412

50. Marat, A. L., Dokainish, H., and McPherson, P. S. (2011) DENN domain proteins: regulators of Rab GTPases. *The Journal of biological chemistry* **286**, 13791-13800

51. Levine, T. P., Daniels, R. D., Wong, L. H., Gatta, A. T., Gerondopoulos, A., and Barr, F. A. (2013) Discovery of new Longin and Roadblock domains that form platforms for small GTPases in Ragulator and TRAPP-II. *Small GTPases* **4**, 62-69

52. Allaire, P. D., Ritter, B., Thomas, S., Burman, J. L., Denisov, A. Y., Legendre-Guillemin, V., Harper, S. Q., Davidson, B. L., Gehring, K., and McPherson, P. S. (2006) Connecdenn, a novel DENN domain-containing protein of neuronal clathrin-coated vesicles functioning in synaptic vesicle endocytosis. *The Journal of neuroscience : the official journal of the Society for Neuroscience* **26**, 13202-13212

53. Marat, A. L., and McPherson, P. S. (2010) The connecdenn family, Rab35 guanine nucleotide exchange factors interfacing with the clathrin machinery. *The Journal of biological chemistry* **285**, 10627-10637

54. Yoshimura, S., Gerondopoulos, A., Linford, A., Rigden, D. J., and Barr, F. A. (2010) Family-wide characterization of the DENN domain Rab GDP-GTP exchange factors. *The Journal of cell biology* **191**, 367-381

55. Ioannou, M. S., Bell, E. S., Girard, M., Chaineau, M., Hamlin, J. N., Daubaras, M., Monast, A., Park, M., Hodgson, L., and McPherson, P. S. (2015) DENND2B activates Rab13 at the leading edge of migrating cells and promotes metastatic behavior. *The Journal of cell biology* **208**, 629-648

56. Hubbs, A. E., Majidi, M., and Lichy, J. H. (1999) Expression of an isoform of the novel signal transduction protein ST5 is linked to cell morphology. *Oncogene* **18**, 2519-2525

57. Matsui, T., Noguchi, K., and Fukuda, M. (2014) Dennd3 functions as a guanine nucleotide exchange factor for small GTPase Rab12 in mouse embryonic fibroblasts. *The Journal of biological chemistry* **289**, 13986-13995

58. Denef, N., Chen, Y., Weeks, S. D., Barcelo, G., and Schupbach, T. (2008) Crag regulates epithelial architecture and polarized deposition of basement membrane proteins in Drosophila. *Developmental cell* **14**, 354-364

59. Recacha, R., Boulet, A., Jollivet, F., Monier, S., Houdusse, A., Goud, B., and Khan, A. R. (2009) Structural basis for recruitment of Rab6-interacting protein 1 to Golgi via a RUN domain. *Structure* **17**, 21-30

60. Miserey-Lenkei, S., Waharte, F., Boulet, A., Cuif, M. H., Tenza, D., El Marjou, A., Raposo, G., Salamero, J., Heliot, L., Goud, B., and Monier, S. (2007) Rab6-interacting protein 1 links Rab6 and Rab11 function. *Traffic* **8**, 1385-1403

61. Linford, A., Yoshimura, S., Nunes Bastos, R., Langemeyer, L., Gerondopoulos, A., Rigden, D. J., and Barr, F. A. (2012) Rab14 and its exchange factor FAM116 link endocytic recycling and adherens junction stability in migrating cells. *Developmental cell* **22**, 952-966

62. Kulasekaran, G., Nossova, N., Marat, A. L., Lund, I., Cremer, C., Ioannou, M. S., and McPherson, P. S. (2015) Phosphorylation-dependent Regulation of Connecdenn/DENND1 Guanine Nucleotide Exchange Factors. *The Journal of biological chemistry* **290**, 17999-18008

63. Xu, J., Fotouhi, M., and McPherson, P. S. (2015) Phosphorylation of the exchange factor DENND3 by ULK in response to starvation activates Rab12 and induces autophagy. *EMBO reports* **16**, 709-718

64. Xu, J., and McPherson, P. S. (2017) Regulation of DENND3, the exchange factor for the small GTPase Rab12 through an intramolecular interaction. *The Journal of biological chemistry*

65. Carney, D. S., Davies, B. A., and Horazdovsky, B. F. (2006) Vps9 domain-containing proteins: activators of Rab5 GTPases from yeast to neurons. *Trends in cell biology* **16**, 27-35

66. Fukuda, M. (2016) Multiple Roles of VARP in Endosomal Trafficking: Rabs, Retromer Components and R-SNARE VAMP7 Meet on VARP. *Traffic* **17**, 709-719

67. Delprato, A., Merithew, E., and Lambright, D. G. (2004) Structure, exchange determinants, and family-wide rab specificity of the tandem helical bundle and Vps9 domains of Rabex-5. *Cell* **118**, 607-617

68. Hattula, K., Furuhjelm, J., Arffman, A., and Peranen, J. (2002) A Rab8-specific GDP/GTP exchange factor is involved in actin remodeling and polarized membrane transport. *Molecular biology of the cell* **13**, 3268-3280

69. Sato, Y., Fukai, S., Ishitani, R., and Nureki, O. (2007) Crystal structure of the Sec4p.Sec2p complex in the nucleotide exchanging intermediate state. *Proceedings of the National Academy of Sciences of the United States of America* **104**, 8305-8310

70. Wang, J., Ren, J., Wu, B., Feng, S., Cai, G., Tuluc, F., Peranen, J., and Guo, W. (2015) Activation of Rab8 guanine nucleotide exchange factor Rabin8 by ERK1/2 in response to EGF signaling. *Proceedings of the National Academy of Sciences of the United States of America* **112**, 148-153

71. Brunet, S., and Sacher, M. (2014) In sickness and in health: the role of TRAPP and associated proteins in disease. *Traffic* **15**, 803-818

72. Fukuda, M. (2011) TBC proteins: GAPs for mammalian small GTPase Rab? *Bioscience reports* **31**, 159-168

73. Fukui, K., Sasaki, T., Imazumi, K., Matsuura, Y., Nakanishi, H., and Takai, Y. (1997) Isolation and characterization of a GTPase activating protein specific for the Rab3 subfamily of small G proteins. *The Journal of biological chemistry* **272**, 4655-4658

74. Du, L. L., and Novick, P. (2001) Purification and properties of a GTPase-activating protein for yeast Rab GTPases. *Methods in enzymology* **329**, 91-99

75. Rak, A., Fedorov, R., Alexandrov, K., Albert, S., Goody, R. S., Gallwitz, D., and Scheidig, A. J. (2000) Crystal structure of the GAP domain of Gyp1p: first insights into interaction with Ypt/Rab proteins. *The EMBO journal* **19**, 5105-5113

76. Pan, X., Eathiraj, S., Munson, M., and Lambright, D. G. (2006) TBC-domain GAPs for Rab GTPases accelerate GTP hydrolysis by a dual-finger mechanism. *Nature* **442**, 303-306

77. Fukuda, M. (2008) Regulation of secretory vesicle traffic by Rab small GTPases. *Cellular and molecular life sciences : CMLS* **65**, 2801-2813

78. Chen, D., Guo, J., Miki, T., Tachibana, M., and Gahl, W. A. (1997) Molecular cloning and characterization of rab27a and rab27b, novel human rab proteins shared by melanocytes and platelets. *Biochemical and molecular medicine* **60**, 27-37

79. Menasche, G., Pastural, E., Feldmann, J., Certain, S., Ersoy, F., Dupuis, S., Wulffraat, N., Bianchi, D., Fischer, A., Le Deist, F., and de Saint Basile, G. (2000) Mutations in RAB27A cause Griscelli syndrome associated with haemophagocytic syndrome. *Nature genetics* **25**, 173-176

80. Van Gele, M., Dynoodt, P., and Lambert, J. (2009) Griscelli syndrome: a model system to study vesicular trafficking. *Pigment cell & melanoma research* **22**, 268-282

81. Tolmachova, T., Anders, R., Stinchcombe, J., Bossi, G., Griffiths, G. M., Huxley, C., and Seabra, M. C. (2004) A general role for Rab27a in secretory cells. *Molecular biology of the cell* **15**, 332-344

82. Fukuda, M. (2013) Rab27 effectors, pleiotropic regulators in secretory pathways. *Traffic* **14**, 949-963

83. Ostrowski, M., Carmo, N. B., Krumeich, S., Fanget, I., Raposo, G., Savina, A., Moita, C. F., Schauer, K., Hume, A. N., Freitas, R. P., Goud, B., Benaroch, P., Hacohen, N., Fukuda, M., Desnos, C., Seabra, M. C., Darchen, F., Amigorena, S., Moita, L. F., and Thery, C. (2010) Rab27a and Rab27b control different steps of the exosome secretion pathway. *Nature cell biology* **12**, 19-30; sup pp 11-13

84. Imai, A., Ishida, M., Fukuda, M., Nashida, T., and Shimomura, H. (2013) MADD/DENN/Rab3GEP functions as a guanine nucleotide

exchange factor for Rab27 during granule exocytosis of rat parotid acinar cells. *Archives of biochemistry and biophysics* **536**, 31-37

85. Tarafder, A. K., Wasmeier, C., Figueiredo, A. C., Booth, A. E., Orihara, A., Ramalho, J. S., Hume, A. N., and Seabra, M. C. (2011) Rab27a targeting to melanosomes requires nucleotide exchange but not effector binding. *Traffic* **12**, 1056-1066

86. Imai, A., Yoshie, S., Nashida, T., Fukuda, M., and Shimomura, H. (2009) Redistribution of small GTP-binding protein, Rab27B, in rat parotid acinar cells after stimulation with isoproterenol. *European journal of oral sciences* **117**, 224-230

87. Coppola, T., Perret-Menoud, V., Gattesco, S., Magnin, S., Pombo, I., Blank, U., and Regazzi, R. (2002) The death domain of Rab3 guanine nucleotide exchange protein in GDP/GTP exchange activity in living cells. *The Biochemical journal* **362**, 273-279

88. Oishi, H. (1998) Localization of the Rab3 Small G Protein Regulators in Nerve Terminals and Their Involvement in Ca2+-dependent Exocytosis. *Journal of Biological Chemistry* **273**, 34580-34585

89. Park, H. H., Lo, Y. C., Lin, S. C., Wang, L., Yang, J. K., and Wu, H. (2007) The death domain superfamily in intracellular signaling of apoptosis and inflammation. *Annual review of immunology* **25**, 561-586

90. Schievella, A. R. (1997) MADD, a Novel Death Domain Protein That Interacts with the Type 1 Tumor Necrosis Factor Receptor and Activates Mitogen-activated Protein Kinase. *Journal of Biological Chemistry* **272**, 12069-12075

91. Miyoshi, J., and Takai, Y. (2004) Dual role of DENN/MADD (Rab3GEP) in neurotransmission and neuroprotection. *Trends in molecular medicine* **10**, 476-480

92. Kurada, B. R., Li, L. C., Mulherkar, N., Subramanian, M., Prasad, K. V., and Prabhakar, B. S. (2009) MADD, a splice variant of IG20, is indispensable for MAPK activation and protection against apoptosis upon tumor necrosis factor-alpha treatment. *The Journal of biological chemistry* **284**, 13533-13541

93. Del Villar, K., and Miller, C. A. (2004) Down-regulation of DENN/MADD, a TNF receptor binding protein, correlates with neuronal cell death in Alzheimer's disease brain and hippocampal neurons. *Proceedings of the National Academy of Sciences of the United States of America* **101**, 4210-4215

94. Zhang, Y., Zhou, L., and Miller, C. A. (1998) A splicing variant of a death domain protein that is regulated by a mitogen-activated kinase is a substrate for c-Jun N-terminal kinase in the human central

nervous system. *Proceedings of the National Academy of Sciences of the United States of America* **95**, 2586-2591

95. Niwa, S., Tanaka, Y., and Hirokawa, N. (2008) KIF1Bbeta- and KIF1A-mediated axonal transport of presynaptic regulator Rab3 occurs in a GTP-dependent manner through DENN/MADD. *Nature cell biology* **10**, 1269-1279

96. Hsu, C., Morohashi, Y., Yoshimura, S., Manrique-Hoyos, N., Jung, S., Lauterbach, M. A., Bakhti, M., Gronborg, M., Mobius, W., Rhee, J., Barr, F. A., and Simons, M. (2010) Regulation of exosome secretion by Rab35 and its GTPase-activating proteins TBC1D10A-C. *The Journal of cell biology* **189**, 223-232

97. Hou, Y., Chen, X., Tolmachova, T., Ernst, S. A., and Williams, J. A. (2013) EPI64B acts as a GTPase-activating protein for Rab27B in pancreatic acinar cells. *The Journal of biological chemistry* **288**, 19548-19557

98. Kimura, T., Kaneko, Y., Yamada, S., Ishihara, H., Senda, T., Iwamatsu, A., and Niki, I. (2008) The GDP-dependent Rab27a effector coronin 3 controls endocytosis of secretory membrane in insulin-secreting cell lines. *Journal of cell science* **121**, 3092-3098

99. Fukuda, M. (2005) Versatile role of Rab27 in membrane trafficking: focus on the Rab27 effector families. *Journal of biochemistry* **137**, 9-16

100. Kuroda, T. S., Fukuda, M., Ariga, H., and Mikoshiba, K. (2002) The Slp homology domain of synaptotagmin-like proteins 1-4 and Slac2 functions as a novel Rab27A binding domain. *The Journal of biological chemistry* **277**, 9212-9218

101. Fukuda, M. (2003) Distinct Rab binding specificity of Rim1, Rim2, rabphilin, and Noc2. Identification of a critical determinant of Rab3A/Rab27A recognition by Rim2. *The Journal of biological chemistry* **278**, 15373-15380

102. Fukuda, M., Saegusa, C., and Mikoshiba, K. (2001) Novel splicing isoforms of synaptotagmin-like proteins 2 and 3: identification of the Slp homology domain. *Biochemical and biophysical research communications* **283**, 513-519

103. Neeft, M., Wieffer, M., de Jong, A. S., Negroiu, G., Metz, C. H., van Loon, A., Griffith, J., Krijgsveld, J., Wulffraat, N., Koch, H., Heck, A. J., Brose, N., Kleijmeer, M., and van der Sluijs, P. (2005) Munc13-4 is an effector of rab27a and controls secretion of lysosomes in hematopoietic cells. *Molecular biology of the cell* **16**, 731-741

104. Zografou, S., Basagiannis, D., Papafotika, A., Shirakawa, R., Horiuchi, H., Auerbach, D., Fukuda, M., and Christoforidis, S. (2012)

A complete Rab screening reveals novel insights in Weibel-Palade body exocytosis. *Journal of cell science* **125**, 4780-4790

105. Izumi, T. (2007) Physiological roles of Rab27 effectors in regulated exocytosis. *Endocrine journal* **54**, 649-657

106. Fukuda, M. (2006) Rab27 and its effectors in secretory granule exocytosis: a novel docking machinery composed of a Rab27.effector complex. *Biochemical Society transactions* **34**, 691-695

107. Waselle, L., Coppola, T., Fukuda, M., Iezzi, M., El-Amraoui, A., Petit, C., and Regazzi, R. (2003) Involvement of the Rab27 binding protein Slac2c/MyRIP in insulin exocytosis. *Molecular biology of the cell* **14**, 4103-4113

108. Cheviet, S., Coppola, T., Haynes, L. P., Burgoyne, R. D., and Regazzi, R. (2004) The Rab-binding protein Noc2 is associated with insulin-containing secretory granules and is essential for pancreatic beta-cell exocytosis. *Molecular endocrinology* **18**, 117-126

109. Guangpu Li, N. S. (2012) Rab GTPases and Membrane Trafficking. *Bentham eBooks*

110. Kuroda, T. S., and Fukuda, M. (2004) Rab27A-binding protein Slp2-a is required for peripheral melanosome distribution and elongated cell shape in melanocytes. *Nature cell biology* **6**, 1195-1203

111. Munafo, D. B., Johnson, J. L., Ellis, B. A., Rutschmann, S., Beutler, B., and Catz, S. D. (2007) Rab27a is a key component of the secretory machinery of azurophilic granules in granulocytes. *The Biochemical journal* **402**, 229-239

112. Holt, O., Kanno, E., Bossi, G., Booth, S., Daniele, T., Santoro, A., Arico, M., Saegusa, C., Fukuda, M., and Griffiths, G. M. (2008) Slp1 and Slp2-a localize to the plasma membrane of CTL and contribute to secretion from the immunological synapse. *Traffic* **9**, 446-457

113. Feldmann, J., Callebaut, I., Raposo, G., Certain, S., Bacq, D., Dumont, C., Lambert, N., Ouachee-Chardin, M., Chedeville, G., Tamary, H., Minard-Colin, V., Vilmer, E., Blanche, S., Le Deist, F., Fischer, A., and de Saint Basile, G. (2003) Munc13-4 is essential for cytolytic granules fusion and is mutated in a form of familial hemophagocytic lymphohistiocytosis (FHL3). *Cell* **115**, 461-473

114. Pastural, E., Barrat, F. J., Dufourcq-Lagelouse, R., Certain, S., Sanal, O., Jabado, N., Seger, R., Griscelli, C., Fischer, A., and de Saint Basile, G. (1997) Griscelli disease maps to chromosome 15q21 and is associated with mutations in the myosin-Va gene. *Nature genetics* **16**, 289-292

115. Griscelli, C., Durandy, A., Guy-Grand, D., Daguillard, F., Herzog, C., and Prunieras, M. (1978) A syndrome associating partial albinism and immunodeficiency. *The American journal of medicine* **65**, 691-702

116. Strom, M., Hume, A. N., Tarafder, A. K., Barkagianni, E., and Seabra, M. C. (2002) A family of Rab27-binding proteins. Melanophilin links Rab27a and myosin Va function in melanosome transport. *The Journal of biological chemistry* **277**, 25423-25430

117. Wu, X., Wang, F., Rao, K., Sellers, J. R., and Hammer, J. A., 3rd. (2002) Rab27a is an essential component of melanosome receptor for myosin Va. *Molecular biology of the cell* **13**, 1735-1749

118. Menager, M. M., Menasche, G., Romao, M., Knapnougel, P., Ho, C. H., Garfa, M., Raposo, G., Feldmann, J., Fischer, A., and de Saint Basile, G. (2007) Secretory cytotoxic granule maturation and exocytosis require the effector protein hMunc13-4. *Nature immunology* **8**, 257-267

119. Stinchcombe, J. C., Barral, D. C., Mules, E. H., Booth, S., Hume, A. N., Machesky, L. M., Seabra, M. C., and Griffiths, G. M. (2001) Rab27a is required for regulated secretion in cytotoxic T lymphocytes. *The Journal of cell biology* **152**, 825-834

120. Westbroek, W., Klar, A., Cullinane, A. R., Ziegler, S. G., Hurvitz, H., Ganem, A., Wilson, K., Dorward, H., Huizing, M., Tamimi, H., Vainshtein, I., Berkun, Y., Lavie, M., Gahl, W. A., and Anikster, Y. (2012) Cellular and clinical report of new Griscelli syndrome type III cases. *Pigment cell & melanoma research* **25**, 47-56

121. Seabra, M. C., Ho, Y. K., and Anant, J. S. (1995) Deficient geranylgeranylation of Ram/Rab27 in choroideremia. *The Journal of biological chemistry* **270**, 24420-24427

122. Mahoney, T. R., Liu, Q., Itoh, T., Luo, S., Hadwiger, G., Vincent, R., Wang, Z. W., Fukuda, M., and Nonet, M. L. (2006) Regulation of synaptic transmission by RAB-3 and RAB-27 in Caenorhabditis elegans. *Molecular biology of the cell* **17**, 2617-2625

123. Tanaka, M., Miyoshi, J., Ishizaki, H., Togawa, A., Ohnishi, K., Endo, K., Matsubara, K., Mizoguchi, A., Nagano, T., Sato, M., Sasaki, T., and Takai, Y. (2001) Role of Rab3 GDP/GTP exchange protein in synaptic vesicle trafficking at the mouse neuromuscular junction. *Molecular biology of the cell* **12**, 1421-1430

124. Yamaguchi, Y., and Hearing, V. J. (2009) Physiological factors that regulate skin pigmentation. *BioFactors* **35**, 193-199

125. Raposo, G., and Marks, M. S. (2007) Melanosomes--dark organelles enlighten endosomal membrane transport. *Nature reviews. Molecular cell biology* **8**, 786-797

126. A., C. M. W. M. S. (2013) Heterogeneity of neural crest-derived melanocytes. *Central European Journal of Biology*

127. Hearing, V. J. (2011) Determination of melanin synthetic pathways. *The Journal of investigative dermatology* **131**, E8-E11

128. Barral, D. C., and Seabra, M. C. (2004) The melanosome as a model to study organelle motility in mammals. *Pigment cell research / sponsored by the European Society for Pigment Cell Research and the International Pigment Cell Society* **17**, 111-118

129. Evans, R. D., Robinson, C., Briggs, D. A., Tooth, D. J., Ramalho, J. S., Cantero, M., Montoliu, L., Patel, S., Sviderskaya, E. V., and Hume, A. N. (2014) Myosin-Va and dynamic actin oppose microtubules to drive long-range organelle transport. *Current biology : CB* **24**, 1743-1750

130. Lavado, A., Matheu, A., Serrano, M., and Montoliu, L. (2005) A strategy to study tyrosinase transgenes in mouse melanocytes. *BMC Cell Biol* **6**, 18

131. Bennett, D. C., Cooper, P. J., Dexter, T. J., Devlin, L. M., Heasman, J., and Nester, B. (1989) Cloned mouse melanocyte lines carrying the germline mutations albino and brown: complementation in culture. *Development* **105**, 379-385

132. Hume, A. N., Tarafder, A. K., Ramalho, J. S., Sviderskaya, E. V., and Seabra, M. C. (2006) A coiled-coil domain of melanophilin is essential for Myosin Va recruitment and melanosome transport in melanocytes. *Molecular biology of the cell* **17**, 4720-4735

133. Jackson, I. J. (1991) Mouse coat colour mutations: a molecular genetic resource which spans the centuries. *BioEssays : news and reviews in molecular, cellular and developmental biology* **13**, 439-446

134. Wilson, S. M., Yip, R., Swing, D. A., O'Sullivan, T. N., Zhang, Y., Novak, E. K., Swank, R. T., Russell, L. B., Copeland, N. G., and Jenkins, N. A. (2000) A mutation in Rab27a causes the vesicle transport defects observed in ashen mice. *Proceedings of the National Academy of Sciences of the United States of America* **97**, 7933-7938

135. Mercer, J. A., Seperack, P. K., Strobel, M. C., Copeland, N. G., and Jenkins, N. A. (1991) Novel myosin heavy chain encoded by murine dilute coat colour locus. *Nature* **349**, 709-713

136. Matesic, L. E., Yip, R., Reuss, A. E., Swing, D. A., O'Sullivan, T. N., Fletcher, C. F., Copeland, N. G., and Jenkins, N. A. (2001) Mutations in Mlph, encoding a member of the Rab effector family, cause the melanosome transport defects observed in leaden mice. *Proceedings of the National Academy of Sciences of the United States of America* **98**, 10238-10243

137. Giacinti, C., and Giordano, A. (2006) RB and cell cycle progression. *Oncogene* **25**, 5220-5227

138. Chin, L., Pomerantz, J., and DePinho, R. A. (1998) The INK4a/ARF tumor suppressor: one gene--two products--two pathways. *Trends in biochemical sciences* **23**, 291-296

139. Bieging, K. T., Mello, S. S., and Attardi, L. D. (2014) Unravelling mechanisms of p53-mediated tumour suppression. *Nature reviews. Cancer* **14**, 359-370

140. Chabrillat, M. L., Wilhelm, C., Wasmeier, C., Sviderskaya, E. V., Louvard, D., and Coudrier, E. (2005) Rab8 regulates the actin-based movement of melanosomes. *Molecular biology of the cell* **16**, 1640-1650

141. Ishida, M., Ohbayashi, N., and Fukuda, M. (2015) Rab1A regulates anterograde melanosome transport by recruiting kinesin-1 to melanosomes through interaction with SKIP. *Scientific reports* **5**, 8238

142. Cerikan, B., Shaheen, R., Colo, G. P., Glasser, C., Hata, S., Knobeloch, K. P., Alkuraya, F. S., Fassler, R., and Schiebel, E. (2016) Cell-Intrinsic Adaptation Arising from Chronic Ablation of a Key Rho GTPase Regulator. *Developmental cell* **39**, 28-43

143. Barral, D. C., Ramalho, J. S., Anders, R., Hume, A. N., Knapton, H. J., Tolmachova, T., Collinson, L. M., Goulding, D., Authi, K. S., and Seabra, M. C. (2002) Functional redundancy of Rab27 proteins and the pathogenesis of Griscelli syndrome. *Journal of Clinical Investigation* **110**, 247-257

144. Allaire, P. D., Marat, A. L., Dall'Armi, C., Di Paolo, G., McPherson, P. S., and Ritter, B. (2010) The Connecdenn DENN domain: a GEF for Rab35 mediating cargo-specific exit from early endosomes. *Molecular cell* **37**, 370-382

145. Johnson, J. L., Ellis, B. A., Noack, D., Seabra, M. C., and Catz, S. D. (2005) The Rab27a-binding protein, JFC1, regulates androgen-dependent secretion of prostate-specific antigen and prostatic-specific acid phosphatase. *The Biochemical journal* **391**, 699-710

146. Levivier, E., Goud, B., Souchet, M., Calmels, T. P., Mornon, J. P., and Callebaut, I. (2001) uDENN, DENN, and dDENN: indissociable domains in Rab and MAP kinases signaling pathways. *Biochemical and biophysical research communications* **287**, 688-695

147. Holz, R. W., Brondyk, W. H., Senter, R. A., Kuizon, L., and Macara, I. G. (1994) Evidence for the involvement of Rab3A in Ca(2+)-dependent exocytosis from adrenal chromaffin cells. *The Journal of biological chemistry* **269**, 10229-10234

148. Murata, T., Delprato, A., Ingmundson, A., Toomre, D. K., Lambright, D. G., and Roy, C. R. (2006) The Legionella pneumophila effector protein DrrA is a Rab1 guanine nucleotide-exchange factor. *Nature cell biology* **8**, 971-977

149. Schoebel, S., Oesterlin, L. K., Blankenfeldt, W., Goody, R. S., and Itzen, A. (2009) RabGDI displacement by DrrA from Legionella is a consequence of its guanine nucleotide exchange activity. *Molecular cell* **36**, 1060-1072

150. Alvarez-Dolado, M., Gonzalez-Moreno, M., Valencia, A., Zenke, M., Bernal, J., and Munoz, A. (1999) Identification of a mammalian homologue of the fungal Tom70 mitochondrial precursor protein import receptor as a thyroid hormone-regulated gene in specific brain regions. *Journal of neurochemistry* **73**, 2240-2249

151. Gerondopoulos, A., Bastos, R. N., Yoshimura, S., Anderson, R., Carpanini, S., Aligianis, I., Handley, M. T., and Barr, F. A. (2014) Rab18 and a Rab18 GEF complex are required for normal ER structure. *The Journal of cell biology* **205**, 707-720

152. Blumberg, P. M. (1988) Protein kinase C as the receptor for the phorbol ester tumor promoters: sixth Rhoads memorial award lecture. *Cancer research* **48**, 1-8

153. Castagna, M., Takai, Y., Kaibuchi, K., Sano, K., Kikkawa, U., and Nishizuka, Y. (1982) Direct activation of calcium-activated, phospholipid-dependent protein kinase by tumor-promoting phorbol esters. *The Journal of biological chemistry* **257**, 7847-7851